Positioning Technology

for

Stepwise Underground Robots

Wei Li

School of Engineering

University of Durham

A thesis submitted in partial fulfilment of the requirements of the University of Durham for the Degree of Doctor of Philosophy (Ph.D.)

March 2003

Abstract

Pipeline robots, borehole robots or exploring robots that work in underground environments can be classified as underground robots. When an underground robot takes a task, tracing and mapping the track of the robot is very important. This project addresses the development of a positioning technique for stepwise underground robots, which have been developed in Durham University. This research is expected to provide a general benefit to stepwise robotic positioning systems rather than a particular robotic or other situation.

The initial period of this project was the most difficult. After a few months of literature searching, no suitable positioning technique had been found. Existing techniques are suitable for surface robots, undersea robots or airborne robots but are far away from the application requirements for underground robots. Positioning technology depends on sensor techniques and measurement technologies. The underground environment restricts the use of absolute measurement technologies. Consequently, underground robotic positioning systems heavily rely on relative measurements, which can cause unbounded accumulation of the positioning errors. Moreover, underground environments restrict the use of many high precision sensors because of restricted space and other factors. Hence, the feasibility of developing high, long-term, accuracy underground robotic positioning systems was problematic.

Since it was found that there was a lack of research on underground robotic positioning, fundamental investigation became necessary. The fundamentals include the dominant error and the characters of the accumulation of positioning errors. After the investigation of the fundamentals the difficulty and feasibility of developing a high long-term accuracy positioning system was understood more clearly and the key factors to improve the accuracy of a positioning system were known. Based on these, a novel parallel linkage mechanism based approach was proposed. This approach has flexibility in terms of geometrical structure and provides the possibility to improve long-term accuracy of a positioning system. Although parallel linkage mechanisms have drawn a great deal of attention from researchers in passed years, this is the first time a parallel linkage mechanism has been applied to a robotic positioning system. Consequently, new problems were generated by this application of parallel linkage

mechanisms. In this project, a Principal Component Analysis (PCA) method is applied to solve the positioning problems and a particular case has been used to show how to solve these problems. Through this case, the advantages of this approach and the feasibility to improve the positioning accuracy is presented. The methodology that can be used to solve the problems for different particular cases can also be used to carry out study for general situations, which have also been illustrated.

Many problems still need to be solved. At the end of this thesis, some further problems are discussed. The author of this thesis believes that the proposed approach can be applied to industrial projects in the near future.

Acknowledgements

I wish to acknowledge my appreciation to all those who helped and assisted during this research project.

Firstly, I would like to thank my supervisor, Professor E. Appleton, who has always encouraged me to think freely, yet gave me good guidance and kept me on the right track.

Secondly, I appreciate Durham University and St Aidan's College for providing me with a Durham University Research Studentship and St Aidan's College Award, which made my PhD study at the School of Engineering, University of Durham, possible.

Notations

D	Step length of a stepwise robot
n	Number (n) of the travelled steps
E_d	Distance measurement error
E_o	Orientation measurement error
E_{ox}	Angular measurement error around the x-axis
E_{oy}	Angular measurement error around the y-axis
E_{oz}	Angular measurement error around the z-axis
E_{oo}	Angular measurement error caused by E_{oz} and E_{oy} is denoted as E_{oo}
E_{od}	Angular measurement error caused by E_{ox} (see page 38)
e_d	Positioning error caused by distance measurement error.
e_o	Positioning error caused by orientation measurement error.
e_{dx}	Positioning error in the travel direction caused by distance measurement error.
e_{dy}	Positioning error in the lateral direction caused by distance measurement error.
e_{ox}	Positioning error in the travel direction caused by orientation measurement error.
e_{oy}	Positioning error in the lateral direction caused by orientation measurement error respectively.
p	Pull force on a spring (in Section 6.1 of this thesis)
l	Length of a spring (in Section 6.1 of this thesis)
p_i	The i-th(i = 1, 2,..., n) sample value of the pull force (p) (in Section 6.1 of this thesis)
l_i	1. the i-th(i = 1, 2,..., n) sample value of the length (l) of a spring (in Section 6.1 of this thesis) 2. The i-th(i = 1, 2,..., n) link in a parallel linkage mechanism (in the rest of this thesis)
$\mathbf{b}_i$	The joint between the i-th (i = 1, 2,..., n) link and the **base** in a parallel linkage mechanism.
$\mathbf{t}_i$.	The joint between the i-th(i = 1, 2,..., n) link and the **top platform** in a parallel linkage mechanism.

$(\alpha_1, \alpha_2, \alpha_3, \alpha_4, \alpha_5, lm)$	Positional variables of a Steward plat form (see the definition on page 61)
$(x_0, y_0, z_0, \alpha, \beta, \gamma)$.	Positional variables of a Steward plat form (see the definition on page 60)
R	Orthogonal rotation matrix
R_{mb}	The orthogonal rotation matrix from the M-frame to the B-frame
R_{tm}	The rotation matrix from the T-frame to the M-frame,
v	Translation vector
F(.)	Any given function
$F^{-1}(.)$	The inverse function of any given function F(.)
Y_k	The *k*th (k = 1, 2,..., n) principal component
Y	Principal component vector $Y = \begin{bmatrix} Y_1 \\ Y_2 \\ \vdots \\ Y_n \end{bmatrix}$;
Y_{ik}	The *i*th (i = 1, 2,..., m) sample value of the *k*th (k = 1, 2,..., *n)* principal component
λ_i	The *i*-th (i = 1, 2,..., n) eigenvalues ($\lambda_1 \geq \lambda_2 \geq \ldots \geq \lambda_n$)
$\mathbf{a}_i$	The *i*-th (i = 1, 2,..., n) eigenvectors corresponding to the *i*-th eigenvalues λ_i
$\{\mathbf{Q}_i\} = \{(y_{i1}, y_{i2}, \ldots, y_{in}) \mid i = 1,2, \ldots, m\}$	Given data set for sampling. Here, m is the size of samples.
$\{\mathbf{P}_i\} = \{(x_{i1}, x_{i2}, \ldots, x_{in}) \mid i = 1,2, \ldots, m\}$	Calculated data set corresponding to data set $\{\mathbf{Q}_i\}$.
ρ	Polar angle in a polar frame
θ	Radius in a polar frame
$(\varepsilon_1, \varepsilon_2, \varepsilon_3, \varepsilon_4, \varepsilon_5, \varepsilon_{lm})$.	Allowable errors of the positional variables (α_1, α_2, α_3, α_4, α, lm)
y_{upper}	Upper value of the variable y
y_{inf}	Inferior vale of the variable y

CONTENTS

PART I

Fundamental Issues in

Underground Robotic Positioning Techniques

Chapter 1

Introduction to Part I

As in the case of other mobile robots, it is very important for an underground robot to know its position. Because the working environments are different, some particular problems in underground robotic positioning systems need to be identified. However, until now there has been a lack of research on underground robotic positioning systems. Therefore, some fundamentals need to be discussed before starting the positioning system design process.

1.1 Objective

In this part, some fundamentals of underground robotic positioning techniques will be discussed. Following that discussion, a parallel linkage mechanisms based approach will be proposed. This approach is based on the understanding of the general characteristic of positioning systems for underground robots, especially for stepwise underground traction.

The task of a positioning system is to know the position and in order to provide information for navigation and robotic control. So, a positioning system is crucially important for a mobile robot. Positioning systems are based on sensors and measurement techniques but the use of sensor signals is different from robot to robot. Surface or undersea robots often need to take action based on the environment. Their control or navigation task is often relative to the environment. So surface or undersea mobile robots often need to use the information from the environment to compare with the known knowledge of the environment in order to identify location. Processing the environmental information needs complicated algorithms. In other words, positioning systems for surface or undersea robots need and can obtain extensive environmental information but the post-processing of the data is complicated and difficult. Underground robots are different. Underground robots do not need to analyse the environment to identify location. It only needs to know the

position relative to a known point or initial starting position. Such machines do not need to collect environmental information to identify location. Comparing underground robots with other mobile robots, their control and navigation are more straightforward but the positioning systems rely more heavily on measurement technologies. If measurement technologies cannot be improved, underground robotic positioning systems will be difficult to improve. Positioning accuracy requirements are also different between underground and other mobile robots. Comparing underground robots with other robots brings out the need for higher long-term and short-term positioning accuracy. Long-term positioning accuracy is more important for underground robots. The definition of 'long-term' or 'short-term' depends on the particular application. In industry, 'long-term' may be 500 meters or longer distances, and 'short-term' may be 10 meters or shorter distances. In this project, the objective is to investigate an improved positioning technique for stepwise underground robot traction. Here, 'long-term' is defined as1000 steps or more, and 'short-term' is defined as 100 steps or less. Between the long-term and short-term is defined as 'medium-term'.

1.2 Positioning Techniques for Mobile Robots

Exact knowledge of the position of a mobile robot is a fundamental problem in mobile robot applications. In researching a solution to determine the position of a robot, researchers and engineers have developed a variety of systems, sensors, and techniques. However, to date, there is no truly elegant solution for this problem. The many partial solutions can roughly be categorised into two groups: relative and absolute position measurement [J. Borenstein 1997]. Because of the lack of a single good method, developers of mobile robots usually combine two methods, one from each group. The two groups can be further divided into the following seven categories:

Group 1. Absolute Position Measurements (also called Reference-Based Systems)

- Active Beacons
- Global Positioning Systems
- Landmark Navigation
- Model Matching

- Magnetic Compasses

Group 2. Relative Position Measurements (also called Dead-reckoning)

- Odometry
- Inertial Navigation

Absolute position measurement techniques normally have higher accuracy but need longer time for sensing and computation. Relative position measurement techniques are suitable for real time measurement but there is a problem with unbounded error accumulation. Normally, relative position measurement needs assistance from absolute position measurement after a robot was travelled a certain distance. A brief introduction to these techniques is as follows.

Active Beacons

Active beacon navigation systems are the most common navigation and are used on aeroplanes and ships, as well as on commercial mobile robot systems. There are two different types of active beacon system: trilateration and triangulation. Active beacons can be detected reliably and provide accurate positioning information and allow high sampling rates and yield high reliability. However, accurate positioning requires accurate mounting and maintenance of beacons.

Global Positioning Systems (GPS)

Global positioning systems comprise of satellites that transmit encoded RF signals. Using advanced trilateration methods, ground-based receivers can compute their position by measuring the travel time of the satellites' RF signal. The use of this technology is limited to outdoor navigation.

Landmark Navigation

In general, landmarks have a fixed and known position and can be recognised by robot sensors. There are two types of landmarks: artificial and natural landmarks.

Map Matching Navigation

In this technique the robot uses its sensors to create a map of its local environment. This local map is then compared to a global map previously stored in memory. If a match is found, then the robot can compute its actual position and orientation in the environment.

Magnetic Compasses

A magnetic compass provides a measure of absolute heading (direction). One disadvantage of any magnetic compass, however, is that the earth's magnetic field is often distorted near power lines or steel structures. This makes the straightforward use of geomagnetic sensors difficult for indoor applications.

Odometry

Odometry is a widely used navigation method for mobile robot positioning. It provides distance travelled by the robot with good short-term accuracy, is inexpensive and allows very high sampling rates. However, the fundamental idea of odometry is the integration of incremental motion information over time, which leads inevitably to the unbounded accumulation of errors. Additionally, orientation errors will cause large lateral positional errors, which increase proportionally with the distance travelled. Despite this limitation, odometry is often an important part of a robot navigation system and the navigation will become simpler when used in conjunction with, for example, accelerometers.

Normally odometers translate wheel revolutions into linear displacement relative to the floor. However, many factors, such as wheel slippage, rough floors and unequal wheel diameter or uncertainty of the length of wheel-base, will influence the accuracy of odometry.

To improve odometry accuracy, there are two generally used methods; one is via calibration experiments to get a centre of gravity of errors before putting the data into use; the other one is via detailed analysis of error sources to obtain error compensation functions.

Inertial Navigation System (INS)

Inertial navigation uses gyroscopes and accelerometers to measure rate of rotation and acceleration respectively. Inertial sensors measure the inertial state of the mobile robot. The associated inertial navigation algorithm is the process of calculating position by integration of velocity and computing velocity by integration of total acceleration. Total acceleration is calculated as the sum of gravitational acceleration, plus the acceleration produced by applied forces.

Historically, inertial navigation systems have been used in aerospace vehicles, military applications, such as ships, submarines and missiles. A few years ago the application of inertial sensing was mainly limited to high-performance high-cost aerospace and

military applications. However, several recent contributions in non-military applications have made use of low-cost inertial systems. In the last couple of years there has been some addressing of the need for a low cost inertial measurement unit based on the progress in the development of low cost gyroscopes. Low cost inertial measurement unit (IMU) research is mainly focused on initial calibration and alignment algorithms to correct for gyroscope errors. Although these methods have greatly improved the accuracy of measurement in some particular applications, its accuracy is still not satisfactory in many other situations.

Apart from gyroscopes and accelerometers, other methods have also been investigated, such as 'Gyroscope Free INS' methods that use six or nine linear accelerometers instead of the usual three gyros and three accelerometers. Although the methods have been found capable of predicting theoretical values they still cannot be put into real systems because they do not have sufficient accuracy and still present a considerable cost.

A major advantage of inertial navigation is that it is nonradiating and nonjammable and may be packaged and sealed from the environment. Its disadvantage is the accumulation of error caused in the double integration processes.

Because of the error properties of inertial navigation systems, it is usually considered necessary to use absolute information provided by external sensors to reinitialise INS during long-term robot motion. Alternatively, mounting a test platform on the robot can also be used to reinitialise INS if the robot is allowed to stop whilst carrying out its task.

Tilt sensors

Tilt sensors are worth mentioning because they are often used to measure robot attitude associated with other positioning techniques. A tilt sensor is a gravity-sensing angle transducer that can measure small deviations of the robot platform from the horizontal plane. Existing tilt sensors provide accurate information only in stationary states because the sensors have a very low ability to deal with inertial disturbance.

1.3 Durham Stepwise Underground Robot

The first of the Durham stepwise underground robots was developed in 1995. It was made for pipeline inspection, and developed in conjunction with British Gas and others. Its general structure is shown in Figure 1-1.

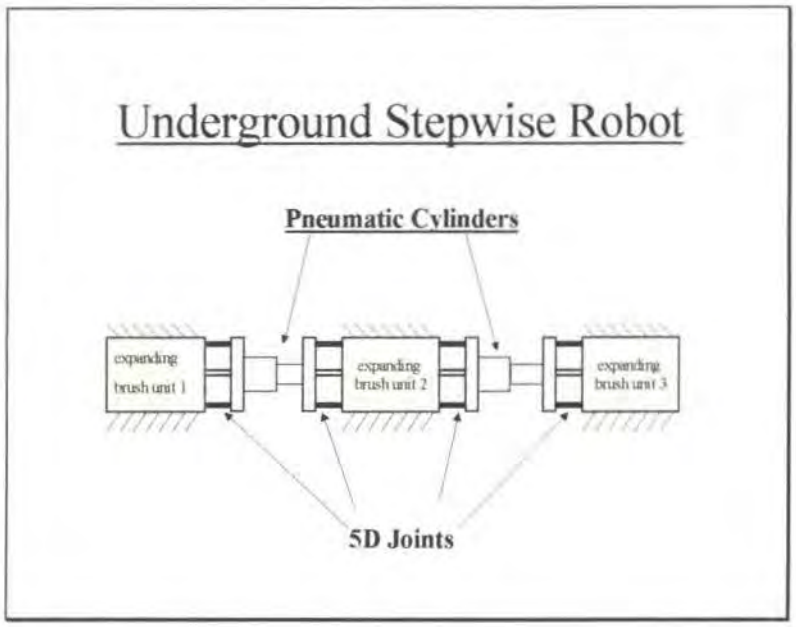

Figure 1-1

A photograph of an actual robot is shown in Figure 1-2.

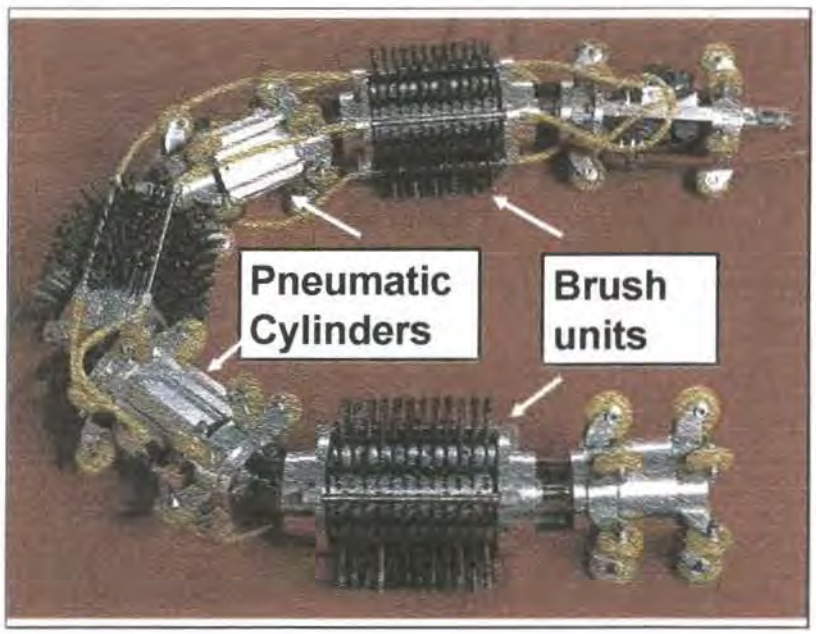

Figure 1-2

This structure comprises three brush units and two expandable cylinders. Its principle of movement is shown in Figure 1-3. When the stepwise robot moves forward one step, the three brush units move forward in turn.

In the first step, the front cylinder expands. This action leads the first brush unit to move forward.

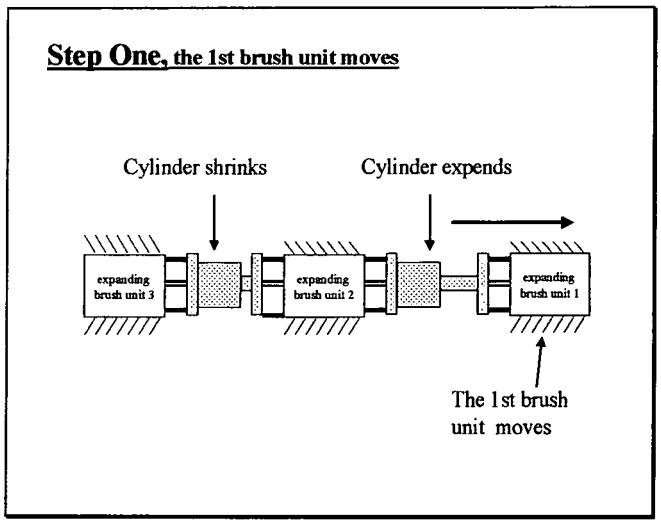

(a)

In the second step, the rear cylinder expands and the front cylinder contracts. This action leads the second brush unit to move forward.

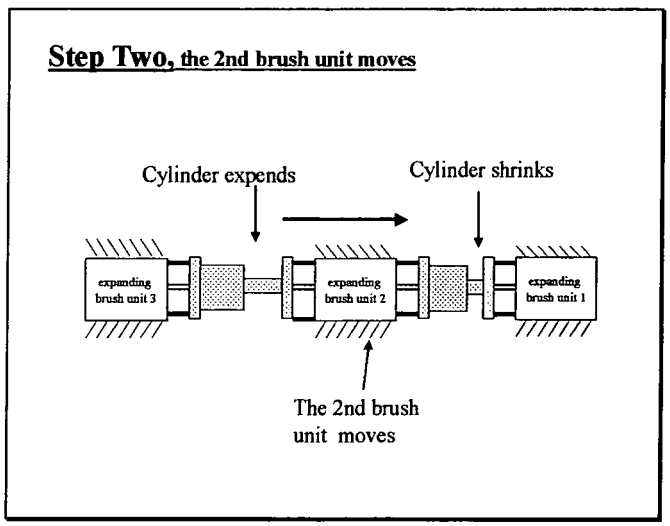

(b)

In the third step, the rear cylinder contracts. This action leads the third brush unit to move forward.

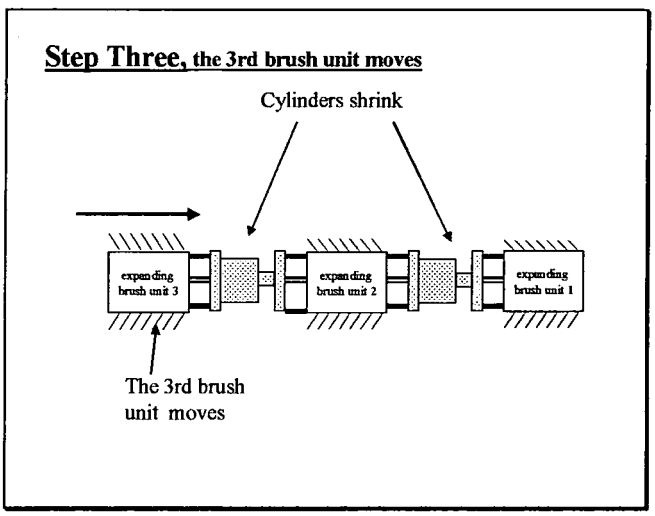

(c)

Figure 1-3

The length of the step depends on the size of the robot actuator (cylinder). Normally, the length of the step is between one and two times of the radius of the brush unit.

1.4 Constraints for Underground Robotic Positioning

Because of the underground environment, the use of sensors and positioning techniques is highly constrained.

The main constraint is that the underground robot cannot use signals from the ground or sky to determine the position of the robot. Also, underground robots cannot transmit signals to receivers on the ground or in the sky to determine their position. This is because signals cannot pass through the strata of the earth or rocks. Thus, the signals will be blocked or greatly distorted especially if a robot is deep beneath the surface of the earth. Consequently, positioning systems can only be mounted on board, and only relative position measurement techniques are available for underground robotic positioning systems.

Restricted space is also a practical constraint. Both pipeline robots and borehole robots move along narrow tubes. The size of an on board positioning system is constrained by the diameter of the tube. This constraint makes it difficult to choose and mount sensors. Generally, the size of a high precision sensor is large. The accuracy of the sensor mounting also affects the measurement accuracy.

There are also other constraints in different applications. For example, robots working in oil exploration drilling often meet high temperature and pressure environments. This also causes difficulty when choosing sensors.

Because of the constraints, only relative position measurement techniques are available in the underground environment. Existing relative position measurement techniques normally cannot provide sufficient positioning accuracy for most mobile robots, especially long-term accuracy. However, underground robots often need to move long distances (more than 1000 steps). Considering the constraint of restricted space, the choice of sensors becomes narrower. Hence, whether the accuracy of positioning systems for underground robots can meet application requirements becomes problematic.

In order to give a base to judge the feasibility of improving the accuracy of positioning systems, quantitative error analysis has been carried out and is as follows.

Chapter 2

Error Analysis and Error Model for Underground Robotic Positioning

The error analysis in this section is based on the application of relative position measurement techniques to stepwise robots. Because the key problem is unbounded error accumulation, the error analysis emphasises error accumulation and the related factors.

2.1 Two-dimensional Error Analysis

To simplify the problem, this discussion of error analysis starts with two-dimensional cases. It is assumed that a point moves along the x-axis from the origin (0,0) of an x-y plane. Also, the distance of every step is a constant, D. After n steps the point moves to (nD,0). If there is measurement error of the step length or the angular orientation, the positional result will not be (nD, 0). Thus positioning accuracy depends upon measurement accuracy.

2.1.1 General Error Analysis

Consider four simple cases:

Case 1, If there is an initial error in step distance, say $+E_d$ in the first measurement, the positional result is ($nD+E_d$, 0). In this situation, the positioning error is a constant and equals $+E_d$.

Case 2, If there is a constant error in distance, say the error in distance is a constant $+E_d$ in each step, the positional result is ($nD+nE_d$, 0). In this situation, the absolute positioning error is $+nE_d$, which increases linearly with the number (n) of steps.

Case 3, If there is an initial error in orientation, say +Eo in the first measurement, the positional result is ($nD\cos(+E_o)$, $nD\sin(+E_o)$), see Figure 2-1. In this situation, the positioning error is $nD\sqrt{2(1-\cos(+E_o))}$, which increases linearly with the number

(n) of steps. Also, for a small angle of error the major part of this error will still be in the direction of y.

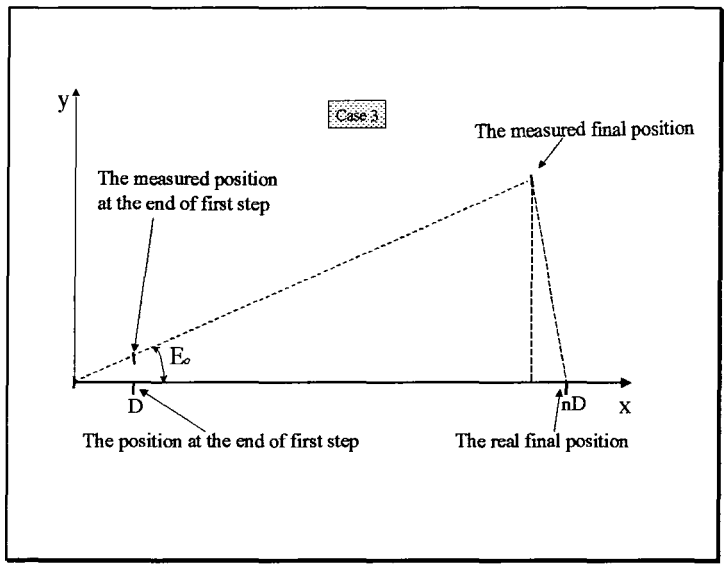

Figure 2-1

Case 4, If there is a constant error in orientation, say the error is a constant $+E_o$ in each step, the positional result is $(nD\sum_{i=1}^{n}\cos(+iE_o), nD\sum_{i=1}^{n}\sin(+iE_o))$

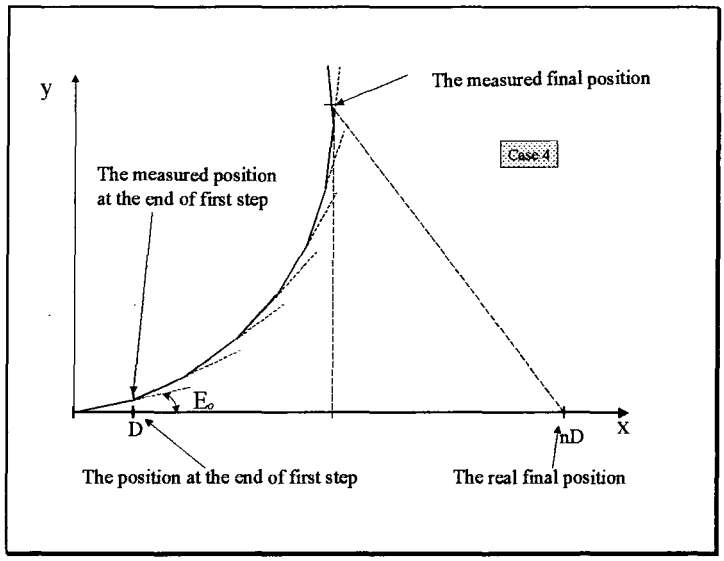

Figure 2-2

Obviously, the orientation error ($+nE_o$) increases with the number (n) of the steps, and the positional error is a second order increase with the number (n) of the steps. Again, the major part of the positioning error is in the direction of y.

Using the above case, error functions were obtained as follows. When a robot moves along an x-axis from the origin, the positioning errors in the travel direction and lateral direction caused by the angular measurement error can be expressed as

$$e_{ox} = nD\sum_{i=1}^{n}\cos(iE_o) \qquad (1\text{-}1)$$

$$e_{oy} = nD\sum_{i=1}^{n}\sin(iE_o) \qquad (1\text{-}2)$$

Here, D is the length of the robotic step; n is the number of the steps the robot has travelled; and E_o is the angular measurement error; e_{ox} and e_{oy} are the positioning errors in the travel direction and lateral direction caused by angular measurement error respectively.

The positioning errors in the travel direction and lateral direction caused by the distance measurement error are

$$e_{dx} = +nE_d, \qquad (1\text{-}3)$$

$$e_{dy} = 0 \qquad (1\text{-}4)$$

Here, D is the length of the robotic step; n is the number of the steps the robot has travelled; and E_d is the distance measurement error; e_{dx} and e_{dy} are the positioning errors in the travel direction and lateral direction caused by distance measurement error respectively.

The estimated position should be in the shadow area shown in Figure 2-3 if there are both angular and distant measurement errors and the range of the angular measurement error is between $-E_o$ and $+E_o$; the range of the distance measurement error is between $-E_d$ and $+E_d$.

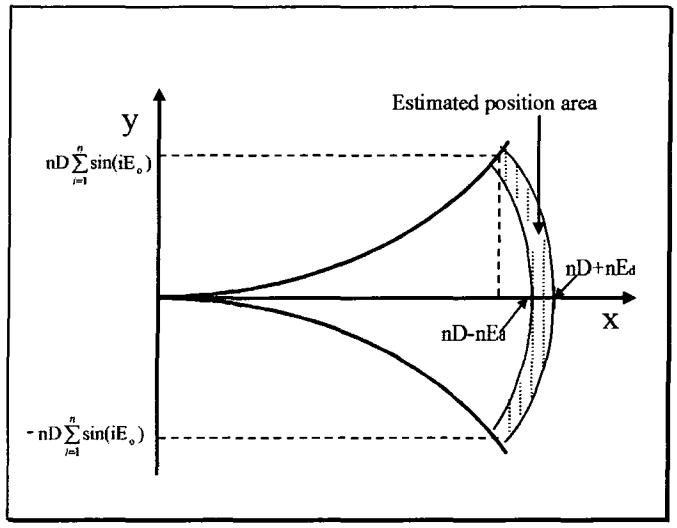

Figure 2-3

In the above discussion, the positioning error was combined by two parts. One is the positioning error caused by the angular measurement error and the other is that caused by the step length measurement error. Normally, these two parts of positioning errors can simply be summed as the total estimate, or the positioning error caused by the step-length measurement error can be ignored.

Through the above figures, it was found that the angular measurement error is the main source of positioning error; the greater the orientation error, the greater the relative positional error. However, the figures only show the tendency, and the error functions (1-1) and (1-2) are not convenience for estimating positional error. Hence, further numerical analysis was required as follows.

2.1.2 Numerical Error Analysis

This numerical error analysis is based on the error functions (1-1), (1-2), (1-3) and (1-4). Formulas (1-3) and (1-4) show the relationship between the positioning errors and distance measurement error very clearly and simply. Hence, the numerical error analysis only focuses on the relationship between the positioning errors and angular measurement error. Obviously, if the orientation error, i.e. the accumulation of the angular error, is greater than 1 radian, the positioning error will be very large. In this situation the result of the positional estimate is unacceptable. Therefore, the numerical analysis in this section emphasises the effect of angular measurement error in the situation where orientation error is less than 1. The orientation error can be easily

obtained by the value nE_{θ}. Also, to carry out the numerical error analysis, cases are given by different values of the length of the step of robot and different values of the angular measurement errors. It is assumed that the length of the step of a robot is 0.1, 0.2 or 0.4 meters. These figures are used because Durham's stepwise robots have

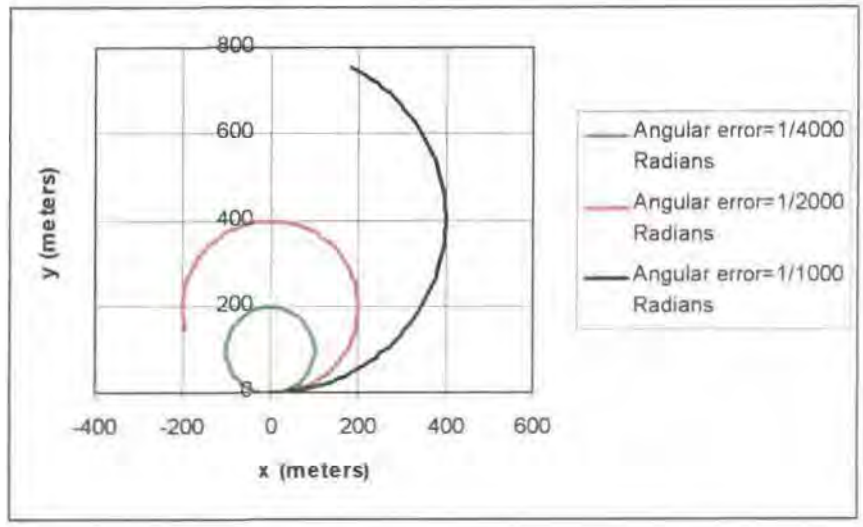

Figure 2-4

similar lengths of step. It is also assumed that the angular error is 1/4000, 1/2000, or 1/1000 radians. This assumption is based upon precision of current commercial angular sensor and the potential techniques to be used. For these nine different cases, the positioning errors for every step can be calculated by using (1-1) and (1-2). The numerical error analysis was carried out based on this calculated data.

Figure 2-4 shows the situation as a robot travels from the origin of the x-y plane to the position (1000, 0). The length of the robotic step is 0.1 meters. The curves in Figure 2-4 are estimated tracks of the positional results when the angular measurement errors are 1/4000 1/2000 and 1/1000 radians respectively.

Through Figure 2-4, it can be seen that even if the angular measurement errors are very small (1/4000 radians), the positioning errors are still unacceptable after 1km of travel. In other words, it is difficult to ensure long-term (500 meters or longer distance) positioning accuracy based on the existing measurement. Also, it is found that the estimated tracks may approximate to circles. To illustrate this, two groups of cases are shown in Figure 2-5. The angular measurement errors are 1/4000, 1/2000

and 1/1000 radians and the length of step is 0.1 and 0.2 meters respectively.

(a) Length of step 0.1 meters.

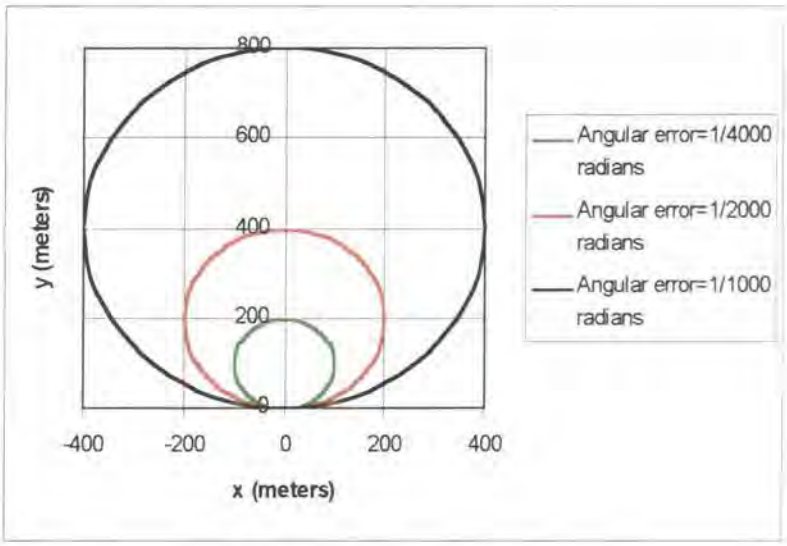

(b) Length of step 0.2 meters

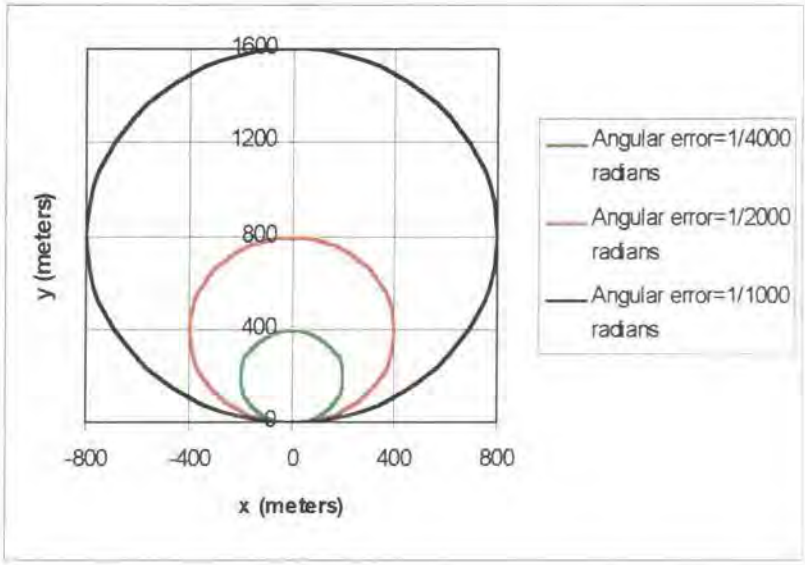

Figure 2-5

Obviously, the estimated tracks are approximately circles if the travelled distance is sufficiently long. The diameters of the circles are in proportion to the length of the step of the robot and also in proportion to the reciprocal of the angular measurement error. This presupposes that the relative positioning error should be in proportion to the orientation error, if the orientation error is not very large. Figure 2-6 illustrates this relationship between the orientation error and the relative positioning error in the y-axis direction, in which the data includes the cases for different angular errors and lengths of step. Obviously, if the orientation error is less than 1, the relationship is

approximately a linear relationship.

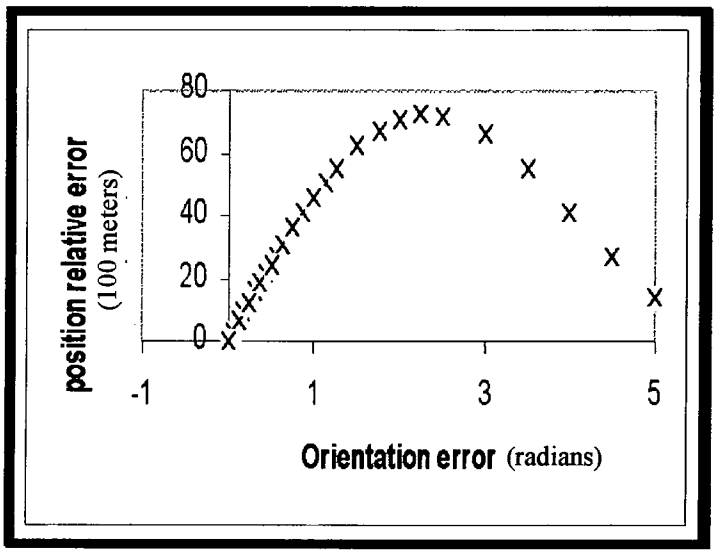

Figure 2-6

Based on this data, the regression function is obtained as (1-5)

$$100\frac{e_0}{nD} = 49nE_o \qquad (1\text{-}5)$$

This is a relative error function. Consequently, the absolute error function is obtained as (1-6)

$$e_o = \frac{49}{100}n^2 E_o D \qquad (1\text{-}6)$$

Formulas (1-5) and (1-6) are the error model on the condition $nE_o<1$. This error model is easy to use. The following are examples to show how to estimate positioning error.

Example 1

It is assumed that the positioning distance is 500 meters; the length of the robotic step (D) is 0.15 meters and the angular measurement error (E_o) is 1/1000 radians.

Firstly, calculating the number of steps by $n = 500/0.15 \approx 3334$

Secondly, calculating the accumulation of the orientation error by $nE_o = 3.334$ radians. Because this orientation error is greater than 1 radian, this positioning error has

already been taken to be unacceptable. Therefore it is not necessary to use (1-5) or (1-6) to estimate the exact positioning error.

Example 2

It is assumed that the positioning distance is 500 meters; the length of the robotic step (D) is 0.25 meter and the angular measurement error (E_o) is 1/2000 radians.

Firstly, calculating the number of steps by n = 500/0.25 =2000

Secondly, calculating the accumulation of the orientation error by nE_o =1

The third step, calculating the relative lateral error by (1-5), i.e. 49×1(%)=49(%)

The third step, calculating the absolute lateral error by (1-6), i.e. 0.49×500= 245(meters)

Therefore, the positioning error is about 245 meters.

Formula (1-5) has been tested by the use of all of the data which was mentioned at the start of Section 2.1.3. The error of the function (1-5) is $|100\frac{e_0}{nD} - 49nE_o|$. In different situations the error of the function (1-5) is also different. In all test situations, the maximum value of the relative error, $|100\frac{e_0}{nD} - 49nE_o|$, was less than 0.375 e.g. 37.5% (see Table A.1 in Appendix A). This formula presents a very high estimated accuracy. The form of the formula is also very simple to use. Approximately, the value of the relative positioning error is half value of the orientation error.

Table A.2 (in Appendix A) shows that the lateral error (e_{oy}) is a major part of the positioning error (e_o). The less the orientation error (E_o), the greater the value e_{oy}/e_o. If orientation error (E_o) is less than 1 radian the value e_{oy}/e_o is greater than 94.5%. Also, the error in the travel direction (e_{ox}) is a small part of the positioning error (e_o). The greater the orientation error (E_o), the greater the value e_{ox}/e_o. If orientation error (E_o) is less than 1 the value e_{ox}/e_o is less than 33%.

Formula (1-6) gives a clear and simple form for understanding the relationships between positioning error and other relative variables. It is very clear that:

- Positioning error (e_o) is in proportion to the angular measurement error (E_o)
- Positioning error (e_o) is in proportion to the square of the number of steps (n^2)
- Positioning error (e_o) is in proportion to the reciprocal of the step length (D) if the travelled distance (nD) is fixed.

If accumulation of angular measurement error is greater than 1 radian, the error functions (1-5) and (1-6) will be invalid. If E_o is given and the number of steps is greater than $1/E_o$, the accumulation of angular measurement will be greater than 1 radian. Consequently, the error functions will be invalid. In other words, if E_o is given, the maximum valid value of the number (n) of steps for the error function (1-5) and (1-6) is known. For the same reason, if E_o and D are given, the maximum valid value of the travel distance (nD) for the error function (1-5) and (1-6) is known. For different values of E_o and D, the maximum valid values of the travel distance (nD) for the error function (1-5) and (1-6) are different, as shown in Table 1-1.

Maximum Valid Values of x, (nD) as a Function of Angular Measurement Error & Step Length

		Maximum Valid Values of x, (nD)		
		Step Length D=0.1 meters	**Step Length D=0.2** meters	**Step Length D=0.4** meters
Angular Measurement Error (radians)	**E_o=1/1000**	100 meters	200 meters	400 meters
	E_o=1/2000	200 meters	400 meters	800 meters
	E_o=1/4000	400 meters	800 meters	1600 meters

Table 1-1

This table indicates that if D=0.1 meters and E_o=1/1000 radians, after the robot has travelled 100 meters the relative positional error (e_o/(nD)) will be 50%. This positioning accuracy is far from the requirement of industrial applications. In particular, it is difficult to meet long-term (longer than 500 meters) accuracy requirements. The other cases shown are better, but still not satisfactory.

Fortunately, sensor errors are normally random values. After a long distance of travel, the probability of high accumulation of angular error should be low. Therefore, it is useful to propose a long-term statistical error model. A statistical model can give a positioning error range with a certain confidence. Here, it should be noted that statistical models are not useful for short-term (less than 100 steps). In particular, statistical models are inappropriate for very short-term travel (less than 10 steps). For short-term travel, exact error models (1-5) and (1-6) are needed.

2.1.3 Error Estimates Using Statistic Models

(a) The estimated trajectory when angular measurement error is 1/4000 radians

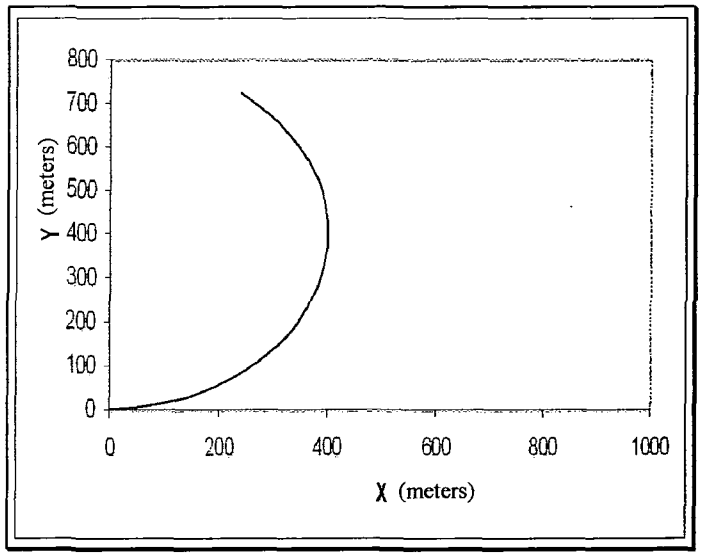

(b) The estimated trajectories when angular measurement error has uniform distribution between −1/4000 and 1/4000 radians

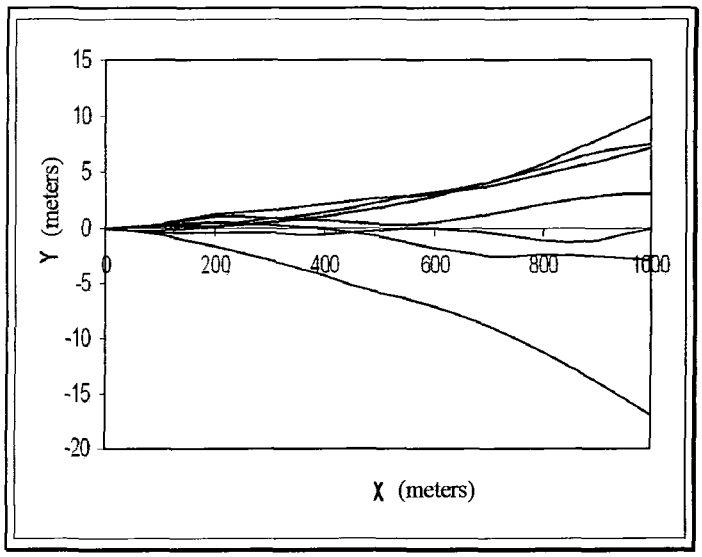

Figure 2-7 Estimated trajectories

Sensor errors are usually random errors. If the precision of an angular sensor is 1/4000 radians and the number (n) of steps of robot travel is very large, the accumulation of

angular measurement error will probably be less than n/4000 radians. Figure 2-7 shows the case in which it is assumed that angular sensor precision is ±1/4000 radians and the length of the robotic step 0.1 meters. Figure 2-7 (a) shows the estimated track by using (1-1) and (1-2). Figure 2-7 (b) shows the tracks, in which the angular measurement error has uniform distribution between –1/4000 and 1/4000 radians.

Obviously, the positioning errors in Figure 2-7(b) are much less than that in Figure 10 (a), which is estimated by using (1-1) or (1-2). Therefore, it is useful to build up a statistical error model for long-term positioning systems.

During the statistical analysis, the assumptions made were the same as those used for building the exact models. That is, the angular measurement accuracy was ±1/4000, ±1/2000 or ±1/1000 radians, and the step length was 0.1, 0.2 or 0.4 meters. In addition, it is assumed that the robot travelled from position (0,0) to (1000,0) in a x-y plane.

In order to build up a statistical model, a data sample was required. Sample data was generated by a digital simulation. Given angular measurement accuracy and step length, the simulation was carried out 1000 times. Every time, one estimated positioning track was obtained. There were 1000 tracks for each given situation. Therefore, there were 9000 tracks for the nine given situations. The sample positions were based on the travelled distance. After each 100-meters travelled, the position result was recorded. That is, when the robot arrived at the positions (xi, 0) (xi = 100, 200, 300, 400, 500, 600, 700, 800, 900, 1000), the estimated positions were collected. For each given situation, at each sample position, there are 1000 data. This data distribution in the x-y plane illustrates the tendency of the error distribution (see Figure 2-8). Consequently, a range of positional errors for each situation, at each sample position, can be determined by using a statistical method. The statistical model can give an estimated positioning error range for different situations. The following paragraphs are discussions of the positional error in the travel direction and the lateral direction respectively.

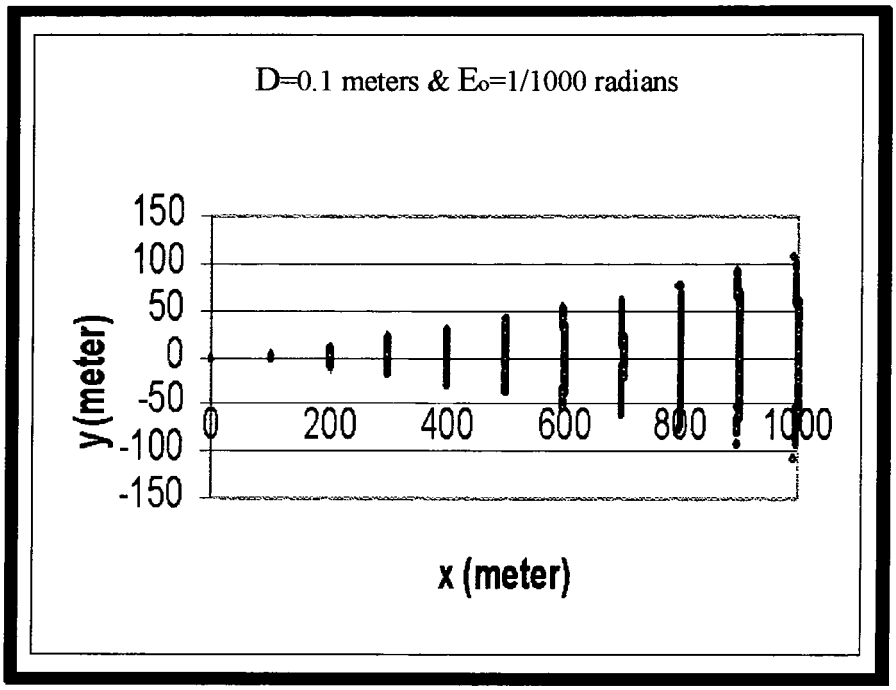

Figure 2-8 Scatter of the positional sample data

Error in lateral direction (y)

Considering for example, the step length is 0.1 and the angular measurement precision is ±1/1000 radians. In addition, the angular measurement error is assumed normally distributed between −1/1000 and 1/1000 radians. After processing, the estimated positions at every sample position were obtained. Figure 2-8 shows the 1000 simulated position results at every sample position. The area of the position results corresponding to each sample position has been shown in Figure 2-8. Figure 2-9 shows the lateral-error frequency of the sample data at the sample positions n=5000, i.e. the travelled distance nD=500 meters. The data distribution is similar to a normal distribution.

Figure 2-10 is a normal Q-Q plot for the sample position n=5000. The Q-Q plot displays a normal probability plot for this group of data. This plot graphically assesses whether the sample data could come from a normal distribution. If the data are normal, the plot will be linear. Other distributions will introduce curvature to the plot. It is obvious that the lateral error distribution is a normal distribution.

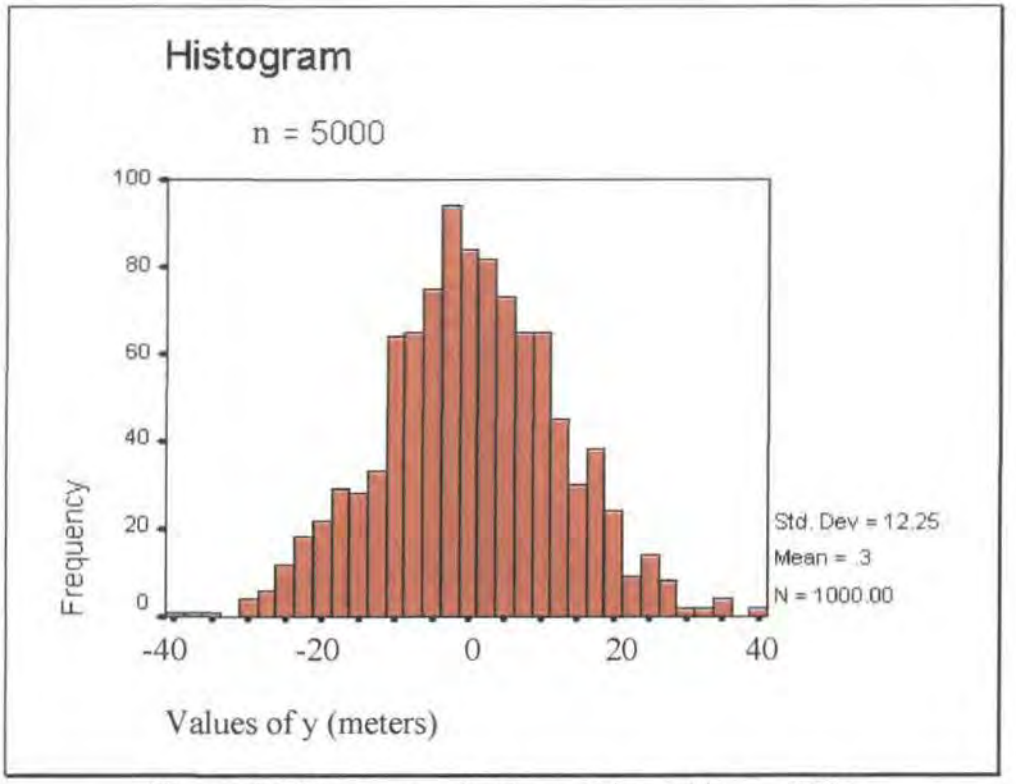

Figure 2-9 Histograms for the sample position, n=5000

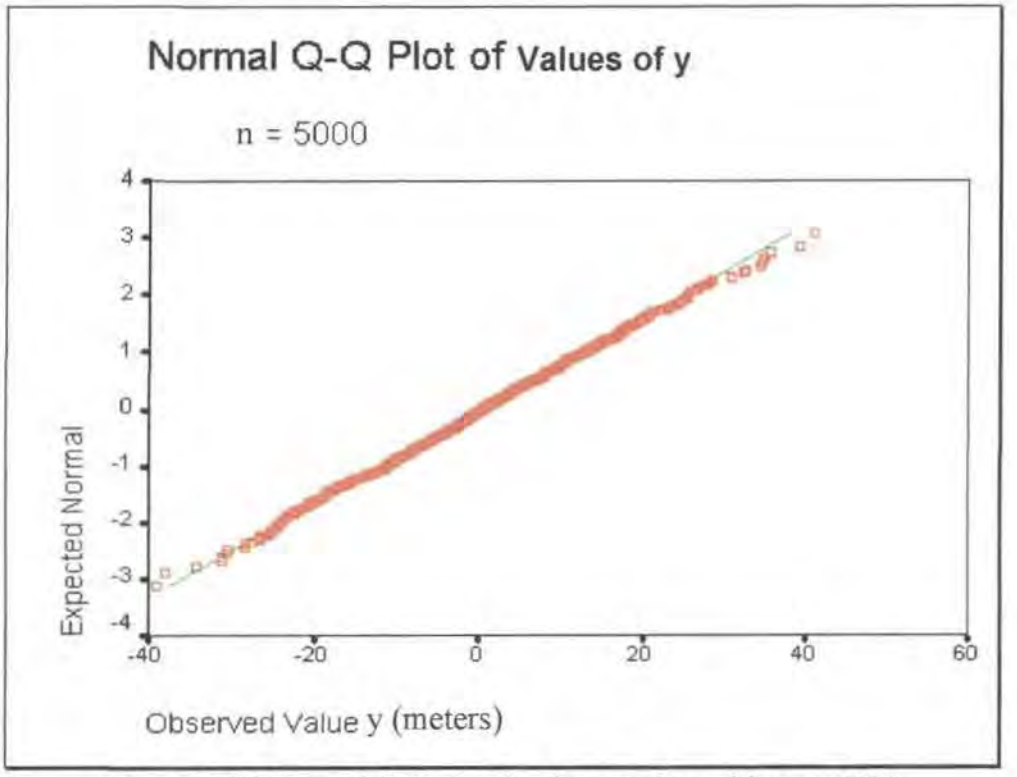

Figure 2-10 Normal Q-Q plot for the sample position, n=5000

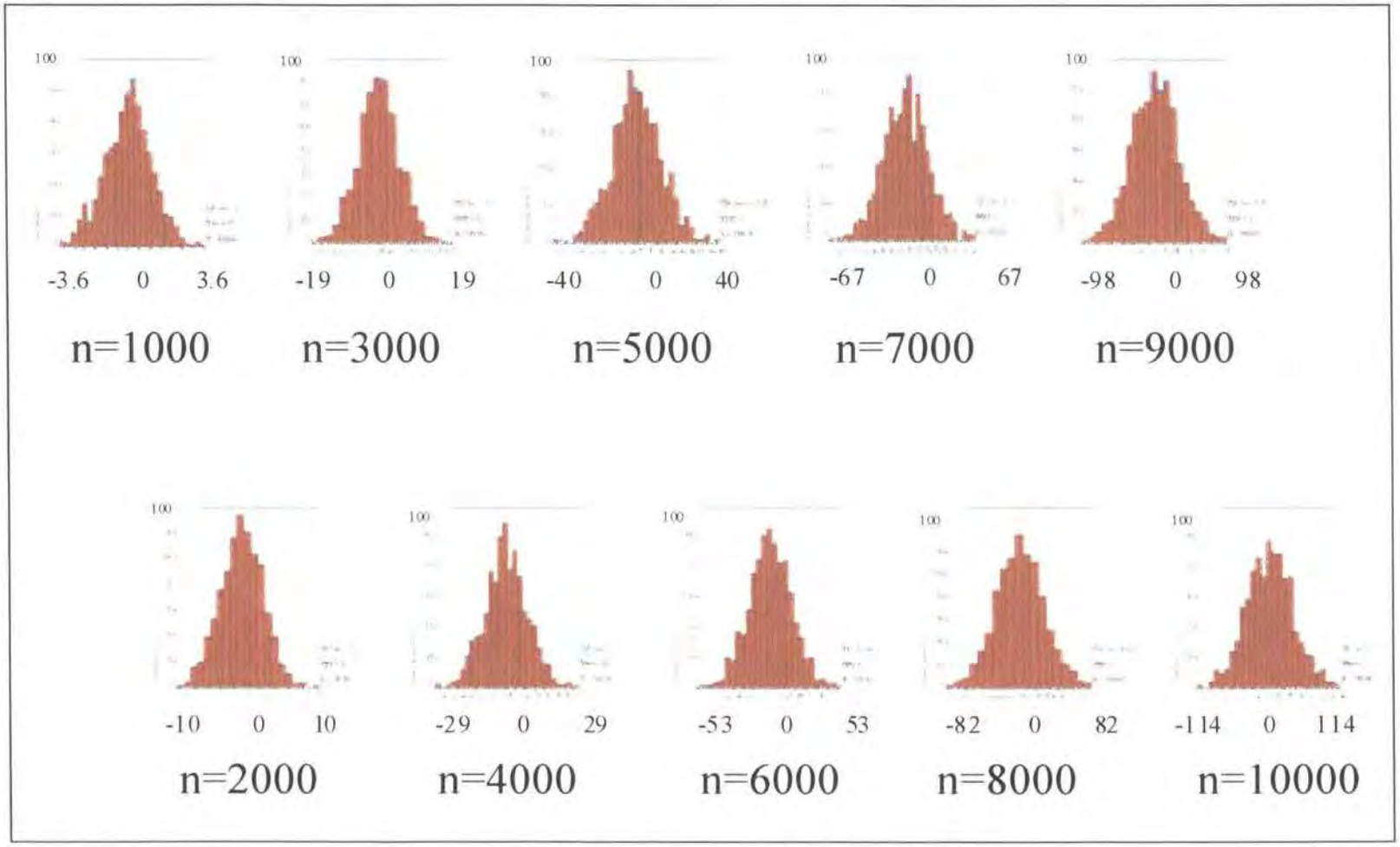

Figure 1-11 Histograms for different sample positions

In the case being considered, sample position is at n=5000, the mean of e_{oy} is 0.34 and the standard deviation is 12.25. The mean of e_{oy} can be viewed as zero because it is very small compared with the travel distance x, for the positioning. From Table B in Appendix B, it is known that the values of a standard normal variable will be greater than –3.3 and less than 3.3 for 99.9% confidence. Consequently, the lateral error will be greater than –3.3×12.25 and less than 3.3×12.25 for 99.9% confidence, i.e. –40.44<y <40.44. This value (40.44) is called the critical value of y for 99.9% confidence.

In this situation, at other sample positions, the lateral error distributions are similar. Figure 2-11 shows the frequency histograms for all sample positions. This figure indicates that the lateral error distributions at different sample positions are normal distribution.

At different sample positions, the means are approximately zero but the deviations are different. Consequently, the critical values of y for 99.9% confidence are different. The values of the means and standard deviations of the lateral error (y) are given in Table 1-2.

n	nD	mean(y)	Std Dev (y)	Critical value (99.9% confidence)
0	0	0	0	0
1000	100	0.0184801	1.087586	3.58903
2000	200	0.648104	3.13933	10.3597
3000	300	0.112391	5.71192	18.8493
4000	400	0.1937944	8.781617	28.97933
5000	500	0.3420512	12.25484	40.4409
6000	600	0.5125174	16.07913	53.0611
7000	700	0.5950634	20.25855	66.8532
8000	800	0.6373955	24.78095	81.7771
9000	900	0.6751322	29.58305	97.6240
10000	1000	0.6801131	34.64108	114.3155

Table 1-2

Based on the critical values in the above table, two curves were obtained, between which the lateral error will be in the enclosed area under 99.9% confidence. The curves are shown in Figure 2-12.

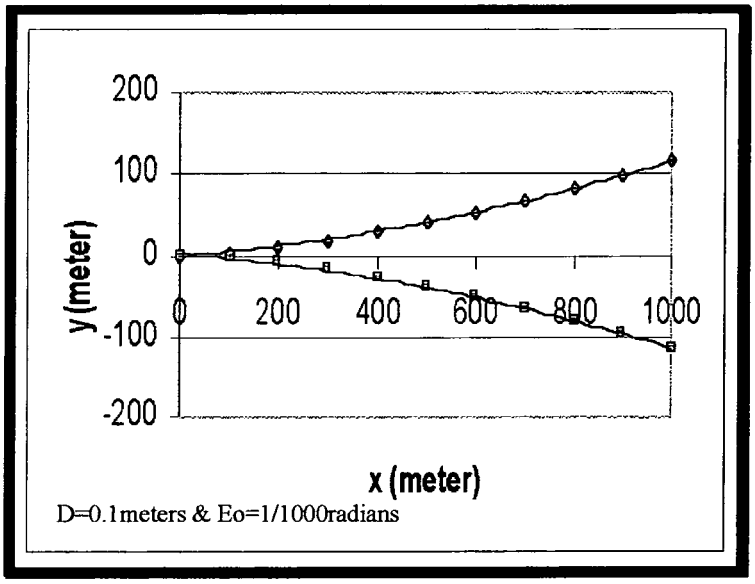

Figure 2-12 Positional error range in two-dimensional space

When D and E_o are fixed, the error in the lateral direction is a function of the travelled distance, y=±f(nD).

The data analyses were also carried out for different lengths of step and different angular measurement accuracy. The means, standard deviations and corresponding critical values of y for the different situations are listed in Table A.3 in Appendix A. For different values of D and E_o, there are different curves similar to Figure 2-12. Based on the critical values in Table A.3, the critical value regression function (1-7) was obtained.

$$CV=E_o\ [0.01625(nD)^2+23(nD)+0.0072n(nD)-15(nD)D] \qquad (1\text{-}7)$$

Here, nD equals the travelled distance. This function is used to estimate the boundary of the lateral error under 99.9% confidence. Therefore, the error estimate function under 99.9% confidence is

$$e_{oy}=\pm E_o\ [0.01625(nD)^2+23(nD)+0.0072n(nD)-15(nD)D] \qquad (1\text{-}8)$$

This function indicates that when the travelled distance (nD) and step length (D) are fixed, the lateral error (e_{oy}) is in proportion to the angular measurement error (E_o). When travelled distance (nD) and angular measurement error (E_o) are fixed, the lateral error (e_{oy}) will decrease with step length (D).

It was found that if E_o is doubled, e_{oy} will be doubled in both error functions (1-8) and (1-6). However, it was found that if D is doubled, e_{oy} will not decrease less than 50% in error functions (1-8). This is different from the error function (1-6). Considering this factor, improving angular measurement accuracy is more important than extension of the step length for long-term positioning accuracy.

Formula (1-7) has been tested by using sample data. Table A.4 in Appendix A shows the result of the estimated errors. In Table A.4, the critical values are the statistical result and the estimated critical values were obtained by using (1-7). The values of CV/nD are the estimated values of the relative error (e_{oy}/nD) by using statistical results. The values of ECV/nD are the estimated values of the relative error (e_{oy}/nD) by using (1-7). The difference between CV/nD and ECV/nD expresses the error of (1-7). Its maximum value is less than 0.61% and the minimum value is greater than −0.23%. This result is satisfactory.

Error in the travel direction

Similar to the error analysis in the lateral direction, the distribution of the positional results (sample data) in the travel direction (x) in the situation D=0.1 meters and Eo=1/1000 radians are shown in Figure 2-13. In particular, at the sample position n=5000 the distribution is shown in Figure 2-14. It was very clear that the error in travel direction is small. Histograms for the sample position n=9000 and n= 10000 are not shown in Figure 2-13. This is because the rate, e_{ox}/x, (x=nD), is too small to be processed by the software, SPSS. The values of x in the sample data for n=9000 and 10000 is taken as constant 900 and 1000.

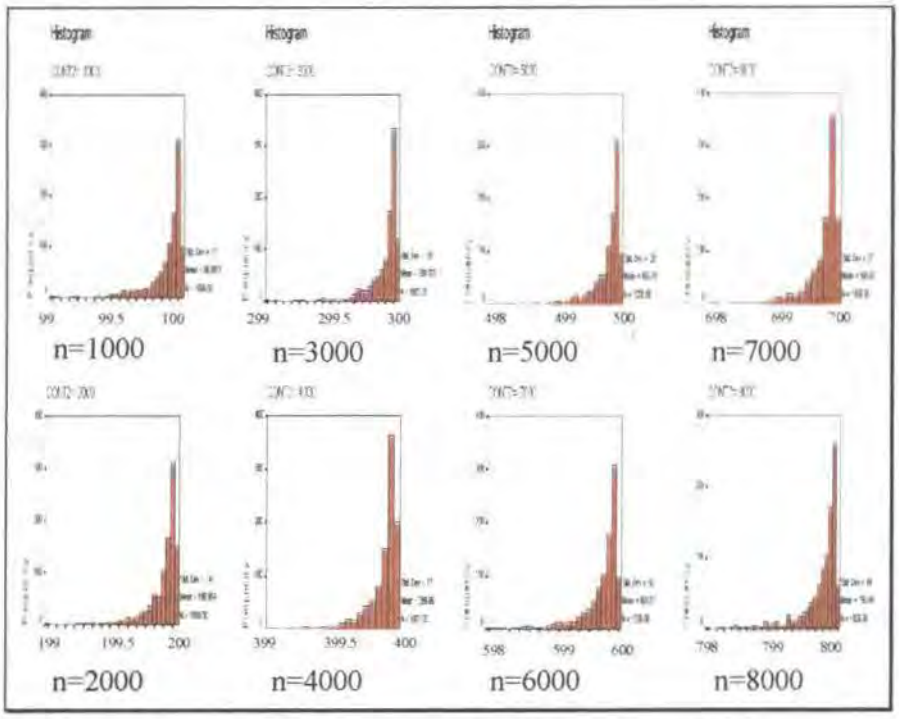

Figure 2-13 Histograms for all sample positions

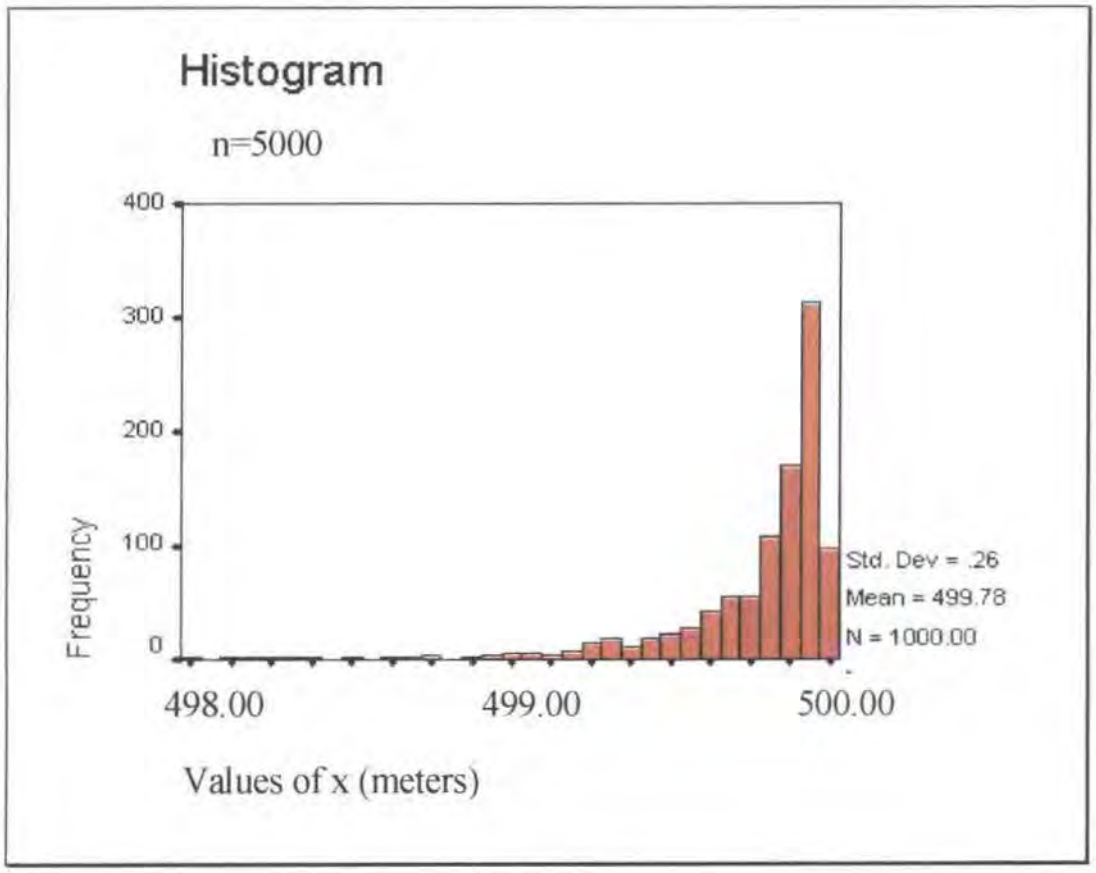

Figure 2-14 Histograms for the sample position, n=5000

For different situations, the statistical analysis results are similar; the error in the travel direction can be ignored. Table 1-3 shows the maximum values of e_{ox}/x, (x=nD) in the sample data.

The Maximum Values of e_{ox}/x, (x=nD) in the Sample Data

		The Maximum Values of e_{ox}/x, (x=nD)		
		Step Length D=0.1meters	**Step Length D=0.2** meters	**Step Length D=0.4** meters
Angular Measurement Error (radians)	**E_o=1/1000**	0.6963%	0.3993%	0.1691%
	E_o=1/2000	0.1571%	0.0999%	0.04228%
	E_o=1/4000	0.0393%	0.02498%	0.0106%

Table 1-3

It was found that the positioning error in the travel direction relative to the travelled distance caused by angular measurement error is less than 0.7%. the higher the positioning accuracy, the lower the maximum value of e_{ox}/x. Compared with the error in the lateral direction, this error can be ignored.

It should be noted that e_{oy} in (1-8) is an estimated maximum value of lateral error for 99.9% confidence. For a particular travel, since the angular measurement error is random, the positional error in the lateral direction may be less than the maximum error estimated by (1-8). Sometime, the lateral error is probably less than the error in the travel direction. This is different from the situation where the angular measurement error is a constant. However, if angular measurement error is random, positional error range in the lateral direction is much greater than the positional error range in the travel direction. Moreover, positional error in the travel direction can be ignored if the angular measurement error is random.

2.1.4 Error estimate functions for the situation where the robotic trajectory is not a straight line

The above discussion of the error functions, exact and statistical, is under the condition that a robot moves along a straight line. If a robot moves along any curve,

the error function might be more complicated. In this section, two cases are discussed, which relate to an understanding of the effect of accumulation of angular measurement error on positioning error in the situation where a robotic trajectory is not a straight line. One case is that the robotic trajectory is a combination of a few lines. The other case is that the robot moves with a constant rotational velocity.

A robotic trajectory is combination of a few lines

Now, considering the case that is shown in Figure 2-15, two robots (robot 1 and robot 2) move from O to A, then robot 1 moves from A to B and robot 2 moves from A to B'. Here the distance $\overline{AB} = \overline{AB'}$.

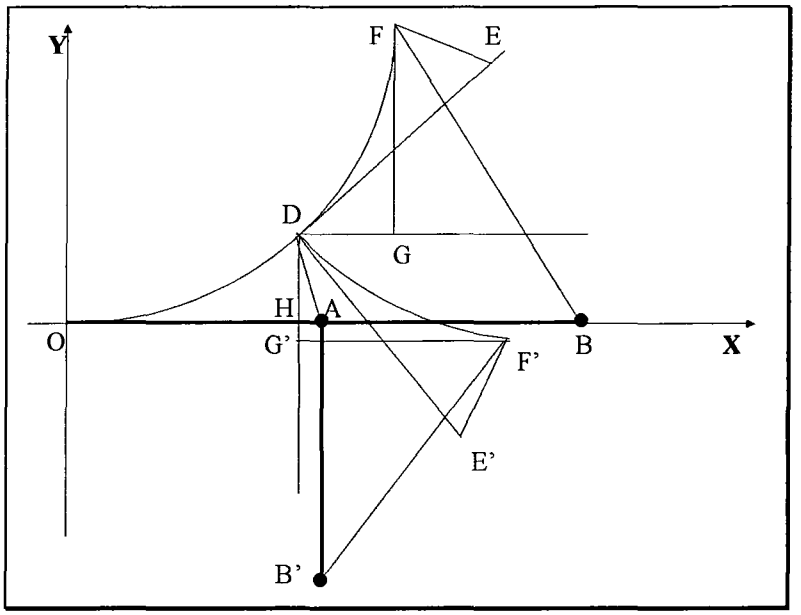

Figure 2-15

Because of angular measurement error, the positional result for robot 1 is the position F rather than B and the positional result for robot 2 is the position F' rather than B'.

For each robot, there are two segments of travel. From O to A, the positional result is identical for the two robots. It is the position D. At this position, the positional error in the lateral direction is $\overline{DH}$ and the positional error in the travel direction is $\overline{AH}$. When robot 1 moves from A to B, the positional result is the position F. At this position, the second segment positioning error in the lateral direction is $\overline{FG}$ and the second segment positioning error in the travel direction is $\overline{AB} - \overline{DG}$. When robot 2 moves from A to B', the positional result is the position F'. At this position, the

second segment positioning error in the lateral direction is $\overline{F'G'}$ and the second segment positioning error in the travel direction is $\overline{AB'} - \overline{DG'}$.

For the positional result of the travel trajectory $\overline{OAB}$, the positional error in the lateral direction is $\overline{FG} + \overline{DH}$. The positional error in the travel direction is $(\overline{AB} - \overline{DG}) + \overline{AH}$. For the positional result of the travel trajectory $\overline{OAB'}$, the positional error in the lateral direction is $\overline{F'G'} - \overline{AH}$. The positional error in the travel direction is $(\overline{AB'} - \overline{D'G'}) + \overline{DH}$. Because $\overline{FG} = \overline{F'G'}$, $\overline{DG} = \overline{D'G'}$ and $\overline{AB} = \overline{AB'}$, the positional errors of $\overline{OAB'}$ in the lateral and travel directions equal $\overline{FG} - \overline{AH}$ and $(\overline{AB} - \overline{DG}) + \overline{DH}$ respectively.

Based on the knowledge that the lateral error is the main part of the positional error when a robot moves along a straight line, it is known that:

$\overline{DH} > \overline{AH}$ (for the segment of the travel trajectory $\overline{OA}$);

$\overline{FG} > \overline{AB} - \overline{DG}$ (for the segment of the travel trajectory $\overline{AB}$);

$\overline{F'G'} > \overline{AB'} - \overline{D'G'}$ (for the segment of the travel trajectory $\overline{AB'}$).

Here, $\overline{FG} = \overline{F'G'}$, $\overline{DG} = \overline{D'G'}$, $\overline{AB} = \overline{AB'}$

Hence,

$\overline{FG} + \overline{DH} > \overline{FG} - \overline{AH}$

(the lateral error for robot 1> the lateral error for robot 2);

$(\overline{AB} - \overline{DG}) + \overline{AH} < (\overline{AB} - \overline{DG}) + \overline{DH}$

(the error in the travel direction for robot 1< the error in that for robot 2);

Hence, the lateral error of robot 1, $\overline{FG} + \overline{DH}$, is greater than the positional errors in the lateral ($\overline{FG} - \overline{AH}$) and travel ($(\overline{AB} - \overline{DG}) + \overline{DH}$) directions of robot 2. In addition, the sum of the positional errors in the lateral and travel directions of robot 2 is less than that of robot 1. In other words, the maximum of the positional errors in the travel and lateral directions of robot 2 is less than that of robot 1. Therefore, the positional error of robot 2 is less than that of robot 1.

If robot 2 turns to another direction as shown in Figure 2-16, the result is similar. The maximum of the positional errors in the lateral and travel directions of robot 2 is less than the lateral error of robot 1. The sum of the positional errors in the lateral and travel directions of robot 2 is less than that of robot 1. Therefore, the positional error of robot 2 is less than that of robot 1.

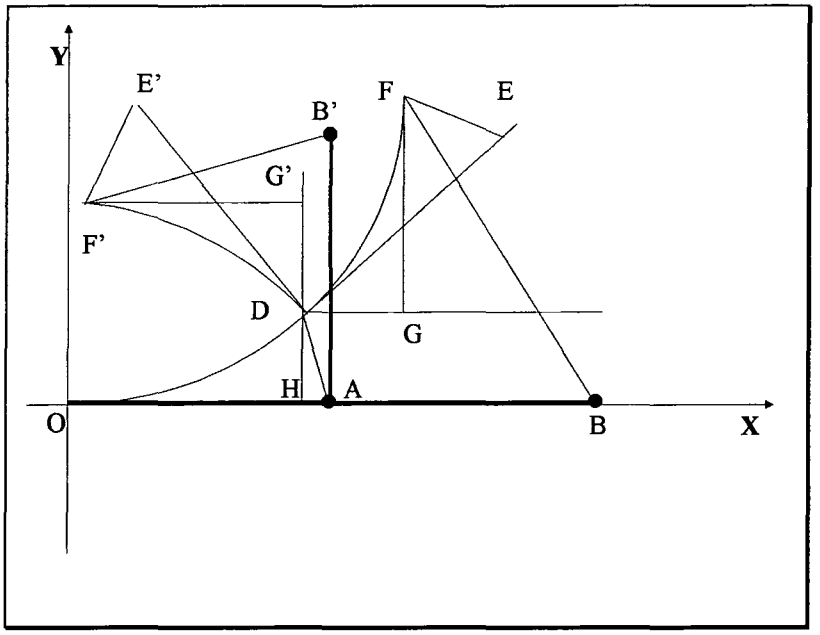

Figure 2-16

If at the position A robot 2 makes a turn which is not 90 degrees, say, the line $\overline{AB'}$ is perpendicular to the line $\overline{DA}$ as shown in Figure 2-17. In this situation, the positional error in the lateral direction ($\overline{F'G'}+\overline{DA}$) of robot 2 is greater than that ($\overline{FG}+\overline{DH}$) of robot 1. Hence, there is possibility that the positional error of robot 2 is greater than that of robot 1. However, $\overline{DA}$ is only slightly greater than $\overline{DH}$. Based on the discussion in Section 2.1.3, the value $\overline{DH}/\overline{DA}$ is greater than 0.95. Moreover, the positional error in the travel direction ($\overline{AB'}-\overline{DG'}$) of robot 2 is less than that ($\overline{AB}-\overline{DG}$)+$\overline{AH}$ of robot 1. Therefore, if the positional error of robot 2 is greater than that of robot 1, the difference between positional errors of robot 1 and 2 is small.

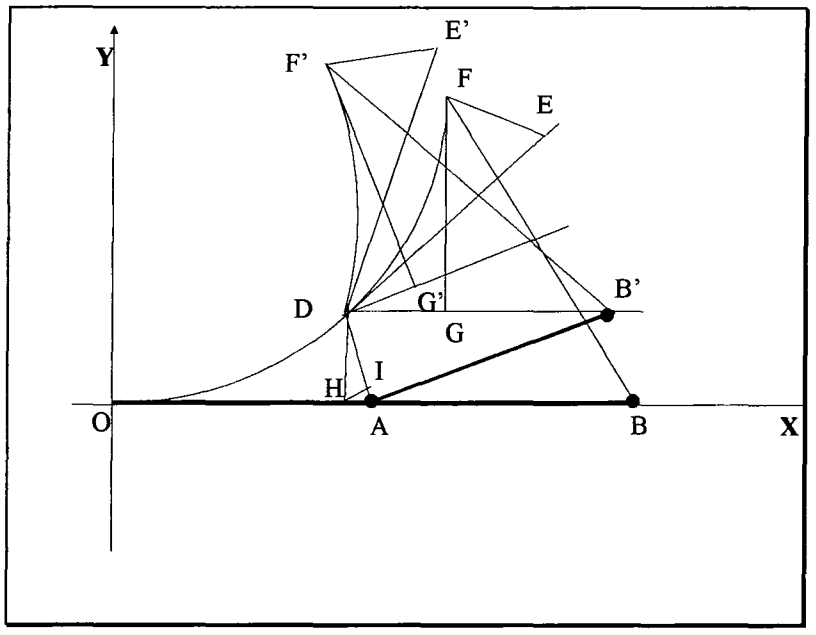

Figure 2-17

In general, if at the position A robot 2 makes a turn which is in any angle, the final positioning error in the lateral direction is the second positioning error in the lateral direction plus or minus the projection of $\overline{DA}$ in the lateral direction of the second travel segment. At the same time, the final positioning error in the travel direction is the second positioning error in the travel direction plus or minus the projection of $\overline{DA}$ in the travel direction of the second travel segment. For the same reason, if the positional error of robot 2 is greater than that of robot 1, the difference between them is small. Therefore, if a robot makes few turns during the travel, the error functions (1-6) and (1-8) are still useful.

Because of making turns, the positional errors in the travel and lateral directions will be different from that in the situation where the robot moves along a straight line. For this general situation, the formula (1-8) can be changed to (1-9).

$$e_o = E_o\ [0.01625(nD)^2 + 23(nD) + 0.0072n(nD) - 15(nD)D] \qquad (1\text{-}9)$$

A robot moves with a constant orientation velocity

Although the positional error is changed very little after the robot makes the turn, if this small change can be accumulated, this accumulation will also affect the final positional result. Considering the case that a robot moves along the x-axis from O to A

as shown in Figure 2-18, because of the angular measurement error $E1_o$ ($E1_o>0$), the positional result is the position E1 rather than A. If the angular measurement error is $E'1_o$ ($E'1_o = -E1_o$), the positional result is the position E'1. If the angular measurement error is $E2_o$ ($E2_o > E1_o$), the positional result is the position E2. Now, if the robot moves with a constant change ($E1_o$) in the orientation, the robot will move along the curve from O to E1. In this situation, if the angular measurement error $\Delta E1_o$ equals $E2_o - E1_o$, the positional result will be E2. For the same reason, if the robot moves along the curve from O to E1 and the angular measurement error is $-E'1_o$, the positional result will be A. According to the discussion of the formula (1-6), if E2<1 and $\Delta E1 = E1$, i.e. $E2 = 2E1$, it was known that;

$$\overline{E2A} / (E1_o + \Delta E1_o) = \overline{E1A} / E1_o$$

so, $\overline{E2A} / (2E1_o) = \overline{E1A} / E1_o$

so, $\overline{E2A} = 2\ \overline{E1A}$

but $\overline{E1A} + \overline{E2E1} > \overline{E2A}$

so, $\overline{E2E1} > \overline{E1A}$

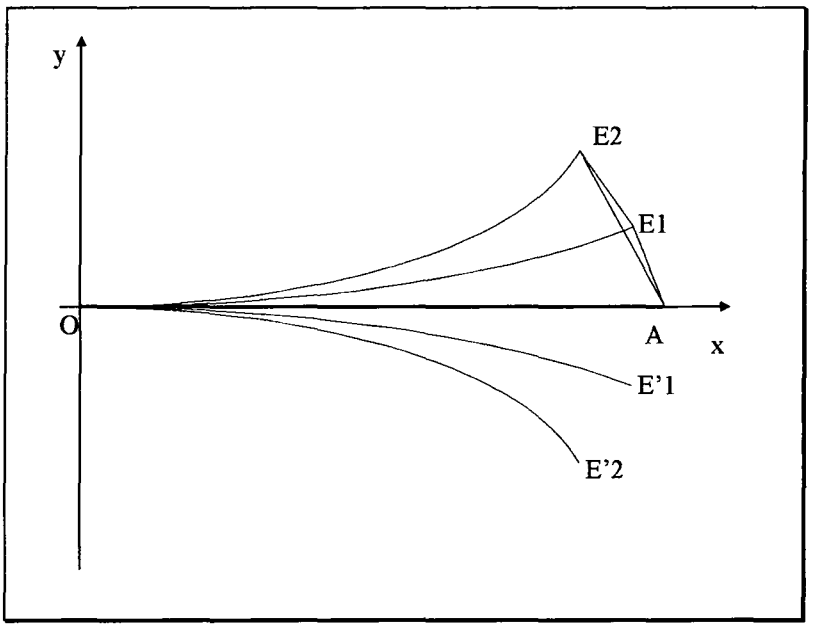

Figure 2-18

This indicates that if the angular measurement error is $E1_o$, the positional error for the situation where the robot moves along the curve from O to E1 is greater than the positional error for the situation where the robot moves along the x-axis from O to A.

However, the difference between $\overline{E1A}+\overline{E2E1}$ and $\overline{E2A}$ is small if $\Delta E1_o+E1_o$ is small.

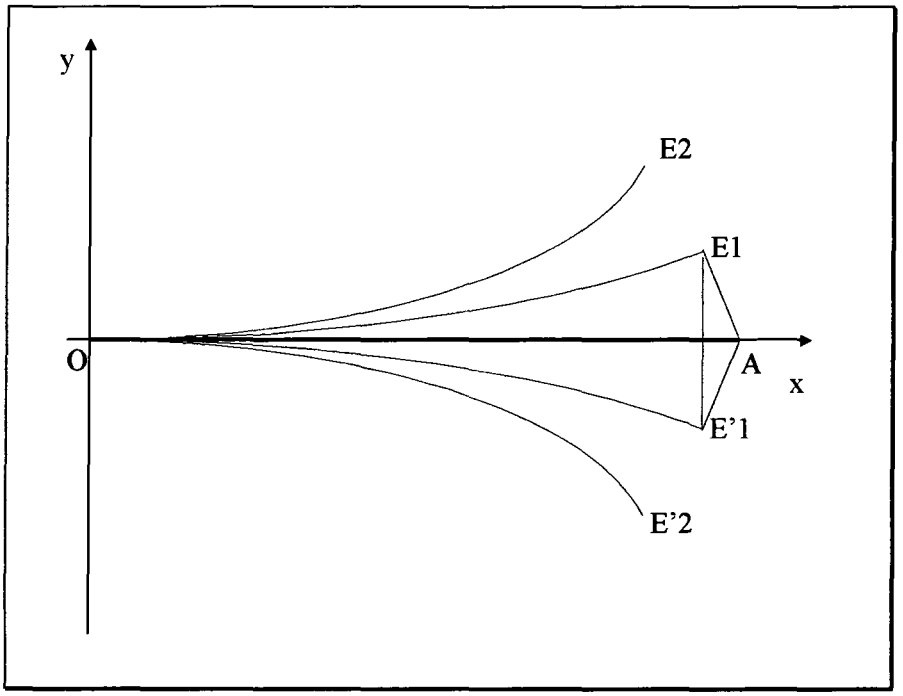

Figure 2-19

Following the above case, if the angular measurement error $\Delta E1_o$ equals –E1 instead of E1, when the robot moves along the curve from O to E1, the positional result is the position A. Therefore, the positional error for the situation where the robot moves along the curve From O to E1 equals the positional error for the situation where the robot moves along the x-axis from O to A, see Figure 2-19.

Moreover, if the angular measurement error $\Delta E1_o$ equals –E2 instead of E1 or –E1, when the robot moves along the curve from O to E1, the positional result is the position E'1. Therefore the positional error for the situation where the robot moves along the curve From O to E1 is less than the positional error for the situation where the robot moves along the x-axis from O to A, see Figure 2-19.

In general, considering the situation where a robot makes turns with a constant angle velocity r_o (radians per step) during travelling and the angular measurement error is E_o, the conclusion obtained was as follows,

If $r_o \times E_o > 0$, then the positional error will be greater than that in the situation where $r_o = 0$. This difference between these two positional errors is small, if the accumulation of $|r_o| + |E_o|$ is small.

If $r_o \times E_o < 0$ and $|r_o| > |E_o|$, then the positional error will be greater than that in the situation where $r_o = 0$. This difference between these two positional errors is small, if the accumulation of $|r_o| + |E_o|$ is small.

If $r_o \times E_o < 0$, $|r_o| \leq |E_o|$ and the accumulation of $|r_o| + |E_o|$ is small, then the positional error will be less than or equal that in the situation where $r_o = 0$;

Based on the above analysis, it is shown that if the sum of the accumulation of the change of the robotic orientation and the accumulation of the angular measurement error is not more than 1 radian, the error functions are valid. Sometimes, the ideal trajectory of the robot is a straight line or a few segments of lines, but because of the uncertain environmental factors, the real trajectory of the robot is near the lines. In this situation, the error functions discussed in this section remain valid.

2.1.5 Summary of the discussion of the two-dimensional error models (exact and statistical)

The above discussion of the two-dimensional error models (exact and statistical) can be summarised as follows.

- There are two sources of positioning error, angular measurement error and step length measurement error.
- Angular measurement error is the dominant error in the two sources of positioning error.
- A positioning error model is a tool to estimate the maximum positioning error based on relative factors. In this project, the relative factors are the angular

measurement error (E_o), the step length measurement error (E_d), length of the step (D) and the number (n) of the travelled steps.

- The estimate of the positioning error can be carried out by two separate parts. One is the estimate of the positioning error caused by the angular measurement error and the other is that caused by the step length measurement error. Normally, these two positioning errors can simply be summed as the total estimate, or the positioning error caused by the step length measurement error can be ignored.

- The positioning error caused by step length measurement error can be estimated by formula (1-3)

$$e_d = \pm nE_d, \qquad (1\text{-}3)$$

- The positioning error caused by angular measurement error can be estimated by formula (1-6) or (1-9)

$$e_o = \frac{49}{100} n^2 E_o D \qquad (1\text{-}6)$$

$$e_o = E_o\ [0.01625(nD)^2 + 23(nD) + 0.0072n(nD) - 15(nD)D] \qquad (1\text{-}9)$$

Here, the formula (1-6) is called the exact model which is a theoretical maximum error estimate function. The formula (1-9) is called the statistical model for 99.9% confidence. The exact model can be viewed as a statistical model for 100% confidence.

- The exact model is for estimating short-term positioning error and the statistical model is for estimating long-term positioning error. Here, the statistical model is under the condition that the angular measurement error is a random error and its possible distribution is a uniform distribution. In fact, if the distribution is a normal distribution, the positioning error will be less than that estimated by (1-10). Hence, this statistical model can still be used if the angular measurement error is a normal distribution error. However, if the mean of the angular measurement error is not zero, this statistical model is not appropriate.

- Based on the exact model, it was found that if the travelled distance (nD) and step length (D) are fixed, the positional error (e_o) is in proportion to the angular

measurement error (E_o). If the travelled distance (nD) and the angular measurement error (E_o) are fixed, the positional error (e_o) is in proportion to the reciprocal of the step length (D). The exact model indicates that if E_o is doubled, e_o will also be doubled. Also, if D is doubled, e_o will be reduced by 50%. Therefore, based on the exact model, improving angular measurement accuracy is of the same importance as the extension of the step length, for positioning accuracy.

- Based on the estimate models, it was found that if the travelled distance (nD) and step length (D) are fixed, the positional error (e_o) is in proportion to the angular measurement error (E_o). If the travelled distance (nD) and angular measurement error (E_o) are fixed, the positional error (e_o) will decrease with step length (D). The error functions (1-9) and (1-6) indicates that if E_o is doubled, e_o will be doubled in both statistical and exact model. However, It was found that if D is doubled, e_o will not decrease by less than 50% in the statistical model, see error function (1-9). This is different from the error function (1-6). Considering this factor, improving angular measurement accuracy is more important than extension of the step length for long-term positioning accuracy.

2.2 Three-dimensional Error Analysis

The error analysis results for the two-dimensional case can be extended to situations of three dimensions. In this section, it is assumed that a robot moves from the origin of a frame x-y-z along the x-axis. The angular measurement error around the x-axis is denoted as Eox. The angular measurement error around the y-axis is denoted as Eoy. The angular measurement error around the z-axis is denoted as Eoz. The measurement error of the step length is denoted as E_d. If Eoz does not equal zero and both Eox and Eoy equal zero, the estimated trajectory remains in the x-axis. In this situation, there is no lateral estimate error. If Eoz equals zero and one value of Eox or Eoy is zero, the situation is a two-dimensional case, which has been discussed in

Section 2.1. The following discussions start with the case that E_{ox} equals zero and both E_{oz} and E_{oy} are not zero. Thus, the case for E_{ox} not equal zero is as follows.

2.2.1 The case for E_{ox} equals zero and both E_{oz} and E_{oy} are not zero

Figure 2-20 shows a simple three-dimensional case which is extended from the two-dimensional case. In this case, the robot moves from O to A. Because of the angular measurement errors around the y-axis and the z-axis, $+E_{oy}$ and $+E_{oz}$, the positioning result is not the position A. If $E_{oz}=0$ and $+E_{oy}$ is a constant, the positioning result is B and the error in the lateral direction is e_{oz} and the error in the travel direction is e_{ox}. Adding the effect of $+E_{oz}$, the positioning result is C and the curve OC is in the plane OAC.

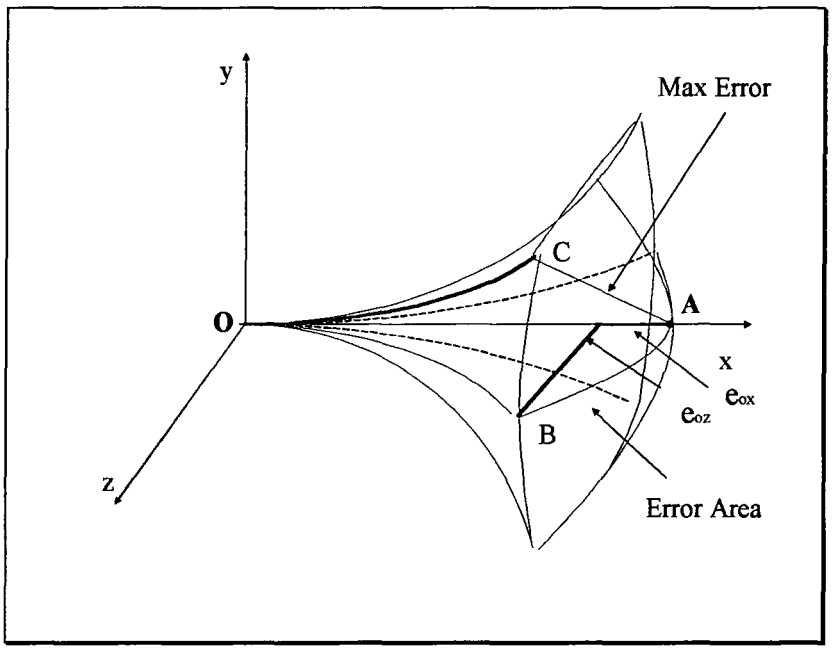

Figure 2-20 Positional error range in three-dimensional space

In fact, this is still a two-dimensional problem. In this case, the key factor for the positioning accuracy is the angular error in the plane OAC caused by E_{oz} and E_{oy}. The angle between the x-y plane and the plane OAC is not affected by the absolute value of the positioning error $|\overline{AC}|$. If the angular measurement errors around the y-axis and the z-axis vary in the range ($-E_{oy}$, E_{oy}) and ($-E_{oz}$ E_{oz}) respectively, the positional error will not be greater than the error $\overline{AC}$.

Considering the plane OAC, the angular measurement error caused by E_{oz} and E_{oy} is denoted as E_{oo} as shown in Figure 2-21. The angular measurement error between the x-y plane and the plane OAC is denoted as E_{od} as shown in Figure 2-21. If E_{od} is a constant, the above case can be viewed as a two-dimensional case. In this situation, the value of E_{od} does not affect the absolute value of the positional error. If E_{od} is not a constant, the above case is a three-dimensional case. The worst positional result of the three-dimensional case is the situation where E_{od} is a constant. Therefore, two-dimensional error functions can be used to estimate the positional error of the above three-dimensional cases where the angular measurement error E_{ox} is zero.

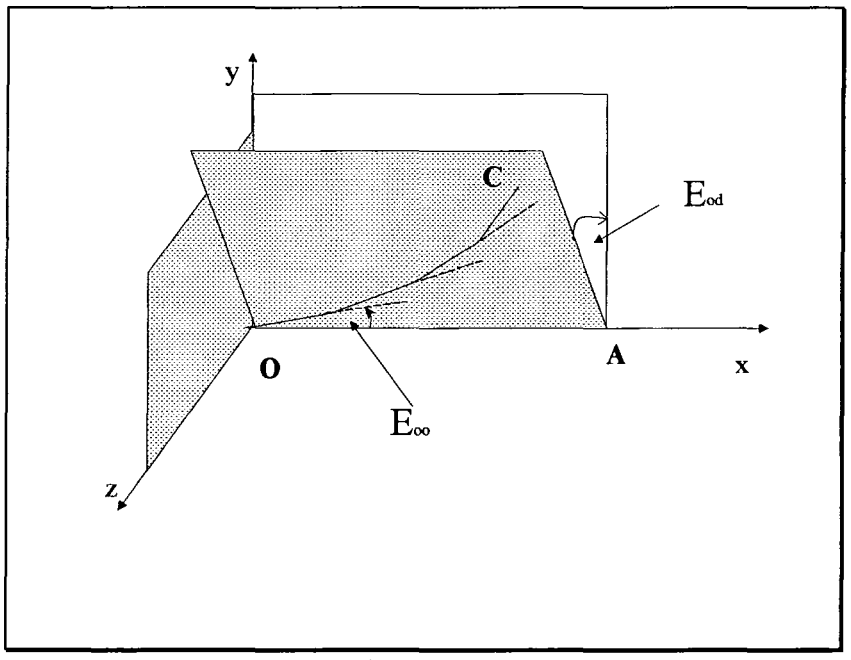

Figure 2-21

2.2.2 The case for E_{ox} does not equal zero

The case for E_{ox} not equal to zero can be viewed as that based on the above case, for which a value of angle E_{ox} is added to E_{od}. If there is only an initial value of E_{ox}, the situation is equivalent to the case where E_{od} is added to a constant value E_{ox}. If there is a constant value of E_{ox}, the situation is equivalent to the case, in which E_{od} increases by a value E_{ox} during each step. Hence, E_{ox} only affects the value of E_{od}. For the investigation of three-dimensional cases, the measurement error can be viewed

as three factors E_{oo}, E_{od} and E_d. If the sensors measure the rotations around the x-axis, y-axis and z-axis, the measurement errors, E_{ox}, E_{oy} and E_{oz}, can be transformed to E_{oo}, E_{od} and E_d. In a similar manner to the two-dimensional case, the key factor for positioning accuracy is the angular measurement error E_{oo}. The effect of the distance measurement error E_d on the positional results can be estimated separately or may be ignored. The effect of the angular measurement error E_{od} on the positional results can be ignored if the accumulation of E_{od} is not very large. The following figures (Figure 2-22, 1-26, 1-27, 1-28 and 1-29) illustrate geometrically the positional results caused by the effect of angular measurement errors E_{oo} and E_{od}. In the cases shown in the following figures, the step length is 1 meter and the travelled distance is 1000 meters.

Figure 2-22 shows the situation where there is a constant error E_{oo}=0.0005 radians and an initial error E_{od} = 0.1 radians

This figure illustrates that the trajectory is in a plane. This can be seen in the y-z plane. In this case, the value of E_{od} can only determine the angle between the projection line of the trajectory on the y-z plane and the y-axis. Only E_{od} can determine the absolute value of the positional error in the lateral direction.

Figure 2-23 shows the situation where there are constant errors E_{oo} = 0.0005 radians and E_{od} = 0.001 radians

This figure illustrates the trajectory is not in a plane. The projection of the trajectory in the y-z plane is a curve. Compared with the case shown in Figure 2-22, the trajectory is in a surface that can be viewed as the plane of trajectory in Figure 2-22 but where the plane of the trajectory is self-curved. Therefore, the positional error in the lateral direction in Figure 2-23 is less than that in Figure 2-22. If the accumulation of E_{od} is not large, the difference in the positional error in the lateral direction between the cases in Figure 2-22 and Figure 2-23 is not large. In Figure 2-23 the accumulation of E_{od} is 1 radian, that is 0.001(radians)×1000. The difference of the positional error in the lateral direction between the cases in Figure 2-22 and Figure 2-23 is not significant.

Figure 2-24 shows the situation where there are constant errors E_{oo}=0.0005 radians and E_{od} = 0.0025 radians.

This figure illustrates the tendency of the robotic trajectory when E_{od} becomes greater than that in Figure1-26. Because the accumulation of E_{od} is larger, that is 0.0025×1000=2.5 radians. The plane of the trajectory is curved more. However, the accumulation of E_{oo} is not very large, that is 0.0005×1000=0.5 radians. Consequently, the positional error in the lateral direction is less.

Figure 2-25 shows the situation where there are constant errors E_{oo}=0.0025 radians and E_{od} = 0.005 radians

In this case, the accumulation of the angular measurement error E_{oo} is 5 radians, that is 0.005(radians)×1000. In the x-y plane, the error between the estimated orientation and the actual orientation is more than 180 degrees. In this situation, the positional error is too large to use the error functions to estimate the positional error.

Figure 2-26 shows the situation where there are constant errors E_{oo}=0.01 radians and E_{od} = 0.01 radians.

This figure illustrates the tendency of the actual trajectory when E_{oo} and E_{od} become large. In this situation, the accumulation of angular measurement error E_{oo} is 10 radians, that is 0.01(radians)×1000. In this situation, the estimated trajectory becomes more complex and the estimated position will be far from the actual position. Hence, the error functions cannot be applied to estimate the positional error.

Through the above figures, it was found that the key factor for the positional accuracy is E_{oo}. The accumulation of E_{od} is not very important. As long as the accumulation of E_{oo} is not large, say less than 1, the positional error of the three-dimensional positioning system can be estimated by the error functions for two-dimensional case.

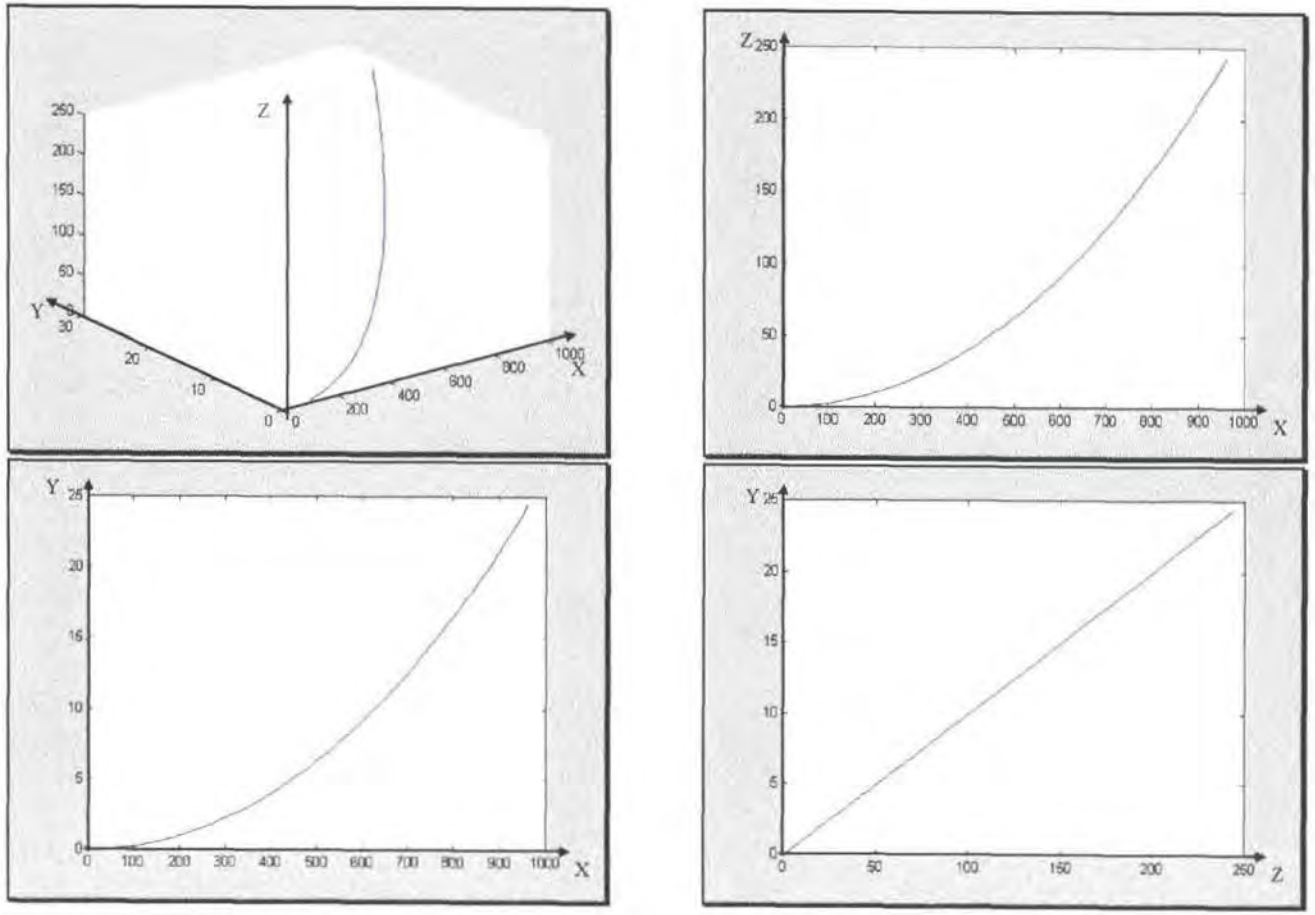

Figure 2-22 Estimated trajectory for the situation where there is a constant error E_{oo}=0.0005 radians and an initial error E_{od}= 0.1 radians

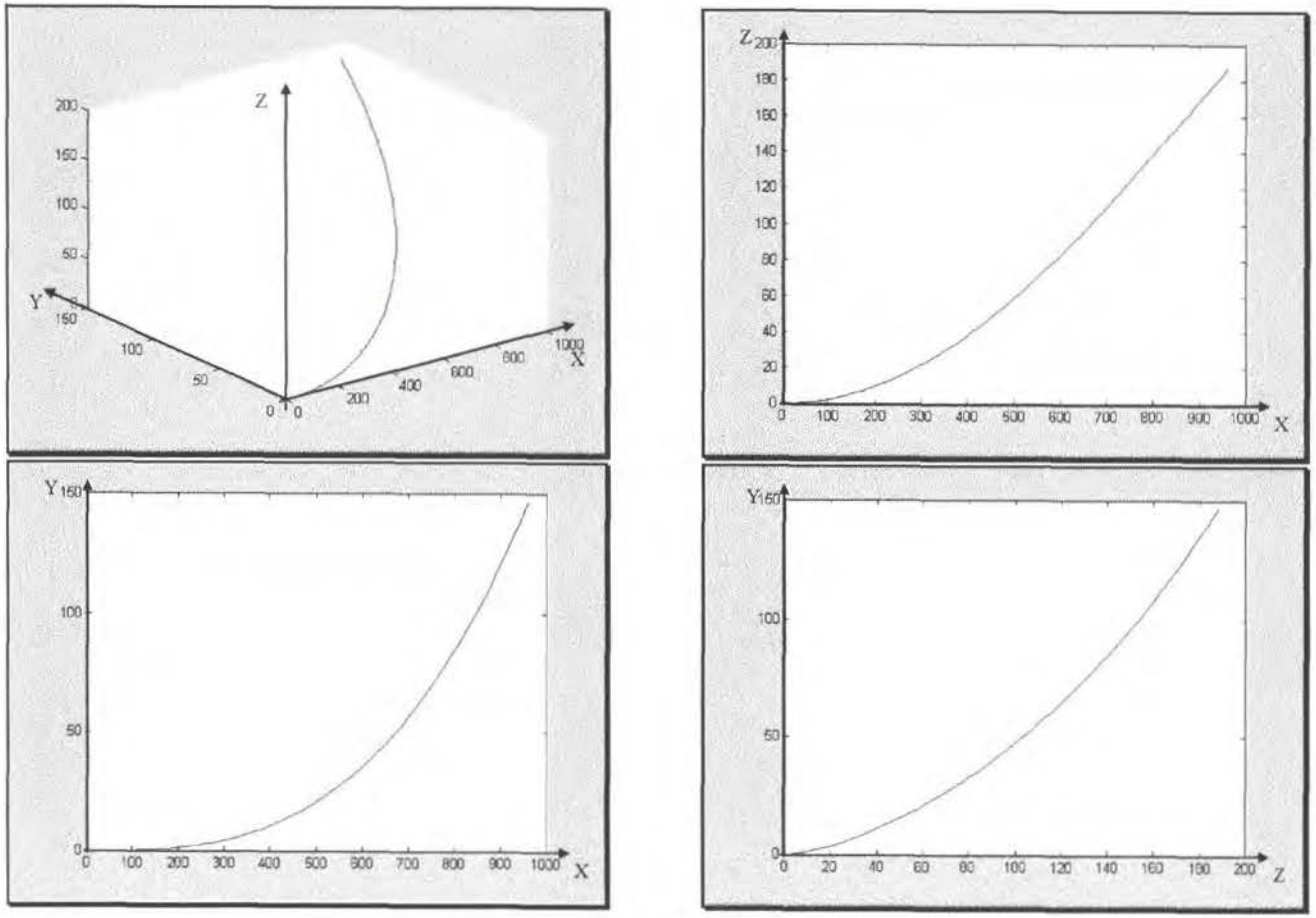

Figure 2-23 Estimated trajectory for the situation where there are constant errors $E_{oo} = 0.0005$ radians and $E_{od} = 0.001$radians

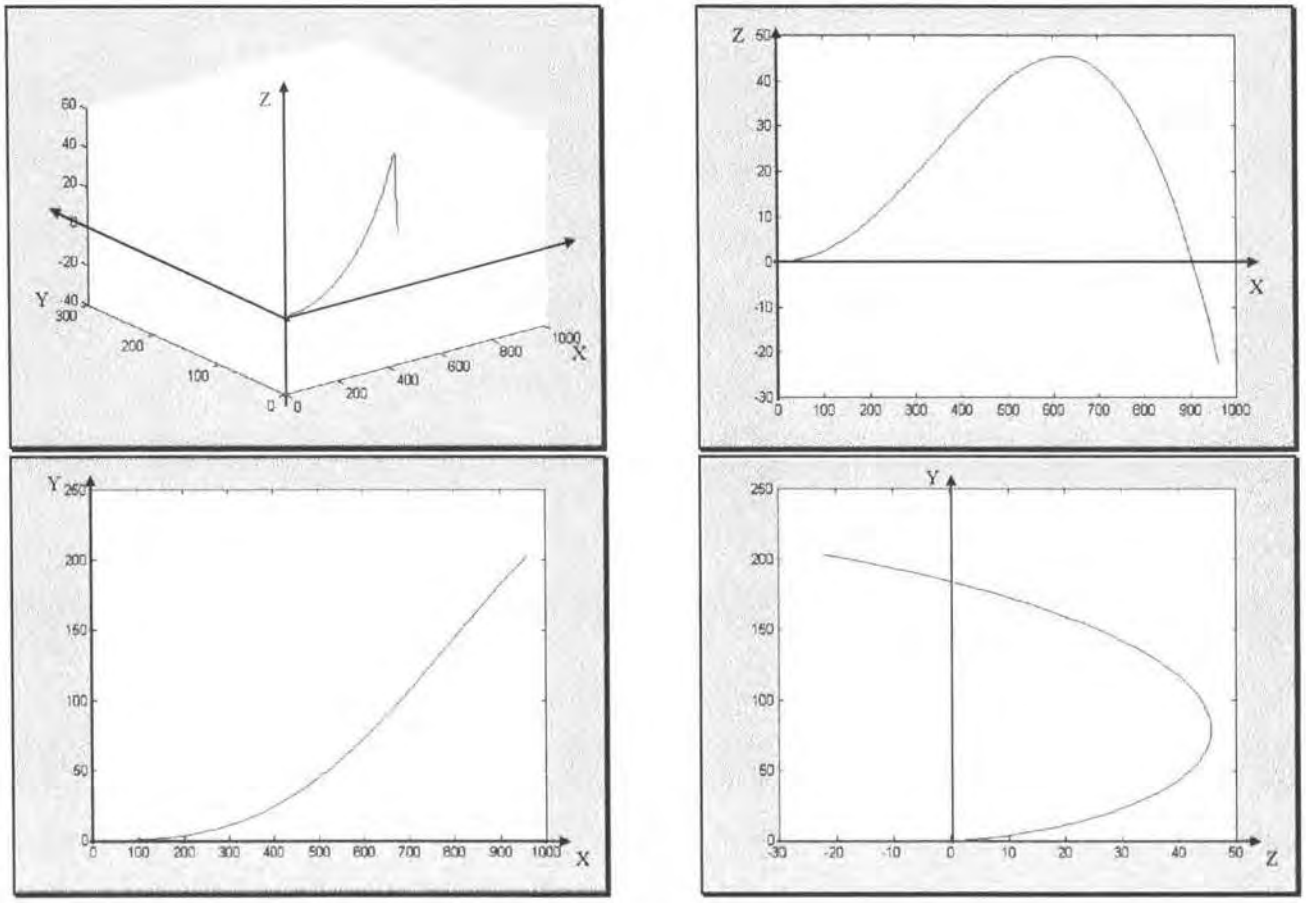

Figure 2-24 Estimated trajectory for the situation where there are constant errors E_{oo}=0.0005 radians and E_{od} = 0.0025 radians

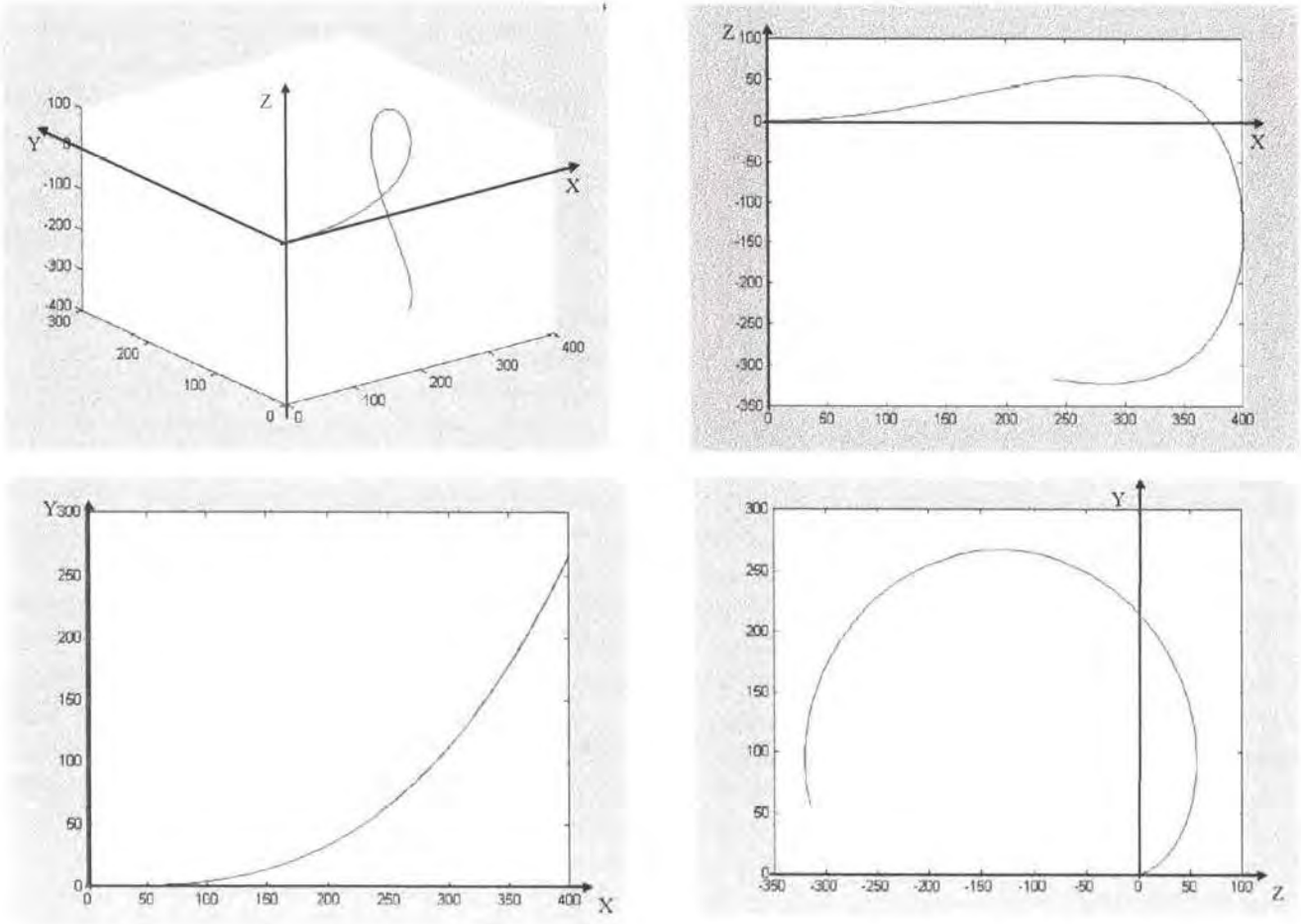

Figure 2-25 Estimated trajectory for the situation where there are constant errors E_{oo} =0.0025 radians and E_{od} = 0.005 radians

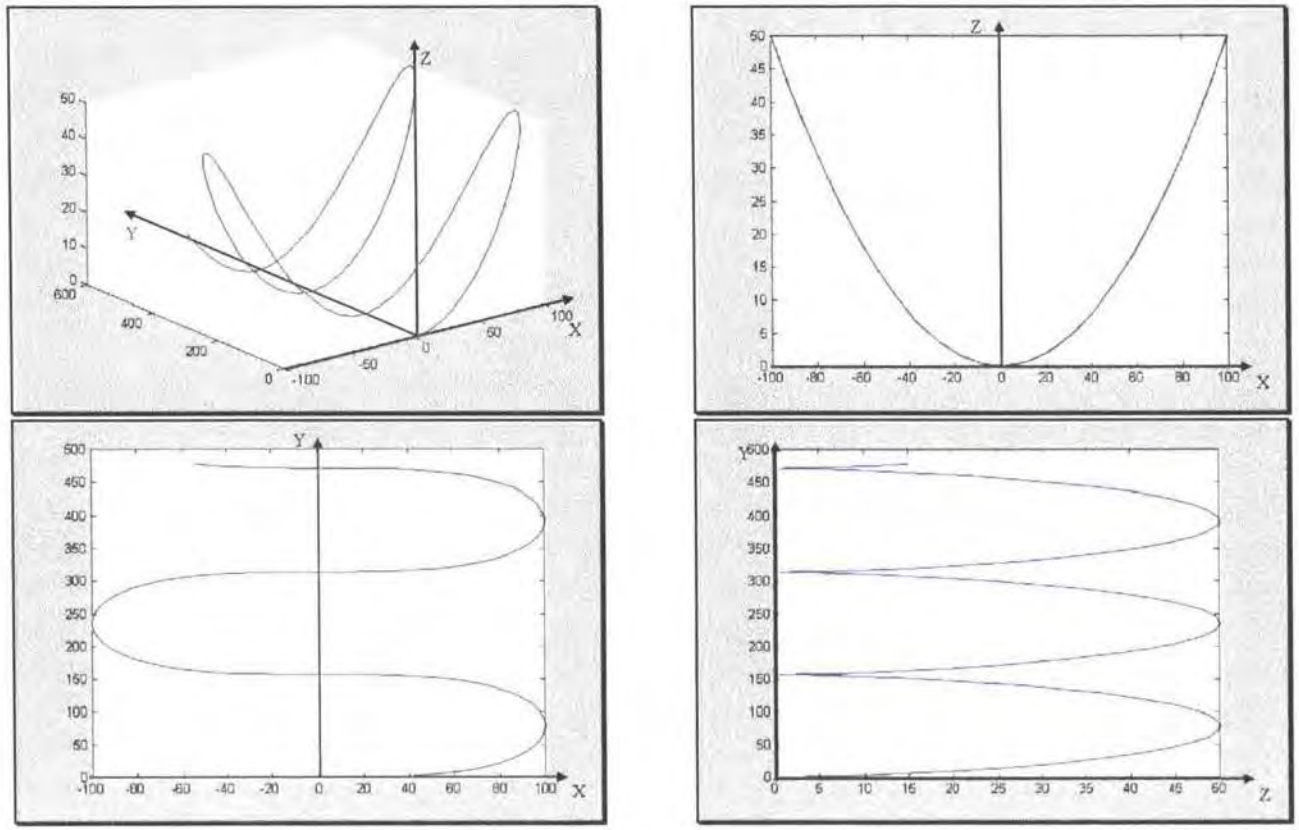

Figure 2-26 Estimated trajectory for the situation where there are constant errors E_{oo}=0.01 radians and E_{od}= 0.01 radians.

2.2.3 Summary of the Three-Dimensional Error Analysis

Based on the above analysis the following conclusions were obtained.

- For three-dimensional cases, the measurement errors, which determine the positional errors, can be viewed as three measurement errors E_{oo}, E_{od} and E_{d}.
- The situation where E_{od} equals zero or only has an initial value is, in fact, a two-dimensional case.
- The positional error in the situation where E_{od} equals a nonzero constant is less than that in the situation where E_{od} equals zero or only has one nonzero initial value.
- The error analysis results for two-dimensional cases can be directly extended to application to three-dimensional cases error estimates. In this situation, E_{od} can be ignored. E_{oo} and E_{d} can be used in the error functions for the two-dimensional case. All conclusions for the two-dimensional cases are suitable for application to three-dimensional cases.

Based on the above discussion, a proposal to improve long-term positioning accuracy for a stepwise underground robot is discussed in the following chapter.

Chapter 3

Proposed Positioning Technique

3.1 Key Factors and Problems

Through the above error analysis, it is known that there are two possibilities to improve long-term positional accuracy. One is to improve angular measurement accuracy. The other is to expand the length of each step of the robot. Considering the factor that measurement errors are normally random errors, improvement of angular measurement accuracy is more important than to expand the step length of a robot.

The step length of a stepwise robot depends upon the robot design. This is beyond the scope of this research. The proposed approach here is to improve angular measurement accuracy.

To improve angular measurement accuracy, high accuracy sensors must be used. However, unfortunately, for existing angular sensors it is difficult to significantly improve their accuracy. In addition, the limited space for mounting sensors has to be considered. Therefore, a parallel linkage mechanisms based approach is proposed.

3.2 Parallel Linkage Mechanism Based Approach for a Positioning System for an Underground Robot

In this section, the proposed parallel linkage mechanism and its application for a positioning system for a stepwise underground robot are described. Then, the advantage and problems of the proposed approach are discussed.

3.2.1 The Structure of the Parallel Linkage Mechanism

To illustrate the basic idea of the parallel linkage mechanism approach, a two-dimensional case is shown in Figure 3-1. In this case, there are two bars. One is called the base bar which is fixed. The other bar is called the top bar. Between the centre points of the two bars, there is a middle bar. One end of the middle bar is fixed to the centre point of the base bar and the other end is jointed at the centre point of the top bar so that the top bar can only change its orientation. This is a one-degree of freedom movement. Hence, one link between the two bars can be used to determine the

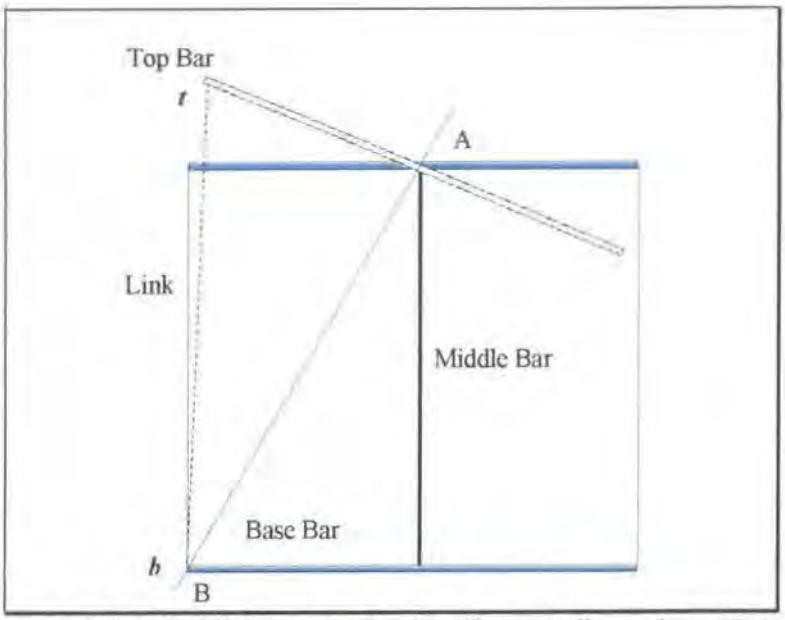

Figure 3-1 Parallel linkage mechanism for two-dimension, 1D, case

orientation of the top bar. The joint between the top bar and the link is denoted as ***t***. The joint between the base bar and the link is denoted as ***b***. If the positions of the joints ***t*** and ***b*** are given, the assembly configuration of the parallel linkage mechanism is given. Obviously, for different assembly configurations, the sensitivities of the mechanisms are different. Consequently, the accuracy of the estimated orientation for the top bar by using the link length will be different. If the joint points are closer to the centre points of the two bars the accuracy of the estimated orientation of the top bar will be lower.

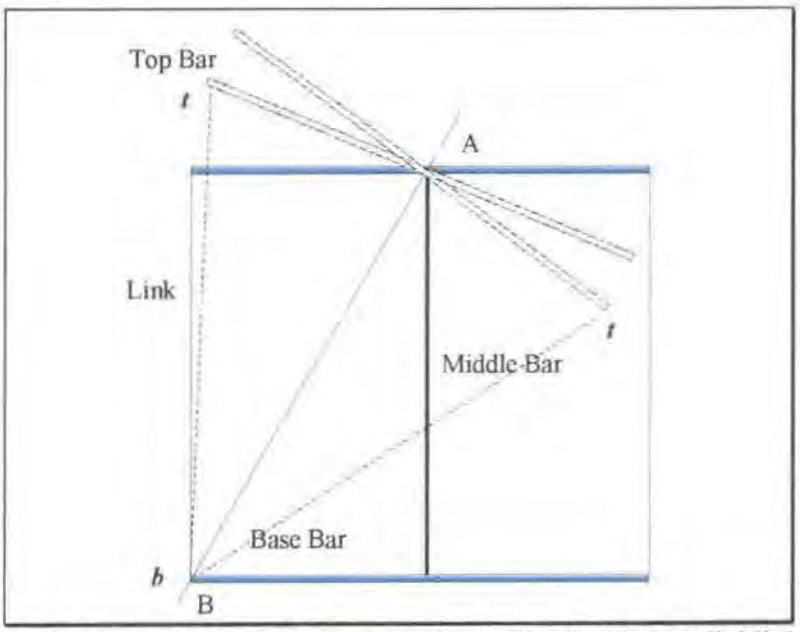

Figure 3-2 two solutions for the two-dimensional, 1D, Parallel linkage mechanism

It should be noted that although the case shown in Figure 3-1 is a 1D case, there may be multiple solutions for a given link length. Figure 3-2 illustrates that the two solutions are mirrored by the line AB. Here, the position A is at the centre of the top bar, and the position B is the joint B.

Following the above case, but there is no middle-bar to fix the centre point of the top bar as shown in Figure 3-3, this case is still in two-dimensional space but becomes a three-degrees of freedom movement case. In this case, at least three sensors are needed to determine the position and orientation of the top bar. Similar to the previous case in Figure 3-1, different assembly configurations will cause different accuracy of

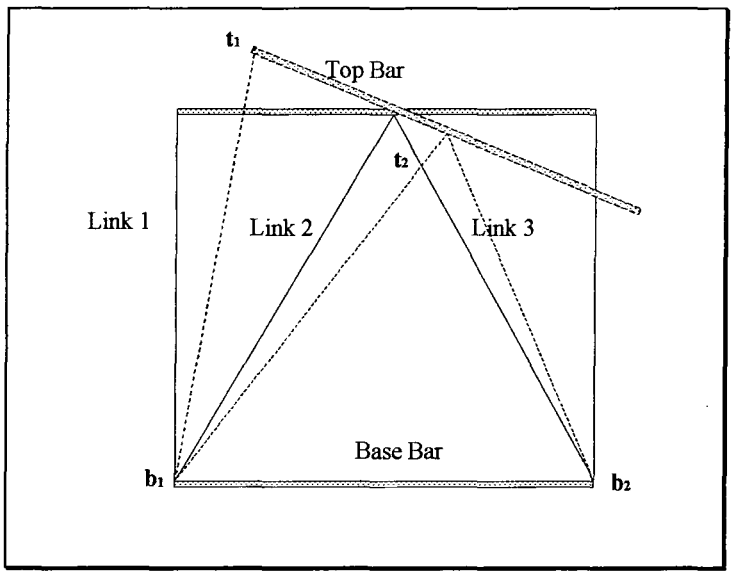

Figure 3-3 Parallel linkage mechanism for two-dimension, 3D, case

the positional result of the top bar. If the joints of link 2 and 3 on the top bar are at the centre point of the top bar, the position of the top bar can be determined by link 2 and 3. When the centre point of the top bar is known, link 1 can determine the orientation of the top bar. In this situation, if the joint of link1 on the top bar is closer to the centre point of the top bar, the accuracy of the estimated orientation of the top bar will be lower. If the lengths of the base bar and the top bar are known, for different link joints on the two bars, the different accuracies of the positioning system can be determined. Consequently, good assembly configuration for high accuracy positioning should be chosen. Since an underground robot has limited space for mounting sensors, the parallel linkage structure provides important flexibility. In the limited space, good joint positions for high accuracy positioning can be chosen.

Again, there may be multiple solutions for given link lengths in the case shown in Figure 3-3. Readers can find that there may be four solutions for a given link lengths.

For the case in three-dimensional space, the situation is similar but the parallel linkage structure becomes more complex. Considering a case shown in Figure 3-4, this structure consists of two disks, which are connected by n (here, $n=6$) linear links.

The bottom disk is called the base and the top disk is called the platform or the top platform. The joint between the i-th ($i = 1, 2, \ldots, n$) link and the **base** is denoted by $\mathbf{b}_i$ and the joint between the i-th link and the **top platform** is denoted by $\mathbf{t}_i$. This is a general structure. The movement of the top platform relative to the base is six-degrees of freedom (6D) movement. Hence, at least six links are needed to determine the position and orientation of the top platform.

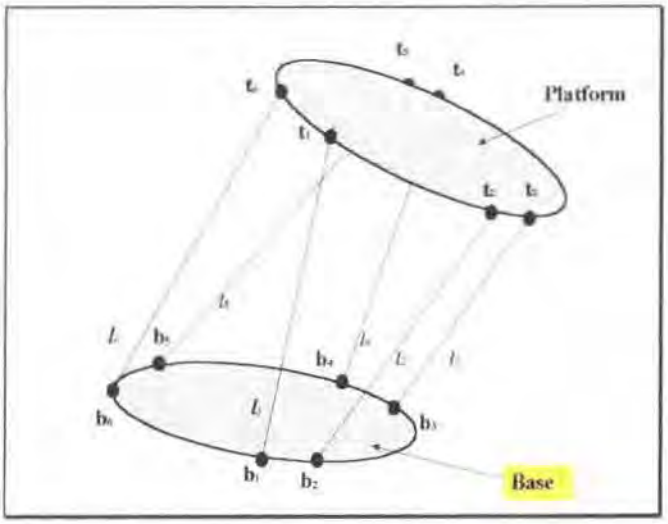

Figure 3-4 Parallel linkage mechanism for three-dimension, 6D, case

For the case of the three-dimensional space shown in Figure 3-4, the problems become much more complex. One of the problems relates to the multiple-solutions. Much literature addresses the multiple solutions for parallel linkage mechanisms [C. Innocenti 1991(*1)], [M. Raghavan, 1993]. However, there is no literature that addresses the sensitivity of displacement of a top platform for the link lengths. In Part II of this thesis, discussion for multiple solutions and the sensitivity of displacement of platform will be presented.

If the accuracy of the positioning system for different assembly configurations is known, a good assembly configuration for high accuracy positioning can be chosen.

Since an underground robot has limited space for mounting sensors, the parallel linkage structure presents advantages in terms of the flexibility for different particular robots.

Because high sensitivity of displacement will lead to high positioning accuracy, when discussing sensitivity of displacement for parallel linkage mechanisms, 'accuracy' will be used instead of 'sensitivity'.

3.2.2 Application of the Structure of the Parallel Linkage to an Underground Robot Positioning System

The structure shown in Figure 3-4 can only estimate the position and orientation of the top platform relative to the base by measuring the lengths of links. For a stepwise underground robot, during the time when the robot moves forward one step, different parts of the robot move forward in turn. Therefore, the parallel links can be mounted to connect a pair of contiguous parts. When the robot moves, the two connected parts can be viewed as the base and the top platform in turn. This procedure is shown in Figure 3-5. Before the front disk moves forward, the front disk is viewed as the top

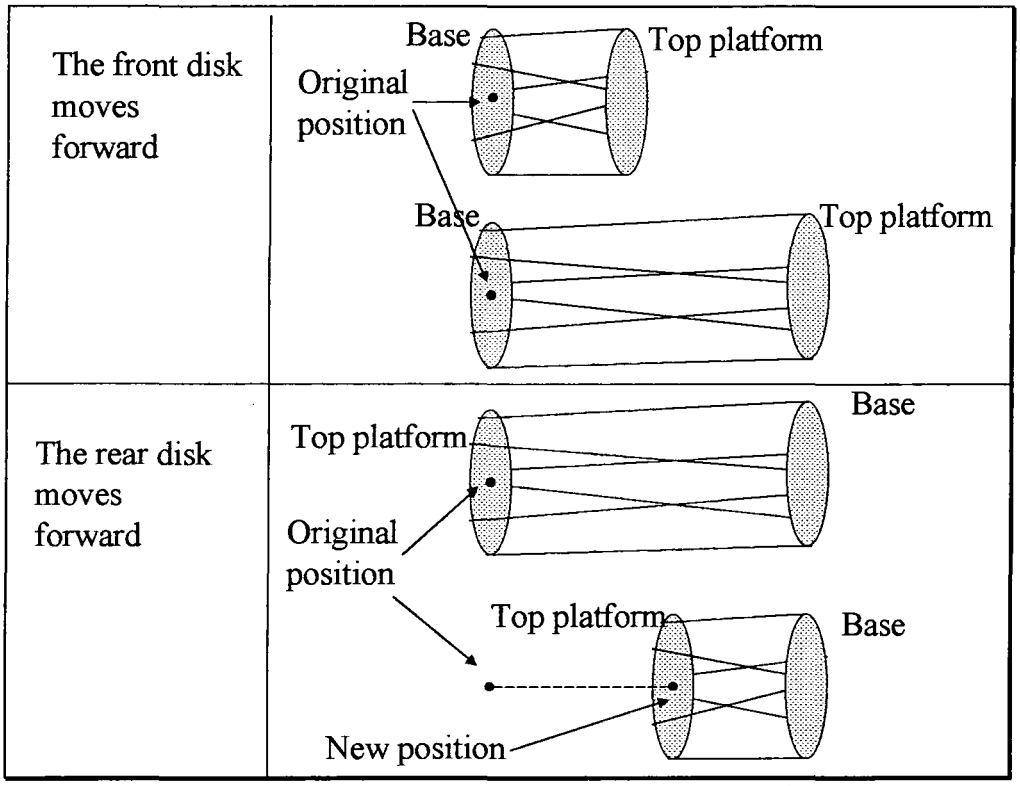

Figure 3-5 Use of parallel linkage mechanism for robot positioning systems

platform and the rear disk is viewed as the base. After the front disk moves forward, the position of the front disk relative to the original position of the rear disk can be

determined. After the front disk moves forward and before the rear disk moves forward, the front disk is viewed as the base and the rear disk is viewed as the top platform. After the rear disk moves forward, the new position of the rear disk relative to the front disk can be determined. Consequently, the new position of the rear disk relative to its original position can be determined.

3.2.3 Advantages and Problems of the Structure of the Parallel Linkage

One of the advantages is that the parallel linkage mechanism can provide flexibility to

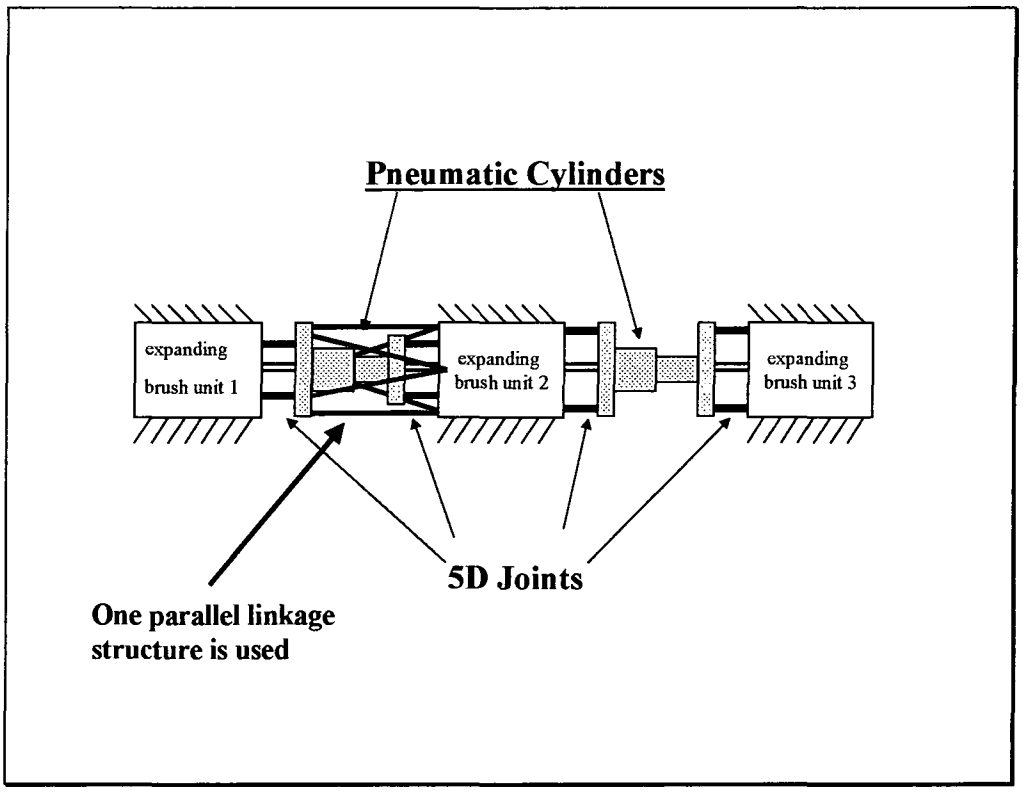

Figure 3-6 One parallel linkage mechanism is used

mount sensors. Figure 3-6 shows the situation where one parallel linkage structure is used. Figure 3-7 shows the situation where it is difficult to mount one parallel linkage structure, because one of the disks occupies the space. Instead, two parallel linkage structures are applied. One is mounted on the 5D joint, which is mainly used to measure the orientation of the robot. The other one is mounted on the expanding cylinder, which is mainly used to measure the step length of the robot.

The flexibility in terms of mounting sensors not only provides the convenience to install the sensors based on a particular structure of a robot but also provides the possibility to improve the positional accuracy. To improve the positioning accuracy,

there are two measures. One is by choosing good joint points of the links if the number of the links is given. The other is by using redundant sensors.

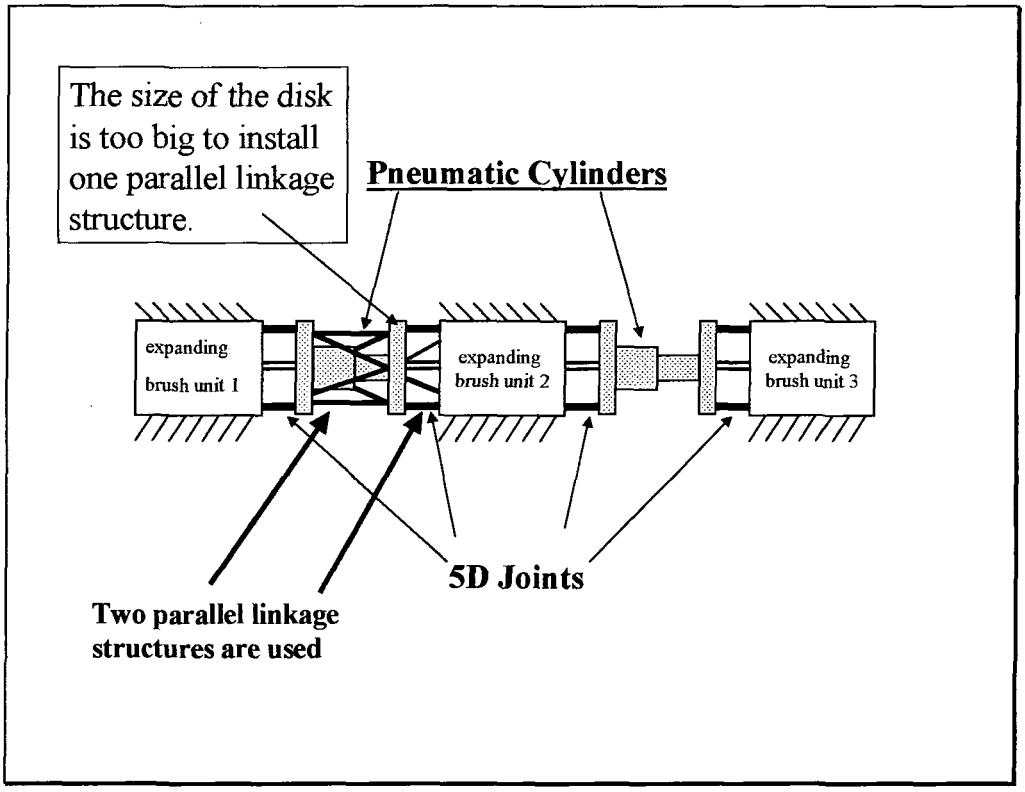

Figure 3-7 Two parallel linkage mechanisms are used

As stated in the previous section, if the accuracy of a parallel linkage mechanism for different joint positions $\mathbf{b}_i$ and $\mathbf{t}_i$ are known, good joint positions for high measurement accuracy can be chosen. For a six links structure, the joint positions can be chosen as shown in Figure 3-4 and Figure 3-8. However, the choice is subject to the particular structure of the robot.

The use of redundant sensors is the other means to improve positioning accuracy. In three-dimensional space, to determine the position and orientation of the top platform, at least six links are needed. Based on measurement technical knowledge, the use of more sensors can improve measurement accuracy. Figure 3-9 shows an eight links structure.

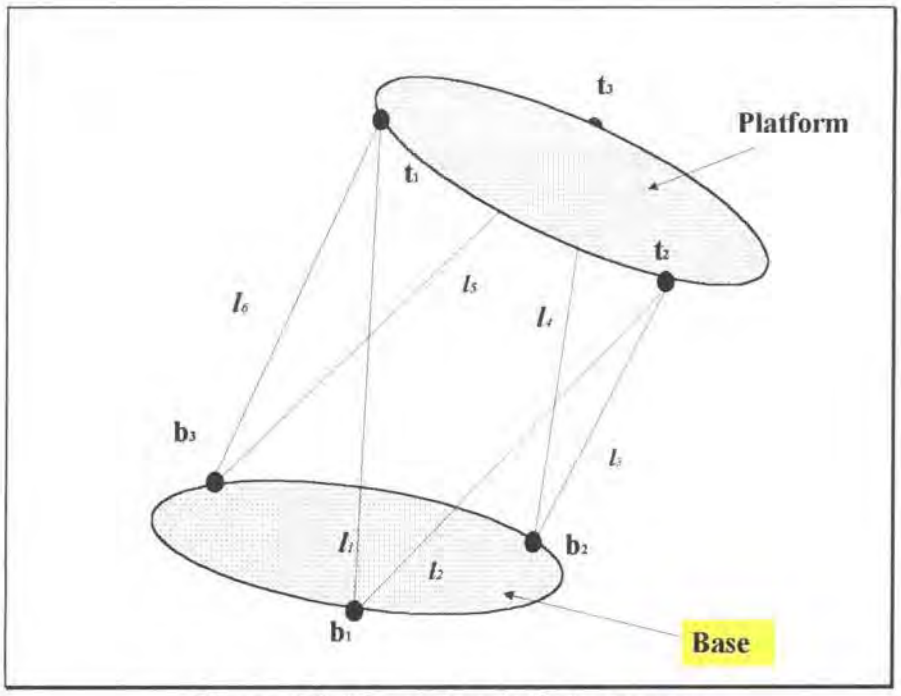

Figure 3-8 Alternative six-link structure.

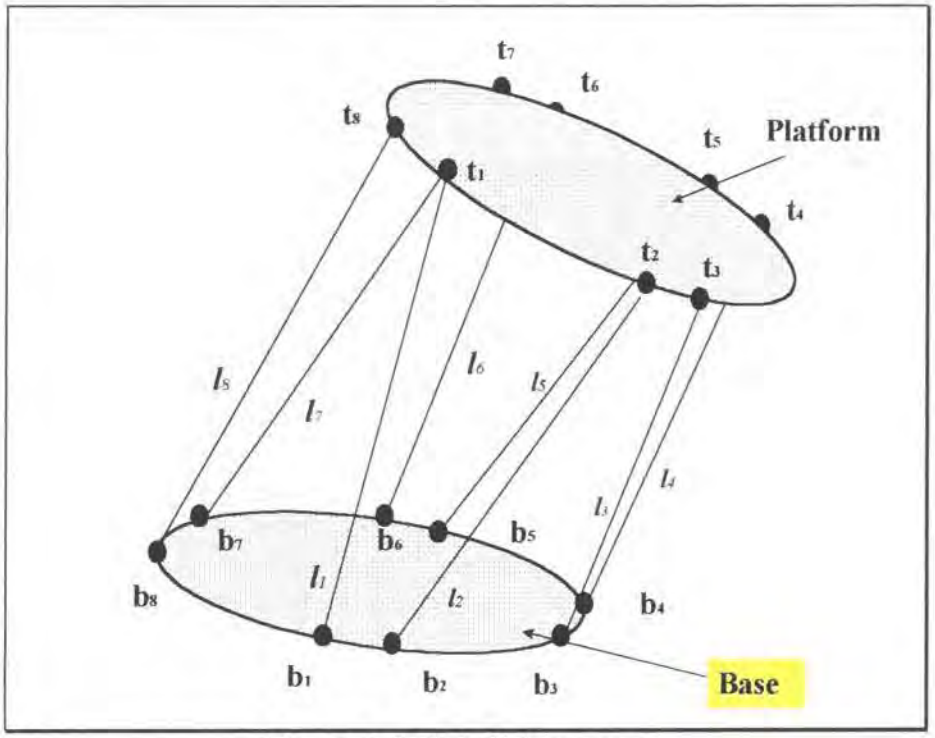

Figure 3-9 Eight-link structure.

Apart from the above advantage, the low cost is also an important advantage for industrial application. Since the parallel linkage mechanism only uses linear sensors to

measure the position and orientation of a robot, there is wider choice for the linear sensors than for rotary sensors. Normally, high-accuracy rotary sensors are more expensive than linear sensors.

In fact, the proposed approach is to improve the measurement accuracy by choosing the particular structure of the parallel linkage mechanism. However, because of the complexity of the parallel linkage mechanism in three-dimensional space, it is difficult to investigate the measurement accuracy for a particular parallel linkage mechanism. This is a disadvantage of the proposed approach.

In the past years, parallel linkage mechanisms have drawn a great deal of attention from many researchers. In this application of the parallel linkage mechanism, some problems have been raised. One problem is how to investigate the measurement accuracy for a particular parallel linkage mechanism. The other problem is how to build an algorithm to compute the position and orientation of the top platform, which has the high performance required to carry out a real-time positioning task.

To solve these problems, a Principal Component Analysis (PCA) based approach is presented in Part II of this thesis.

Chapter 4

Summary of Part I

In Part I, some fundamentals of underground robotic positioning techniques have been discussed. These characteristics can be summarised as follows.

- Underground robot positioning systems heavily rely on relative positional measurement techniques. For general cases, only relative positioning techniques are available.
- Because of relying heavily on relative position measurement techniques, long-term positional accuracy is the most important problem for an underground robot positioning system.
- Limited space strongly restricts the choice and installation of a positioning system and their sensors for an underground robot. This causes a difficult constraint in any attempt to improve the accuracy of a positioning system.
- The dominant measurement error for a positioning system is the angle between the actual orientation of the robot and the estimated orientation. This measurement error and the step length measurement error can be used to estimate the three-dimensional positioning error by using the two-dimensional error functions (1-6) and (1-9).
- Considering the exact error estimate function (1-6), existing positional techniques and sensors cannot absolutely guarantee to meet a long-term accuracy requirement for an underground robot. However, using the statistical error function (1-9), the long-term positional error estimated is lower than that estimated by (1-6). This is a very important characteristic for underground robot positioning systems. Because of this characteristic, the improvement of long-term positioning for an underground robot becomes possible. Statistical error estimate functions cannot guarantee 100% to meet a long-term accuracy but can meet the accuracy under a given confidence. The confidence of the statistical error estimate function (1-9) is 99.9%. This means that there is 99.9% possibility

to ensure that the positional error is in the range estimated by using the function (1-9). If the confidence of a statistical error estimate function is less than 99.9%, the estimated positional error will be lees than that estimated by using the function (1-9).

- Based on the exact error function (1-6), improving the angular measurement accuracy and enlarging the step length of a stepwise robot are significant for improving positioning accuracy. If the accuracy of the angular measurement is doubled, the positional accuracy will be doubled for a fixed travelled distance of a robot. If the step length is doubled, the positional accuracy will also be doubled for a fixed travelled distance of a robot. However, it should be noted that the exact error function (1-6) is mainly for short-term positioning. Based on the statistical error function (1-9), improving the angular measurement accuracy is more important than enlarging the step length of a stepwise robot. If the accuracy of the angular measurement accuracy is doubled, the positional accuracy will be doubled for a fixed travelled distance of a robot. If the step length is doubled, the positional accuracy will be higher but less than double for a fixed travelled distance of a robot. Therefore, the first important factor for improving long-term positional accuracy is to improve the angular measurement accuracy, especially, the accuracy of measuring the angle between the actual orientation of the robot and the estimated orientation. The second important factor for improving long-term positional accuracy is to enlarge the step length of the robot.

Based on the characteristics of underground robot positioning systems, a parallel linkage mechanism based approach is proposed. This approach has many advantages for matching the characteristics of a positioning system for an underground robot. It should be noted that this approach only gives a direction to improve angular measurement accuracy. Different parallel linkage mechanisms may have different measurement accuracy. The analysis of the measurement accuracy of a parallel linkage mechanism is very important. The improvement of the performance of an algorithm to carry out a real-time positioning task is also important. Some preparatory work in this area is presented in Part II of this thesis. A particular parallel linkage mechanism used to improve positional accuracy for underground robots is also presented in Part II.

PART II

The PCA Based Approach for Forward Displacement Measurement of the Stewart Platform

Chapter 5

Introduction to Part II

In past years, parallel linkage mechanisms have drawn a great deal of attention from many researchers. This popularity results from the fact that parallel mechanisms have attractive characteristics for robotic applications. The research of the displacement kinematic problem for parallel mechanisms is one of the important branches of parallel linkage mechanism research. The inverse displacement kinematic problem for parallel mechanisms, as found in robot control, is straightforward. However, the forward displacement kinematic problem is a more challenging task. Hence, in past year, many published papers addressed this problem. As mentioned in Part I, the use of a parallel linkage mechanism can provide many technical advantages to an underground robotic positioning system. To establish a parallel mechanism based positioning system requires the solution of the forward displacement kinematic problem. In addition, the accuracy of the solution for the forward displacement kinematic problem in a given solution range needs analysis. A Principal Component Analysis (PCA) based approach for the analysis of relationships between the linkage and the positional variables of the platform of a parallel mechanism was proposed in this research. Thus, as a consequence, the PCA based approach was used for the relationship analysis and accuracy analysis for a particular forward displacement measurement. Based on the results of the PCA based analysis, a PCA based numerical algorithm for forward displacement measurement was also developed.

5.1 Displacement Kinematic Problems for Parallel Mechanisms

The very basic kinematic problem for parallel mechanisms can be roughly divided into two categories: direct displacement analysis (forward kinematics) and inverse kinematics. The direct displacement kinematic problem is to compute the position and orientation of the top platform relative to the base when the link lengths are given. On

the other hand, the inverse kinematic problem can be expressed as 'given the position and orientation of the top platform, calculate the link lengths' [J.J. Craig, 1986].

Geometrically, the forward displacement problem is equivalent to the problem of placing a rigid body such that ***n*** of its given points lie on ***n*** given spheres. Denoting the *i*-th **base** point by $\mathbf{b}_i$ and the *i*-th **top platform** point by $\mathbf{t}_i$, it is required to solve the kinematic equations

$$\| \mathbf{v} + \mathbf{R}\mathbf{t}_i - \mathbf{b}_i \|^2 = l_i^2 \qquad \text{for } i = 1,\ldots,n \qquad (1)$$

for the translation vector **v** and the orthogonal rotation matrix R, where the link lengths l_i (i =1,..., n) are given.

When ***n*** equals six, the parallel mechanism is known as a Stewart Platform, which was introduced by Stewart [D. Stewart, 1965]. A special structure with ***l*** and ***m*** distinct joint-points at the base and at the platform was referred to as an ***l-m*** Stewart Platform, the simplest being the 3-3 case (the octahedral structure) and the general structure being the 6-6 Stewart Platform. During the late 1980's and early 1990s, the forward displacement problem enjoyed a central status in the research on the Stewart Platform [B. Dasgupta, 2000]. In this project, the purpose of studying the forward displacement problem is not only to get a good solution for a particular mechanism, but also, more importantly, to obtain the properties of the solutions in a certain range for designing a good positioning system.

5.2 Geometrical Model of the 6-6 Stewart Platform

In Eq (1) the orientation of the platform is represented by the orthogonal direction cosine matrix. Since, in this project, the geometrical properties of the Stewart Platform need to be analysed, the geometrical model is introduced as follow.

5.2.1 General Model

A geometrical model of the 6-6 Stewart Platform is illustrated in Figure 5-1. This is a general model, in which two disks are connected by six linear links. The bottom disk is called the base and the top disk is called the platform or top platform. There are also two coordinate frames on the two disks. One frame is on the base and called the base frame. The other one is on the top platform and is called the top frame. The origin of

the base frame is at the centre of the base disk. The x-y plane of the base frame is in the plane of the base and the direction of the z-axis of the base frame is upward. The origin of the top frame is at the centre of the platform disk. The x-y plane of the top frame is in the plane of the platform and the direction of the z-axis of the top frame is upward. In Figure 5-1, (x_0,y_0,z_0) are the coordinate values of the centre of the top platform in the base frame coordinate system, and the variables α, β and γ are the rotational angles of the top frame relative to the base frame. Corresponding to Eq (1), the position vector (x_0,y_0,z_0) is the vector (**v**) in Eq (1) and the rotational angles α, β, γ determine the rotation matrix R in Eq (1).

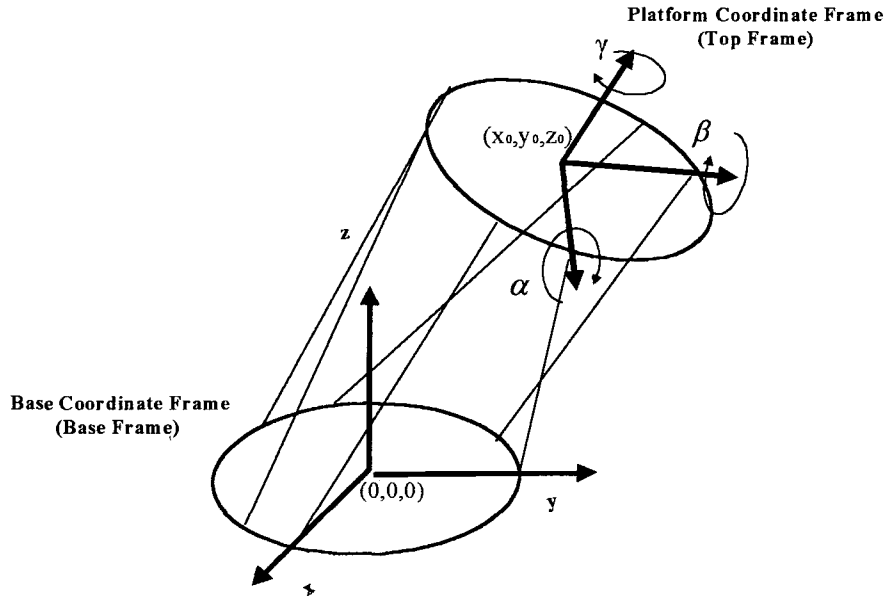

Figure 5-1 Basic Geometrical model of Stewart platform

5.2.2 Equivalent Model

In this research, the Principal Component Analysis (PCA) method is used to find the relationship between the six link-lengths and the position and orientation of the platform. To carry out the analysis more easily and to illustrate the relationship more clearly, an equivalent model is used. In this model, an extensible virtual bar has been added between the two disk centres. This bar is denoted as the M-bar (see Figure 5-2). Consequently, another coordinate frame, the M-frame, is also introduced. The origin of the M-frame is at the bottom of the M-bar and the z-axis is in the centreline of the

M-bar. The T-frame and B-frame are the same as Top Frame and Base Frame, respectively in the general model shown in Figure 5-2.

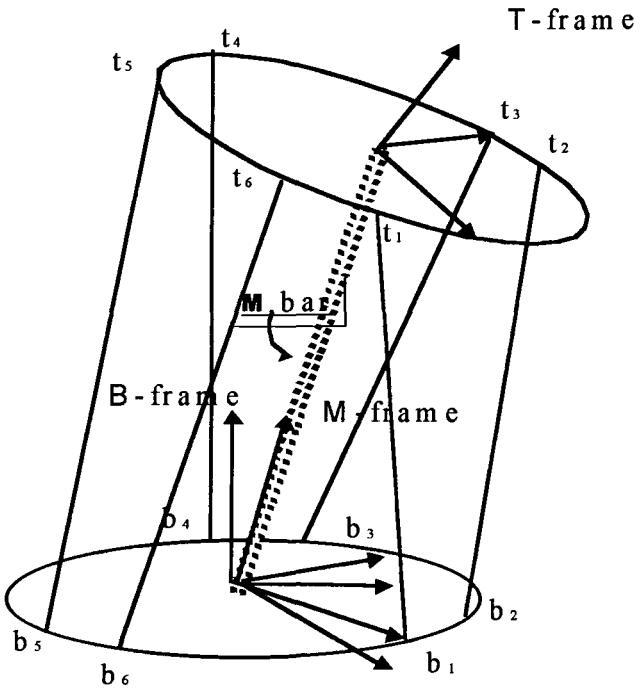

Figure 5-2 Equivalent geometrical model of Stewart platform

Here, a set of variables (α_1, α_2, α_3, α_4, α_5, *lm*) is chosen as the positional variables to express the position and orientation of the platform relative to the base instead of the variable set ($x_0, y_0, z_0, \alpha, \beta, \gamma$). These new variables are defined as follows:

lm: Length of the M-bar. α_1 *:* Angle 1 is the angle between the z-axis of the M-frame and the z-axis of the B-frame. α_2 *:* Angle 2 is the angle between the X-Z plane of the B-frame and the plane constructed by the z-axis of the M-frame and the z-axis of the B-frame.	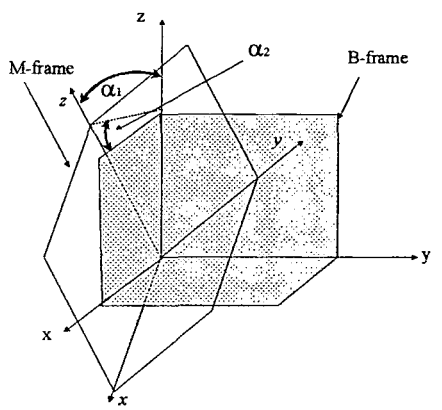

α_3: Angle 3 is the angle between the z-axis of the M'-frame and the z-axis of the T-frame.

α_4: Angle 4 is the angle between the X-Z plane of the M'-frame and the plane constructed by the z-axis of the T-frame and the z-axis of the M'-frame,

α_5: Angle 5 is the platform's rotation angle around z-axis of the T-frame, which is defined by the difference of two angles. One is the angle between the axis of the T-frame and the intersection line that is constructed by the x-y plane of the T-frame and the x-y plane of the M'-frame. The other one is the angle between the x-axis of the M'-frame and the intersection line that is constructed by the x-y plane of the T-frame and the x-y plane of the M'-frame.

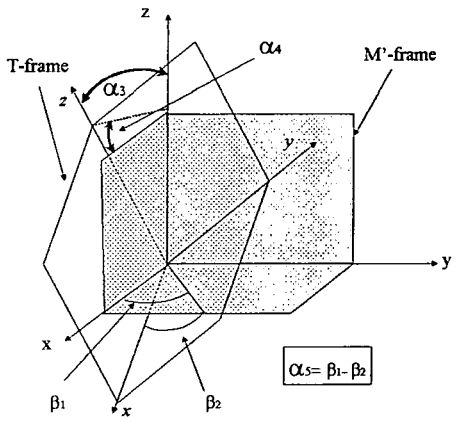

Note: The M'-frame is transformed from the M-frame by moving the origin of the M-frame to the origin of the T-frame.

In this model, it is assumed that the M-bar cannot roll around the z-axis of the M-frame.

Since the three coordinate frames are applied, Eq (1) can be transformed to the equivalent equations (2) as follows.

$$\| \mathrm{R}_{mb}\mathbf{w} + \mathrm{R}_{mb}\mathrm{R}_{tm}\mathbf{t}_i - \mathbf{b}_i \|^2 = l_i^2 \qquad \text{for } i = 1,\ldots,6 \qquad (2)$$

Here, $\mathbf{w}$ = (0, 0, lm) is the coordinate of the centre of the top platform in the M-frame. Comparing Eq (2) with the vector $\mathbf{v}$ and the rotation matrix R from the T-frame to B-frame in Eq(1),

$\mathbf{v} = R_{mb} * \mathbf{w}$ and

the rotation matrix $R = R_{mb} R_{tm}$.

Here R_{mb} is the rotation matrix from the M-frame to the B-frame, which is determined by the angles 1 and 2. Also R_{tm} is the rotation matrix from the T-frame to the M-frame, which is determined by the angles 3, 4 and 5.

5.3 Approaches for the Forward Displacement Problem of a Stewart Platform

As the complete solution of the forward displacement problem for a Stewart Platform was quite challenging, numerous approaches were made by various researchers, which fall into the following categories.

5.3.1 *Closed-form solutions of special cases*

It was known that coalescence of some of the joint-points at the platform or the base or both simplifies the closed-form solution of the problem and reduces the maximum number of possible solutions. In this way, there are three sorts of approaches. One of the approaches [M. Griffis, 1989] [W. lin, 1992, 1994] is based on the use of the input-output equations of spherical four-bar mechanisms to solve the 3-3 case and extend it to more difficult (6-3, 4-4, 4-5) cases. In another approach [C. Innocenti, 1990,1995], [P. Nanua, 1990], [V. Murthy, 1992], [J.-P. Merlet, 1992], [N.-X. Chen,1994], [Q. Liao, 1995], the platform is first removed, then the loci of the coalesced platform are imposed to derive the equations for further simplification. In a third approach [C. Innocenti, 1992, 1993(*1), [M.Husain, 1994], [K. Wohlhart, 1994], used approach which is slightly different from the second one, as a part of the entire structure is reduced to an equivalent serial mechanism and constraints on its joint angles are imposed by the constraints of the remaining parts to obtain the equations. Apart from coalescence of joint-points, other geometrical conditions like collinearity of some joint-points or similarity of the base and platform polygons also facilitate the solution of the problem in closed form, as demonstrated by various authors[C-de Zhang, 1991], [W. Guozhen, 1992], [J.P. Yin, 1994], [S.V. Sreenivasan, 1994].

5.3.2 *Numerical schemes*

The numerical approach [H. McCallion, 1979], [G. Deshmukh, 1990], [C.C. Nguyen, 1991], [L.-C.T. Wang, 1993] that directly resorts to nonlinear-equation-solving algorithms has computational advantages. This is true in most practical situations where only one real solution is required and a good starting point is available in the form of a neighbouring solution. However, the approach is not suitable for a theoretical investigation aimed at determining all the possible solutions. For finding all real solutions, approaches [C. Innocenti, 1991(*1)], [M. Ait-Ahmed, 1993] are employed to reduce the problem by geometrical or algebraic methods to that of solving a system of three equations the solutions of which can be trapped by a three-dimensional search. A unidimensional search algorithm for finding all real solutions was developed [C. Innocenti, 1993(*2)]. This algorithm temporarily replaces one of the legs of a general 6-6 Stewart Platform by a fictitious leg of variable length to convert it into a 5-5 Stewart Platform. The approach then solves the modified structures by a specialised method and re-imposed the constraint due to the original removed leg. A predictor-corrector algorithm [B. Dasgupta, 1996] used an efficient 3D search strategy for trapping the real solutions purely from geometrical considerations. For finding all solutions in the complex domain, an algorithm was also developed [M. Raghavan, 1993].

5.3.3 *Analytical approaches*

If the orientation of the platform is represented by the orthogonal direction cosine matrix (rather than a presentation like Euler angles etc.), the six kinematic equations obtained from Eq. (1) are all quadratic and the quadratic terms appear only in a few groups thus facilitating linearisation of some of those equations. A number of analytical approaches [S.V. Srinivasan, 1992], [A. Dhingra, 1992], [C.-de Zhang, 1994], [B. Dasgupta, 1994] to the forward displacement problem exploited this fact to reduce the total degree of the resulting polynomial system.

5.3.4 *Approaches for on-line operations*

For purposes of on-line operation, it is essential that (1) out of all possible solutions, a particular one (the actual one) is determined unambiguously and (2) the solution is fast enough for real-time implementation. To meet these two ends, redundant sensing

has been proposed and analysed [L. Baron, 1994(*1), 1994(*2), 1995(*1)], [K. Han 1996], [V. Parenti, 1999] for resolving ambiguity on one hand and decoupling and linearising the problem on the other, leading to fast computation.

5.3.5 *Other approaches*

There is also other work, such as neural network solutions [Z. Geng, 1991], polynomial network solutions [R. Boudreau,1998], [V. Parenti-Castelli, 1992], [C. Gosselin, 1992]. The use of a camera for obtaining extra information has also been suggested [L. Baron, 1995(*2)].

For the application of parallel mechanisms in this project, the solution for forward displacement problem is required to meet the purposes of on-line operation. However, as a part of the foundational research for underground robotic positioning systems, no particular redundant sensing approach was considered in this research. Instead, good understanding of parallel mechanisms for positioning system is desired, so that more information for designing a positioning system using redundant sensors can be obtained.

Chapter 6

The Methodology

For the application of parallel mechanisms to a stepwise robotic positioning system, a PCA based approach to solve the forward displacement problem and analyse its accuracy was applied. The PCA method is a multivariate statistical method. To illustrate the principle of the PCA based approach, the introduction starts by a general outline of statistical methods to find such relationships. After that, the principle of PCA and its particular application for analysis of mechanical relationships are introduced.

6.1 Statistic Method for Relationship Analysis

Statistical methods are often used for data analysis in research. In the present research, statistical principles are applied for analysis to find the relationship between two important sets of variables. This procedure of statistical analysis is similar to that of experimental analysis.

Experimental methods are often used in science and engineering research. The objective of an experiment is to find the relationship between two or more objects or variables. When an experiment is being carried out, test data is recorded. In some simple cases, the relationship can be directly illustrated by the experimental data. However, most application cases need some data processing of the experimental data before a relationship is obtained.

Statistical methods are often used to process experimental data. In these situations, the whole procedure of an experiment can be viewed as a statistical analysis procedure. The following is a simple example. The purpose of the experiment is to discover the relationship between the length (l) of a spring and the pull force (p) acting on it. Here the variable p is a function of the variable l and the experiment needs to find the function $p = F(l)$. The procedure is as follows:

1. Decide a set of test values, say, the pull force $p_1, p_2, \ldots, p_n$

2. Get the test values, say, the spring length l_1, l_2, ... l_n, corresponding to $p_1, p_2, \ldots, p_n$
3. Analyse the relationship between the variables l and p to get the function p = F(l).

This can be expressed diagrammatically as shown in Figure 6-1

The region in the left ellipse represents the whole variable space of p and the elements $p_1, p_2, \ldots, p_n$ are the decided test values. The region in the right ellipse represents the whole variable space of l and the elements $l_1, l_2, \ldots, l_n$ are the measured values. The arrows present the one to one map in the sample space, p_1 to l_1, , p_2 to l_2 ....., p_n to l_n. This map is established through the second step in each of the tests. The arrow p = F(l) is the usual way of expressing this relationship. The arrow l = G(p) is an inverse function of the function p = F(l), which uses the spring length to determine the force.

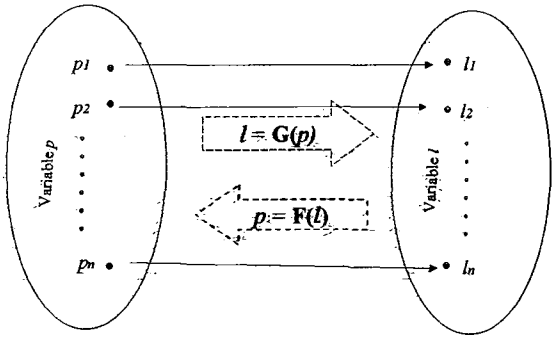

Figure 6-1

Continuing with the spring example, this experiment can be viewed as a statistical analysis. Step 1 is deciding the sample method, step 2 is doing the sample and step 3 is data processing. When the function is not known, the experiment provides a measure to bridge the two variables in the sample space. The result of the analysis based on the sample space can then be extended to the whole variable space.

Comparing experimental analysis with statistical analysis, they are similar in terms of basic procedure and their functions. Statistical analysis is based on the sample data. When statistical analysis is used to find a relationship between two variables, the function of the sample is to obtain a map in a sample space. This is the same as the function of the "test" in an experiment. Before taking a sample, the sample method

needs to be decided. This is also similar to deciding a set of test point in an experiment. The following table compares the tasks between experimental and statistical analysis on a step-by-step basis.

Experiment	Statistics
1. Deciding a set of test points Task: Deciding the value range of the variable p and tested points p_1, p_2, ... p_n	**1. Deciding sample method** Task: 1. Deciding the value range of the variable p; 2. Deciding sample method (random, equal interval or other sample methods); 3. Deciding how many sampling points
2. Carrying out experiment Task: 1 Testing; 2. Recording the results	**2. Sampling** Task: 1 Collecting the sample data; 2. Recording the sample data.
3. Experimental data process Task: Discovering the relationship	**3. Statistical data analysis** Task: Discovering the relationship

Table 2-1 Comparisons between experiment and statistics

Here, Step 1 of an experiment is a special situation of the application of statistics. Test points in an experiment have been decided before the test starts. In Step 2, testing can be viewed as collecting the sample data. In Step 3, experimental data may be processed by various sorts of methods and statistical analysis is only one of the methods available.

Although experiments might provide a measure to discover a relationship, sometimes it is difficulty to carry out an experiment in theoretical research. The problem becomes how to complete the task of step 2 in the above table. When the investigated object is an unknown function F(.) and the inverse function G(.) is computable, the inverse function G(.) can be used to replace the role of the testing in step 2, to bridge the two variables in the sample space. In this situation, it is a non-experimental method but is similar to an experiment. Therefore, it is a necessary condition that there is a known and computable inverse function G(.) in order to use statistical analysis to find the relationship of a function F(.). A very simple example is shown as follows:

The problem is calculation of the function y = F(x), in the area 0<=x<=1.

Now, the function is $F(x)=\sqrt{x}$ and the inverse function x = G(y) is known as $G(y) = y^2$. In practice it is difficult to compute $\sqrt{x}$ but much less difficult to compute y^2. Thus, in this situation, the inverse function G(.) can be used to bridge the two variables in the sample space, say y = 0.00, 0.10, ..., 1.00.

Thus, Table 2-2 is:-

y	→	x
0.00	→	0.00
0.10	→	0.01
0.20	→	0.04
0.30	→	0.09
0.40	→	0.16
...	...	...
1.00	→	1.0.

Table 2-2 The map from y to x

Further data analysis can be carried out based on this table.

In this example, if the inverse function were unknown or too difficult to compute, it would be difficult to establish the map. Consequently, the data analysis could not be carried out.

Regarding the problem of the Stewart platform forward displacement, it is equivalent to solving the equations (1). The inverse problem can be easily solved by resolving the inverse equations (1), so it meets the necessary condition to use statistical analysis methods. That is, if the lengths of the six links are known it is difficult to determine the relative corresponding positions and orientations of the platforms. However, if the positions and orientations of the platforms are known the computation of the lengths of the links is merely a matter of geometry.

It should be noted that the data generated by experiments or numerical calculation in Step 2 would normally involve errors. Consequently, the analysis result based on the experimental data also has an error range. Therefore, the impact of the testing error or sampling error should be considered. Sometimes an approximate closed form result, that meets certain accuracy, in a certain range of the variables, can be obtained. Also, sometimes, the analysis result is not a closed form result but it can provide enough

information to establish a numerical solution of function F(.) In this research, a statistical analysis method is used to provide information to build up a numerical solution for the Stewart platform forward displacement problem.

It is obvious that multiple-variable analysis is more complex than single-variable analysis. The complexity mainly appears in Step 3, the data analysis. There are many methods available for different data analysis applications. The Stewart platform forward displacement problem has six known variables (l_1, l_2, ... l_6), and six unknown positional variables (α_1, α_2, α_3, α_4, α_5, lm). To solve this complex problem, the Principal Component Analysis (PCA) method has been introduced.

6.2 Principal Component Analysis (PCA) Method

The PCA, as a multivariate statistical method, is widely applied in many different fields, such as business, science and engineering research. It is often applied to measure a characteristic of an object by using a group of measurement variables. In this situation, the characteristic of the object can be viewed as a function of the measurement variables. Sometimes a group of measurement variables can also be used to measure several different characteristics of an object. Therefore, in this situation, several functions of the group of variables need to be found. Under the model in Figure 5-2, the values of the variables α_1, α_2, α_3, α_4, α_5 and lm can be determined by the lengths of the six links. This means that α_1, α_2, α_3, α_4, α_5 and lm are functions of the group of the measurement variables l_1, l_2, ... l_6. However, these functions are difficult to express in general closed-form. Even if there were general closed-form expressions of the functions, they would be too complex to be used[†]. Using the PCA, the measurement variables l_1, l_2, ... l_6 can be transformed to another six variables, called principal components, which are the linear combinations of the measurement variables l_1, l_2, ... l_6. These six principal components are used to approximately express the positional variables α_1, α_2, α_3, α_4, α_5, lm respectively. The basic principle of the PCA is introduced as follows:

[†] The author used Maple to find a general closed-form solution for a 3D parallel structure. However, every expression for a single positional variable is longer than 1000 lines. This result is not valuable for a real-time system.

6.2.1 Mathematical Definition of the PCA

Considering an *n*-dimensional set of data, the data are modelled as usual by a swarm of *m* points in *n*-dimensions, each axis corresponding to a measurement variable. A line OY_1, in this space such can be found, such that the spread of the *m* points when projected on this line is a maximum. This operation defines a derived variable of the form $Y_1 = a_1X_1 + a_2X_2 + \ldots a_nX_n$, with coefficients a_i satisfying $\sum_{i=1}^{n} a_i^2 = 1$, and determined by the requirement that the variance of Y_1 be maximised. Having obtained OY_1, consider the (*n*-1) dimensional subspace orthogonal to OY_1, and look for the line OY_2 in this subspace such that the spread of points when projected on to this line is a maximum. Having obtained OY_2, then consider the (*n*-2) dimensional subspace orthogonal to both OY_1 and OY_2. Thus, look for a line OY_3 which is at right angles to both OY_1 and OY_2, such that the spread of points when they are projected on to OY_3 is as large as possible after the spreads on OY_1 and OY_2 have been taken into account. This process can be continued until *n* mutually orthogonal lines OY_i (i= 1, ..., *n*) have been obtained. Each of these lines defines a derived variable $Y_i = a_{i1}X_1 + a_{i2}X_2 + \ldots a_{ip}X_n$ (i= 1, ..., *n*). The Y_i thus obtained are called the (sample) ***principal components*** of the system, and the process of obtaining them is called ***principal component analysis***.

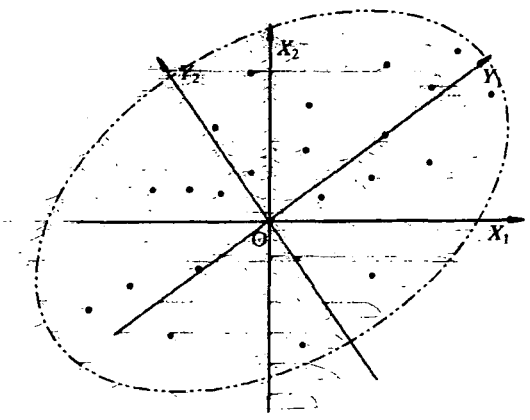

Figure 6-2

Through the above definition of principal components, it is shown that the principal components Y_i (i = 1,2, ... *n*) are variables, which are derived from the original

variables X_i (i = 1,2, ... n). Geometrically, the distribution of the sample points in the n-dimension variable space can be viewed as a hyper-ellipsoid area, and the lines OY_i, (i = 1,2, ... n) are the axes of the ellipsoid. The direction of the first principal component (Y_1) is in the longest axis and the direction of the second principal component (Y_2) is in the second longest axis. In general, the direction of the kth principal component (Y_k) is in the kth longest axis. By way of example, Figure 6-2 is a 2-dimensional case. The measurement variables are X_1 and X_2. The direction of the first principal component (Y_1) is the longer axis and the direction of the second principal component (Y_2) is the shorter axis.

6.2.2 Procedure for Obtaining the Principal Components of a System

After giving the definition of principal components, the consequent problem is how to obtain principal components of a system. Many textbooks [W.J. Krzanowski 1988] have described and proved this method. Here is a brief summary of the processing steps of the PCA.

Step 1: Data sampling: According to a particular application requirement, a set of sample data, say $p_i = (x_{i1}, x_{i2}, \ldots, x_{in})$, when i =1,2, ...,m (m>n), is collected.

The sample data can be expressed in the form of a matrix

$$P = \begin{bmatrix} p_1 \\ p_2 \\ \vdots \\ p_n \end{bmatrix} = \begin{bmatrix} x_{11} & x_{12} & \cdots & x_{1n} \\ x_{21} & x_{22} & \cdots & x_{2n} \\ \cdots & \cdots & \cdots & \cdots \\ x_{m1} & \cdots & \cdots & x_{mn} \end{bmatrix}$$

Every row in the data matrix P corresponds to a sample and every column corresponds to a data set of one variable in different samples.

Step 2: The scatter matrix: The scatter matrix S is set by the sample data matrix as below:

$$S = P'P = \begin{bmatrix} x_{11} & x_{21} & \cdots & x_{m1} \\ x_{12} & x_{22} & \cdots & x_{m2} \\ \cdots & \cdots & \cdots & \cdots \\ x_{1n} & \cdots & \cdots & x_{mn} \end{bmatrix} \begin{bmatrix} x_{11} & x_{12} & \cdots & x_{1n} \\ x_{21} & x_{22} & \cdots & x_{2n} \\ \cdots & \cdots & \cdots & \cdots \\ x_{m1} & \cdots & \cdots & x_{mn} \end{bmatrix} \quad (2\text{-}1)$$

Where P' is the diagonal rotation of the matrix P.

Step 3: Obtaining the principal components of the system

In fact, this step is a procedure of computing the eigenvalues and the eigenvectors of the scatter matrix S. The eigenvalues are denoted as $\lambda_1 \geq \lambda_2 \geq \ldots \geq \lambda_n$, and the correspondent eigenvectors are denoted as $\mathbf{a}_1$, $\mathbf{a}_2, \ldots \mathbf{a}_n$, and

$\mathbf{a}_k = (a_{k1}, a_{k2}, \ldots a_{kn})'$ $k = 1,2, \ldots, n$

Then, the *k*th principal component (Y_k) of the system is:-

$$Y_k = a_{k1} X_1 + a_{k2} X_2 + \ldots + a_{kn} X_n \quad k = 1,2, \ldots, n \qquad \textbf{(2.2-2)}$$

It should be noted that the principal component corresponding to the greatest eigenvalue is the first principal component. Its direction is in the longest elliptic axis of the data distribution. In general, the principal component corresponding to the *k*th greatest eigenvalue is the *k*th principal component. For more details, [W.J. Krzanowski 1988] can be referenced.

If the principal component vector is denoted as $Y = \begin{bmatrix} Y_1 \\ Y_2 \\ \vdots \\ Y_n \end{bmatrix}$;

the eigenvector matrix is denoted as $A = \begin{bmatrix} \mathbf{a}_1 \\ \mathbf{a}_2 \\ \vdots \\ \mathbf{a}_n \end{bmatrix} = \begin{bmatrix} a_{11} & a_{12} & \ldots & a_{1n} \\ a_{21} & a_{22} & \ldots & a_{2n} \\ \ldots & \ldots & \ldots & \ldots \\ a_{n1} & a_{n2} & \ldots & a_{nn} \end{bmatrix}$ and

the measurement variable vector is denoted $\mathbf{X} = \begin{bmatrix} X_1 \\ X_2 \\ \vdots \\ X_n \end{bmatrix}$;

Then the formula (2.2-2) can be expressed in matrix form as follow:

$$\mathbf{Y} = \mathbf{AX} \qquad \textbf{(2.2-3)}$$

Where Y_1, Y_2, ... Y_n are principal components and X_1, X_2, ... X_n are measurement variables.

6.2.3 Understanding the PCA applied to geometry

Understanding the PCA applied geometry is very helpful to apply the PCA to the analysis for mechanical relationships. Since the eigenvectors are orthogonal unit vectors and the matrix A is an orthogonal matrix, the transformation from **X** to **Y** is an orthogonal transformation. The distance between any two points in the **X** space is the same as the distance between the two points in the **Y** space, which are transformed from the same two points in the **X** space. Therefore, this transformation can be viewed as a coordinate frame transformation from the original frame to the principal component frame. This new coordinate frame i.e. principal component coordinate frame, provides a different view of the sample point distribution from the original frame. Sometimes, a distribution of points transformed to a different frame will produce a more easily identified envelope shape and orientation. These different envelope surfaces may indicate different characteristics of a system. Therefore, in the new frame, characteristics of a system can be interpreted as a function of the new coordinate variables. For example, consider a 3-dimension system as in Figure 6-3(a), in which there are 3 links from the three fixed points (b_1, b_2, b_3) to the movable point P. When the point P is moved, the three link-lengths (l_1,l_2,l_3) will change. Different positions of the point P in the natural 3D space correspond to different link-lengths (l_1,l_2,l_3). Consequently, different positions of the point P in the natural 3D space (Figure 6-3(a)) correspond to different positions in the 3D frame l_1-l_2-l_3 (Figure 6-3(b)). When the point P moves along a circle in a horizontal plane shown in Figure 6-3(a), the circle corresponds to another circle in the 3D frame l_1-l_2-l_3. The different circles in the natural 3D space (Figure 6-3(a)) correspond to different circles in the 3D frame l_1-l_2-l_3 (Figure 6-3(b)). Moreover, when the circles form a tube, there is also a shape similar to a tube in the frame l_1-l_2-l_3 (see Figure 6-3 (b)). If sample data comes from the situation shown in Figure 6-3 and the length of this tube in Figure 6-3(a) is significantly greater than the diameter of the circle, the first principal component (Y_1) will be in the direction of the centre line of the tube in Figure 6-3(b). Consequently, the plane (Y_2-Y_3) formed by the second (Y_2) and the third (Y_3) principal components is perpendicular to Y_1. Obviously, any single variable l_1, l_2 or l_3 cannot express the length of the tube in Figure 6-3(b). However, the first principal component Y_1 can directly express the length of the tube. Because

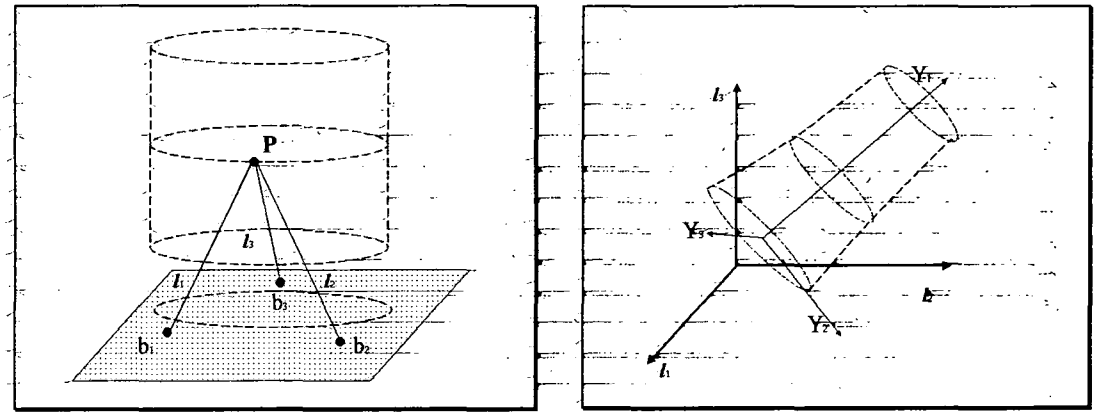

Figure 6-3 PCA can be used to analyse mechanical relationship

the length of the tube shown in Figure 6-3(b) relates to the length of the tube shown in Figure 6-3(a), as long as the relationship between the lengths of these two tubes is identified, the first principal component Y_1 can be used to express the length of the tube. For the same reason, any one or two of the variables (l_1, l_2. l_3) cannot express a position in the top circle of the tube in Figure 6-3(b), but the combination of Y_2 and Y_3 can directly express any position in the top circle of the tube. Because the top circle of the tube shown in Figure 6-3(a) relates to the top circle shown in Figure 6-3(b), as long as the relationship between the position in the top circle in Figure 6-3(a) and the corresponding position in the top circle in Figure 6-3(b) is identified, the combination of Y_2 and Y_3 can be used to express any position in the top circle in Figure 6-3(a). In summary, the length of the tube in Figure 6-3(b) can be expressed by Y_1 more easily than by the three variables (l_1, l_2. l_3). For the same reason, the point in the top circle of the tube in Figure 6-3(b) can be expressed by the combination of Y_2 and Y_3 more easily than by the three variables (l_1, l_2. l_3). To identify the relationship between Y_1 and the length of the tube in Figure 6-3(b) and to identify the relationship between the combination of Y_2 and Y_3 and the point in the top circle of the tube in Figure 6-3(b), the principal component frame provides better views than using the frame l_1-l_2-l_3. This is because a circle in Figure 6-3(a) corresponds to a circle in the plane Y_2-Y_3, but corresponds to an ellipse in the plane l_1 - l_2, plane l_2 -l_3 or plane l_3 - l_1.

This is somewhat similar to the use of views in mechanical design drawing. Sometime, three views are used to illustrate the geometrical characteristics of an object.

Through the example shown in Figure 6-3, it is also clear that the data sample is very important for a successful application of the PCA. If the range of the movement in the vertical direction is very small, i.e. the length of the tube in Figure 6-3(a) is very short, the length of the corresponding tube in Figure 6-3(b) will be very short. According to the definition in Section 6.2.1, the first principal component Y_1 would not be in the direction of the centre line of the tube shown in Figure 6-3(b). In this situation, the above discussions are not true.

6.3 PCA Based Relationship Analysis

As discussed earlier, the use of the PCA method to analyse relationships is a statistical approach. Since this particular multivariate statistical application is a complex application, the particular procedure of this method and the analysis skills are discussed as follows.

6.3.1 Procedure of Using PCA to Analyse a Relationship

The discussions in this section are not restricted in the PCA application to relationship analysis for parallel mechanisms. The procedure of using PCA to analyse a relationship, discussed here, is a general procedure. This procedure can be applied to any mechanical relationship analysis using the PCA approach.

It is supposed that an n-dimensional vector function $\mathbf{y} = F(\mathbf{x})$ is unknown. The n-dimensional independent variable $\mathbf{x} = (x_1, x_2, \ldots, x_n)$ is measurable. The inverse function $\mathbf{x} = F^{-1}(\mathbf{y})$ is known and computable. Relating this general function to the Stewart platform problem, the independent variable $\mathbf{x}$ is link lengths $(l_1, l_2, l_3, l_4, l_5, l_6)$ and the positional variable $\mathbf{y}$ is platform position i.e. the variables $(\alpha_1, \alpha_2, \alpha_3, \alpha_4, \alpha_5, lm)$ which have been defined in Section 2.1.3.2. The general function $F(.)$ corresponds to the forward displacement problem and the inverse function $F^{-1}(.)$ corresponds to the inverse displacement problem. The Stewart platform forward displacement problem is the one needs to be solved. The inverse displacement is easy to compute. Therefore, the Stewart platform problem meets the

initial supposition, $\mathbf{y} = F(\mathbf{x})$ is unknown, and the inverse function $\mathbf{x} = F^{-1}(\mathbf{y})$ is known and computable. Under this supposition, the problem is how to use the PCA to determine the value of the positional variable $\mathbf{y} = (y_1, y_2, \ldots, y_n)$ when the value of the independent variable $\mathbf{x}$ is given. An application of the PCA is to use the principal components Y_i (i =1,2, ...,n) instead of the measurement variables to solve the problem. Here the measurement variables are the independent variables x_i (i =1,2, ...,n) and the principal components Y_i are derived from the independent x_i. Therefore the problem becomes how to determine the value of the positional variable $\mathbf{y} = (y_1, y_2, \ldots, y_n)$ when the value of the principal component vector $\mathbf{Y} = (Y_1, Y_2, \ldots, Y_n)$ is given and how to obtain the principal components $\mathbf{Y} = (Y_1, Y_2, \ldots, Y_n)$. The following are the steps to solve this problem.

Step 1. Data sampling: As in other statistical applications, the first step of using the PCA to analyse relationships is data sampling. Since the investigated relationship is between the positional variables $\{y_1, y_2, \ldots, y_n\}$ of the function F(.) (corresponding to the Stewart platform forward displacement problem in Figure 5-2, the positional variables are $\{\alpha_1, \alpha_2, \alpha_3, \alpha_4, \alpha_5, lm\}$) and the principal components $\{Y_1, Y_2, \ldots, Y_n\}$, the data sampling starts with a given data set of the positional variables $\{y_1, y_2, \ldots, y_n\}$. This data set is denoted as $\{\mathbf{Q}_i\} = \{y_1, y_2, \ldots, y_n\}_i | i=1,2,\ldots,m\} = \{(y_{i1}, y_{i2}, \ldots, y_{in}) | i =1,2, \ldots,m\}$. Here, m is the size of samples. This number m should at least equal or be greater than two times of the number of dimension ($2\times n$). This is because every positional variable should at least have two different given values. Normally it should have three or more different given values to show the relationships with the independent variables. Generally speaking, the greater the sample number, the easier it is to illustrate the relationships. However, if the sample size is too big, the data processing will require more time and computer memory. Therefore, the sample size and every point in the data set $\{\mathbf{Q}_i\}$ should be determined based upon the need of a particular application. For example, in the case of the spring test used earlier, the force values $\{p_i\}$ are used to determine the test points. These test points should be chosen based on the range of applied force in a particular application and the requirement of the accuracy before the test is carried out. Since the inverse function $\mathbf{x}$

$= F^{-1}(\mathbf{y})$ is known and computable, then, the given data set $\{\mathbf{Q}_i\}$ is used to carry out the calculation to obtain the corresponding sample data set of the variables $\{x_1, x_2, \ldots, x_n\}$. This calculated sample data set is denoted as $\{\mathbf{P}_i\} = \{x_1, x_2, \ldots, x_n\}_i | i=1,2,\ldots,m\} = \{(x_{i1}, x_{i2}, \ldots, x_{in}) | i = 1,2, \ldots, m\}$ corresponding to data set $\{\mathbf{Q}_i\}$. Relating the general approach to what is done on the Stewart platform, the platform is set to a series of different positions, i.e. different values of $(\alpha_1, \alpha_2, \alpha_3, \alpha_4, \alpha_5, lm)$ then using formula (2) to compute the corresponding values of link lengths $(l_1, l_2, l_3, l_4, l_5, l_6)$. To complete this step, a data sample table as follows is used.

Sample No. (i)	Given Data $\{\mathbf{Q}_i\}$				Calculated Data $\{\mathbf{P}_i\}$				Principal Components $\{\mathbf{Y}_i\}$			
	y_{i1}	y_{i2}	.....	y_{in}	x_{i1}	x_{i2}	.....	X_{in}	Y_{i1}	Y_{i2}	.....	Y_{in}
1	y_{11}	y_{12}	.....	y_{1n}	x_{11}	x_{12}	.....	X_{1n}				
2	y_{21}	y_{22}	.....	y_{2n}	x_{21}	x_{22}	.....	X_{2n}				
.....	.....	.....	.....	.....	.....	.....	.....	.....				
m	y_{m1}	y_{m2}	.....	y_{mn}	x_{m1}	x_{m2}	.....	X_{mn}				

Table 2.2-3 An example of data sampling table

This table consists of three parts; given data $\{\mathbf{Q}_i : \{y_1, y_2, \ldots, y_n\}_i | i=1,2,\ldots,m\}$, calculated data $\{\mathbf{P}_i : \{x_1, x_2, \ldots, x_n\}_i | i=1,2,\ldots,m\}$, and the principal components $\{\mathbf{Y}_i : \{Y_1, Y_2, \ldots, Y_n\}_i | i=1,2,\ldots,m\}$. The data set $\{\mathbf{Q}_i\}$ is given before carrying out the sample. The calculated data set $\{\mathbf{P}_i\}$ is obtained during the sampling, and the corresponding principal component values will be calculated after obtaining the formula of the principal components of the system.

Step 2. Obtaining the formula of the principal components of the system

This is a standard procedure of the PCA, which has been described in Section 6.2.2. The task of this step is to obtain the constants for every principal component.

$$Y_k = a_{k1} x_1 + a_{k2} x_2 + \ldots + a_{kn} x_n, (k = 1,2, \ldots, n)$$

Step 3. Calculating the principal component values for every point in $\{\mathbf{Q}_i\}$ and filling the above table. The value of the ith sample's kth principal component (Y_{ik}) is

$$Y_{ik} = a_{k1} x_{i1} + a_{k2} x_{i2} + \ldots + a_{kn} x_{in} \quad \text{for } k=1,2, \ldots, n. \; i = 1,2, \ldots, m$$

Step 4. Analysing the relationships between $\{\mathbf{Y}_i\}$ and $\{\mathbf{Q}_i\}$in the sample space. The result of this step can be directly extended to the whole component variable space and positional variable space. The tools and skills of this step are discussed in the following section.

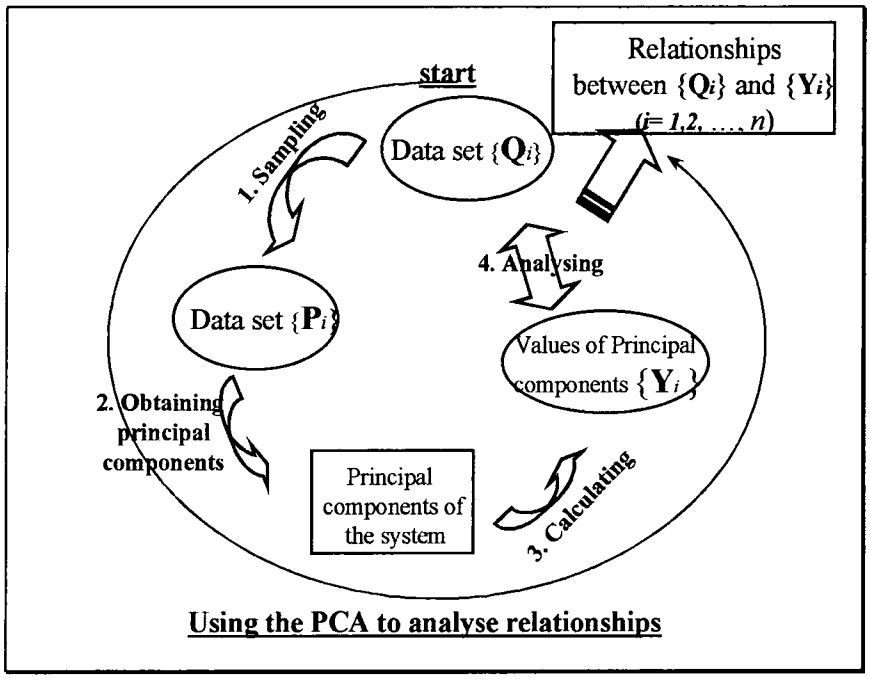

Figure 6-4 Procedure of using PCA to analyse relationship

The whole procedure of using the PCA to analyse relationships can be illustrated by Figure 6-4.

6.3.2 Analysis of the Relationship between Principal Components and Positional Variables

The discussions in this section address mechanical relationship analyses rather than analysis for a general relationship as an abstract function F(.) shown in Section 6.3.1. Corresponding to the general discussion in the previous section, data set $\{\mathbf{Q}_i\}$ is the sample data set of the positional variables; the data set $\{\mathbf{P}_i\}$ is the sample data set of the measurement variables; and the data set $\{\mathbf{Y}_i\}$ is the data set of the principal components corresponding to the sample data.

The purpose of the analysis of the relationship between the principal component data set $\{\mathbf{Y}_i\}$ and the data set $\{\mathbf{Q}_i\}$ of the positional variables is to provide sufficient information to build up an algorithm. This algorithm can be used to compute the

values of the positional variables using principal component values. Through a relationship analysis, the following results should be obtained:

(1) Every positional variable can be determined by a function in which the independent variables are principal components only. At least, this is true when other positional variables are given.

(2) If a positional variable can be determined by a function in which the independent variables are principal components only, when other positional variables vary in a certain range, the change of the characteristics of this function with the change of the values of the other positional variables can also be identified.

To obtain the above two results, the relationship analysis starts by use of one-to-one relationship analysis. That is to try to find the relationship between every one positional variable and every principal component. If every positional variable can be determined by one principal component, the result (1) has been obtained. However, normally, some positional variables are difficult to determine by a single principal component. After a part of positional variables is identified by some one-to-one relationships, the remained part of positional variables cannot be determined by single principal component. In this situation, pair-to-pair relationship analysis is required. That is, for the remained positional variables, to try to find the relationship between every pair of positional variables and every pair of principal components. Sometime, a pair-to-pair relationship can be transformed to two one-to-pair relationships. That is, one positional variable can be expressed by a pair of principal components, which will be discussed later in this section. For most situations, the relationship analysis can be based on these two sorts of analyses, one-to-one and pair-to-pair relationship analyses. Following this, to know the effect on every obtained relationship of other positional variables, further analyses are also required.

The tools used for the relationship analysis are 2-dimensional graphs. For one-to-one relationship analysis, one coordinate axis is one of the positional variables and the other axis is one of the principal components. Further details are given later. For pair-to-pair relationship analysis, the two coordinate axes are two of the principal components and, once again, detail discussion is in a later section. The data in the 2-dimensional graph is taken from the sample data table, Table 2.2-3.

During the development of the PCA based approach, some typical situations have

been considered. Studying these typical cases should be helpful for relationship analyses for other mechanisms. The following is a brief discussion.

6.3.2.1 One-to-one Relationship Analysis

After filling up Table 2.2-3, the data analysis normally should start by looking for one-to-one relationships between the positional variables y_i and the principal components Y_i ($i = 1, 2, \ldots, n$). During this period, 2-dimensional coordinate graphs, which consist of one positional variable axis and one principal component axis, are used. In such a graph, the data of the positional variable is from one column of the data $\{\mathbf{Q}_i\}$ in Table 2.2-3 and the data of the corresponding principal component is from one column of the principal component $\{\mathbf{Y}_i\}$ in the same table. If all the sample data from Table 2.2-3 forms one increase or decrease curve or line (see Figure 6-5), it means that this principal component can directly express this positional variable and this relationship is not affected by other positional variables. That is, for any given value of the principal component, there is only a single value of the corresponding positional variable, no matter what the values of the other positional variables. Figure 6-5 (a) and (b) are examples in which the positional variable is y_1 and the principal component is Y_1.

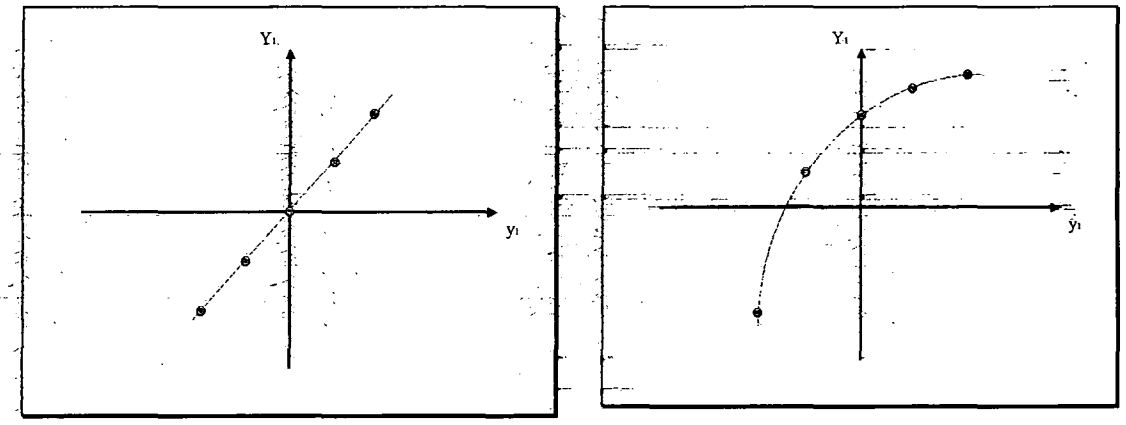

(a) (b)

Figure 6-5 Unambiguous one-to-one relationships

Here, it should be explained that each given value of a positional variable corresponds to several rows in Table 2.2-3. That is, each given value of a positional variable

corresponds to several different values of other positional variables. Sometimes, the given positional variable with the different values of other positional variables correspond only one value of the related principal component. In this situation, the relationship graph is a single curve or line as shown in Figure 6-5. This means that other positional variables do not affect this relationship. However, in most situations, any given value of a positional variable with different values of other positional variables correspond to different values of the principal components and show different points in the 2-dimensional graph, as shown in Figure 6-6. In this situation, the relationship graph will be several curves. Every one of the curves corresponds to given values of other positional variables. The difference from curve to curve is the effect on the relationship by other positional variables.

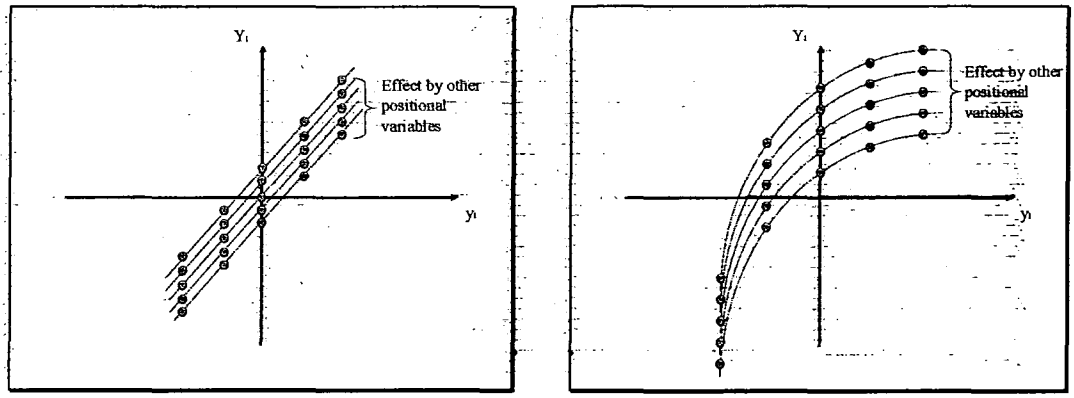

(a) (b)

Figure 6-6 one-to-one relationships with effect by other positional variables

To find what positional variable affects the invested relationship, the same coordinate system is used but the data shown in the graph needs to be filtered. For example, if the relationship between the positional variable y_1 and the principal component Y_1 is being investigated and the graph of the relationship is as shown in Figure 6-6, the task is to find what positional variables affect this relationship. In the first step, every positional variable from y_2 to y_n is fixed so that the sample points in the graph form a single curve or line similar to Figure 6-5. Then, these fixed variables from y_2 to y_n are in turn given different sample values to show what differences are caused. When one of these positional variables, say y_2, is given different values and every value of the positional variable y_1 corresponds to one value of the principal component Y_1, it

means that this positional variable y_2 does not affect this relationship. When one of these positional variables, say y_2, is given different values and every value of the positional variable y_1 corresponds to different values of the principal component Y_1, it means that this positional variable y_2 affects this relationship. After analysing the effect of the positional variable y_2, then the effect of another one of the positional variables, say y_3, should be analysed. This processing does not stop until it is known whether every one of the positional variables from y_2 to y_n affects this relationship or not.

It should be noted that, since the data shown in the graph is from the sample data in Table 2.2-3, rather than from the whole data range, the curves or lines shown in Figure 6-5 or 6-6 are formed by several sample data instead of actual curves or lines. Some knowledge of the particular application background can be used to judge whether the curve or line is increasing or decreasing among the sample data. In most mechanical application situations, if the sample data shows an increase along a curve in a graph as shown in Figure 6-5, the actual curve corresponding to the sample data should be an increasing curve. Sometimes if the points shown in the graph are not sufficient to determine the increase or decrease of the curve as shown in Figure 6-7, some new sample points should be inserted into Table 2.2-3 and appear in the corresponding 2-dimensional relationship graph.

The procedure of exploring one-to-one relationships does not stop until every positional variable has been compared with every principal component. This process of comparison needs to be carried out *n(the number of positional variables)* × *n(the number of principal components)* times.

However, sometimes 2-dimensional graphs used to show one-to-one relationships are more complex than the simple increase or decrease curves or lines discussed here. In this situation, one given principal component value may correspond to several values of the different positional variable. Therefore, this principal component cannot determine the positional variable. Moreover, the curve of the investigated one-to-one relationship, sometimes, is significantly affected by another positional variable as shown in Figure 6-7. This situation was met in the Stewart platform analysis. For example, as the positional variable α_2 of the Stewart platform shown in Figure 5-2

changes from 0 to 2π, the values of the measurement variables $(l_1, l_2, l_3, l_4, l_5, l_6)$ are changed from their initial values to other values and then change back to the initial values. Therefore, the corresponding points in the measurement variable space $(l_1, l_2, l_3, l_4, l_5, l_6)$, and consequently, in the principal component space $(Y_1, Y_2, Y_3, Y_4, Y_5, Y_6)$, form a closed curve. Moreover, the diameter of the closed curve significantly depends on the value of α_1. If α_1 equals zero, this closed curve becomes one point. If α_1 becomes bigger, the diameter of the closed curve will become bigger. Hence, any graph which consists of one of the principle component axes and the axis of the positional variable α_2 will show a curve including increase and decrease segments in the value range of α_2 between 0 and 2π as shown in Figure 6-7. In this situation, pair-to-pair relationship analysis is needed.

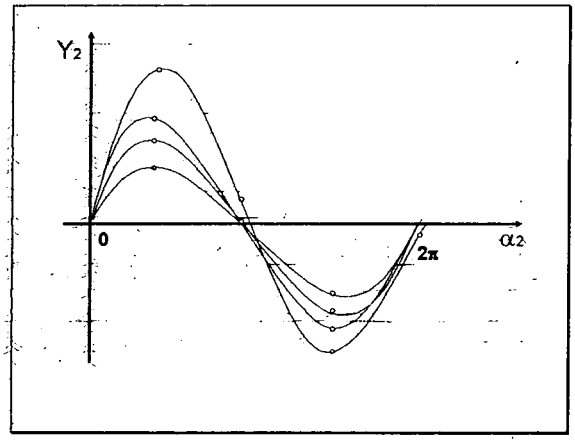

Figure 6-7

6.3.2.2 Pair-to-Pair Relationship Analysis

During pair-to-pair relationship analysis, the two coordinate axes in the graphs are two of the principal components (say Y_1 and Y_2), and the data is from two columns of the principal components $\{\mathbf{Y}_i\}$ in Table 2.2-3 (say $Y_{11} \sim Y_{m1}$ and $Y_{12} \sim Y_{m2}$). To find which two positional variables correspond to these two principal components, every two of the positional variables are in turn chosen for investigation. To show the relationships more clearly, all of the positional variables, with the exception of the two investigated positional variables, should be fixed during the pair-to-pair relationship analysis. Normally, this graph shows two families of curves, which

mainly correspond to two of the positional variables. Through the analysis of the type and array of the curves, it can be found whether this pair of principal components can express the chosen pair of positional variables and their relationships. After obtaining the pair-to-pair relationships, the effects of the other positional variables should also be investigated. The following are some typical types of curve families in 2-dimemensional principal component space.

Type 1. The two families of curves are two families of parallel lines and these two families of lines are perpendicular to each other. One family of lines is arrayed by the increment of one of the positional variables and the other family of lines is arrayed by the increment of the other positional variable.

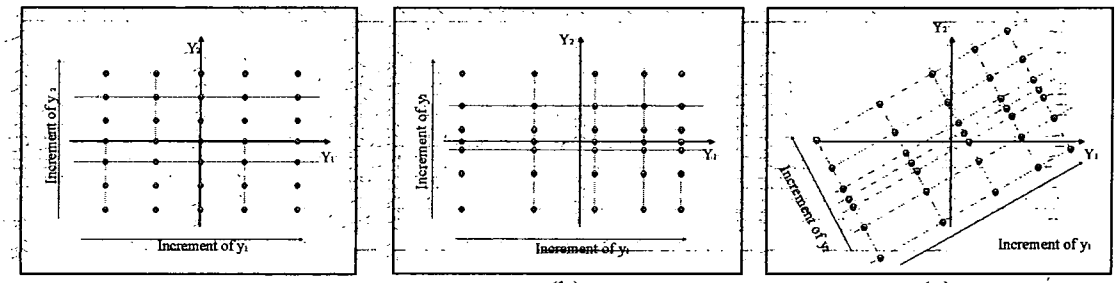

(a) (b) (c)

Figure 6-8 Type 1

Figure 6-8 shows examples, in which, the two axes are Y_1 and Y_2 and the lines are arrayed by the increment of the positional variables y_1 and y_2 respectively.

In fact, this kind of relationship can also be found through one-to-one analysis. In Figure 6-8 (a), the relationship between y_1 and Y_1 or between y_2 and Y_2 is a linear relationship as shown in Figure 6-6(a). In Figure 6-8(b), the relationship between y_1 and Y_1 or between y_2 and Y_2 is a non-linear relationship as shown in Figure 6-6(b). In the situation as shown in Figure 6-8(a) or (b), the relationship between y_1 and Y_1 is not affected by y_2, and the relationship between y_2 and Y_2 is not affected by y_1. In Figure 6-8(c), the relationship between y_1 and Y_1 or between y_2 and Y_2 is a non-linear relationship as shown in Figure 6-8(b). The relationship between y_1 and Y_1 is affected by y_2, and the relationship between y_2 and Y_2 is affected by y_1. It should be noted that in the situation, as shown in Figure 6-8(c), the principal components' directions can be changed via a coordinate rotation to the same direction as the

increment of positional variable y_1 or y_2. After the coordinate rotation, the situation, as shown in Figure 6-8(c) will be changed to the situation as shown in Figure 6-8(a) or (b).

Type 2: The two curve families are two families of general open curves. The curves in each family do not cross each other. The sample points in principal component space are arrayed in two families of curves rather than lines seen in Type 1. One family of curves is arrayed by the increment of one of the positional variables. The other family of curves is arrayed by the increment of the other positional variable. Figure 6-9 is an example, in which the two axes are Y_1 and Y_2 and the curves are arrayed by the increment of the positional variables y_1 and y_2 respectively.

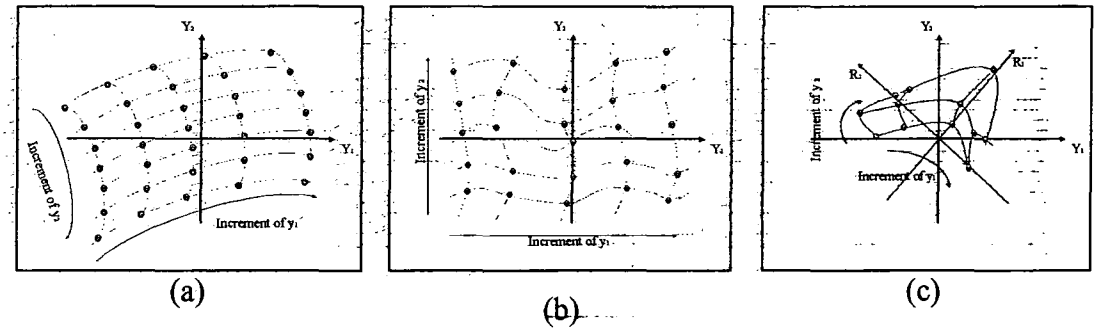

Figure 6-9 Type 2

There are two situations in Figure 6-9. In the situation shown in Figure 6-9(a) and (b), the positional variable y_1 mainly relates to the principal component Y_1 and the positional variable y_2 mainly relates to the principal component Y_2. Therefore, the principal component Y_1 can be used to express the positional variable y_1 and the principal component Y_2 can be used to express the positional variable y_2. In fact, this kind of relationship can also be found through one-to-one analysis but the figures used in pair-to-pair analysis show the relationships more clearly. The situation shown in Figure 6-9(c) is when Y_1 or Y_2 is given a value, and there may be more than one corresponding point in a curve. Therefore, Y_1 and Y_2 cannot express y_1 or y_2 respectively. However, after giving a rotation of the coordinate frame Y_1-Y_2, the situation can be changed to be the same as Figure 6-9(a) or (b). Hence, y_2 can be expressed by R_1, and y_1 can be expressed by R_2 in the new frame R_1-R_2. This means that y_1 and y_2 can be expressed by the different linear combinations of Y_1 and

Y_2 respectively.

Type 3: The sample points in principal component space are arrayed in a family of closed concentric curves, which cross with a family of curves from a centre point, radiating outward (see Figure 6-10). Around the closed curves, the clockwise or anti-clockwise direction is the increment of one of the positional variables and the radius of the closed curve increases with the increment of the other positional variable. Figure 6-10 is an example, in which the two axes are Y_1 and Y_2 and the curves are arrayed by the increment of the positional variables y_1 and y_2 respectively.

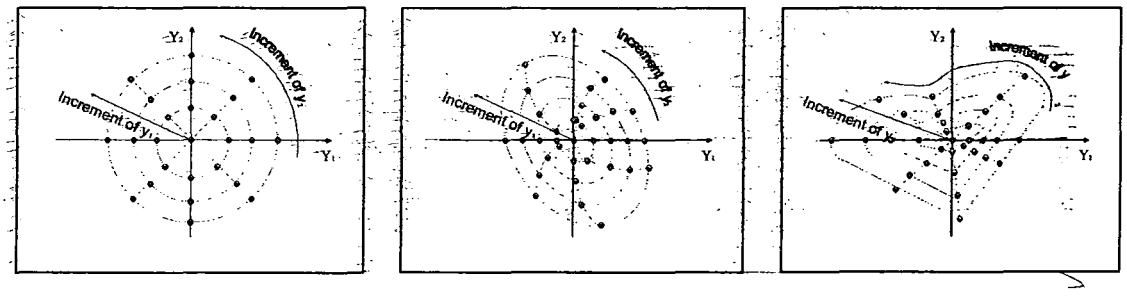

(a) (b) (c)

Figure 6-10 Type 3

This situation can easily be transformed to the distribution of Type 1 or Type 2 but where the coordinate axes are polar angle and radius, instead of orthogonal principal components (see Figure 6-11).

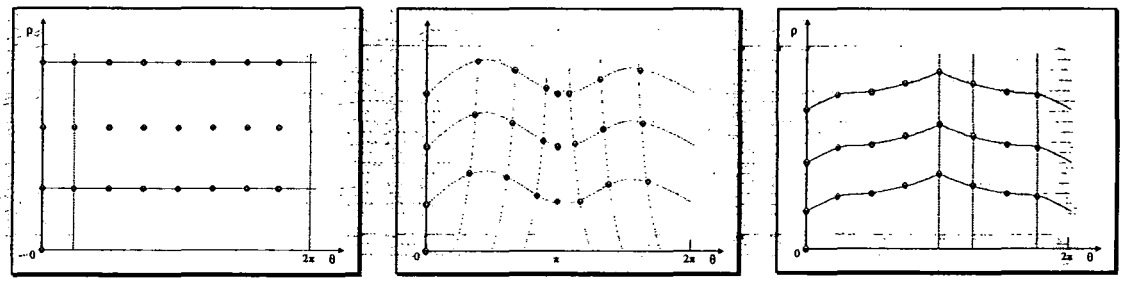

(a) (b) (c)

Figure 6-11 Type 3 can be transformed to Type 1 or Type 2

Therefore, the positional variable y_1 can be expressed by the radius $\rho=\sqrt{Y_1^2+Y_2^2}$ in Figure 6-11 and the positional variable y_2 can be expressed by the polar angle $\theta=\text{atan}(Y_2/Y_1)$. Since the transformation from the principal components Y_1 and Y_2 to the polar angle and the radius (ρ , θ) is a trigonometric transformation, the

positional variables y_1 and y_2 can be expressed by two different functions of the principal components Y_1 and Y_2 respectively. It also means that the positional variables y_1 and y_2 can be expressed by the principal components Y_1 and Y_2.

Type 4: The sample points in principal component space are arrayed in two families of curves, but some curves in one of the two families cross each other (see Figure 6-12).

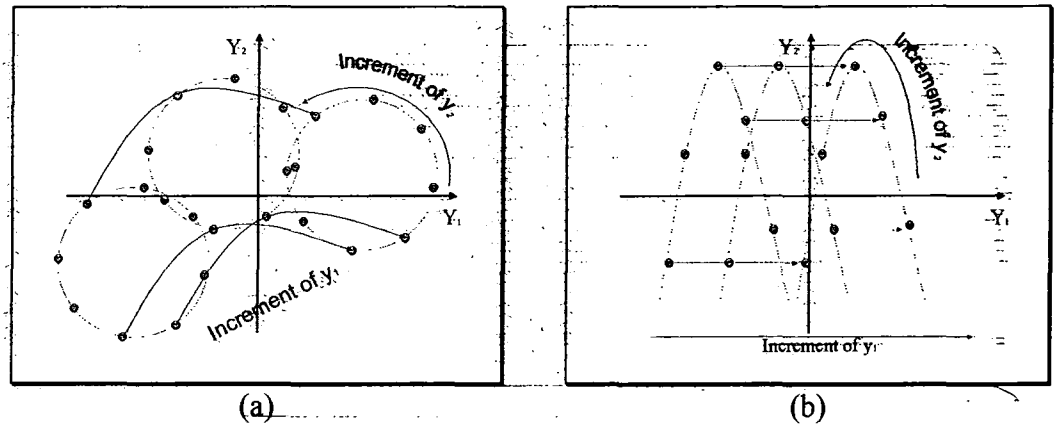

Figure 6-12 the situation is difficult to directly analyse the relationship

The situation shown in Figure 6-12 is more difficult to analyse. Normally, in this situation, the positional variables (y_1, y_2) are inappropriate to be expressed by the principal components (Y_1, Y_2).

Chapter 7

PCA Based Relationship Analysis for a 6-6 Stewart Platform

This section shows how to use the PCA approach to obtain the PCA based measurement solution using a real case.

7.1 The Assembly Configuration of the 6-6 Stewart Platform

This real case is a 6-6 Stewart platform, which has already been shown in Figure 2.1-1. That is a structure, which consists of two disks and six links. Additionally, the dimensions of the disks and the positions of the link joint points on the disks are given in Figure 7-1.

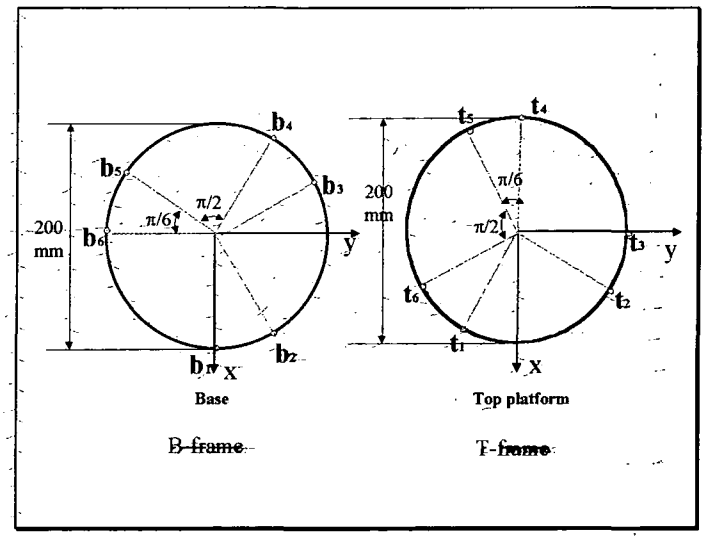

Figure 7-1 the positions of the joint points of the links

The diameters of the two disks are 200 mm. The joint points on the base are fixed relative to the base coordinate frame system the B-frame. The joint points on the top platform are fixed relative to the top platform coordinate system, the T-frame. Hence, the coordinate values of the joints on the base in the B-frame and the coordinate values of the joints on the top platform in the T-frame coordinate systems are constant. These coordinated values are listed as follows:

Joint points b_i of links on the base (in B-frame) are

$b_1 = (100, 0, 0)$;

$b_2 = (100\cos(\pi/6), 100\sin(\pi/6), 0)$;

$b_3 = (100\cos(\pi 4/6), 100\sin(\pi 4/6), 0)$;

$b_4 = (100\cos(\pi 5/6), 100\sin(\pi 5/6), 0)$;

$b_5 = (100\cos(\pi 8/6), 100\sin(\pi 8/6), 0)$;

$b_6 = (100\cos(\pi 9/6), 100\sin(\pi 9/6), 0)$.

Joint points t_i of links on the top platform (in T-frame) are

$t_1 = (100\cos(\pi 11/6), 100\sin(\pi 11/6), 0)$;

$t_2 = (100\cos(\pi 2/6), 100\sin(\pi 2/6), 0)$;

$t_3 = (100\cos(\pi 3/6), 100\sin(\pi 3/6), 0)$;

$t_4 = (100\cos(\pi 6/6), 100\sin(\pi 6/6), 0)$;

$t_5 = (100\cos(\pi 7/6), 100\sin(\pi 7/6), 0)$;

$t_6 = (100\cos(\pi 10/6), 100\sin(\pi 10/6), 0)$.

Initial position

In the above configuration, the relative position of the top platform is to be measured. This initial position is defined such that the corresponding axes and the origin of the T-frame and the B-frame are coincident. At this initial position, all of the positional variables (α_1, α_2, α_3, α_4, α_5, lm) are zero. At this initial position the joint point's (t_i) coordinate values in the B-frame are

$t_1 = (100\cos(\pi 11/6), 100\sin(\pi 11/6), 0)$;

$t_2 = (100\cos(\pi 2/6), 100\sin(\pi 2/6), 0)$;

$t_3 = (100\cos(\pi 3/6), 100\sin(\pi 3/6), 0)$;

$t_4 = (100\cos(\pi 6/6), 100\sin(\pi 6/6), 0)$;

$t_5 = (100\cos(\pi 7/6), 100\sin(\pi 7/6), 0)$;

$t_6 = (100\cos(\pi 10/6), 100\sin(\pi 10/6), 0)$.

They are the same as the coordinate values in the T-frame because the T-frame and the B-frame are coincident.

7.2 The PCA Based Forward Displacement Measurement Solution

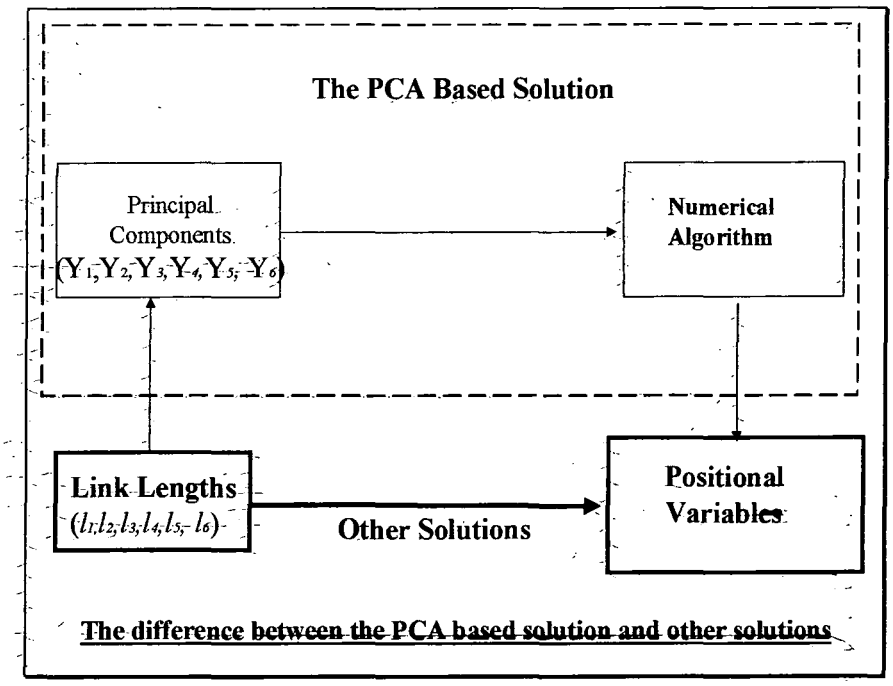

Figure 7-2 The difference between the PCA based solution and other solutions

The PCA based solution makes use of the principal components of the system as a bridge to solve the problem. When the link lengths of the Stewart platform are given, the values of the link lengths are first transformed to the values of the principal components. Then a numerical algorithm completes the calculation of the positional variables using the principal component values. These positional variables are a set of variables representing the position and orientation of the Stewart platform, which have been defined in Chapter 5. The numerical algorithm in the PCA based solution is based on the relationship between the principal components and the positional variables. The above procedure, which progresses from given link lengths to principal component values and then to the positional variables, is called ***the PCA based forward displacement measurement solution.*** In Figure 7-2, the process is indicated by the arrows.

The PCA based solution consists of two parts; calculation of the principal components of the system and the numerical algorithm for computing the positional variables. A Stewart platform with different assembly configurations has different principal components and numerical algorithms. The technical key to the PCA based solution is the transformation from six link-lengths to six principal components. If the transformation is successful, the relationship between the principal components and the positional variables can be identified. Consequently, a numerical algorithm can be established, based on the identified relationship. The methodology to develop the PCA based forward displacement solutions for different assembly configurations is called ***the PCA based forward displacement measurement method***. Every PCA based solution is for a particular case with a particular assembly configuration. The PCA based method can be used to develop different solutions for different assembly configurations.

The PCA based forward displacement measurement solution is an on-line procedure. It has high accuracy and computational efficiency. The PCA based forward displacement measurement method is an off-line procedure. It is a methodology for obtaining PCA based solutions. The following sections show a real case in which the PCA based forward displacement measurement method was applied to obtain a solution for a 6-6 Stewart platform. The assembly configuration of this particular Stewart platform has been described in Section 5.1.

7.3 Principal Component Analysis

The principal component analysis is a standard procedure. However, some particular application background factors need to be considered.

7.3.1 Data Sample

As mentioned in Chapter 6, the first task of sample is to give several particular values of the positional variables. This operation is called determining the sample condition. The sample condition values correspond to the data set $\{\mathbf{Q}_i\}$ in Table 2.2-3. In this case, the following factors were considered before determining the sample conditions:

Factor 1: The data sample should cover as much of the value range of the positional variables. The requirement of this application is that the robot can make turning in any

direction but the degree of the turning is not more than $\pi/4$ during one step of movement. The length of the step is between 150 and 200mm. During the robot moves, there is only very little roll. Therefore, the value range of the positional variables in this application is given as: $\alpha_1 : \in [0, \pi/4)$; $\alpha_2 \in [0, 2\pi)$; $\alpha_3 \in [0, \pi/4)$; $\alpha_4 \in [0, 2\pi)$; $\alpha_5 \in [-\pi/6, \pi/6]$; $lm \in [150, 200]$. There is a constraint that is: $\alpha_1 + \alpha_3 < \pi/2$.

Factor 2: Every positional variable should have at least two different values so that it is probable to show the relationships between the positional variables and the principal components. Normally, every positional variable should have at least 3 different values, so that it is able to show the linearity or non-linearity of the relationships between the positional variable and principal components. Some circular variables*, such as α_2 and α_4, should have at least 4 different values, so that it is able to show the change of the data distribution in the principal component space.

Factor 3: Some variable values such as α_2, α_4 and α_5 can be chosen to show the symmetry of the top platform the positions. The variables α_2, α_4 and α_5 should be chosen by geometry symmetrical points, so that it is able to show the symmetry of the distribution of sample points in a principal component subspace. This symmetry information is also helpful in the stage of relationship analysis.

Based on the above considering, the given values of the positional variables are:

Angle 1 (α_1): 0, $\pi/6$, $\pi/12$, $\pi/6$, $\pi/4$
Angle 2 (α_2): 0, $\pi/4$, $\pi/2$, $\pi\times3/4$, π, $\pi\times5/4$, $\pi\times6/4$ $\pi\times7/4$;
Angle 3 (α_3): 0, $\pi/6$, $\pi/12$, $\pi/6$, $\pi/4$
Angle 4 (α_4): 0, $\pi/4$, $\pi/2$, $\pi\times3/4$, π, $\pi\times5/4$, $\pi\times6/4$ $\pi\times7/4$;
Angle 5 (α_5): $-\pi/12$, $-\pi/24$, 0, $\pi/24$, $\pi/12$,
Length of M-bar (*lm*): 150,200

Therefore, the sample size is determined. That is, the sample covers the number of all possible combinations of the above values of the positional variables, which gave different positions and orientations of the Stewart platform. Corresponding to Table 2.2-3 in Chapter 6, the values of $\{\mathbf{Q}_i\}$ were given. Then, for each given position and orientation of the Stewart platform, the corresponding lengths of the linkages were

* Here, the circular variable means the value of the variable varies in a circle, e.g. between 0 and 2π.

calculated. Corresponding to Table 2.2-3 in Chapter 6, the values of $\{\mathbf{P}_i\}$ were obtained. Then the computation of the principal components of the system was required for calculating the corresponding values of $\{\mathbf{Y}_i\}$.

7.3.2 Computation of the Principal Components of the System

This procedure has been introduced in Chapter 6. According to Eq (2.2-1), the scatter matrix can be obtained and then the eigenvalues and the corresponding eigenvectors of the scatter matrix can be obtained. One eigenvalue with corresponding eigenvector corresponds to one principal component. Every scale value of the eigenvectors corresponds to a factor of the principal component formula (2.2-2). After the computation, the following eigenvalues and eigenvectors were obtained.

Eigenvalues	**Eigenvectors**
λ_1 =1281077815	$\mathbf{a}_1$ = {0.40825, 0.40825, 0.40825, 0.40825, 0.40825, 0.40825}
λ_2 =41040737	$\mathbf{a}_2$ = {0.28868, 0.57735, 0.28868, -0.28868, -0.57735, -0.28868}
λ_3 =41038068	$\mathbf{a}_3$ = {0.5, 0, -0.5, -0.5, 0, 0.5}
λ_4 =3242860	$\mathbf{a}_4$ = {-0.28868, 0.57735, -0.28868, -0.28868, 0.57735, -0.28868}
λ_5 =3240898	$\mathbf{a}_5$ = {-0.5, 0, 0.5, -0.5, 0, 0.5}
λ_6 =495051.4	$\mathbf{a}_6$ = {-0.40825, 0.40825, -40825, 0.40825, -0.40825, 0.40825}

So, the principal components of the system are:

$$Y_1 = 0.40825\, l_1 + 0.40825\, l_2 + 40825\, l_3 + 0.40825\, l_4 + 0.40825\, l_5 + 0.40825\, l_6 \quad \textbf{(2.3-1)}$$

$$Y_2 = 0.28868 l_1 + 0.57735 l_2 + 0.28868\, l_3 - 0.28868\, l_4 - 0.57735\, l_5 - 0.28868 l_6 \quad \textbf{(2.3-2)}$$

$$Y_3 = 0.5\, l_1 - 0.5 l_3, -0.5\, l_4 + 0.5 l_6 \quad \textbf{(2.3-3)}$$

$$Y_4 = -0.28868 l_1 + 0.57735 l_2 - 0.28868\, l_3 - 0.28868\, l_4 + 0.57735\, l_5 - 0.28868 l_6 \quad \textbf{(2.3-4)}$$

$$Y_5 = -0.5\, l_1 + 0.5 l_3, -0.5\, l_4 + 0.5 l_6 \quad \textbf{(2.3-5)}$$

$$Y_6 = - -0.40825\, l_1 + 0.40825\, l_2 - 40825\, l_3 + 0.40825\, l_4 - 0.40825\, l_5 + 0.40825\, l_6 \quad \textbf{(2.3-6)}$$

According to the above formulas, the corresponding principal component values $\{\mathbf{Y}_i : (Y_1\, Y_2, Y_3, Y_4, Y_5, Y_6)_i \,|i=1, 2, \ldots, m\}$ (here, m is the sample size) were calculated. Then, analysis for identifying the relationships between the positional variables and the principal components was carried out. This analysis was based on the sample data; the positional variable values $\{\mathbf{Q}_i : (\alpha_1, \alpha_2, \alpha_3, \alpha_4, \alpha_5, lm)_i \,|i=1,$

2, ..., m } and the principal component values $\{\mathbf{Y}_i:(Y_1\ Y_2, Y_3, Y_4, Y_5, Y_6)_i | i=1, 2, ..., m\}$.

It should be noted that in the symmetries in the eigenvectors represent symmetries in the assembly configuration[□]. The repeated eigenvalues $(\lambda_2, \lambda_3, \lambda_4, \lambda_5)$ represent the symmetries in the assembly configuration and data sampling. It is very difficult to give a complete physical explanation of the eigenvalues and the eigenvectors for a particular application. In this case, some physical explanation will be discussed in the following sections but the complete physical explanation is till an open question.

7.3.3 Analysis of the Relationship between the Principal Components and the Positional Variables

The procedure of the analysis of the relationship between the principal components and the positional variables has been introduced in Section 6.3.2. The relationship analysis starts by the one-to-one relationship analysis. If one-to-one relationship analysis cannot obtain satisfactory results, pair-to pair relationship analysis will be carried out. During this analysis, two one-to-one relationships were identified. Those are the relationship between the first principal component (Y_1) and the length of the M-bar (*lm*) and the relationship between the sixth principal component (Y_6) and Angle 5 (α_5). However, the relationship between (Y_2, Y_3, Y_4, Y_5) and (α_1, α_2, α_3, α_4) is very complex. Hence, pair-to-pair relationships were identified. Then, the combinations of the pair-to-pair relationships were also identified. These identified relationships are discussed as follows.

7.3.3.1 One-to-one Relationship Analysis

After comparing every principal component with each positional variable, two relationships have been identified. One is the relationship between the first principal component Y_1 and the length of the M-bar *lm*. The other is the relationship between the sixth principal component (Y_6) and the angle 5 (α_5).

[□] The author used non-symmetry assembly configurations, which leaded to non-symmetry eigenvectors.

7.3.3.1.1 The relationship between the 1st principal component and the length of the M-Bar

According to the formula (2.3-1) of the first principal component,

$$Y_1 = 0.40825\, l_1 + 0.40825\, l_2 + 40825\, l_3 + 0.40825\, l_4 + 0.40825\, l_5 + 0.40825\, l_6$$

$$= 0.40825\,(l_1 + l_2 + l_3 + l_4 + l_5 + l_6)$$

$$= 2.4495\,(l_1 + l_2 + l_3 + l_4 + l_5 + l_6)/6$$

(a) The relationship between Y_1 and *lm*

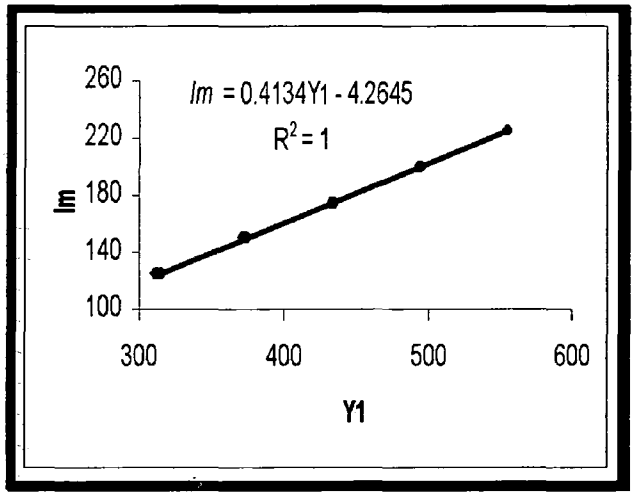

(b) The error of the regression function

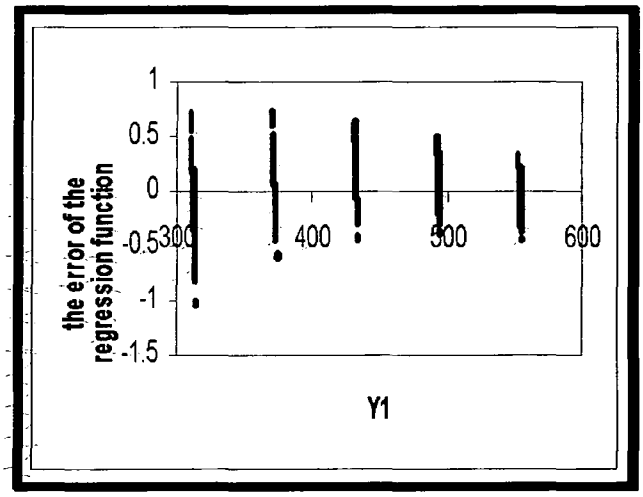

Figure 7-3 The relationship between Y_1 and *lm*

In fact, the first principal component is an arithmetic average of the six link lengths with a constant factor. It is obvious that the first principal component value increases with the length of the M-bar (*lm*). Normally, the arithmetic average of the six link lengths is greater than the length of the M-bar. But, when the length of the M-bar

approaches infinite, the difference between the arithmetic average of the six link lengths and the length of the M-bar approaches zero. Figure 7-3(a) illustrates the relationship between Y_1 and *lm* using all of the sample data. To show the relationship more clearly, more sample data (for *lm*= 125, 150, 175, 200 and 225) was inserted in the figure. Also, the regression line is added.

The regression function is:

$$lm=0.4134Y_1 - 4.2645 \qquad (2.3\text{-}7)$$

When the other positional variables (α_1, α_2, α_3, α_4, α_5) are given, there is an increasing function $lm=f(Y_1)$. When the other positional variables have different values, the corresponding functions $lm=f(Y_1)$ may be different. However, these differences are very small. This can be illustrated by Figure 7-3. Figure 7-3(b) is a scatter figure in which every difference between every sample datum value and the value calculated by the regression function (2.3-7) is shown using all of the sample data. To give a closed form expression to the function $lm=f(Y_1)$ with the parameters (α_1, α_2, α_3, α_4, α_5), $lm=f[Y_1, (\alpha_1, \alpha_2, \alpha_3, \alpha_4, \alpha_5)]$, is very difficult. However, the properties of the functions $lm=f(Y_1)$ have been identified. They are increasing functions, hence, the value of *lm* can be obtained by using a numerical algorithm, if the principal component Y_1 and position variables α_1, α_2, α_3, α_4, α_5 are known. Also, the regression function (2.3-7) can be used to set the initial value of *lm* in the computing algorithm. Figure 7-3(b) shows that if *lm* varies between 150 and 200, the error of the regression function is less than ±1mm. The relative error is less than 0.5% when α_1, α_2, α_3, α_4, α_5 vary in the value range described in 2.3.3.1. Therefore, the initial value given by the regression function has high accuracy. It is also known through Figure 7-3(b), that the position variable *lm* has only small variance (less than ±1%) when α_1, α_2, α_3, α_4, α_5 have different values. Therefore, the value of *lm* can be determined by the value of Y_1 only using the regression function for some applications, in which accuracy requirement is less than ±1%. Considering the fact that the errors of the regression function shown in Figure 7-3(b) include all of the sample data, it is known that for different values of the positional variables (α_1, α_2, α_3, α_4, α_5), the quantity relationship between *lm* and Y_1 has only very small

change. In other words, the positional variables (α_1, α_2, α_3, α_4, α_5) only have a very small effect on the relationship between *lm* and Y_1.

Conclusions for the relationship between Y_1 and lm :

- The first principal component is mainly relative to the positional variable *lm*. The first principal component increases with the increase of the variable *lm*.
- If the other positional variables (α_1, α_2, α_3, α_4, α_5) are given, there is an increasing function $lm=f(Y_1)$.
- If the other positional variables have different values, the corresponding functions $lm=f(Y_1)$ may be different, but this difference is very small. In the range $125<=lm<=225$, there is a regression function:

  $$lm=0.4134Y_1-4.2645$$

  The error of this regression function in the given value range of *lm* is less than ±1%.

  This fact indicates that the positional variables α_1, α_2, α_3, α_4, α_5 only have very small effects on the relationship between *lm* and Y_1.

7.3.3.1.2 The Relationship between the 6th principal component (Y_6) and the angle 5 (α_5)

The formula (2.3-6) of the 6th principal component is:

$$\mathbf{Y}_6 = -0.40825\, l_1 + 0.40825\, l_2 - 40825\, l_3 + 0.40825\, l_4 - 0.40825\, l_5 + 0.40825\, l_6$$

$$= 0.40825(-l_1 + l_2 - l_3 + l_4 - l_5 + l_6)$$

$$= 1.22475\,[(l_2 - l_1) + (l_4 - l_3) + (l_6 - l_5)]/3$$

In fact, the sixth principal component is an arithmetic average of the three differences, $(l_2 - l_1)$, $(l_4 - l_3)$ and $(l_6 - l_5)$, with a constant coefficient. Figure 7-4(a) and (b) are the top view and 3D view of the Stewart platform respectively. If α_5 increases, that

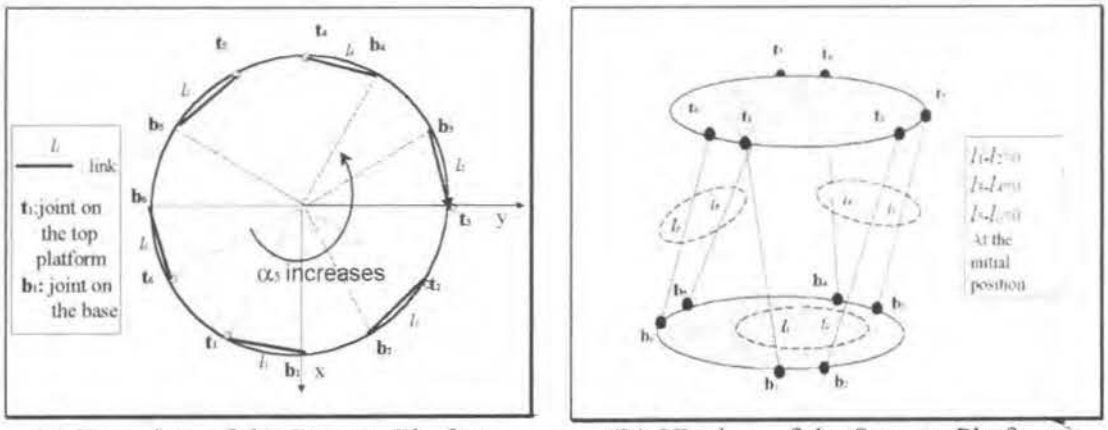

(a) Top view of the Stewart Platform **(b)** 3D view of the Stewart Platform

Figure 7-4

is, the top platform rotates in an anti-clockwise direction, the lengths of l_2, l_4, l_6 will increase and the lengths of l_1, l_3, l_5 will decrease. If α_5 decreases, the lengths of l_2, l_4, l_6 will decrease and the lengths of l_1, l_3, l_5 will increase. Therefore, the average of the three differences, $(l_2 - l_1)$, $(l_4 - l_3)$ and $(l_6 - l_5)$, can be used to express the rotational angle α_5. Consequently, the sixth principal component (Y_6) can be used to express α_5.

Figure 7-5 illustrates the relationship between the 6th principal component (Y_6) and the positional variable α_5 when α_5 is between $-\pi/12$ and $\pi/12$. Figure 7-5(a) shows the situation when α_1, α_2, α_3, α_4 are zero and lm equals 150. The regression function corresponding to the sample data shown in Figure 7-5(a) is:-

$$Y_6 = 76.383\alpha_5$$

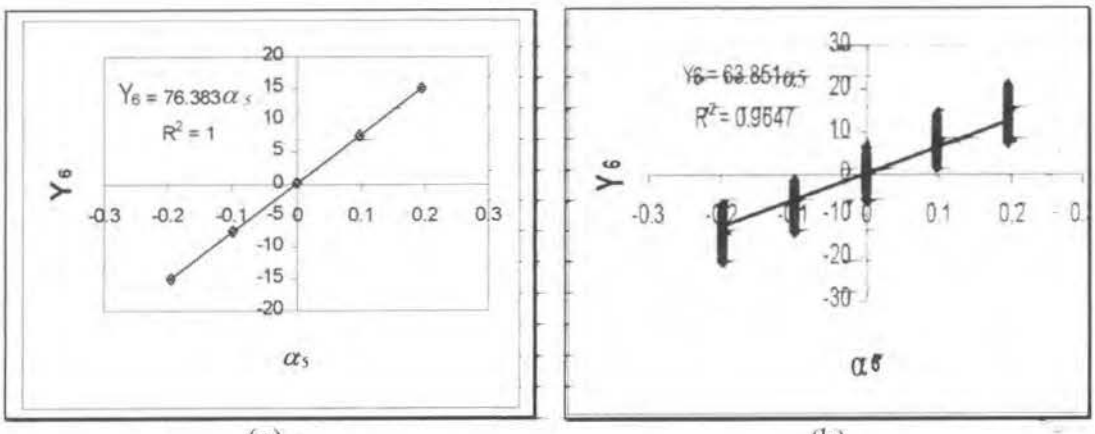

(a) (b)

Figure 7-5 The relationship between Y_6 and α_5

Here, the intercept is zero and the slope is 76.383. When α_1, α_2, α_3, α_4 and *lm* are given different values, the relationship between Y_6 and α_5 is still an approximate linear relationship but the corresponding regression linear function for each situation has different intercepts and slopes. Each individual regression function for every individual situation will not be discussed. Instead, a linear regression function for all situations is given in Figure 7-5(b). Figure 7-5(b) is a scatter figure showing the relationship between Y_6 and α_5 using all of sample data. For any given value of α_5, there are many different values of Y_6 corresponding to the same given α_5 but different values of (α_1, α_2, α_3, α_4, *lm*). For example, when α_5 equals 0, the values of Y_6 are between –7 and 7, which correspond to different values of the other positional variables α_1, α_2, α_3, α_4 and *lm*. These differences of the values of Y_6 are effects on the relationship between Y_6 and α_5 caused by the other positional variables (α_1, α_2, α_3, α_4, *lm*). The linear regression function for all of the sample data is

$$Y_6 = 63.851\alpha_5.$$

This function can be used to estimate the approximate value of α_5, but the error is relative large.

Conclusions for the relationship between Y_6 and α_5:

- The sixth principal component is mainly related to the positional variable α_5.
- The sixth principal component increases with the positional variable α_5.
- The relationship between Y_6 and α_5 is an approximately linear relationship when the other positional variables are fixed. The linear regression function for this case is,

$$Y_6 = 63.851\alpha_5$$

- Impact of other positional variables: When the values of α_1, α_2, α_3, α_4 and *lm* vary in the range given in Section 7.3.2, the quantity relationship between Y_6 and α_5 has relatively large change. However, the quality relationship between Y_6 and α_5 is still the same no matter the values of (α_1, α_2, α_3, α_4, *lm*). That is when α_5 increases, Y_6 will increase.

7.3.3.2 Pair-to-Pair Relationship Analysis

During the one-to-one relationship analysis, the relationships between the 2nd, 3rd, 4th and 5th principal components (Y_2, Y_3, Y_4, Y_5) and positional variables ($\alpha_1,\alpha_2,\alpha_3,\alpha_4$) are still difficult to identify. Hence, pair-to-pair relationship analyses were carried out. Through the pair-to-pair analyses, it is clear that both of the two pair variables (α_1,α_2) and (α_3,α_4) significantly affect both of the pairs of the principal components (Y_2, Y_3) and (Y_4, Y_5).

7.3.3.2.1 The pair-to-pair relationships (Y_2, Y_3)-to-(α_1,α_2) and (Y_2, Y_3)-to-(α_3,α_4)

According to the formula (2.3-2) and (2.3-3), the 2nd and 3rd principal components are:

$$\mathbf{Y}_2 = 0.28868 l_1 + 0.57735 l_2 + 0.28868 l_3 - 0.28868 l_4 - 0.57735 l_5 - 0.28868 l_6$$

$$\mathbf{Y}_3 = 0.5 l_1 - 0.5 l_3, -0.5 l_4 + 0.5 l_6$$

Because the relationships (Y_2,Y_3)-to-(α_1,α_2) and (Y_2,Y_3)-to-(α_3,α_4) are difficult to directly identify, analysis was carried out in two steps. The first step is to analyse two pair-to-pair relationships, (Y_2,Y_3)-to-(α_1,α_2) and (Y_2,Y_3)-to-(α_3,α_4), based on a special condition. The second step is a synthetic analysis to combine these two pair-to-pair relationships. This process is discussed as follows.

The basic relationship of (Y_2,Y_3)-to-(α_1, α_2)

To show the relationship more clearly, it is assumed that $\alpha_3 = 0$, $\alpha_4 = 0$, $\alpha_5 = 0$, and *lm* = 150. The relationship (Y_2,Y_3)-to-(α_1, α_2) based on this assumption is called

basic relationship of (Y_2, Y_3)-to-(α_1, α_2). The Figure 7-6 shows the basic relationship of (Y_2, Y_3)-to-(α_1, α_2) using the sample data.

(a) The sample data distribution in the principal component plane Y_2-Y_3

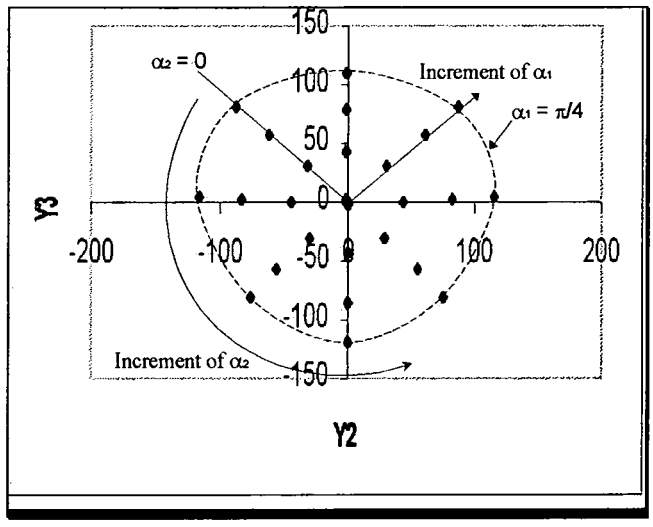

(b) The sample data distribution in the θ_{23} –ρ_{23} coordinate plane

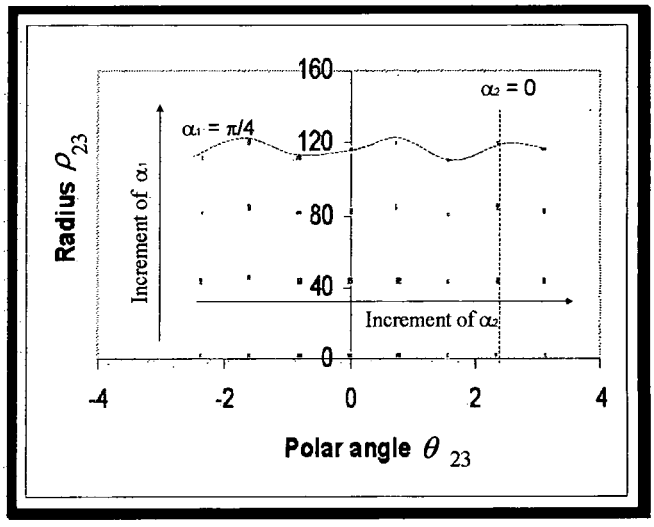

(c) The relationship between ρ_{23} and α_1.shown by using the sample data

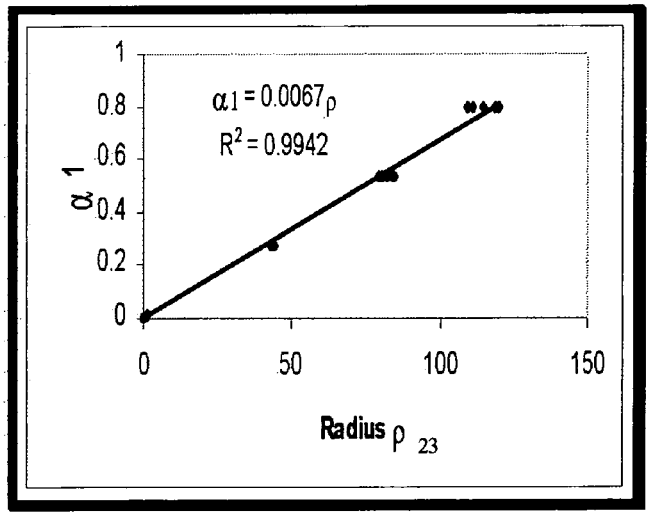

(d) The relationship between θ_{23} and α_2 shown by using the sample data

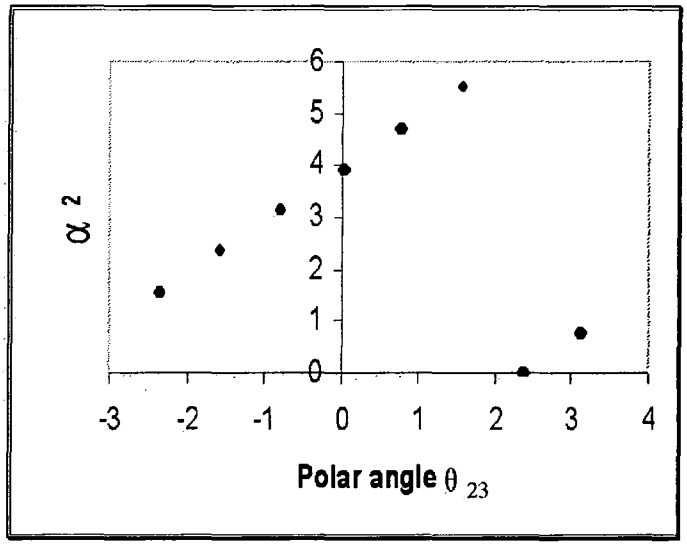

(e) The relationship between θ_{23} and α_2

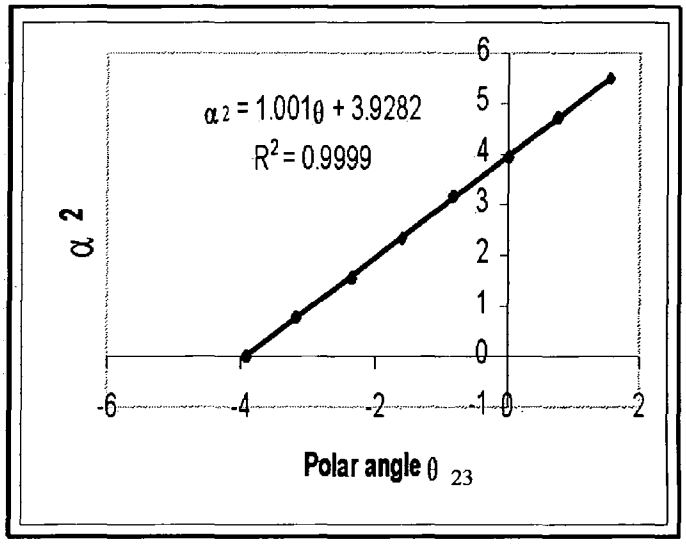

Figure 7-6 The relationship between (Y_2, Y_3) and (α_1, α_2)

Figure 7-6(a) shows the sample data distribution corresponding to all of the sample values of α_1 and α_2. This type of distribution is Type 3 of which has been discussed in Section 6.3.2.2. The sample points in principal component plane Y_2-Y_3 are arrayed in a family of closed concentric curves, which cross with a family of curves from a centre point, radiating outward. Around the closed curves (θ_{23}), the anti-clockwise direction is the increment of the variables α_2 and the radius of the closed

curve (ρ_{23}) increases with the increment of the variable α_1. Here, $\theta_{23} = \text{atan}(Y_3/Y_2)$ and $\rho_{23} = \sqrt{Y_2^2 + Y_3^2}$.

As mentioned in Section 6.3.2.2, Type 3 can be transformed to Type 1 or Type 2. Figure 7-6(b) shows the sample data distribution in the θ_{23} –ρ_{23} coordinate plane. This type of the sample data distribution is Type 2 which has been discussed in Section 6.3.2.2. It obviously illustrates that ρ_{23} increases with α_1 and θ_{23} increases with α_2. For the same value of α_1, the value of ρ_{23} is a wave. This means that the data points corresponding to the same value of α_1, in the plane Y_2-Y_3 is not in an exact circle.

Figure 7-6(c) shows the relationship between ρ_{23} and α_1 using the sample data. This has a linear regression function,

$$\alpha_1 = 0.0067\rho_{23} = 0.0067\sqrt{Y_2^2 + Y_3^2}$$

Figure 7-6(d) shows the relationship between the θ_{23} and α_2 when θ_{23} is between [-π, π] and α_2 between [0, 2π]. There is a jump at the point α_2=2π and α_2=0. Since the variables α_2 and θ_{23} are circular variables, θ_{23} can be in the value range [-5π/4, 3π/4] instead of [-π, π]. Therefore, Figure 7-6(e) shows the linear relationship between θ and α_2. This linear regression function is

$$\begin{aligned}\alpha_2 &= 1.001\,\theta_{23} + 3.9282 \\ &\approx \theta_{23} + 5\pi/4 \\ &= \text{atan}(Y_3/Y_2) + 5\pi/4\end{aligned}$$

When the variables α_5 and *lm* varies, the sample data distribution in the plane Y_2-Y_3 is almost the same as Figure 7-6. Therefore, the above analysis result is still suitable for different values of α_5 and *lm*.

The basic relationship of (Y_2, Y_3)-to(α_3, α_4)

To show the relationship more clearly, it is assumed that $\alpha_1 = 0$, $\alpha_2 = 0$, $\alpha_5 = 0$, and $lm = 150$. The relationship (Y_2, Y_3)-to-(α_3, α_4) based on this assumption is called basic relationship of (Y_2, Y_3)-to-(α_3, α_4). The Figure 7-7 shows the basic relationship of (Y_2, Y_3)-to-(α_3, α_4) using the sample data. It is interesting that the sample data distribution in the principal component plane Y_2-Y_3 is almost the same as that in the Figure 7-6.

(a) The sample data distribution in the principal component plane Y_2-Y_3

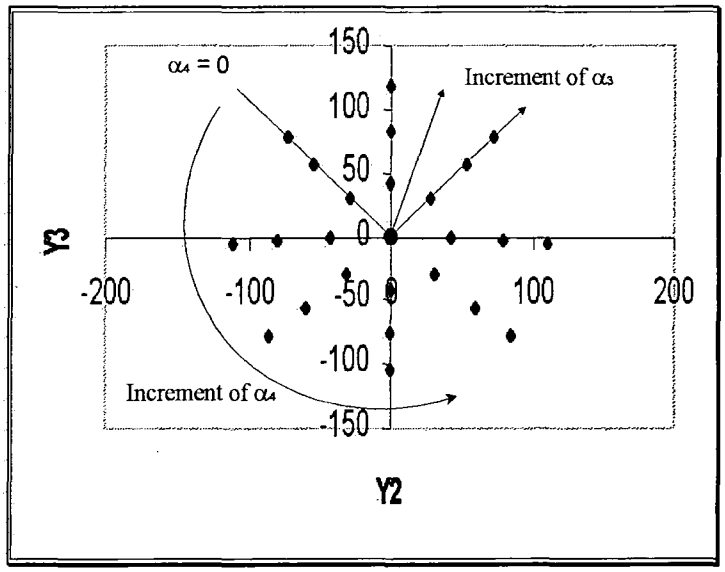

(b) The relationship between ρ_{23} and α_3 shown by using the sample data

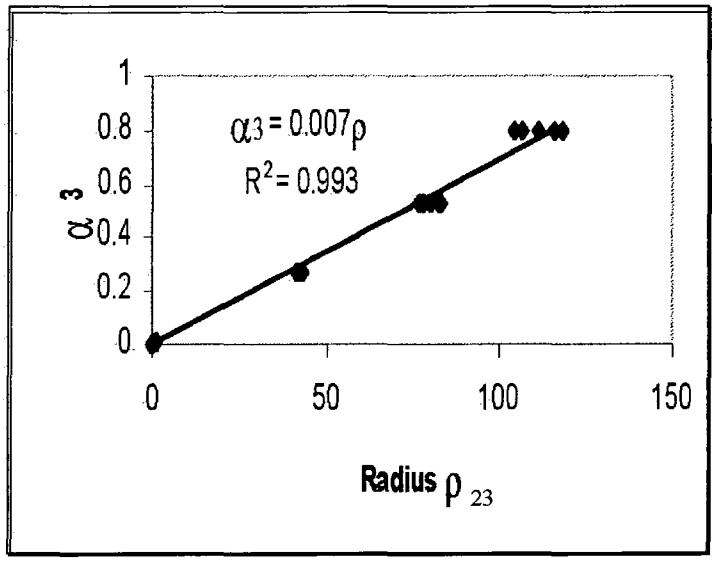

(c) The relationship between the θ_{23} and α_4 shown by using the sample data

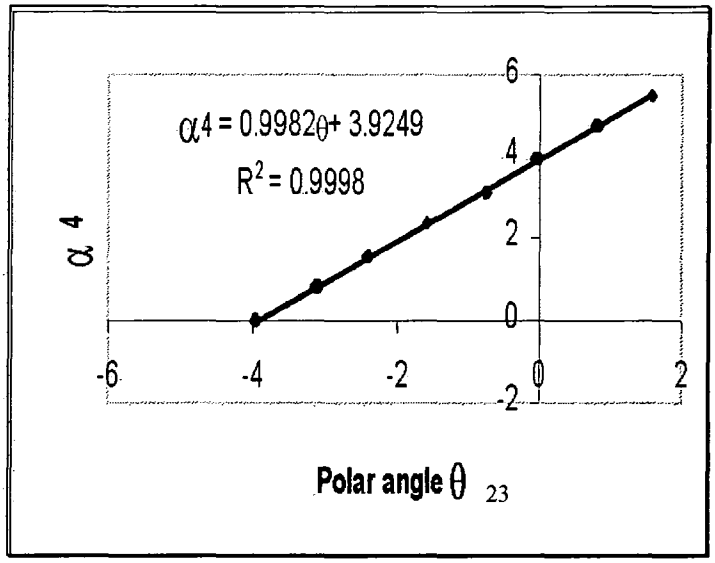

Figure2.3-7 The relationship of (Y_2, Y_3) and (α_3, α_4)

Figure 7-7(a) shows the data distribution corresponding to all values of α_3 and α_4. This type of distribution is Type 3 of which has been discussed in Section 6.3.2.2. Similar to the discussion on Figure 7-6, Figure 7-7(b) shows the relationship between ρ_{23} and α_3. This has a linear regression function:

$$\alpha_3 = 0.007\rho_{23} = 0.007\sqrt{Y_2^2 + Y_3^2}$$

Figure 7-7(c) shows the linear relationship between θ_{23} and α_4. This has a linear regression function,

$$\alpha_4 = 0.9982\theta + 3.9249 \approx \theta_{23} + 5\pi/4 = \text{atan}(Y_3/Y_2) + 5\pi/4$$

When the variables α_5 and *lm* vary, the data distribution is almost the same as the sample data distribution in Figure 7-7. Therefore the above analysis result is still suitable for different values of α_5 and *lm*.

Synthetic analysis

Relationship between (Y_2, Y_3) and $(\alpha_1, \alpha_2, \alpha_3, \alpha_4)$

The (Y_2, Y_3)–to-(α_1, α_2) relationship under the condition $\alpha_3 = 0$ and $\alpha_4 = 0$ is called (Y_2, Y_3)–to-(α_1, α_2) basic relationship. The (Y_2, Y_3)–to-(α_3, α_4) relationship under the condition $\alpha_1 = 0$ and $\alpha_2 = 0$ is called (Y_2, Y_3)–to-(α_3, α_4)

basic relationship. It was found that when both of (α_1, α_2) and (α_3, α_4) are not (0,0), the relationship between (Y_2, Y_3) and $(\alpha_1, \alpha_2, \alpha_3, \alpha_4)$ can be expressed by the combination of these two basic relationships.

Figure 7-8 shows the combination of the basic relationships, (Y_2, Y_3)–to-(α_1, α_2) and (Y_2, Y_3)–to-(α_1, α_2), using the sample data. The sample data in Figure 7-8 includes three data sets:-

$\{(\alpha_1, \alpha_2, \alpha_3, \alpha_4, \alpha_5, lm) \mid \alpha_3 = 0, \alpha_4 = 0, \alpha_5 = 0, lm = 150\}$;

$\{(\alpha_1, \alpha_2, \alpha_3, \alpha_4, \alpha_5, lm) \mid \alpha_1 = \pi/4, \alpha_2 = 0, \alpha_3 = \pi/12, \alpha_5 = 0, lm = 150\}\}$;

$\{(\alpha_1, \alpha_2, \alpha_3, \alpha_4, \alpha_5, lm) \mid \alpha_1 = \pi/4, \alpha_2 = \pi/4, \alpha_3 = \pi/12, \alpha_5 = 0, lm = 150\}$.

If $\alpha_1 = \pi/4$, the centre of the circle corresponding to $\alpha_3 = \pi/12$ has been moved on the circle corresponding to $\alpha_1 = \pi/4$, instead of being at the origin of the Y_2-Y_3 plane.

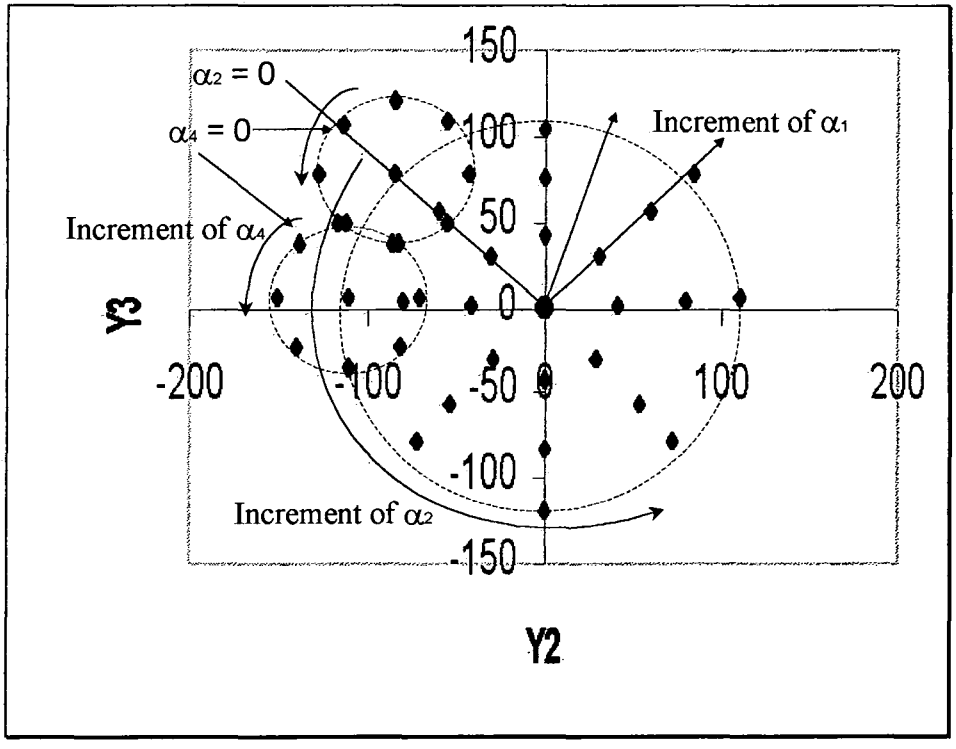

Figure 7-8 The combination of the basic relationships (Y_2, Y_3)–to-(α_1, α_2) and (Y_2, Y_3)–to-(α_3, α_4) shown by using the sample data

Figure 7-9 illustrates the combination of the basic relationships using vectors. If the values of (α_1, α_2) are given, the value of (Y_2, Y_3) can be determined by the basic relationship (Y_2, Y_3)-to-(α_1, α_2). The value of (Y_2, Y_3) can be expressed by a vector. This vector is denoted as $v_{(23,b12)}(\alpha_1, \alpha_2)$. Also if the values of (α_3, α_4) is given, the value of (Y_2, Y_3) can be determined by the basic relationship (Y_2, Y_3)-to-(α_3, α_4). The value of (Y_2, Y_3) can also be expressed by a vector. This vector is denoted as $v_{(23,b34)}(\alpha_3, \alpha_4)$. Therefore, the relationship between (Y_2, Y_3) and $(\alpha_1, \alpha_2, \alpha_3, \alpha_4)$ can be approximately expressed by

$$(Y_2, Y_3) = v_{23}(\alpha_1, \alpha_2, \alpha_3, \alpha_4) = v_{(23,b12)}(\alpha_1, \alpha_2) + v_{(23,b34)}(\alpha_3, \alpha_4)$$

Here, $v_{23}(\alpha_1, \alpha_2, \alpha_3, \alpha_4)$ is a vector expression of the values of (Y_2, Y_3) which is determined by $(\alpha_1, \alpha_2, \alpha_3, \alpha_4)$.

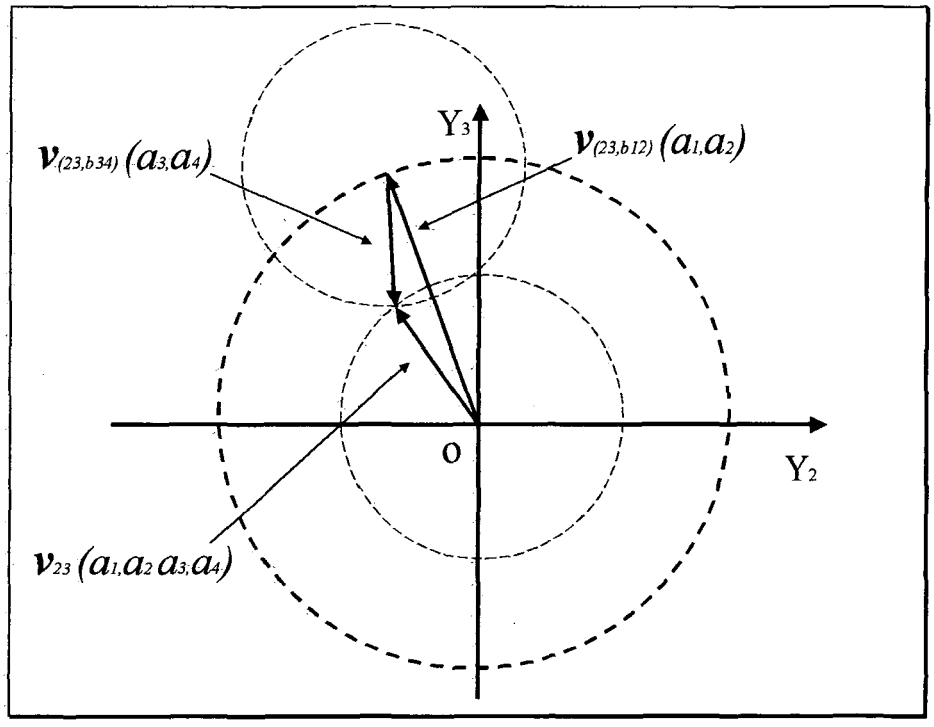

Figure 7-9 The combined relationship shown using vectors

It should be noted that the above vector expression is an approximate expression which results from the sample data analysis. However, the accuracy of the expression is not given. In this project, the accuracy of the expression is not very important. The important result of the analysis is that the qualitative relationship between (Y_2, Y_3)

and $(\alpha_1, \alpha_2, \alpha_3, \alpha_4)$ is identified. That is, there are two closed curve families in the plane Y_2-Y_3, which are Type 3 curves discussed in Section 6.3.2.2. If the values of $(\alpha_1, \alpha_2, \alpha_3, \alpha_4)$ are given, the values of (Y_2, Y_3) can be determined by the cross point of the two curves in the plane Y_2-Y_3, from the two curve families. This important characteristic can be used to build up a numerical algorithm to search the value of $(\alpha_1, \alpha_2, \alpha_3, \alpha_4)$, which will be discussed in the next chapter. In the algorithm, the approximate vector expression of the relationship can be used to set initial values.

If the positional variables α_5 and *lm* are fixed, it is known that any given values of $(\alpha_1, \alpha_2, \alpha_3, \alpha_4)$ can determine the values of (Y_2, Y_3). However, given values of (Y_2, Y_3) cannot determine values of $(\alpha_1, \alpha_2, \alpha_3, \alpha_4)$. In other words, given vector $\boldsymbol{v}_{23}(\alpha_1, \alpha_2, \alpha_3, \alpha_4)$ corresponds to a set of values of $(\alpha_1, \alpha_2, \alpha_3, \alpha_4)$. Geometrically, this set of values of $(\alpha_1, \alpha_2, \alpha_3, \alpha_4)$ corresponds to a set of geometrical statuses of the top platform. Based on the above analysis for the combined relationship, these geometrical statuses can be approximately viewed as a set of statuses of the platform that have the same tilt direction and degree of the top platform relative to the base. The length of the vector $\boldsymbol{v}_{23}$ ($\rho_{23} = \| \boldsymbol{v}_{23} \| = \sqrt{Y_2^2 + Y_3^2}$) corresponds to the tilt degree of the top platform relative to the base. The polar angle of the vector $\boldsymbol{v}_{23}$ ($\theta_{23} = \text{atan}(Y_3/Y_2)$) corresponds to the tilt direction of the top platform relative to the base. In summary, any given vector $\boldsymbol{v}_{23}$ $(\alpha_1, \alpha_2, \alpha_3, \alpha_4)$ expresses a set of statuses of the top platform, which have the same tilt direction and degree relative to the base. Here, some special situations are as follows:

Firstly, if $\boldsymbol{v}_{23}(\alpha_1, \alpha_2, \alpha_3, \alpha_4) = \mathbf{0}$, e.g. $(Y_2, Y_3) = (0,0)$, the top platform is parallel with the base (see Figure 7-10(a)). It is known that if $\alpha_1 = \alpha_3$ and $\alpha_2 = \alpha_4$, $\boldsymbol{v}_{(23,b12)}$ $(\alpha_1, \alpha_2) = \boldsymbol{v}_{(23,b34)}(\alpha_3, \alpha_4)$. It is also known that $\boldsymbol{v}_{(23,b12)}$ $(\alpha_1, \alpha_2 \pm \pi) = -\boldsymbol{v}_{(23,b12)}$ (α_1, α_2). Hence, if $\alpha_1 = \alpha_3$ and $\alpha_2 = \alpha_4 \pm \pi$, then $\boldsymbol{v}_{(23,b12)}(\alpha_1, \alpha_2) = -\boldsymbol{v}_{(23,b34)}(\alpha_3, \alpha_4)$, and then $\boldsymbol{v}_{23} = \boldsymbol{v}_{(23,b12)}$ $(\alpha_1, \alpha_2) + \boldsymbol{v}_{(23,b34)}(\alpha_3, \alpha_4) = 0$. This indicates the fact, if $\boldsymbol{v}_{23} = 0$ and $\alpha_1 = \alpha_3$ then $\alpha_2 = \alpha_4 \pm \pi$. This means that the M-bar and the top platform

tilt in contrary directions by the same tilt angle. That is, the top platform is parallel with the base (see Figure 7-10(a)).

If $v_{23}(\alpha_1, \alpha_2, \alpha_3, \alpha_4)$ is given a non-zero value but $\alpha_2 = \alpha_4$, then the length of the vector $v_{23}(\alpha_1, \alpha_2, \alpha_3, \alpha_4)$ equals the sum of the length of the vector $v_{(23,612)}(\alpha_1, \alpha_2)$ and the length of the vector $v_{(23,634)}(\alpha_3, \alpha_4)$. This means that $\alpha_1 + \alpha_3 =$ a constant. In this situation, the M-bar and the top platform tilt in contrary directions ($\alpha_2 = \alpha_4 \pm \pi$) and the top platform has a constant tilt angle ($\alpha_1 + \alpha_3 =$ a constant) relative to the base (see Figure 7-10(b)). All the orientations of the platform in this situation are the same.

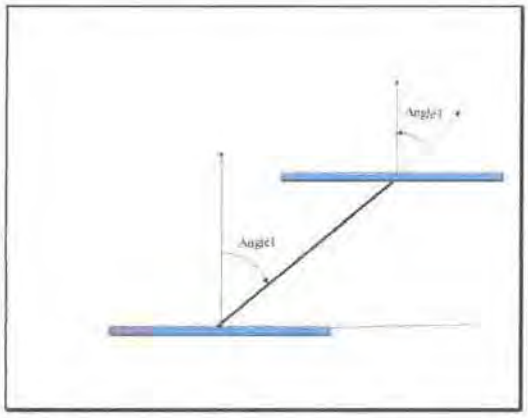

(a) The situations where $(Y_2, Y_3)=(0,0)$

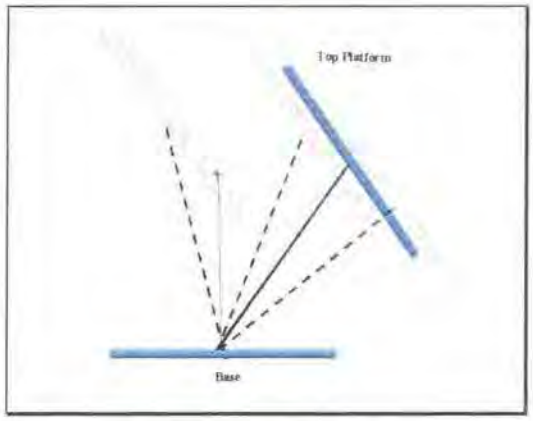

(b) The situations where $(Y_2, Y_3)\neq(0,0)$ but $\alpha_2 = \alpha_4$ is a constant, and $\alpha_1 + \alpha_3 =$ a constant

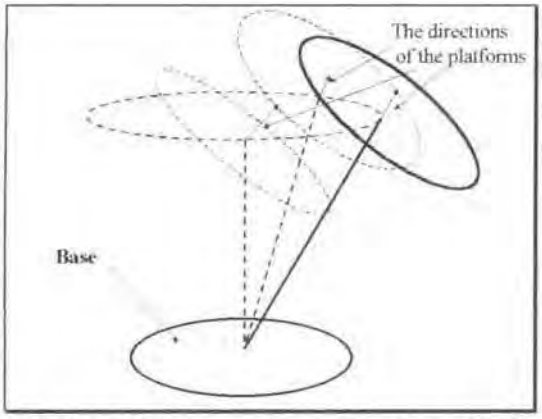

(c) The situations where $(Y_2, Y_3)\neq(0,0)$ but $\alpha_1 =$ a constant (3D view)

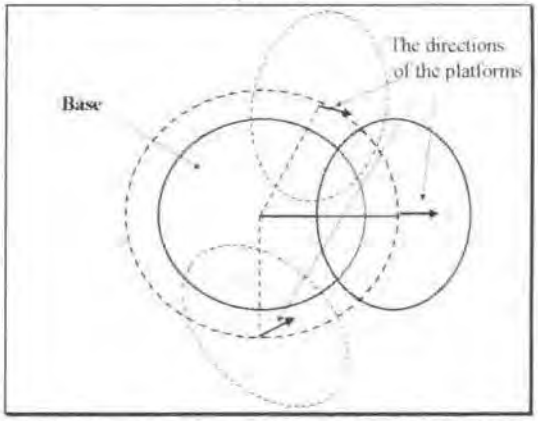

(d) The situations where $(Y_2, Y_3)\neq(0,0)$ but $\alpha_1 =$ a constant (top view)

Figure 7-10 Given (Y_2, Y_3) corresponds to a set of statuses of the platform

The situation where $v_{23}(\alpha_1, \alpha_2, \alpha_3, \alpha_4)$ is given a non-zero value but α_1 equals a constant will not be discussed, but the corresponding geometrical statuses are shown in Figure 7-10 (c) and (d). In this set of the statuses of the platform, there is one status corresponding to $\alpha_2 = \alpha_4$, or $\alpha_2 = \alpha_4 \pm \pi$, which is the green platform in Figure 7-10 (c) and (d). Other statuses of the platform in this status set of the platform are approximately parallel to this status with a small angular difference forward to this green platform.

Conclusions for the relationship between (Y_2, Y_3) and $(\alpha_1, \alpha_2, \alpha_3, \alpha_4)$:

- Generally, the principal component pair (Y_2, Y_3) mainly relates to the positional variable pairs (α_1, α_2) and (α_3, α_4).
- The geometrical meaning of a vector in the principal component plane Y_2-Y_3 can be interpreted as:
  a) The direction of the vector expresses the tilt direction of the top platform;
  b) The length of the vector expresses the tilt degree of the top platform
- Any given vector v_{23} in the principal component plane Y_2-Y_3 can be viewed as a combination of other two vectors $v_{(23,b12)}(\alpha_1, \alpha_2)$ and $v_{(23,b34)}(\alpha_3, \alpha_4)$. That is, $v_{23} = v_{(23,b12)}(\alpha_1, \alpha_2) + v_{(23,b34)}(\alpha_3, \alpha_4)$. Here, the two vectors $v_{(23,b12)}(\alpha_1, \alpha_2)$ and $v_{(23,b34)}(\alpha_3, \alpha_4)$ are determined by the basic relationships between the pair (Y_2, Y_3) and one of the positional variable pairs (α_1, α_2) and (α_3, α_4).

7.3.3.2.2 The pair-to-pair relationships (Y_4, Y_5)-to-(α_1, α_2) and (Y_4, Y_5)-to-(α_3, α_4)

The formula (2.3-4) and (2.3-5) for the 4th and 5th principal components are:

$$\mathbf{Y}_4 = -0.28868 l_1 + 0.57735 l_2 - 0.28868 l_3 - 0.28868 l_4 + 0.57735 l_5 - 0.28868 l_6$$

$$\mathbf{Y}_5 = -0.5 l_1 + 0.5 l_3, -0.5 l_4 + 0.5 l_6$$

The procedure of the analysis for identifying the relationship the relationships $((Y_4, Y_5)$-to-(α_1, α_2) and (Y_4, Y_5)-to-(α_3, α_4) is the same as in the discussions in

the previous section (Section 7.3.3.2.1). However, the results are slightly different from the previous section. The detailed discussions are as follows.

The basic relationship of (Y_4, Y_5)-to-(α_1, α_2)

To show the relationship more clearly, it is assumed that $\alpha_3 = 0$, $\alpha_4 = 0$, $\alpha_5 = 0$, and lm = 150. The relationship (Y_4, Y_5)-to-(α_1, α_2) based on this assumption is called the basic relationship of (Y_4, Y_5)-to-(α_1, α_2). The Figure 7-11 shows the basic relationship of (Y_4, Y_5)-to-(α_1, α_2) using the sample data.

(a) The sample data distribution in the principal component plane Y_4-Y_5

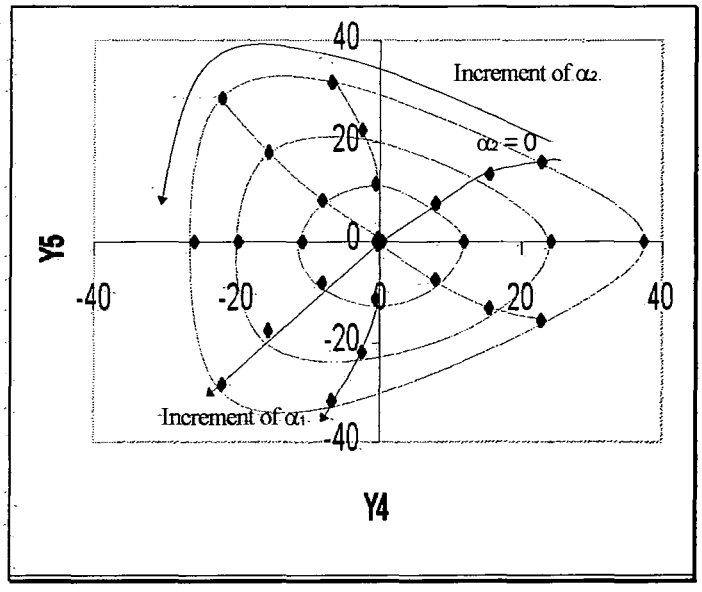

(b) The sample data distribution in the θ_{45} –ρ_{45} coordinate plane

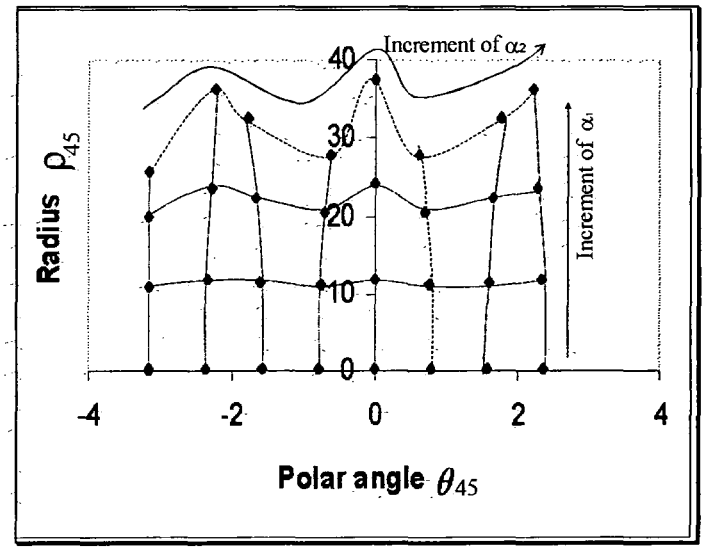

(c) The relationship between ρ_{45} and α_1 shown by using the sample data

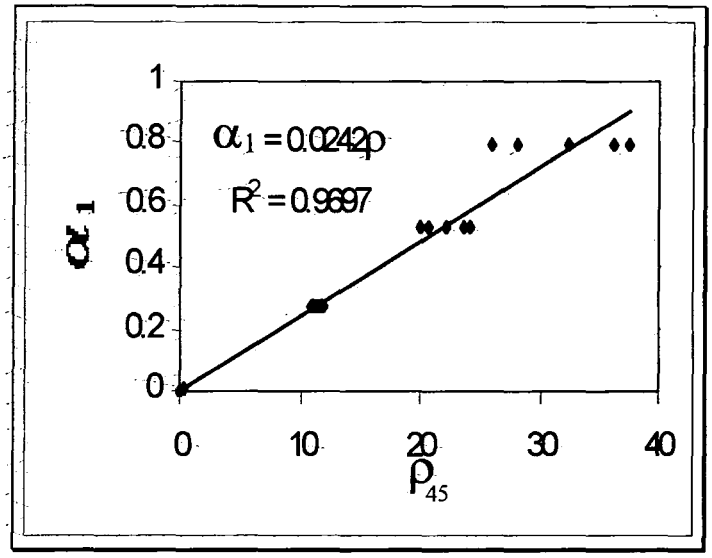

(d) The relationship between θ_{45} and α_2 shown by using the sample data

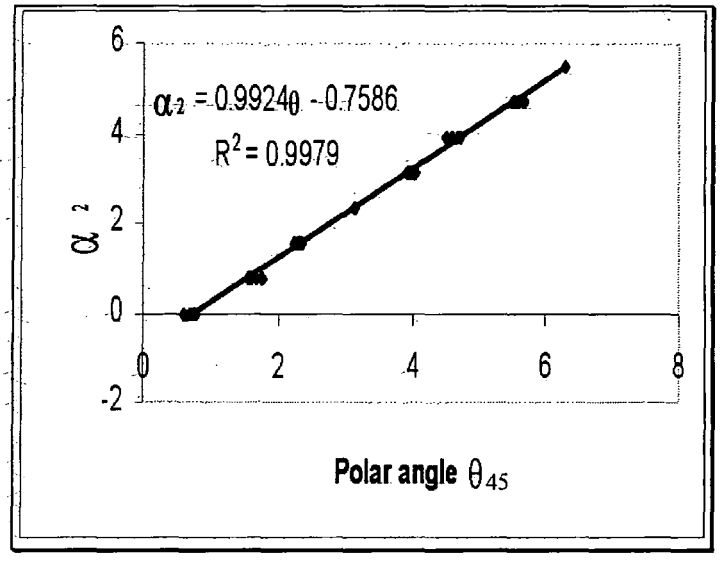

Figure 7-11 the relationship between (Y_4, Y_5) and (α_1, α_2)

In the principal components plane Y_4-Y_5, the sample data distribution (Figure 7-11(a)) is similar to Figure 7-6(a) which has been discussed in the previous section. The sample points in the principal component plane Y_4-Y_5 are arrayed in a family of closed concentric curves, which cross with a family of curves from a centre point, radiating outward. Around the closed curves (θ_{45}), the anti-clockwise direction is the increment of the variable α_2 and the radius of the closed curve (ρ_{45}) increases with the increment of the variable α_1. However, the closed curves in Figure 7-6(a) are more like circle. Here, in Figure 7-11(a), the outside closed cure is more similar to a triangle.

Figure 7-11(b) shows the sample data distribution in the θ_{45} –ρ_{45} coordinate plane. It illustrates that the increment of α_1 is mainly in the direction of the ρ_{45} axis. The increment of α_2 is mainly in the direction of the θ_{45} axis. Here, $\theta_{45} = \text{atan}(Y_5/Y_4)$ and $\rho_{45} = \sqrt{Y_4^2 + Y_5^2}$ For any given value of α_1, the value ρ_{45} is a wave. This means that the sample data points corresponding to the same value of α_1, in the plane Y_4-Y_5 are not on an exact circle. Also, the sample data points corresponding to the same value of α_2, in the plane Y_4-Y_5 do not have the same polar angle θ_{45}. Compared with Figure 7-6(b), the waves of the curves in Figure 7-11(b) are higher.

Figure 7-11(c) shows the relationship between ρ_{45} and α_1 using the sample data. A linear regression function was obtained.

$$\alpha_1 = 0.0242\rho_{45}$$

Figure 7-11(d) shows the relationship between θ_{45} and α_2 using the sample data. A linear regression function was obtained,

$$\alpha_2 = 0.9924\,\theta_{45} - 0.7586$$

$$\approx \theta_{45} - \pi/4$$

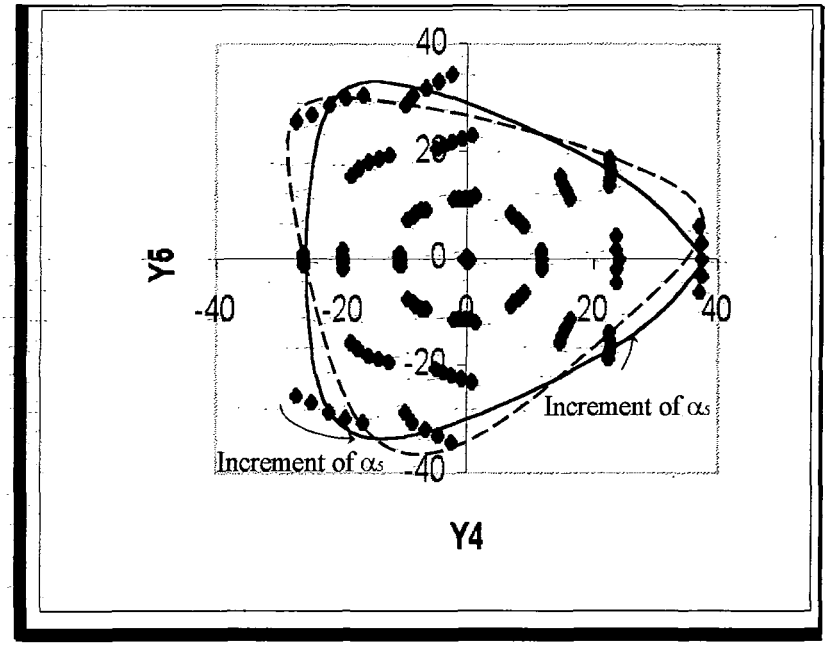

Figure 7-12 the effect α_5 on the relationship of (Y_4, Y_5)-to-(α_1, α_2)

When the variable *lm* varies, the sample data distribution in plane Y_4-Y_5 is almost the same as the distribution in Figure 7-11. This fact indicates that the results of the above analysis are suitable for different values of *lm*.

However, when the variable α_5 is given a nonzero value, the sample data distribution in the plane Y_4-Y_5 is obviously changed. Compared with Figure 7-11, the closed corves have a rotation (see Figure 7-12). The angle of the rotation is approximately the given value of α_5. This change is the effect of α_5 on the relationship of (Y_4,Y_5)-to-(α_1, α_2). Figure 7-12 shows the sample data distribution in which α_5 is given different values ($-\pi/12$, $-\pi/24$, 0, $\pi/24$, $\pi/12$). This figure shows that when α_5 increases, the closed curves formed by the sample points in the plane Y_4-Y_5 rotate in the anti-clockwise direction.

The basic relationship of (Y_4,Y_5)-to(α_3, α_4)

To show the relationship more clearly, it is assumed that $\alpha_1 = 0$, $\alpha_2 = 0$, $\alpha_5 = 0$, and *lm* = 150. The relationship (Y_4,Y_5)-to-(α_3, α_4) based on this assumption is called the basic relationship of (Y_4,Y_5)-to-(α_3, α_4). The Figure 7-13 shows the basic relationship of (Y_4,Y_5)-to-(α_3, α_4) using the sample data.

(a) The sample data distribution in the principal component plane Y_4-Y_5

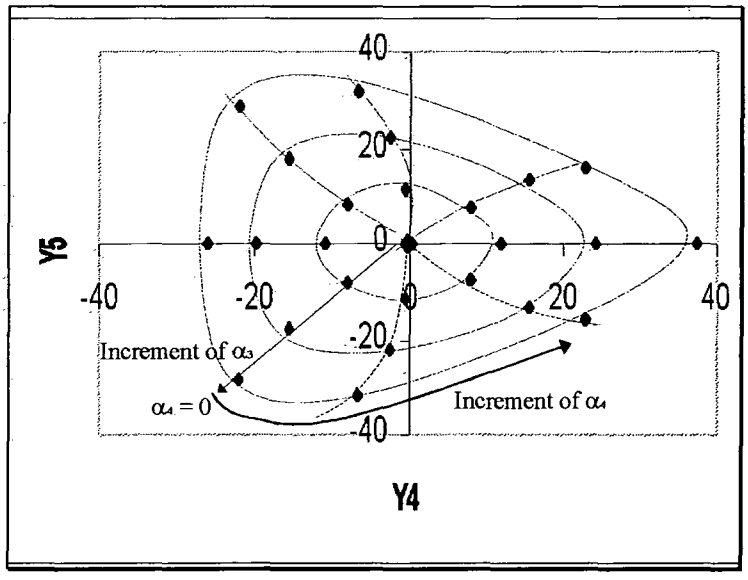

(b) The relationship between ρ_{45} and α_3 shown by using the sample data

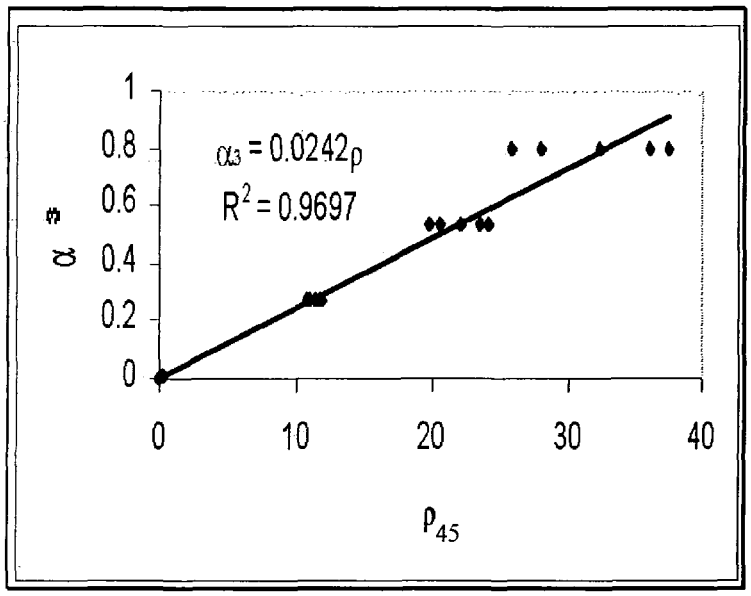

(c) The relationship between θ_{45} and α_4 shown by using the sample data

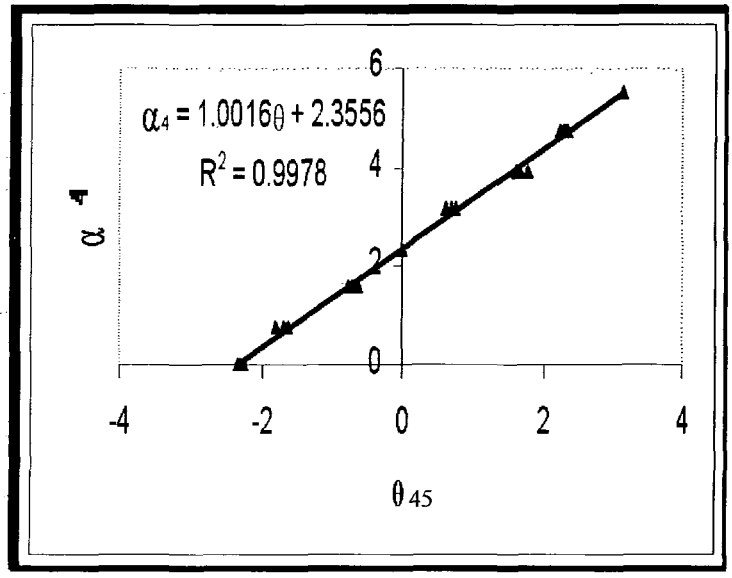

Figure 7-13 the relationship between (Y_4, Y_5) and (α_3, α_4)

Figure 7-13(a) is the sample data distribution in the plane Y_4-Y_5. It is similar to Figure 7-11(a), but if $\alpha_4 = 0$, the corresponding polar angle is $-3\pi/4$ instead of $\pi/4$. The difference between $-3\pi/4$ and $\pi/4$ is π.

Figure 7-13(b) shows the relationship between ρ_{45} and α_3 using the sample data. A linear regression function was obtained,

$$\alpha_3 = 0.0242\rho_{45}$$

Figure 7-13(c) shows the relationship between θ_{45} and α_4 using the sample data. A linear regression function was also obtained,

$$\alpha_4 = 1.0016\,\theta_{45} + 2.3556$$

$$\approx \theta_{45} + 3\pi/4$$

Comparing the situation shown in Figure 7-13 with that shown in Figure 7-11, it was found that the relationship α_1-to-ρ_{45} is almost the same as α_3-to-ρ_{45}, but between the relationships α_2-to-θ_{45} and α_4-to-θ_{45} there is phase difference (approximate π).

When the variable *lm* varies, the sample data distribution in plane Y_4-Y_5 is almost the same as that in Figure 7-13(a). This fact indicates that the above analysis is suitable for different values of *lm*.

However, when the variable α_5 is given a nonzero value, the sample data distribution in the plane Y_4-Y_5 is similar to Figure 7-13, but the closed curves have a rotation. In aspect, it is similar to the discussion on Figure 7-12 and, hence, will not be repeated.

Synthetic analysis

The (Y_4, Y_5)-to-(α_1, α_2) relationship under the condition $\alpha_3 = 0$ and $\alpha_4 = 0$ is called the (Y_4, Y_5)-to-(α_1, α_2) basic relationship. The (Y_4, Y_5)-to-(α_3, α_4) relationship under the condition $\alpha_1 = 0$ and $\alpha_2 = 0$ is called the (Y_4, Y_5)-to-(α_3, α_4) basic relationship. It was found that when both of (α_1, α_2) and (α_3, α_4) are not (0,0), the relationship between (Y_4, Y_5) and $(\alpha_1, \alpha_2, \alpha_3, \alpha_4)$ can be expressed by the combination of these two basic relationships.

To show the relationship more clearly, Figure 7-14 shows the sample data distribution in the plane Y_4-Y_5. This sample data includes three data sets:-

$\{(\alpha_1, \alpha_2, \alpha_3, \alpha_4, \alpha_5, lm) \mid \alpha_3 = 0, \alpha_4 = 0, \alpha_5 = 0, lm = 150\}$;

$\{(\alpha_1, \alpha_2, \alpha_3, \alpha_4, \alpha_5, lm) \mid \alpha_1 = \pi/4, \alpha_2 = 0, \alpha_3 = \pi/12, \alpha_5 = 0, lm = 150\}\}$;

$\{(\alpha_1, \alpha_2, \alpha_3, \alpha_4, \alpha_5, lm) \mid \alpha_1 = \pi/4, \alpha_2 = \pi/4, \alpha_3 = \pi/12, \alpha_5 = 0, lm = 150\}$.

If $\alpha_1 = \pi/4$, the centre of the circle corresponding to $\alpha_3 = \pi/12$ is moved on to the circle corresponding to $\alpha_1 = \pi/4$, instead of being at the origin of the Y_4-Y_5 plane. It should be noted that there is slight a difference between the two small closed curves corresponding to $\alpha_1 = \pi/4$ and $\alpha_3 = \pi/12$ in Figure 7-14. However, these two closed curves are approximately the same as the small curve corresponding to $\alpha_1 = 0$ and $\alpha_3 = \pi/12$ in Figure 7-13(a). Hence, the relationship between (Y_4, Y_5) and $(\alpha_1, \alpha_2, \alpha_3, \alpha_4)$ can be approximately expressed by the combination of these two basic relationships.

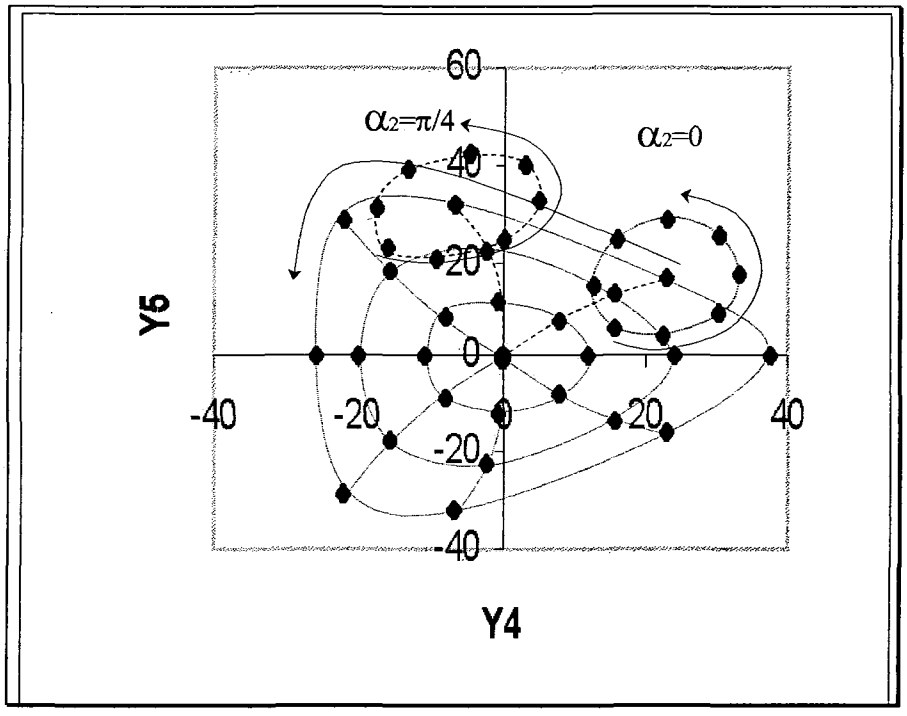

Figure 7-14 The combination of the basic relationships (Y_4,Y_5)-to-(α_1, α_2) and (Y_4,Y_5)-to-(α_3, α_4) shown by the sample data

Figure 7-15 illustrates the combination of the basic relationships using vectors. If the values of (α_1, α_2) are given, the values of (Y_4,Y_5) can be determined by the basic relationship (Y_4,Y_5)-to-(α_1, α_2). The values of (Y_4,Y_5) can be expressed by a vector. This vector is denoted as $v_{(45,b12)}(\alpha_1, \alpha_2)$. Also, if the values of (α_3, α_4) are given, the values of (Y_4,Y_5) can be determined by the basic relationship (Y_4,Y_5)-to(α_3, α_4). The values of (Y_4,Y_5) can also be expressed by a vector. This vector is

denoted as $v_{(45,b34)}(\alpha_3, \alpha_4)$. Therefore, the relationship between (Y_4, Y_5) and $(\alpha_1, \alpha_2, \alpha_3, \alpha_4)$ can be approximately expressed by

$$(Y_4, Y_5) = v_{45}(\alpha_1, \alpha_2, \alpha_3, \alpha_4) = v_{(45,b12)}(\alpha_1, \alpha_2) + v_{(45,b34)}(\alpha_3, \alpha_4)$$

Here, $v_{45}(\alpha_1, \alpha_2, \alpha_3, \alpha_4)$ is a vector expression of the values of (Y_4, Y_5) which is determined by $(\alpha_1, \alpha_2, \alpha_3, \alpha_4)$.

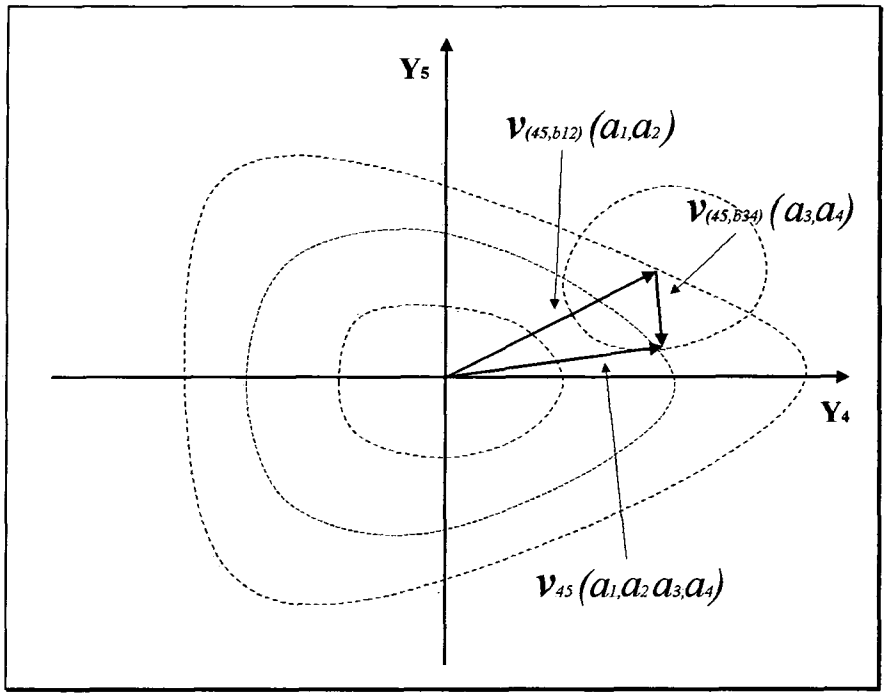

Figure 7-15 the vector expression of the combination of the two basic relationships

It should be noted that the above vector expression is an approximate expression which results from the sample data analysis. However, the accuracy of the expression is not given. In this project, the accuracy of the expression is not very important. The important result of the analysis is that the qualitative relationship between (Y_4, Y_5) and $(\alpha_1, \alpha_2, \alpha_3, \alpha_4)$ is identified. That is, there are two closed curve families in the plane Y_4-Y_5, which are Type 3 curves discussed in Section 6.3.2.2. If the values of $(\alpha_1, \alpha_2, \alpha_3, \alpha_4)$ are given, the values of (Y_4, Y_5) can be determined by the cross point of the two curves in the plane Y_4-Y_5, from the two curve families. This important characteristic can be used to build up a numerical algorithm to search the value of $(\alpha_1, \alpha_2, \alpha_3, \alpha_4)$, which will be discussed in the next chapter. In the

algorithm, the approximate vector expression of the relationship can be used to set initial values.

If the positional variables α_5 and *lm* are fixed, it is known that any given values of $(\alpha_1, \alpha_2, \alpha_3, \alpha_4)$ can determine the values of (Y_4, Y_5). However, given values of (Y_4, Y_5) cannot determine values of $(\alpha_1, \alpha_2, \alpha_3, \alpha_4)$. In other words, a given vector $v_{45}(\alpha_1, \alpha_2, \alpha_3, \alpha_4)$ corresponds to a set of values of $(\alpha_1, \alpha_2, \alpha_3, \alpha_4)$. Geometrically, this set of values of $(\alpha_1, \alpha_2, \alpha_3, \alpha_4)$ corresponds to a set of geometrical statuses of the top platform. The following discussions are an approximate geometrical explanations for given values of (Y_4, Y_5) in some particular situation.

Situation 1, $[v_{45}(\alpha_1, \alpha_2, \alpha_3, \alpha_4) = 0$, *e.g.* $(Y_4, Y_5) = (0,0)]$:

In Situation 1, if (α_1, α_2)=(0, 0), it is known that (α_3, α_4) = (0, 0). Geometrically, this corresponds to the status that the M-bar is perpendicular to the platform and the base.

In Situation 1, but $(\alpha_1, \alpha_2) \neq (0, 0)$, the discussion is as follows.

- According to the basic relationship (Y_4, Y_5)-to-(α_1, α_2), it is known that if $\alpha_1 \neq 0$, say, $\alpha_1 = \alpha_0$, there is a nonzero vector $v_{(45,b12)}$ (α_1, α_2) in the plane Y_4-Y_5 (see Figure 7-16(a')). Geometrically, this corresponds to the status that there is an angle between the M-bar and the z-axis of the Base frame (see Figure 7-16(a)).

- In addition, according to the basic relationship (Y_4, Y_5)-to-(α_3, α_4), it is known that if $\alpha_3 \neq 0$ say $\alpha_3 = \alpha_0$, there is a nonzero vector $v_{(45,b34)}$ (α_3, α_4) in the plane Y_4-Y_5 (see Figure 7-16(b')). Geometrically, this corresponds to the status that there is an angle between the z-axis of the Platform frame and the M-bar (see Figure 7-16(b)).

- Moreover, according to the combination of the basic relationships (Y_4, Y_5)-to-(α_1, α_2) and (Y_4, Y_5)-to-(α_3, α_4), it is known that if $\alpha_3 = \alpha_1 = \alpha_0$ and $\alpha_2 = \alpha_4$, then $v_{(45,b12)}(\alpha_1, \alpha_2) \cong -v_{(45,b34)}(\alpha_3, \alpha_4)$. Combining the situations shown in Figure 7-16(a) and 6(b), it is known that if $(\alpha_1, \alpha_2) \neq (0, 0)$ but $\alpha_3 = \alpha_1$ and $\alpha_2 = \alpha_4$ then $v_{45}(\alpha_1, \alpha_2, \alpha_3, \alpha_4) = v_{(45,b12)}(\alpha_1, \alpha_2) + v_{(45,b34)}(\alpha_3, \alpha_4) \cong \mathbf{0}$ (see Figure 7-16(b')). Geometrically, this corresponds to the status that the angle between the z-axis of the Platform frame and the M-bar is the same as the angle between the M-bar and the z-axis of the Base frame. Also, the plane formed by the M-bar and the z-axis of the Base frame and the plane formed by the z-axis of the Platform frame and the M-bar are in one plane (see Figure 7-16(c)).

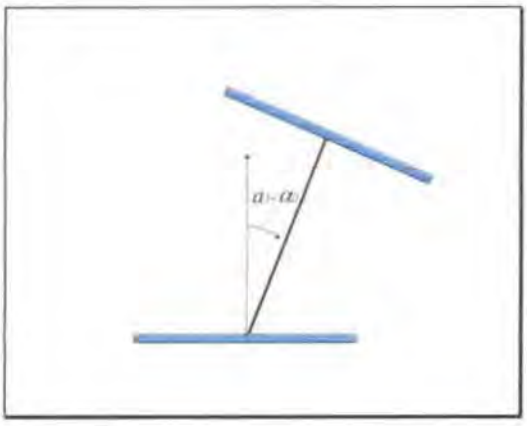

(a)

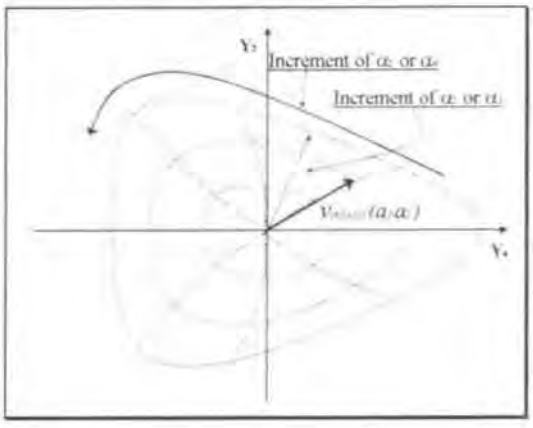

(a')

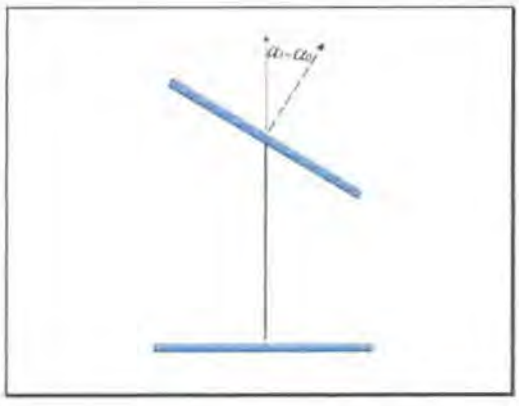

(b)

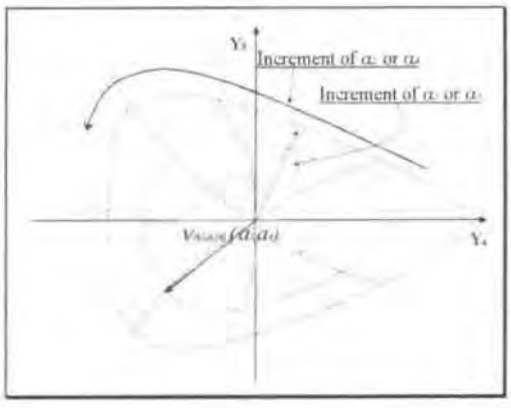

(b')

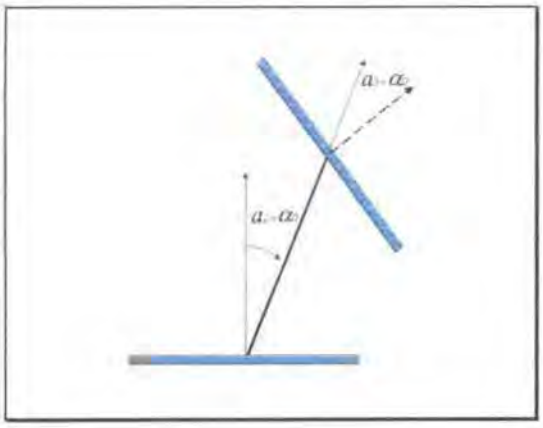

(c)

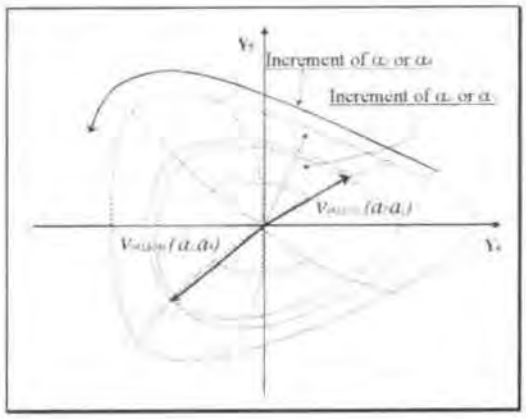

(c')

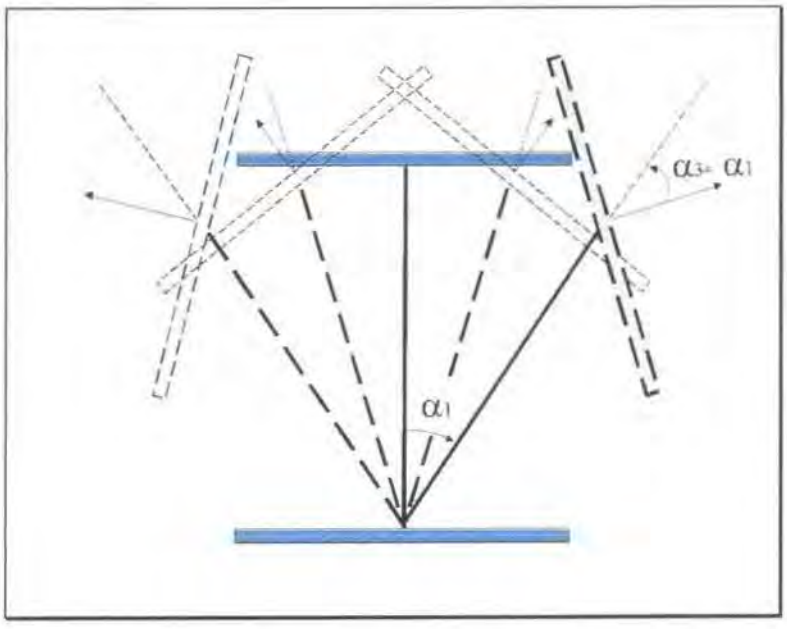

(d)

Figure 7-16 Given (Y_4, Y_5)=(0,0) corresponds to a set of statuses of the platform

Hence, if $\boldsymbol{v}_{45}(\alpha_1, \alpha_2, \alpha_3, \alpha_4) = 0$ but $(\alpha_1, \alpha_2) \neq (0, 0)$, then $\alpha_3 \cong \alpha_1$ and $\alpha_2 \cong \alpha_4$. For $\boldsymbol{v}_{45}(\alpha_1, \alpha_2, \alpha_3, \alpha_4) = 0$ and different values of (α_1, α_2), the set of the statuses of the platform are shown in Figure 7-16(d).

Situation 2, *[$\boldsymbol{v}_{45}(\alpha_1, \alpha_2, \alpha_3, \alpha_4) \neq \boldsymbol{0}$, e.g. $(Y_4, Y_5) \neq (0,0)$]:*

The discussions for the situation $\boldsymbol{v}_{45}(\alpha_1, \alpha_2, \alpha_3, \alpha_4) \neq \mathbf{0}$, say $\boldsymbol{v}_{45}(\alpha_1, \alpha_2, \alpha_3, \alpha_4) = \bar{v}_{45} \neq \mathbf{0}$, are as follows.

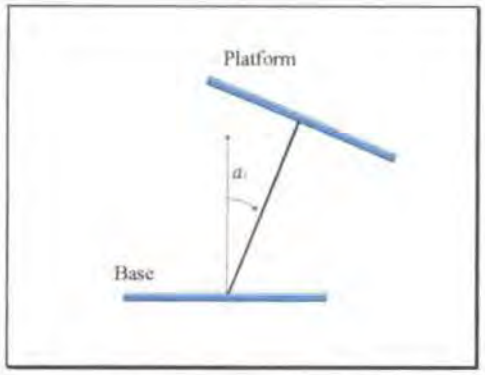

(a)

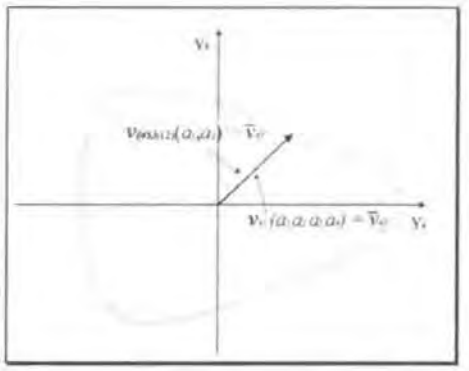

(a')

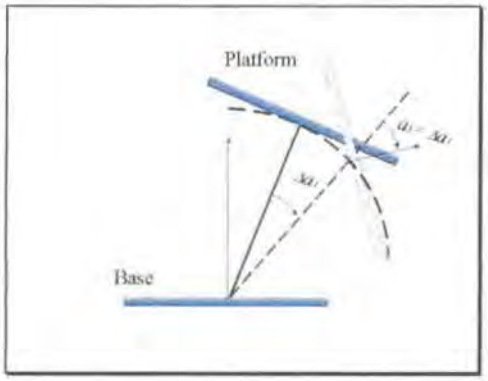

(b)

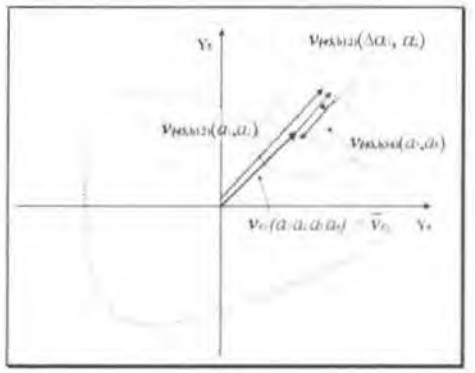

(b')

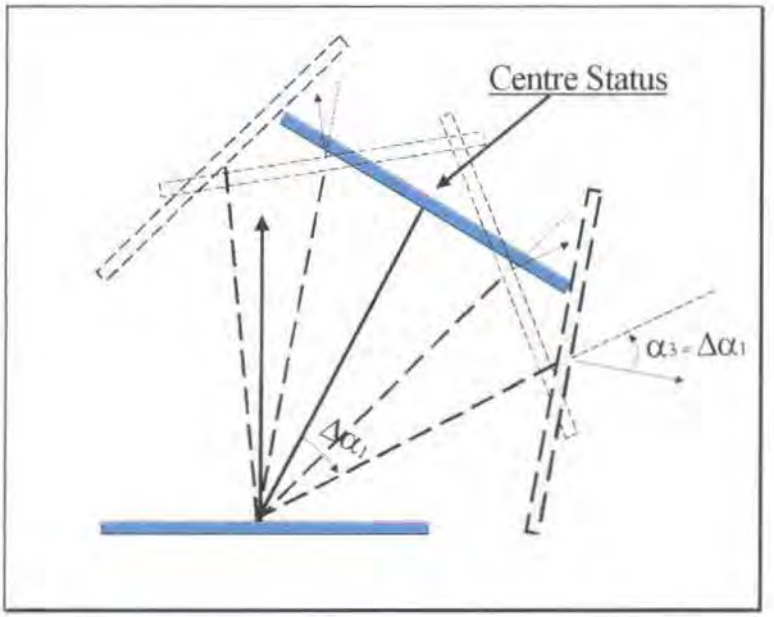

(c)

Figure 7-17 Given (Y_4, Y_5), the corresponding set of statuses of the platform

In Situation 2, if $(\alpha_3, \alpha_4) = (0, 0)$, it is known that $\alpha_1 \neq 0$. According to the basic relationship (Y_4, Y_5)-to-(α_1, α_2), it is known that there is a nonzero vector $v_{(45,b12)}(\alpha_1, \alpha_2) = \bar{v}_{45}$ in the plane Y_4-Y_5 (see Figure 7-16(a')). Geometrically, this corresponds to the status that the M-bar is perpendicular to the platform but there is an angle between the z-axis of the Base frame and the M-bar (see Figure 7-17(a)). The status of the platform corresponding to $v_{45}(\alpha_1, \alpha_2, \alpha_3, \alpha_4) = \bar{v}_{45}$ and $(\alpha_3, \alpha_4) = (0, 0)$ is called the centre status of $v_{45}(\alpha_1, \alpha_2, \alpha_3, \alpha_4) = \bar{v}_{45}$.

For the situation $v_{45}(\alpha_1, \alpha_2, \alpha_3, \alpha_4) = \bar{v}_{45} \neq \mathbf{0}$ and $(\alpha_3, \alpha_4) \neq (0, 0)$, the discussions are based on the centre status of $v_{45}(\alpha_1, \alpha_2, \alpha_3, \alpha_4) = \bar{v}_{45}$. Here, the situation based on the centre status where α_2 is fixed and α_1 is changed will be discussed.

Based on the centre status of $v_{45}(\alpha_1, \alpha_2, \alpha_3, \alpha_4) = \bar{v}_{45}$ if α_2 is fixed and α_1 is changed, it is known that the length of the vector $v_{(45,b12)}(\alpha_1, \alpha_2)$ in the plane Y_4-Y_5 will be changed, but the direction of the vector $v_{(45,b12)}(\alpha_1, \alpha_2)$ will not be changed. If α_1 increases $(\Delta\alpha_1)$, then $v_{(45,b12)}(\alpha_1, \alpha_2)$ will become $\bar{v}_{45} + v_{(45,b12)}(\Delta\alpha_1, \alpha_2)$ (see Figure 7-17(b')). According to the combination of the basic relationships (Y_4, Y_5)-to-(α_1, α_2) and (Y_4, Y_5)-to-(α_3, α_4), it is known that if $\alpha_3 = \Delta\alpha_1$ and $\alpha_4 = \alpha_2$, then $v_{(45,b34)}(\alpha_3, \alpha_4) \cong v_{(45,b12)}(\Delta\alpha_1, \alpha_2)$. That is, if $\alpha_3 = \Delta\alpha_1$ and $\alpha_4 = \alpha_2$, then $v_{45}(\alpha_1, \alpha_2, \alpha_3, \alpha_4) \cong v_{(45,b12)}(\alpha_1, \alpha_2) + v_{(45,b34)}(\alpha_3, \alpha_4) \cong \bar{v}_{45}$.

Geometrically, this corresponds to the statuses of the platform, in which the angle between the actual M-bar and the M-bar of the centre status equals the angle between the z-axis of the Platform frame and the M-bar. Also, the plane formed by the actual M-bar and the M-bar of the centre status and the plane formed by the z-axis of the Platform frame and the M-bar are in one plane (see Figure 7-17(c)).

Generally, given $v_{45}(\alpha_1, \alpha_2, \alpha_3, \alpha_4) = \bar{v}_{45}$, the corresponding geometrical status of the platform can be approximately viewed as that the platform tilts from the centre

status of $v_{45} = \bar{v}_{45}$ outward with the same angle as the angle between the actual M-bar and the M-bar of the centre status. Although much further discussion is possible, this section has its purpose to approximately illustrate the relationship between the values of (Y_4, Y_5) and the corresponding geometrical statuses. Although further discussion is possible this section has now served its purpose to illustrate two of the important structures

Conclusions for the relationship between (Y_4, Y_5) and $(\alpha_1, \alpha_2, \alpha_3, \alpha_4)$:

- Generally, the principal component pair (Y_4, Y_5) mainly relates to the position variable pair (α_1, α_2) and (α_3, α_4).

- Any given vector v_{45} in the principal component plane Y_4-Y_5 can be viewed as a combination of two other vectors $v_{(45,b12)}$ and $v_{(45,b34)}$ that is,

$$(Y_4, Y_5) = v_{45}(\alpha_1, \alpha_2, \alpha_3, \alpha_4) = \mathbf{v}_{(45,b12)}(\alpha_1, \alpha_2) + \mathbf{v}_{(45,b34)}(\alpha_3, \alpha_4)$$

  Here, the vector, $\mathbf{v}_{(45,b12)}(\alpha_1, \alpha_2)$, is determined by the basic relationship(Y_4, Y_5)-to-(α_1, α_2) and the vector $\mathbf{v}_{(45,b34)}$ is determined by the basic relationship (Y_4, Y_5)-to-(α_3, α_4).

- The geometrical meaning of a vector in the principal component plane Y_4-Y_5 can be approximately interpreted as a set of platform statuses. Every vector value corresponds to one set of statuses. Every one set of statuses has one centre status. Around this centre status, the platforms tilt from the centre status outward.

7.3.3.2.3 The relationship between the relative change of (α_1, α_2) and the relative change of (Y_4, Y_5)

It is known that the position of the M-bar can be determined by the variables $(\alpha_1\ \alpha_2)$. It is also known that the basic relationship between $(\alpha_1\ \alpha_2)$ and (Y_4, Y_5) can be expressed by a closed-curve family as shown in Figure 7-11(a). However, if the position of the M-bar is changed, the positional change of the M-bar relative to its previous position will cause a change of (Y_4, Y_5). Because of the requirement of the

numerical algorithm that will be discussed in Chapter 8, the relationship between the relative change of $(\alpha_1\ \alpha_2)$ and the relative change of (Y_4, Y_5) needs to be identified.

Figure 7-18 shows a relative change of the position of the M-bar (a) and the corresponding relative change of the principal components (Y_2, Y_3) (b).

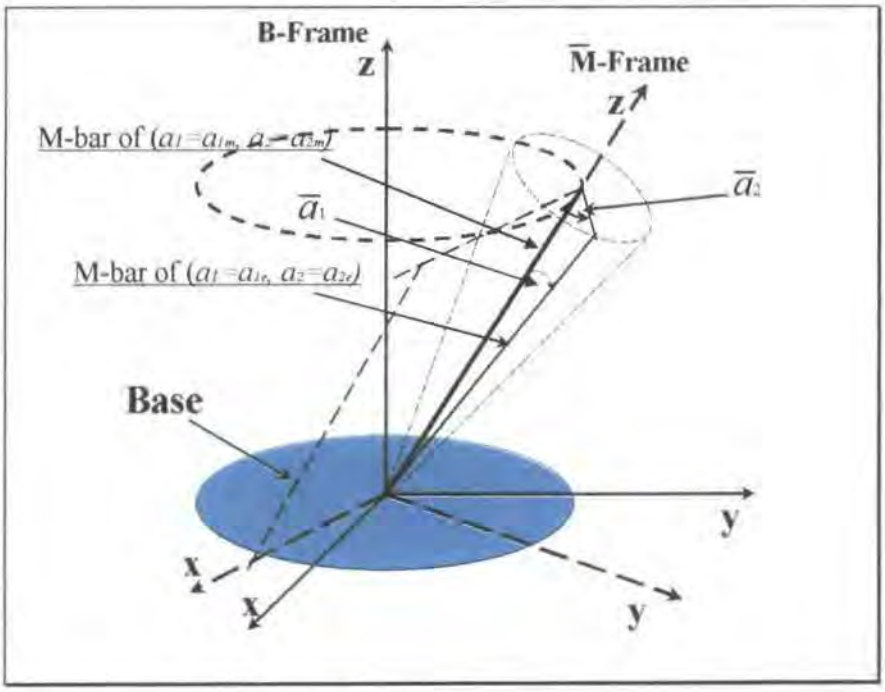

Figure 7-18(a)

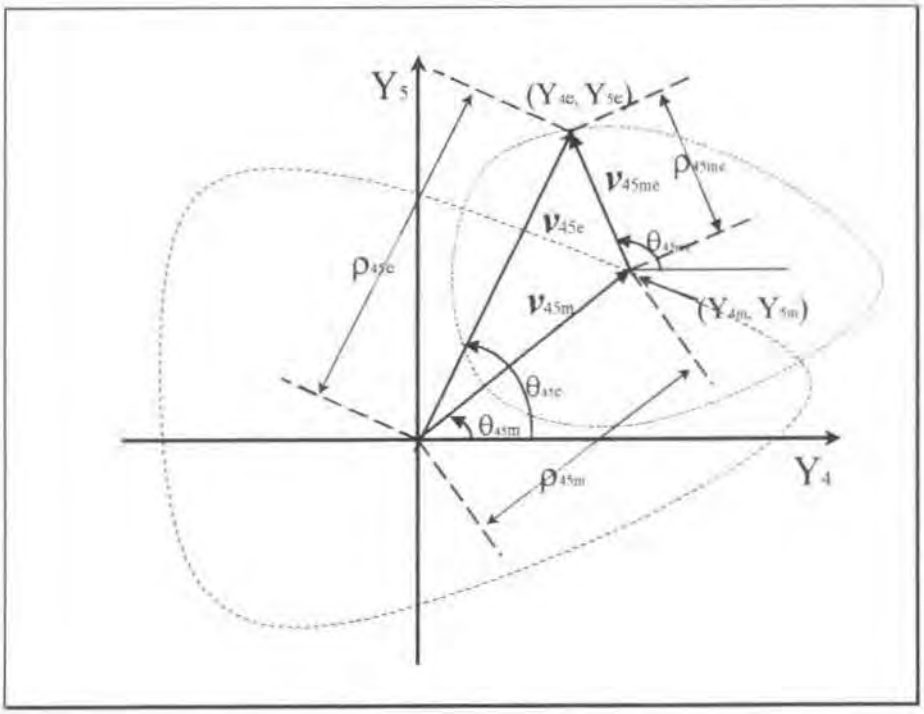

Figure 7-18(b)

If the M-bar moves from (α_1=0, α_2=0) to (α_1= α_{1m}, α_2= α_{2m}) (see Figure 7-18 (a)), there is a vector v_{45om} in the Y_4-Y_5 plane corresponding to the new position of (α_1= α_{1m}, α_2= α_{2m}) (see Figure 7-18 (b)). If the M-bar moves from (α_1= α_{1m}, α_2= α_{2m}) to (α_1= α_{1e}, α_2= α_{2e}), there is a vector v_{45oe} in the Y_4-Y_5 plane corresponding to the new position α_1= α_{1e}, α_2= α_{2e}. Based on the basic relationship (Y_4,Y_5)-to-(α_1 α_2), the values of vectors v_{45om} and v_{45oe} can be determined by the values (α_{1m}, α_{2m}) and (α_{1e}, α_{2e}) respectively. However, the relationship between the positional difference (α_{1e}, α_{2e}) -(α_{1m}, α_{2m}) and the vector difference v_{45me}= v_{45oe} - v_{45om} has not yet been discussed. Here, a new frame and new variables, which are used to measure the positional difference, introduced as follows.

Once again, referring to Figure 7-18(a), the $\overline{M}$ -Frame is defined by the M-Frame in which the M-bar is at the position α_1= α_{1m}, α_2= α_{2m}.

The variable $\bar{a}_1$ is defined as the angle between the M-bar and the z-axis of the $\overline{M}$ -Frame.

The variable $\bar{a}_2$ is defined as the angle between the x-z plane of the $\overline{M}$ -Frame and the plane formed by the z-axis of M-bar and the z-axis of the $\overline{M}$ -Frame.

Here the definition of the new variables $\bar{a}_1$ and $\bar{a}_2$ is similar to the definition of the variables α_1 and α_2, but the reference frame is the $\overline{M}$ -Frame instead of the usual B-Frame. Therefore, the variables $\bar{a}_1$ and $\bar{a}_2$ express the M-bar position relative the $\overline{M}$ -Frame and the variables α_1 and α_2 express the M-bar position relative the B-Frame.

Obviously, if α_{1m}= 0 and α_{2m}= 0 the relationship (Y_4,Y_5)-to-($\bar{a}_1$, $\bar{a}_2$) is the same as the basic relationship(Y_4,Y_5)-to-(α_1 α_2). In fact, if $\alpha_{1m} \neq 0$ the relationship (Y_4,Y_5)-to-($\bar{a}_1$, $\bar{a}_2$) can be viewed as the combination of the relationship(Y_4,Y_5)-to-(α_{1m}, α_{2m}) and the relationship (Y_4,Y_5)-to-($\bar{a}_1$, $\bar{a}_2$). Because the discussion of this combination is similar to the discussion of the combination of the basic relationships (Y_4, Y_5)-to-(α_1, α_2) and (Y_4, Y_5)-to-(α_3, α_4), the details will not be

repeated. Thus, here only the results of the analysis are given. If the differences Y_{4e} - Y_{4m} and Y_{5e} - Y_{5m} are denoted as $Y_{4me} = Y_{4e} - Y_{4m}$ and $Y_{5me} = Y_{5e} - Y_{5m}$ respectively, the relationship between (Y_{4me}, Y_{5me}) and ($\bar{a}_1$, $\bar{a}_2$) can be expressed as follows.

$$\bar{a}_1 = 0.0242\,\bar{\rho}_{45me} = 0.0067\sqrt{Y_{4me}^2 + Y_{5me}^2}$$

$$= 0.0067\sqrt{(Y_{4e} - Y_{4m})^2 + (Y_{5e} - Y_{5m})^2}$$

$$\bar{a}_2 = 0.9924\,\bar{\theta}_{45me} - 0.7586$$

$$\approx \bar{\theta}_{45me} - \pi/4$$

$$= \mathrm{atan}(Y_{5me}/Y_{4me}) - \pi/4$$

$$= \mathrm{atan}\left(\frac{Y_{5e} - Y_{5m}}{Y_{4e} - Y_{4m}}\right) - \pi/4$$

Chapter 8

The PCA Based Numerical Algorithm for a 6-6 Stewart Platform

Through the PCA based analysis, the relationships between the principal components and the positional variables have been identified. Based on the relationships, the principal components can be used to determine the values of the positional variables. The PCA based numerical algorithm is an algorithm which searches the positional variable values using given principal component values. Because every principal component is a linear combination of the lengths of the six links, the PCA based numerical algorithm is a numerical approach to obtain the values of the positional variables using the lengths of the six links. For different assembly configurations, the relationships between the principal components and the positional variables may be different. Consequently, the numerical algorithms must also be different. The following is a numerical algorithm for the case discussed in the last section.

8.1 The Top-level Framework of the Numerical Algorithm

Through the PCA based analysis, two one-to-one relationships have been identified. Those are the relationship between the length of the M-bar (*lm*) and the first principal component (Y_1) and the relationship between the angle 5 (α_5) and the sixth principal component (Y_6). By using these two one-to-one relationships, *lm* and α_5 can be determined using the first or the sixth principal components (Y_1 or Y_6) respectively, if the other five of the six positional variables are known. Also, it is known that the values of the positional variables α_1, α_2, α_3 and α_4 can be determined by the principal components Y_2, Y_3, Y_4, Y_5, if the variables *lm* and α_5 are known. However, any one of the positional variables α_1, α_2, α_3 and α_4 cannot be determined by only one of the principal components Y_2, Y_3, Y_4, Y_5. Thus, the numerical algorithm consists of three search blocks. These three blocks are; the block for searching for the value of the variable *lm*, the block for searching for the value of

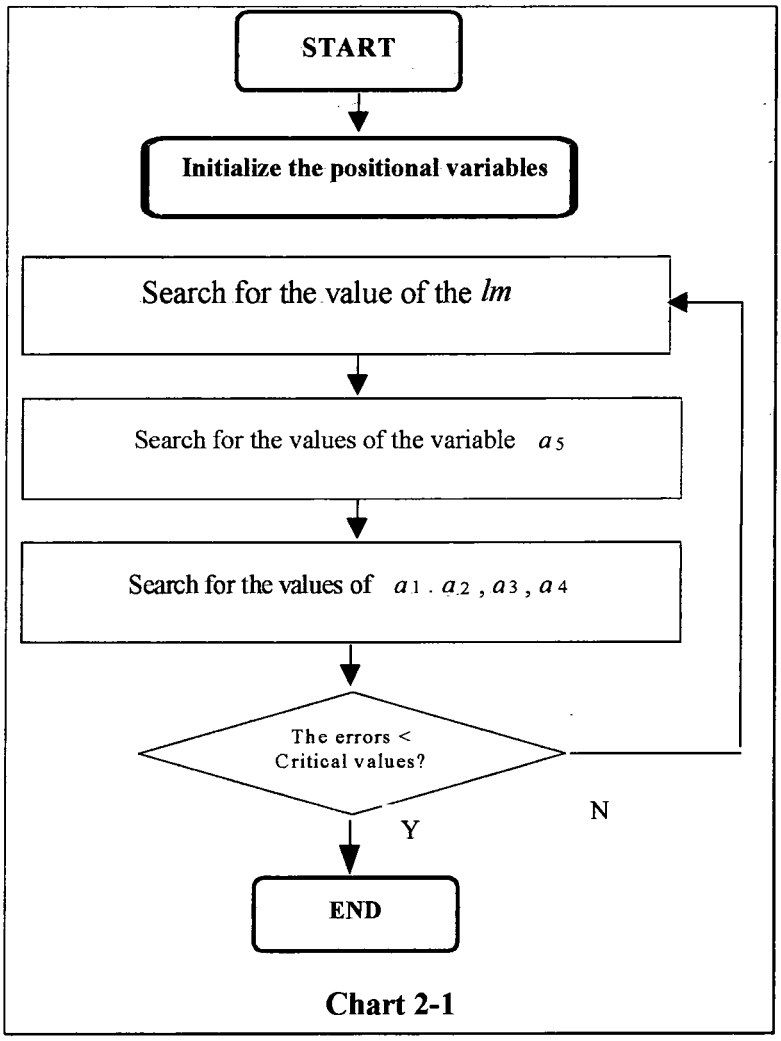

Chart 2-1

the variable α_5 and the block for searching for the values of the variables α_1, α_2, α_3 and α_4 (see Chart 2-1). At the beginning of the search, every positional variable is given an initial value. There is no special requirement for the initial values in this algorithm, as long as the given initial values are in the range in which the relationships are identified. During the computing simulation, the initial values were given by $\alpha_1 = \alpha_2 = \alpha_3 = \alpha_4 = \alpha_5 = 0$ and $lm = 150$. After initialising the positional variables, the corresponding initial principal component values can be obtained. Therefore, the algorithm decides its searching directions based on the difference of the principal components between the initial values and the given values. In this algorithm, three searching blocks work in turn until the errors of all the positional variables α_1, α_2, α_3, α_4, α_5 and *lm* are less than previously given critical values. In this algorithm, the critical values of the errors are based on the principal component values. That is, if one of the differences between the given values of the principal

components and the obtained principal component values is greater than the corresponding critical value, the obtained values of variables α_1, α_2, α_3, α_4, α_5 and *lm* become the new initial values for the next search loop. In fact, every searching block has its own critical value or values. When a block stops searching, the searched result output will meet the accuracy requirement. However, after the next search block output a new result, the principal component value corresponding to the positional variable output by the previous block, may be changed. So when the main search program checks the critical value, the positional variables α_1, α_2, α_3, α_4 meet their critical values, but α_5 or *lm* may not meet its critical value. If this is the case, the main search program will continue searching. It should be noted that this algorithm is for application to a stepwise robotic positioning system. Hence, the critical value setting should be based on the accuracy requirement of the measurement and the relationships between the principal components and the positional variables. In this case, critical values of every bottom level sub-algorithm are directly based on the positional variable. This is because, during the search in a bottom level sub-algorithm, the values of the positional variable in different steps of the search can directly be used. This will be clearer after discussing the details of the sub-algorithm in the next sections. However, at the main output of the algorithm, the critical values are based on the principal components. According to the relationships between the principal components and the positional variables, the measurement accuracy requirement can be transformed to critical values of principal components. Here, it is supposed that the allowable errors of the positional variables (α_1, α_2, α_3, α_4, α_5, *lm*) are (ε_1,ε_2,ε_3,ε_4,ε_5, ε_{lm}). Also, the given principal component values are Y_{1o}, Y_{2o}, Y_{3o}, Y_{4o}, Y_{5o}, Y_{6o}. According to the regression functions which has been described in Chapter 7, the critical values are given as follows:

$|Y_{1o}-Y_1| < \varepsilon_{lm}$,

$|Y_{6o}-Y_6| < 76\varepsilon_5$,

$|\sqrt{Y_{2o}^2+Y_{3o}^2} - \sqrt{Y_2^2+Y_3^2}| < 149\varepsilon_1$

$|\text{atan}(Y_{3o}/Y_{2o}) - \text{atan}(Y_3/Y_2)| < \varepsilon_2$

$$|\sqrt{Y_{4o}^2 + Y_{5o}^2} - \sqrt{Y_4^2 + Y_5^2}| < 4\varepsilon_3$$

$$|\text{atan}(Y_{5o}/Y_{4o}) - \text{atan}(Y_5/Y_4)| < \varepsilon_4$$

The two one-to-one relationships have the property such that if the principal component (Y_1 or Y_6) increases, the corresponding positional variable (*lm* or α_5) increase. Therefore, an algorithm for searching the value of a single-variable increasing function can be used to search the values of the variables *lm* and α_5 respectively. However, to search the values of the positional variables (α_1, α_2, α_3, α_4), a special algorithm needs to be given. The next two sections are the details of the above algorithms.

8.2 An Algorithm for Searching for the Value of a Single-variable Increasing Continuous Function

It is generally assumed that a single-variable, increasing, continuous function is y = f(x). Here, y is a dependent variable corresponding to the positional variable *lm* or α_5

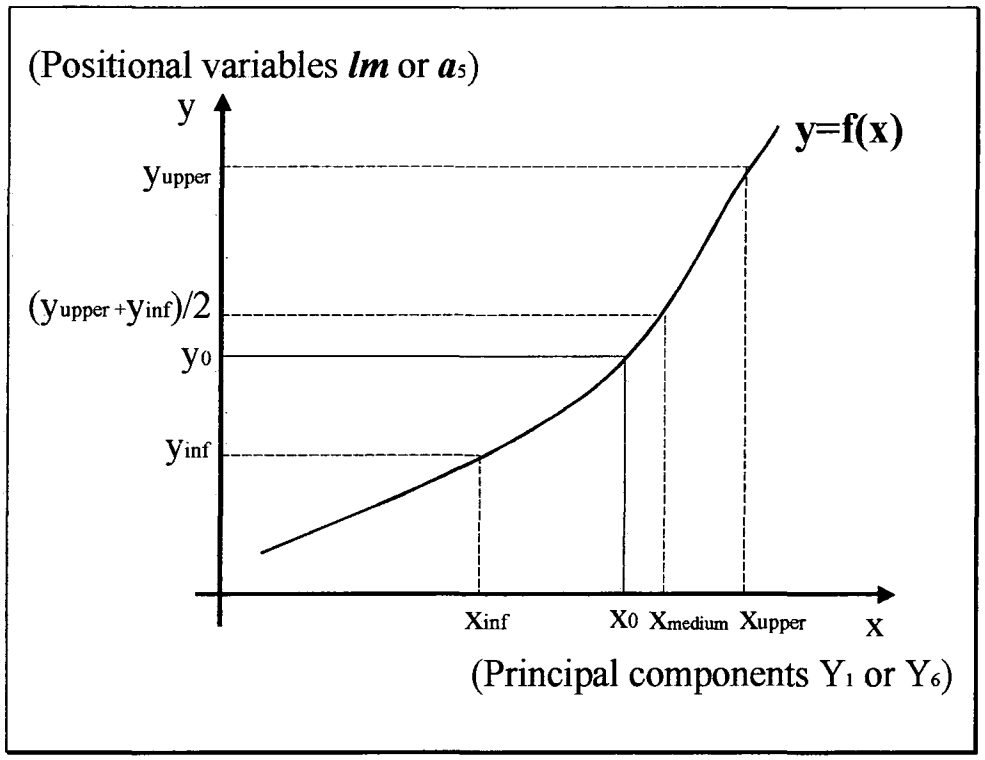

Figure 8-1 A single-variable, increasing and continuous function

in this case, and x is an independent variable corresponding to the principal

component Y_1 or Y_6 in this case. It is also assumed that the inverse function x = f^{-1}(y) is computable. When the independent variable x is given a value x_0, the dependent variable y should have a corresponding value $y_0 = f(x_0)$. The problem is how to obtain the approximate value of y_0, when x_0 is given

In this algorithm, a closed interval $[y_{inf}, y_{upper}]$ along the y-axis is applied (see Figure 8-1).

If $y_0 \in [y_{inf}, y_{upper}]$ i.e. $y_{inf} \le y_0 \le y_{upper}$, the closed interval $[y_{inf}, y_{upper}]$ can be split into two closed intervals $[y_{inf}, (y_{inf} + y_{upper})/2]$ and $[(y_{inf} + y_{upper})/2, y_{upper}]$. The value y_0 must be in one of these two closed interval, say $y_{inf} \le y_0 \le (y_{inf} + y_{upper})/2$. Then this closed interval is denoted as a new $[y_{inf}, y_{upper}]$. This process cuts off half of the closed interval $[y_{inf}, y_{upper}]$, and y_0 is always in the remaining new closed interval $[y_{inf}, y_{upper}]$. This process will continue until the value $y_{upper} - y_{inf}$ is less than the given allowable error. The details of the algorithm are as follows.

Firstly, the dependent variable y is given two different initial values $y_{inf} < y_{upper}$, then the two corresponding values x_{inf}, x_{upper} ($x_{inf} < x_{upper}$) can be calculated by using the inverse function $x=f^{-1}(y)$. At this moment, there are three possible situations (case 1,2,3).

- Case 1: One of the values of x_{inf}, x_{upper} equals the value x_0, say $x_{inf} = x_0$. The corresponding value $y_{inf} = f(x_{inf})$ is the solution, i.e. $y_{inf} = y_0$. In this situation, the algorithm stops the search and outputs the search result.
- Case 2: The values of x_{inf} and x_{upper} do not equal the value x_0, and $x_0 \notin [x_{inf}, x_{upper}]$ (i.e. $x_{inf} < x_{upper} < x_0$ or $x_0 < x_{inf} < x_{upper}$). Correspondingly, the value of y is $y_0 \notin [y_{inf}, y_{upper}]$ (i.e. $y_{inf} < y_{upper} < y_0$ or $y_0 < y_{inf} < y_{upper}$). In this situation, the interval $[y_{inf}, y_{upper}]$ should be expanded, so that y_0 can be finally in a new interval $[y_{inf}, y_{upper}]$. In this algorithm, the length of the interval is doubled each time. If $x_{inf} < x_{upper} < x_0$, then $y_{inf\ (new)} \leftarrow y_{inf}$ and $y_{upper\ (new)} \leftarrow y_{upper} + (y_{upper} - y_{inf})$.

If $x_0 < x_{inf} < x_{upper}$, then $y_{upper\ (new)} \leftarrow y_{upper}$ and $y_{inf\ (new)} \leftarrow y_{inf} - (y_{upper} - y_{inf})$. Then $y_{inf\ (new)}$ is denoted as y_{inf} and $y_{upper\ (new)}$ is denoted as y_{upper}. Then, the algorithm loops to the start point to calculate the values x_{inf} and x_{upper}.

- Case 3: The values of x_{inf} and x_{upper} do not equal the value x_0, but $x_0 \in [x_{inf}, x_{upper}]$ (i.e. $x_{inf} < x_0 < x_{upper}$). Correspondingly, the values of y are $y_0 \in [y_{inf}, y_{upper}]$ (i.e. $y_{inf} < y_0 < y_{upper}$). In this situation, the new value of y is given by $y_{(new)} = (y_{inf} + y_{upper})/2$ and the corresponding value of x, $x_{(new)}$ is computed by $x_{(new)} = f^{-1}(y_{(new)})$. If $x_{(new)} < x_0$, then $y_{(new)}$ is denoted as y_{inf}. If $x_{(new)} > x_0$, then $y_{(new)}$ is denoted as y_{upper}. Then, the algorithm loops to the start point to calculate the values x_{inf} and x_{upper}.

After an initial interval $[y_{inf}, y_{upper}]$ is given, the above process will continue until the value $y_{upper} - y_{inf}$ is less than a critical value. There is no special requirement for setting the initial interval. As long as, the initial interval is in a range, in which the relationship analysis has been carried out, the algorithm will be convergent. Therefore, the initial interval can be chosen randomly. In this case, the regression functions that have been obtained during the relationship analysis can be used to set the initial interval, so that the initial values y_{inf} and y_{upper} are likely to be closer to the solution y_0 than that which was randomly selected. It should be noted that the regression function that has been obtained during the relationship analysis is approximately true for all positional variable values (α_1, α_2, α_3, α_4, α_5, *lm*). However, it is not exactly true for particular values of the positional variables (α_1, α_2, α_3, α_4, α_5 *lm*). For example, during the data analysis, the relationship between the positional variable *lm* and the principal component Y_1 has been analysed. The regression function obtained was (Chapter 7)

$$lm = 0.4134 Y_1 - 4.2645$$

It approximately expresses the relationship between *lm* and Y_1 for all values of α_1, α_2, α_3, α_4, α_5. However, for different values of α_1, α_2, α_3, α_4, α_5, the actual

relationships between *lm* and Y_1 are different (see Figure 8-2). The regression function is an approximate expression of the relationship between the variable *lm* and the principal component Y_1. Therefore, the regression function cannot directly determine the actual value of *lm*, but it can be used to give an approximate value of *lm* as an initial value. Because the algorithm needs an initial interval, it needs two initial values. The following shows how to use the regression function to set the initial interval of *lm*. If the principal component Y_1 is given a value, say Y_{1o}. The estimated value $lm_{ini} = 0.4134Y_{1o} - 4.2645$ can be obtained. Normally, this value lm_{ini} is not the solution lm_o because the regression function is only an approximate function that has an estimating error (see Figure 8-2).

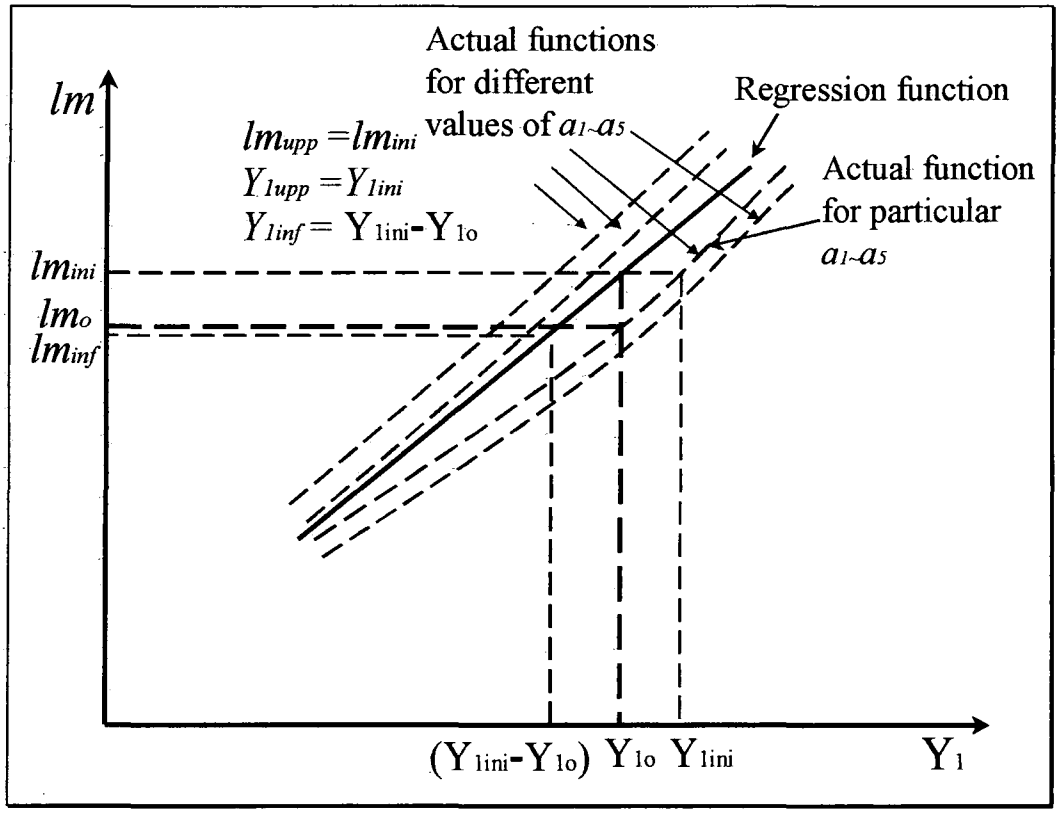

Figure 8-2 the functions for different values of $(\alpha_1, \alpha_2, \alpha_3, \alpha_4, \alpha_5)$

It is known that if the positional variables (*lm*, α_1, α_2, α_3, α_4, α_5) are known, the principal components can be obtained easily. Hence, after obtaining lm_{ini}, the

principal component value Y_{1ini} can be easily computed. If $Y_{1ini} > Y_{1o}$, it means that $lm_{ini} > lm_o$. In this situation, lm_{upper} is given the value of lm_{ini}, i.e.

$$lm_{upper} = lm_{ini}$$

and lm_{inf} is given by

$$lm_{inf} = 0.4134[Y_{1o} + (Y_{1o} - Y_{1ini})] - 4.2645$$

If $Y_{1ini} < Y_{1o}$, it means that $lm_{ini} < lm_o$. In this situation, lm_{inf}, is given the value of lm_{ini}, i.e.

$$lm_{inf} = lm_{ini}$$

and lm_{upper} is given by

$$lm_{upper} = 0.4134[Y_{1o} + (Y_{1o} - Y_{1ini})] - 4.2645$$

Summarising the above two cases, the initial interval can be set by

$$lm_{inf} = \min\{0.4134Y_{1o}, 0.4134[Y_{1o} + (Y_{1o} - Y_{1ini})]\} - 4.2645$$

$$lm_{upper} = \max\{0.4134Y_{1o}, 0.4134[Y_{1o} + (Y_{1o}, - Y_{1ini})]\} - 4.2645$$

The following is the flow diagram of the algorithm for searching the value of a single-variable, increasing and continuous function.

Start

Initialisation of the interval of y: $[y_{inf}, y_{upp}]$

Loop

Calculation of the value of $x_{inf} = f^{-1}(y_{inf})$, $x_{upp} = f^{-1}(y_{upp})$

Case 1 $(x_0 - x_{inf})(x_0 - x_{upp}) = 0$

If $x_0 = x_{inf}$, **then** $y_0 \leftarrow y_{inf}$

If $x_0 = x_{upp}$, **then** $y_0 \leftarrow y_{upp}$

End

Case 2 $(x_0 - x_{inf})(x_0 - x_{upp}) > 0$

If $x_0 < x_{inf}$, **then** $y_{inf} \leftarrow y_{inf} - (y_{upp} - y_{inf})$

If $x_0 > x_{upp}$, **then** $y_{upp} \leftarrow y_{upp} + (y_{upp} - y_{inf})$

Case 3 $(x_0 - x_{inf})(x_0 - x_{upp}) < 0$

If $x_0 < (x_{inf} + x_{upp})/2$, **then** $y_{upp} \leftarrow (y_{inf} + y_{upp})/2$

Else $y_{inf} \leftarrow (y_{inf} + y_{upp})/2$

If $|y_{upp} - y_{inf}| < \varepsilon$, **then** $y_0 \leftarrow (y_{inf} + y_{upp})/2$, **End**

Else $y_{inf} \leftarrow (y_{inf} + y_{upp})/2$

End Loop

End

Here, ε is a critical value. The variable x corresponds to the principal component (Y_1 or Y_6). The variable y corresponds to the positional variable (*lm* or α_5). Function $f^{-1}(.)$ corresponds to the calculation for the inverse problem solution. The symbol, '←', means 'is given a value'

8.3 Algorithm for Searching for the Values of the Positional Variable α_1, α_2, α_3 and α_4

Searching for the values of the variables α_1, α_2, α_3 and α_4 by using the values of the principal components Y_2, Y_3, Y_4 and Y_5 needs to make use of the relationships between (α_1, α_2, α_3, α_4) and (Y_2, Y_3, Y_4, Y_5), which have been discussed in Chapter 7. It is known that the relationship between (α_1, α_2, α_3, α_4) and (Y_2, Y_3, Y_4, Y_5) can be expressed by two sub-relationships. These are the relationship between (Y_2, Y_3) and (α_1, α_2, α_3, α_4) and the relationship between (Y_4, Y_5) and (α_1, α_2, α_3, α_4). The value of (α_1, α_2, α_3, α_4) cannot be determined by use of only one of these two sub-relationships. To determine the value of (α_1, α_2, α_3, α_4), these two relationships need to be conjunct. Here, two, two-dimension planes (the planes of Y_2-Y_3, and Y_4-Y_5), in which the two relationships can be expressed graphically, are used to explain the search algorithm.

8.3.1 The Framework of the Algorithm for Searching for the Values of the Positional variable α_1, α_2, α_3 and α_4

If the principal components (Y_2,Y_3, Y_4, Y_5) are given any constant values ($\overline{Y}_2$, $\overline{Y}_3$, $\overline{Y}_4$, $\overline{Y}_5$) respectively, the vector variable v_{23} in the planes of Y_2-Y_3, and the vector variable v_{45} in the plane Y_4-Y_5 respectively are known (see Figure 8-3 (a1) (a2)), i.e. $v_{23} = \overline{v}_{23}$, $v_{45} = \overline{v}_{45}$. Here, $\overline{v}_{23}$ and $\overline{v}_{45}$ are known values of the vectors v_{23} and v_{45}. The vectors $\overline{v}_{23} = (\overline{Y}_2, \overline{Y}_3)$ and $\overline{v}_{45} = (\overline{Y}_4, \overline{Y}_5)$. Here, the vector $v_{23} = \overline{v}_{23}$ in the plane of Y_2-Y_3 can be viewed as a combination of two vectors $\overline{v}_{23} = v_{(23,b12)}(\alpha_1, \alpha_2) + v_{(23,b34)}(\alpha_3, \alpha_4)$ (see Figure 8-3 (b1)). The vector $v_{(23,b12)}(\alpha_1, \alpha_2)$ is determined by values (α_1, α_2) based on the basic relationship between (Y_2, Y_3)-to-(α_1, α_2), which have been discussed in Chapter 7. Also, the vectors $v_{(23,b34)}(\alpha_3, \alpha_4)$ is determined by (α_3, α_4) based on the basic relationship between (Y_2, Y_3)-to-(α_3, α_4), which have been discussed in Chapter 7. There are many different values of $(\alpha_1, \alpha_2, \alpha_3, \alpha_4)$ that satisfy the equation $\overline{v}_{23} = v_{(23,b12)}(\alpha_1, \alpha_2) + v_{(23,b34)}(\alpha_3, \alpha_4)$. Geometrically, the vector $v_{23} = \overline{v}_{23}$ approximately corresponds to a status set of the platform (see Figure 8-3 (c1)), which have the same orientation but different centre positions of the platform. The vector $v_{45} = \overline{v}_{45}$ in the plane of Y_4-Y_5 can also be viewed as a combination of two vectors $\overline{v}_{45} = v_{(45,b12)}(\alpha_1, \alpha_2) + v_{(45,b34)}(\alpha_3, \alpha_4)$ (see Figure 8-3 (b2)). The vector $v_{(45,b12)}(\alpha_1, \alpha_2)$ is determined by values (α_1, α_2) based on the basic relationships (Y_4, Y_5)-to-(α_1, α_2), which have been discussed in Chapter 7. Also, the vector $v_{(45,b34)}(\alpha_3, \alpha_4)$ is determined by values (α_3, α_4) based on the basic relationships (Y_4, Y_5)-to-(α_3, α_4), which have been discussed in Chapter 7. There are also many different values of $(\alpha_1, \alpha_2, \alpha_3, \alpha_4)$ that satisfy the equation $\overline{v}_{45} = v_{(45,b12)}(\alpha_1, \alpha_2) + v_{(45,b34)}(\alpha_3, \alpha_4)$. Geometrically, the vector $v_{45} = \overline{v}_{45}$ approximately corresponds to a status set of the platform (see Figure 8-3 (c2)), which have different orientations and different centre positions of the platform.

The problem is how to find a value (a'_1, a'_2, a'_3, a'_4) of the variable $(\alpha_1, \alpha_2, \alpha_3, \alpha_4)$ to satisfy the equations simultaneously,

$$\bar{v}_{23} = v_{(23;b12)}(a'_1, a'_2) + v_{(23,b34)}(a'_3, a'_4) \quad (2.4\text{-}1)$$

$$\bar{v}_{45} = v_{(45,b12)}(a'_1, a'_2) + v_{(45,b34)}(a'_3, a'_4) \quad (2.4\text{-}2)$$

Here, $\bar{v}_{23}$ and $\bar{v}_{45}$ are any given constant vectors $\bar{v}_{23} = (\bar{Y}_2, \bar{Y}_3)$ and $\bar{v}_{45} = (\bar{Y}_4, \bar{Y}_5)$.

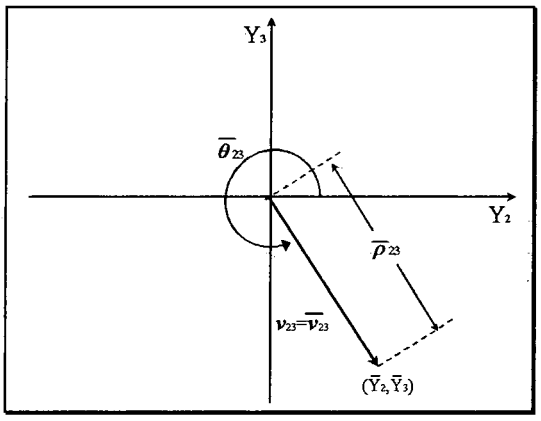

(a1) $v_{23} = \bar{v}_{23}$

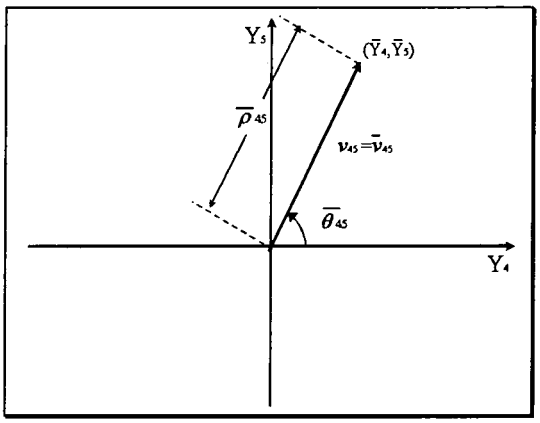

(a2) $v_{45} = \bar{v}_{45}$

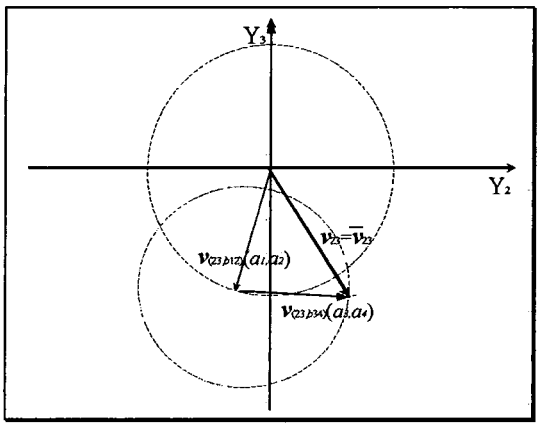

(b1) $\bar{v}_{23} = v_{(23,b12)}(\alpha_1, \alpha_2) + v_{(23,b34)}(\alpha_3, \alpha_4)$

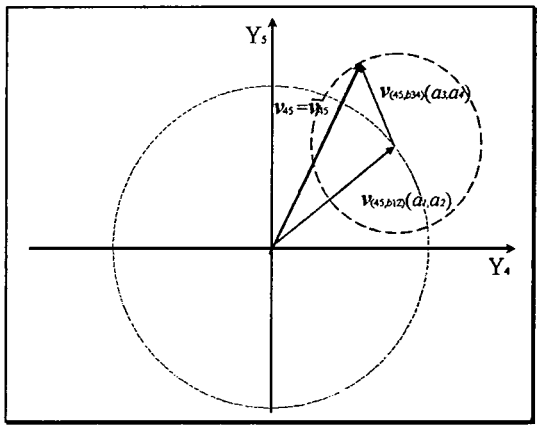

(b2) $\bar{v}_{45} = v_{(45,b12)}(\alpha_1, \alpha_2) + v_{(45,b34)}(\alpha_3, \alpha_4)$

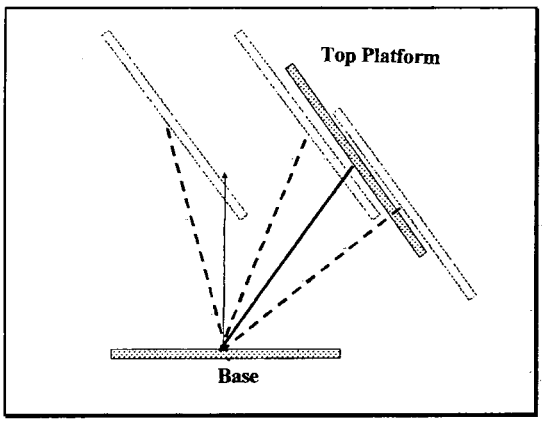

(c1) status set of $v_{23} = \bar{v}_{23}$

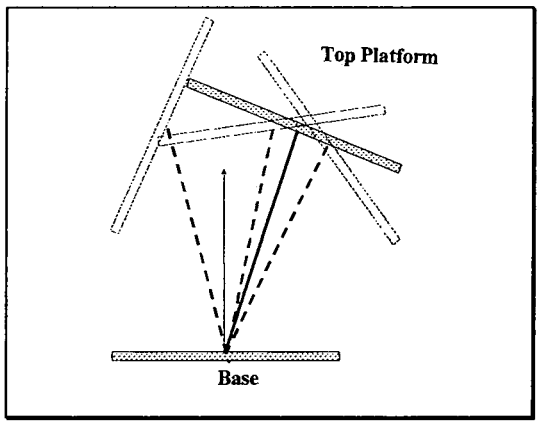

(c2) status set of $v_{45} = \bar{v}_{45}$

Figure 8-3 The situation where the principal components (Y_2, Y_3, Y_4, Y_5) are given

Geometrically, this problem is equivalent to finding a status that belongs to the two sets of the status of the platform in Figure 8-3 (c1) and (c2).

Corresponding to equations (2.4-1) and (2.4-2), the vectors $v_{(23,b12)}(a'_1, a'_2)$, $v_{(23,b34)}(a'_3, a'_4)$ and $\bar{v}_{23}$ are shown in Figure 8-4(a1) and the vectors $v_{(45,b12)}(a'_1, a'_2)$, $v_{(45,b34)}(a'_3, a'_4)$ and $\bar{v}_{45}$ are shown in Figure 8-4 (a2). The basic idea of this algorithm is as follows.

Firstly, it gives a value of $(\alpha_1, \alpha_2, \alpha_3, \alpha_4)$ as an initial value to meet equation (2.4-2) but may not meet equation (2.4-1). Correspondingly, the initial value of v_{45} is $\bar{v}_{45}$, but the initial value of v_{23} may not be $\bar{v}_{23}$, (See Figure 8-4 (a1) (a2));

It then finds a different value of $(\alpha_1, \alpha_2, \alpha_3, \alpha_4)$ but the value still meets equation (2.4-2) and is nearer to meeting the equation (2.4-1). Correspondingly, the new value of v_{45} is still $\bar{v}_{45}$ (see Figure 8-4 (b2)), and the new value of v_{23} is closer to $\bar{v}_{23}$ than the previous value (see Figure 8-4 (b1)). This procedure repeats until the value of $(\alpha_1, \alpha_2, \alpha_3, \alpha_4)$ is 'very close' to satisfying equations (2.4-1) and (2.4-2). Correspondingly, the values of v_{45} are always $\bar{v}_{45}$, and the new values of v_{23} are closer and closer to $\bar{v}_{23}$ (see Figure 8-4 (c)).

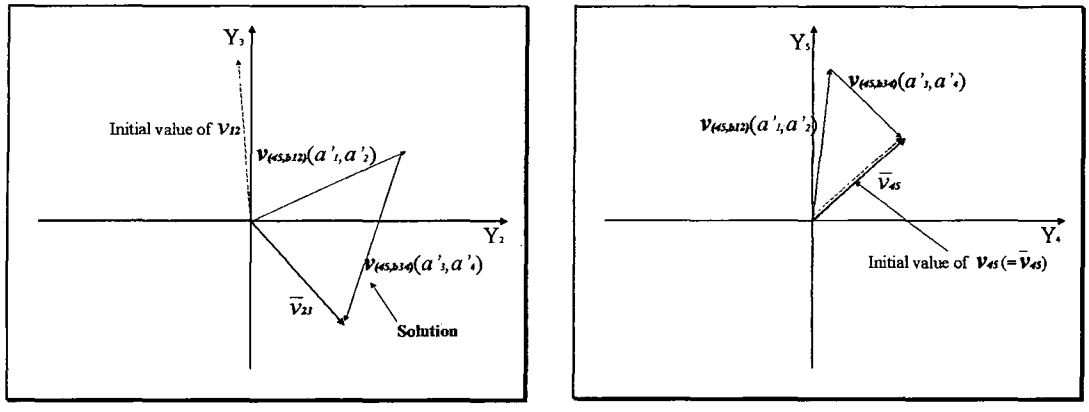

(a1) **(a2)**

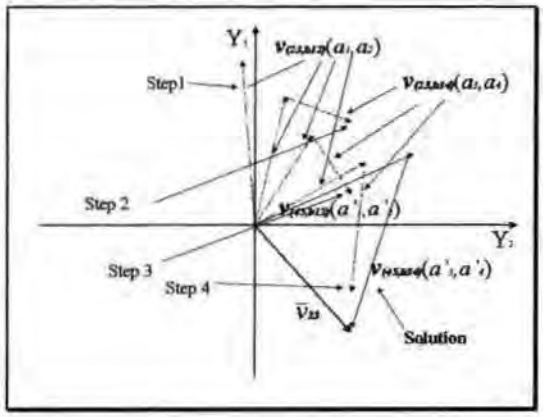

(b1)

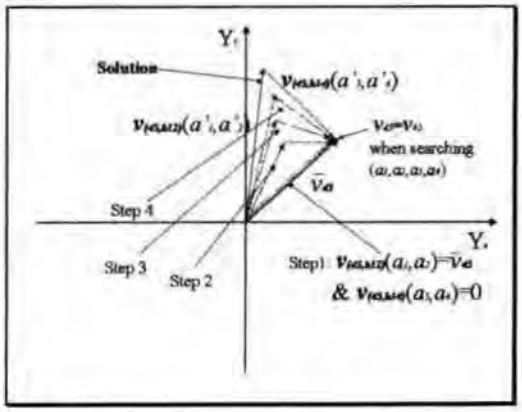

(b2)

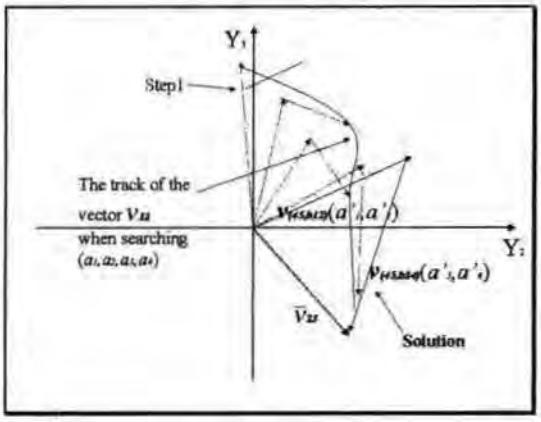

(c)

Figure 8-4 Searching the value of $(\alpha_1, \alpha_2, \alpha_3, \alpha_4)$ corresponding to

$$(Y_2, Y_3, Y_4, Y_5) = (\overline{Y}_2, \overline{Y}_3, \overline{Y}_4, \overline{Y}_5)$$

In this algorithm, the search starts from the centre status of the status set of $v_{45} = \overline{v}_{45}$. The centre status is where the M-bar is perpendicular to the platform in the status set of $v_{45} = \overline{v}_{45}$. That is, the values (α_3, α_4) are zero (0,0). Correspondingly, vector value $v_{(45,b34)}(\alpha_3, \alpha_4)$ in Y_4-Y_5 plane is zero and the vector value $v_{(45,b12)}(\alpha_1, \alpha_2)$ in Y_4-Y_5 plane is $\overline{v}_{45}$ in Figure 8-4 (b2). Corresponding to this status, there is a vector value, $v_{23} = v_{(23,b12)}(\alpha_1, \alpha_2) + v_{(23,b34)}(\alpha_3, \alpha_4)$, in the Y_2-Y_3 plane. Based on the relationship between (Y_2, Y_3) and $(\alpha_1, \alpha_2, \alpha_3, \alpha_4)$, it is known that $v_{(23,b34)}(\alpha_3, \alpha_4) = 0$, so that $v_{23} = v_{(23,b12)}(\alpha_1, \alpha_2)$ (see Figure 8-4 (b1)). The search will then be carried out around the centre status of $v_{45} = \overline{v}_{45}$.

To continue the search, the vectors v_{23} corresponding to the centre status of $v_{45}=\bar{v}_{45}$ is denoted as v_{23c}, $v_{23c}=(Y_{2c},Y_{3c})$ (see Figure 8-5 (b1)). Also, the relative positional variables $\bar{a}_1$, $\bar{a}_2$, $\bar{a}_3$ and $\bar{a}_4$, which were introduced in Chapter 7 are applied. Here, the relative position is the position relative to the centre status of $v_{45}=\bar{v}_{45}$. It is known that if the tilt angle ($\bar{a}_1$) of the M-bar relative to the M-bar of the centre status of $v_{45}=\bar{v}_{45}$ is fixed and the tilt direction ($\bar{a}_2$) of the M-bar relative to the centre status varies (see Figure 8-5 (a)), the end of the vector $v_{(45,b12)}(\alpha_1, \alpha_2)$ will be in a circle (see Figure 8-5 (b2)). To keep $v_{45}=\bar{v}_{45}$, the vector $v_{(45,b34)}(\alpha_3, \alpha_4)$ should be from the end of the vector $v_{(45,b12)}(\alpha_1, \alpha_2)$ to $\bar{v}_{45}$, that is, from a point on the circle to the end of the vector $\bar{v}_{45}$. In this situation, the vector $v_{(45,b12)}(\alpha_1, \alpha_2)$ obviously equals $\bar{v}_{45}+v_{(45,b12)}(\bar{a}_1, \bar{a}_2)$, and $v_{(45,b34)}(\alpha_3, \alpha_4)$ equals $v_{(45,b34)}(\bar{a}_3, \bar{a}_4)$. Similarly, when $\bar{a}_1$ is fixed and $\bar{a}_2$ varies, the vector v_{23} in the Y_2-Y_3 plane will also be changed. In this situation, $v_{23}=v_{23c}+v_{(23c,b12)}(\bar{a}_1, \bar{a}_2)+v_{(23c,b34)}(\bar{a}_3, \bar{a}_4)$, $v_{(23c,b12)}(\alpha_1, \alpha_2)=v_{23c}+v_{(23c,b12)}(\bar{a}_1, \bar{a}_2)$ and $v_{(23c,b34)}(\alpha_3, \alpha_4)=v_{(23c,b34)}(\bar{a}_3, \bar{a}_4)$, (see Figure 8-5(b1)).

The searching procedure is as follows. Firstly, $\bar{a}_1$ is fixed, and $\bar{a}_2$ is given different values. For any given value of $\bar{a}_2$, there is one pair of values ($\bar{a}_3$, $\bar{a}_4$), which meet the equation $v_{45}=\bar{v}_{45}$. For different given values of $\bar{a}_2$, there are different corresponding pairs of values ($\bar{a}_3$, $\bar{a}_4$), which satisfy the equation $v_{45}=\bar{v}_{45}$ but have different values of v_{23}. The value of ($\bar{a}_1$, $\bar{a}_2$, $\bar{a}_3$, $\bar{a}_4$) corresponding to the vector v_{23}, that is the closest to $\bar{v}_{23}$, is the result of the first step of the search. In the second step, $\bar{a}_2$ is fixed, and $\bar{a}_1$ is given different values. For any given value of $\bar{a}_1$, there is one pair of values ($\bar{a}_3$, $\bar{a}_4$), which satisfies the equation $v_{45}=\bar{v}_{45}$. For different given values of $\bar{a}_1$, there are different corresponding pairs of values ($\bar{a}_3$, $\bar{a}_4$), which satisfy the equation $v_{45}=\bar{v}_{45}$ but may not satisfy the equation $v_{23}=\bar{v}_{23}$. The

value of ($\bar{a}_1$, $\bar{a}_2$, $\bar{a}_3$, $\bar{a}_4$) corresponding to the vector v_{23} that is the closest to $\bar{v}_{23}$ is the result of the second step of the search. Then, $\bar{a}_1$ and $\bar{a}_2$ are in turn fixed in the following search steps until a solution is obtained.

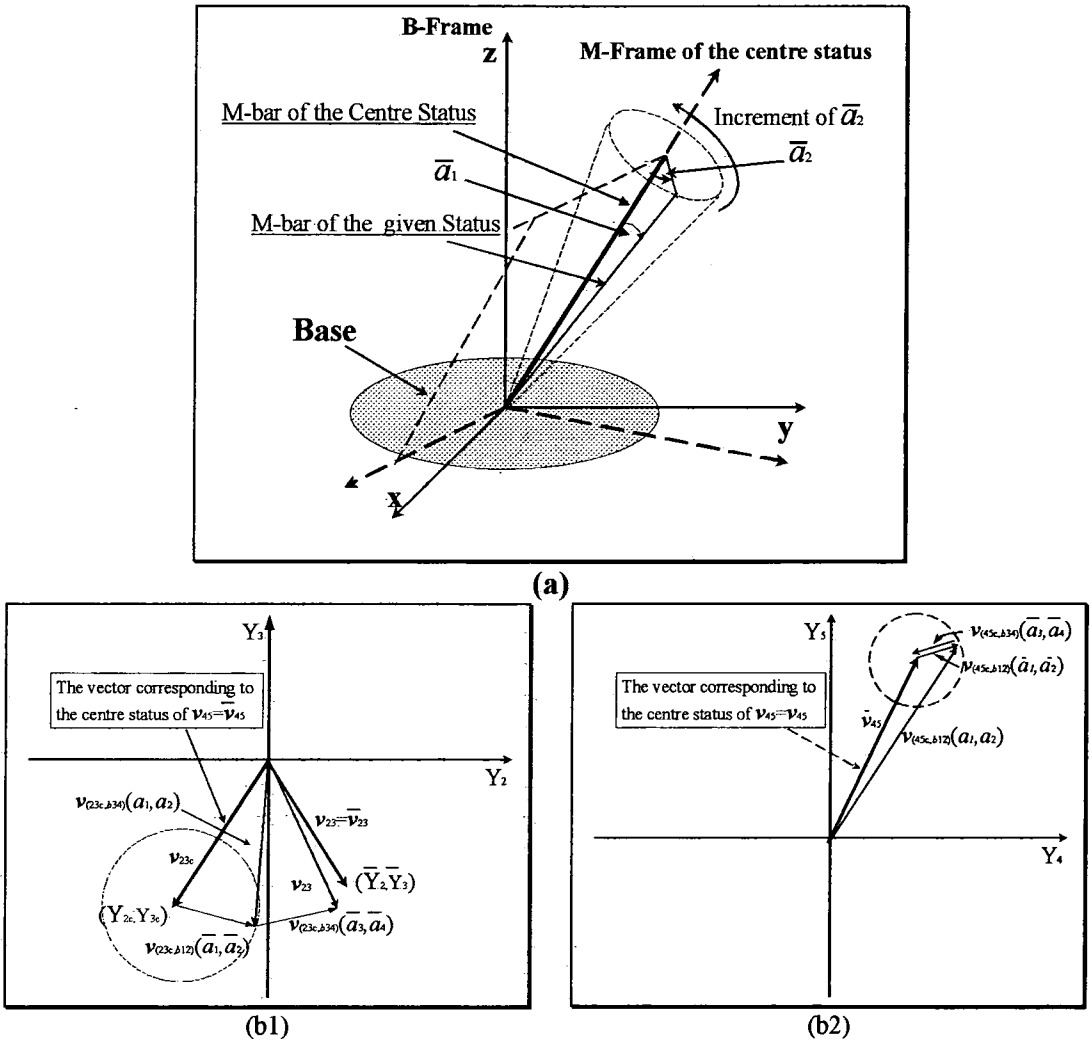

Figure 8-5

The following is the flow diagram of the main program for searching for the values α_1, α_2, α_3, and α_4.

Start

Calculating the values (α_1, α_2, α_3, α_4) corresponding to the centre status of $v_{45}=\bar{v}_{45}$, and then calculating the value of v_{23c}

If $v_{23c}=\bar{v}_{23}$ ***then*** **End**

Endif

Initialising the variables $\bar{a}_1$ and $\bar{a}_2$, and searching for the value α_3, α_4

corresponding to $v_{45}=\bar{v}_{45}$, and at the same time obtaining the value of v_{23c}

Loop

Searching $\bar{a}_2$ ($\bar{a}_1$ is fixed)

Searching $\bar{a}_1$ ($\bar{a}_2$ is fixed)

If the value of Δv_{23c} is less than the critical value ***then*** **End**

Endif

Endloop

End

In the above diagram the task of 'Searching $\bar{a}_2$' is taken by a sub-program. During the process of 'Searching $\bar{a}_2$', every step search needs to call a sub-sub-program once. This sub-sub-program is for searching for the value of $(\bar{a}_3, \bar{a}_4)$ corresponding to $v_{45}=\bar{v}_{45}$, and at the same time the value of v_{23c} is updated. The process of 'Searching $\bar{a}_1$' is similar.

This sub-sub-program for searching for the value of $(\bar{a}_3, \bar{a}_4)$ corresponding to $v_{45}=\bar{v}_{45}$ will be discussed in Section 8.3.5.

Through the above flow diagram, the framework of the algorithm for searching for the values of the variables $(\alpha_1, \alpha_2, \alpha_3, \alpha_4)$ has been constructed. In detail, two problems still remain. The first problem is how to obtain the value of $(\alpha_1, \alpha_2, \alpha_3, \alpha_4)$ corresponding to the centre status of $v_{45}=\bar{v}_{45}$, and at the same time, how to obtain the vector v_{23} corresponding to the centre status of $v_{45}=\bar{v}_{45}$. The second problem is how to search for the values of $\bar{a}_1$ and $\bar{a}_2$ if the vector v_{23} corresponding to the centre status of $v_{45}=\bar{v}_{45}$ does not equal $\bar{v}_{23}$. The second problem can be split into two sub-problems. One is how to initialise the variables $\bar{a}_1$ and $\bar{a}_2$ to start the search around the centre status of $v_{45}=\bar{v}_{45}$. The other is how to search for the values of $\bar{a}_1$ and $\bar{a}_2$ in the two sub-programs. The following sections discuss these problems.

8.3.2 Searching for the value $(\alpha_1,\alpha_2,\alpha_3,\alpha_4)$ corresponding to the centre status of $v_{45}=\bar{v}_{45}$

It is known that $\alpha_3 = 0$ and $\alpha_4=0$ according to the definition of the centre status of $v_{45}=\bar{v}_{45}$. Hence, the task becomes a search for the values, (α_1,α_2), corresponding to the centre status of $v_{45}=\bar{v}_{45}$. Based on the basic relationship between (Y_2,Y_3) and (α_1,α_2), it is known that the variable α_1 increases with the length (ρ_{23}) of the vector v_{23} in the Y_2-Y_3 plane. Here, $\rho_{23} = \sqrt{Y_2^2+Y_3^2}$. Also, the variable α_2 increases with the polar angle (θ_{23}) of the vector v_{23} in the Y_2-Y_3 plane. Here, θ_{23} =atan(Y_3/Y_2). Similar to the discussion in Section 8.2, the values of α_1 and α_2 can be obtained by using the algorithm for searching for the value of a single-variable increasing continuous function. The programs for searching for the values of α_1 and α_2 will run in turn until both the results for α_1 and α_2 have sufficient accuracy.

8.3.3.*Initialisation of the relative positional variables* $\bar{a}_1,\bar{a}_2,\bar{a}_3$, *and* $\bar{a}_4$

After obtaining the value of $(\alpha_1,\alpha_2,\alpha_3,\alpha_4)$ corresponding to the centre status of $v_{45}=\bar{v}_{45}$, the corresponding vector v_{23c} in the Y_2-Y_3 plane can also be obtained at the same time. If $v_{23c}\neq\bar{v}_{23}$ the search will continue. Setting a good initial value of $(\bar{a}_1,\bar{a}_2,\bar{a}_3,\bar{a}_4)$ to enhance the performance of the search program is very helpful. This work is based on the difference between v_{23c} and $\bar{v}_{23}$, and is also based on the knowledge of the relationship between $(\bar{a}_1,\bar{a}_2,\bar{a}_3,\bar{a}_4)$ and (Y_2, Y_3, Y_4, Y_5) that was obtained in Chapter 7,

It is known that if $\bar{a}_1=\bar{a}_3$ and $\bar{a}_2=\bar{a}_4$, then,

$$v_{(23c,b12)}(\bar{a}_1,\bar{a}_2)\approx v_{(23c,b34)}(\bar{a}_3,\bar{a}_4)$$

$$v_{(45c,b12)}(\bar{a}_1,\bar{a}_2)\approx -v_{(45c,b34)}(\bar{a}_3,\bar{a}_4).$$

Hence, if given $v_{(23c,b12)}\ (\bar{a}_1, \bar{a}_2) = \Delta v_{23c}/2$ and $\bar{a}_1 = \bar{a}_3$ and $\bar{a}_2 = \bar{a}_4$, then the vector $v_{23c} + v_{(23c,b12)}\ (\bar{a}_1, \bar{a}_2) + v_{(23c,b34)}\ (\bar{a}_3, \bar{a}_4) \approx \bar{v}_{23}$ (see Figure 8-7)

$v_{45c} + v_{(45c,b12)}(\bar{a}_1, \bar{a}_2) + v_{(45c,b34)}(\bar{a}_3, \bar{a}_4) \approx \bar{v}_{45}$ (see Figure 8-6)

Here, $\Delta v_{23c} = \bar{v}_{23} - v_{23c}$

According to the basic relationship between (Y_2, Y_3) and the relative positional variables $(\bar{a}_1, \bar{a}_2)$ to let the value $v_{(23c,b12)}\ (\bar{a}_1, \bar{a}_2) \approx \Delta v_{23c}/2$, initial values of $\bar{a}_1$ and $\bar{a}_2$ can be given an approximate value by using the regression functions, which were obtained in Chapter 7

$$\bar{a}_1 = 0.0067\bar{\rho}_{23c}/2$$

$$= 0.00335\sqrt{(\bar{Y}_2 - Y_{2c})^2 + (\bar{Y}_3 - Y_{3c})^2}$$

$$\bar{a}_2 = 1.001\ \bar{\theta}_{23c} + 3.9282$$

$$\approx \bar{\theta}_{23c} + 5\pi/4$$

$$= \text{atan}(\bar{Y}_{3c}/\bar{Y}_{2c}) + 5\pi/4$$

$$= \text{atan}\left(\frac{\bar{Y}_3 - Y_{3c}}{\bar{Y}_2 - Y_{2c}}\right) + 5\pi/4$$

Here, $\bar{\rho}_{23c}$ is the length of Δv_{23c} and $\bar{\theta}_{23c}$ is the polar angle of Δv_{23c}. $\bar{Y}_2$ and $\bar{Y}_3$ are given values of Y_2 and Y_3 respectively. Y_{2c} and Y_{3c} are the values of Y_2 and Y_3 corresponding to the centre status of $v_{45} = \bar{v}_{45}$ (see Figure 8-6).

After giving the initial value of $(\bar{a}_1, \bar{a}_2)$, a program for searching for the value of $(\bar{a}_3, \bar{a}_4)$ needs to be called. At this time, an initial value of $(\bar{a}_3, \bar{a}_4)$ is required by the search program. According to the basic relationship between (Y_2, Y_3) and the relative positional variables $(\bar{a}_3, \bar{a}_4)$, the initial values of $\bar{a}_3$ and $\bar{a}_4$ can be given by.

$$\bar{a}_3 = \bar{a}_1$$

$$\bar{a}_4 = \bar{a}_2$$

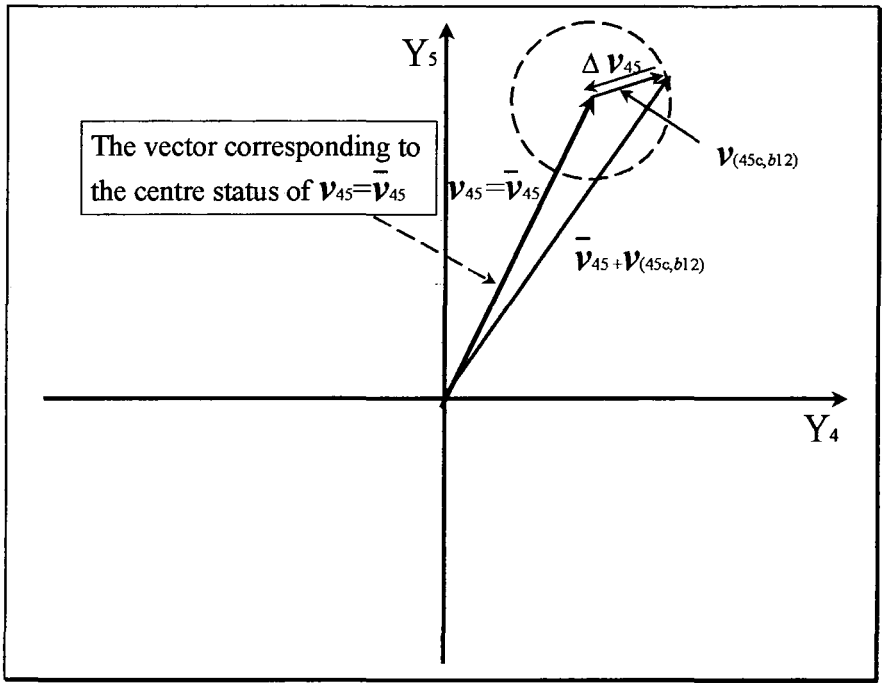

Figure 8-6

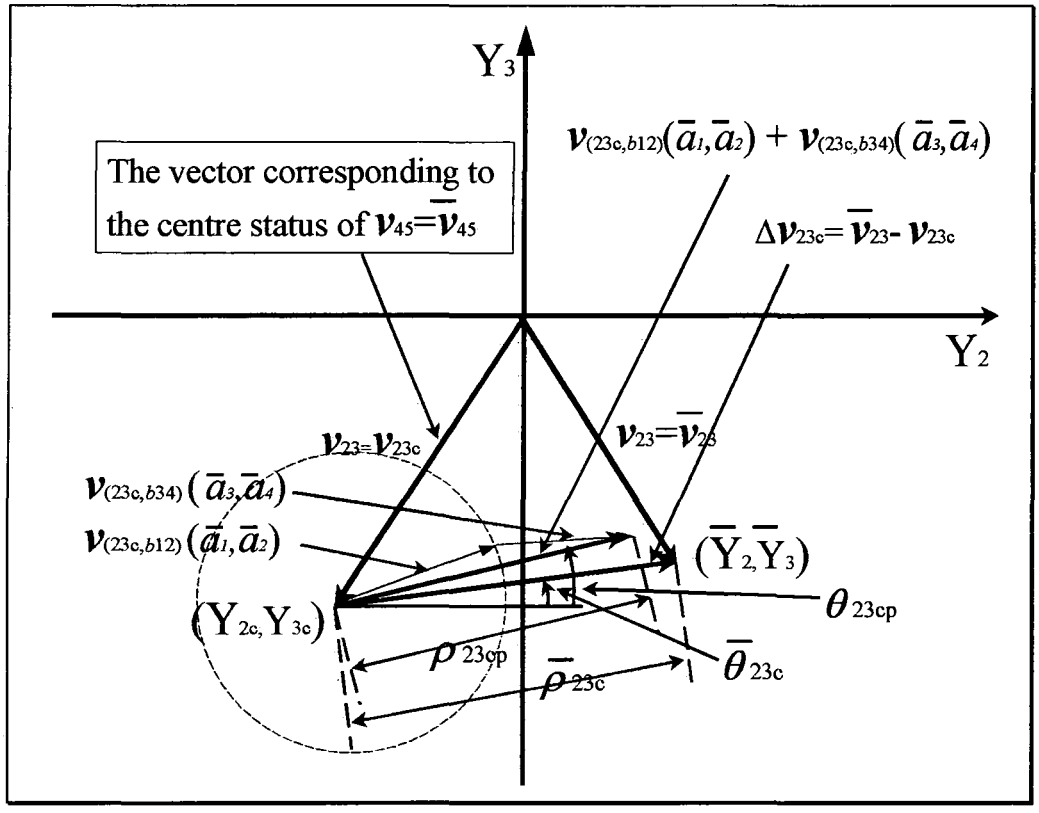

Figure 8-7

After running the program for searching for the value of $(\bar{a}_3, \bar{a}_4)$, the value of v_{23} is also obtained. The difference between v_{23} and $\bar{v}_{23}$ is used to determine whether the program for searching the value of $(\alpha_1, \alpha_2, \alpha_3, \alpha_4)$ should stop.

8.3.4 The sub-algorithm for searching for the value of $\bar{a}_1$ and $\bar{a}_2$:

In the main program for searching the values of α_1, α_2, α_3 and α_4, there are two sub-programs. These are the programs for searching for the value of $\bar{a}_1$ and for searching for the value of $\bar{a}_2$. There is a slight difference between these two algorithms when initialising the searched values and outputting the search result. The following is a detailed explanation of the algorithm for searching for the value of $\bar{a}_2$ and the flow diagrams of these algorithms.

The sub-algorithm for searching for the value of $\bar{a}_2$:

When $\bar{a}_1$ is fixed and $\bar{a}_2$ varies, geometrically, the M-bar has a constant angle relative to the M-bar of the centre status of $v_{45} = \bar{v}_{45}$. In the Y_2-Y_3 plane, the polar angle of the corresponding vector, $v_{(23c,b12)}(\bar{a}_1, \bar{a}_2)$, varies and the length is fixed. The objective of this search is to find the value of $\bar{a}_2$ that lets the $\| [\bar{v}_{23} - v_{23c}] - [v_{(23c,b12)}(\bar{a}_1, \bar{a}_2) + v_{(23c,b34)}(\bar{a}_3, \bar{a}_4)] \|$ value become the minimum. Now, the polar angle of the vector sum, $v_{(23c,b12)}(\bar{a}_1, \bar{a}_2) + v_{(23c,b34)}(\bar{a}_3, \bar{a}_4)$, is denoted as θ_{23cp} and the length is denoted as ρ_{23cp} (see Figure 8-7). In this algorithm, if the $|\bar{\theta}_{23c} - \theta_{23cp}|$ value is less than a critical value, it stops the search. Since there is a constraint $v_{45} = \bar{v}_{45}$, based on the relationship between (Y_4, Y_5) and $(\bar{a}_1, \bar{a}_2, \bar{a}_3, \bar{a}_4)$, it is known through Figure 8-5 that if the value of $\bar{a}_2$ increases, the polar angle of $v_{(45c,b12)}(\bar{a}_1, \bar{a}_2)$ will increase, and consequently the polar angle of $v_{(45c,b34)}(\bar{a}_3, \bar{a}_4)$ and the value of $\bar{a}_4$ will also increase. Consequently, based on the relationship between (Y_2, Y_3) and $(\bar{a}_1, \bar{a}_2, \bar{a}_3, \bar{a}_4)$, it is known through Figure 8-6 that the value of θ_{23cp} will increase with the value of $\bar{a}_2$. Hence, the search algorithm for a

single-variable increasing continuous function that has been discussed in Section 8.2 can be applied for searching the value of $\bar{a}_2$. The flow diagram of the algorithm is given as follows:

Start

Initialisation of the interval of $\bar{a}_2$: $[\bar{a}_{2\inf}, \bar{a}_{2upp}]$

Loop

Computation of the values $\theta_{23c\inf} = f^{-1}(\bar{a}_{2\inf})$, $\theta_{23cupp} = f^{-1}(\bar{a}_{2upp})$

Case 1 $(\bar{\theta}_{23c} - \theta_{23c\inf})(\bar{\theta}_{23c} - \theta_{23cupp}) = 0$

If $\bar{\theta}_{23c} = \theta_{23c\inf}$, **then** $\bar{a}_2 \leftarrow \bar{a}_{2\inf}$

If $\bar{\theta}_{23c} = \theta_{23cupp}$, **then** $\bar{a}_2 \leftarrow \bar{a}_{2upp}$

End

Case 2 $(\bar{\theta}_{23c} - \theta_{23c\inf})(\bar{\theta}_{23c} - \theta_{23cupp}) > 0$

If $\bar{\theta}_{23c} < \theta_{23c\inf}$, **then** $\bar{a}_{2\inf} \leftarrow \bar{a}_{2\inf} - (\bar{a}_{2upp} - \bar{a}_{2\inf})$

If $\bar{\theta}_{23c} > \theta_{23cupp}$, **then** $\bar{a}_{2upp} \leftarrow \bar{a}_{2upp} + (\bar{a}_{2upp} - \bar{a}_{2\inf})$

Case 3 $(\bar{\theta}_{23c} - \theta_{23c\inf})(\bar{\theta}_{23c} - \theta_{23cupp}) < 0$

If $\bar{\theta}_{23c} < (\theta_{23c\inf} + \theta_{23cupp})/2$, **then** $\bar{a}_{2upp} \leftarrow (\bar{a}_{2\inf} + \bar{a}_{2upp})/2$

Else $\bar{a}_{2\inf} \leftarrow (\bar{a}_{2\inf} + \bar{a}_{2upp})/2$

If $|\bar{a}_{2upp} - \bar{a}_{2\inf}| < \varepsilon$, **then** $\bar{a}_2 \leftarrow (\bar{a}_{2\inf} + \bar{a}_{2upp})/2$, **End Loop**

Else $\bar{a}_{2\inf} \leftarrow (\bar{a}_{2\inf} + \bar{a}_{2upp})/2$

End Loop

Output Result

End

Here $f^{-1}()$ is a function of $\bar{a}_2$ for computing of the value of θ_{23cp}. There are three steps in this computation: searching for the value of $\bar{a}_3$ and $\bar{a}_4$ to keep $v_{45} = \bar{v}_{45}$; transforming the relative positional variables $(\bar{a}_1, \bar{a}_2, \bar{a}_3, \bar{a}_4)$ to positional variables $(\alpha_1, \alpha_2, \alpha_3, \alpha_4)$; and calculating the link lengths and the principal components by using $(\alpha_1, \alpha_2, \alpha_3, \alpha_4)$.

The sub-algorithm for searching for the value of $\bar{a}_1$*:*

The sub-algorithm for searching for the value of $\bar{a}_1$ is almost the same as the algorithm for searching for the value of $\bar{a}_2$. The difference is at the initial value and

the critical value setting, which is discussed in this section. The following is the flow diagram.

Start

Initialisation of the interval of $\bar{a}_1$: $[\bar{a}_{1\inf}, \bar{a}_{1upp}]$

Loop

Computation of the values $\theta_{23c\inf} = f^{-1}(\bar{a}_{1\inf})$, $\theta_{23cupp} = f^{-1}(\bar{a}_{1upp})$

Case 1 $(\bar{\rho}_{23c} - \rho_{23c\inf})(\bar{\rho}_{23c} - \rho_{23cupp}) = 0$

If $\bar{\rho}_{23c} = \rho_{23c\inf}$, **then** $\bar{a}_1 \leftarrow \bar{a}_{1\inf}$

If $\bar{\rho}_{23c} = \rho_{23cupp}$, **then** $\bar{a}_1 \leftarrow \bar{a}_{2upp}$

End

Case 2 $(\bar{\rho}_{23c} - \rho_{23c\inf})(\bar{\rho}_{23c} - \rho_{23cupp}) > 0$

If $\bar{\rho}_{23c} < \rho_{23c\inf}$, **then** $\bar{a}_{1\inf} \leftarrow \bar{a}_{1\inf} - (\bar{a}_{1upp} - \bar{a}_{1\inf})$

If $\bar{\rho}_{23c} > \rho_{23cupp}$, **then** $\bar{a}_{1upp} \leftarrow \bar{a}_{1upp} + (\bar{a}_{1upp} - \bar{a}_{1\inf})$

Case 3 $(\bar{\rho}_{23c} - \rho_{23c\inf})(\bar{\rho}_{23c} - \rho_{23cupp}) < 0$

If $\bar{\rho}_{23c} < (\rho_{23c\inf} + \rho_{23cupp})/2$, **then** $\bar{a}_{1upp} \leftarrow (\bar{a}_{1\inf} + \bar{a}_{1upp})/2$

Else $\bar{a}_{1\inf} \leftarrow (\bar{a}_{1\inf} + \bar{a}_{1upp})/2$

If $|\bar{a}_{1upp} - \bar{a}_{1\inf}| < \varepsilon$, **then** $\bar{a}_1 \leftarrow (\bar{a}_{1\inf} + \bar{a}_{1upp})/2$, **End Loop**

Else $\bar{a}_{1\inf} \leftarrow (\bar{a}_{1\inf} + \bar{a}_{1upp})/2$

End Loop

Output Result

End

Here $f^{-1}()$ is a function of $\bar{a}_1$ for computing of the value of θ_{23cp}. Once again, there are three steps in this computation: searching for the value of $\bar{a}_3$ and $\bar{a}_4$ to keep $v_{45} = \bar{v}_{45}$; transforming the relative positional variables $(\bar{a}_1, \bar{a}_2, \bar{a}_3, \bar{a}_4)$ to positional variables $(\alpha_1, \alpha_2, \alpha_3, \alpha_4)$; and calculating the link lengths and the principal components by using $(\alpha_1, \alpha_2, \alpha_3, \alpha_4)$.

8.3.5 Searching for the values of $\bar{a}_3$ and $\bar{a}_4$ to keep $v_{45} = \bar{v}_{45}$;

If $\bar{a}_1$ and $\bar{a}_2$ are given, there is a vector $v_{(45c,b12)}(\bar{a}_1, \bar{a}_2)$. At this moment, $v_{45c} + v_{(45c,b12)}(\bar{a}_1, \bar{a}_2)$ does not equal $\bar{v}_{45}$. The difference, $\Delta v_{45} = \bar{v}_{45} - (v_{45c} +$

$v_{(45c,b12)}(\bar{a}_1, \bar{a}_2)$), can be obtained see Figure 8-6. Then, based on the polar angle of Δv_{45}, the variable $\bar{a}_4$ can be determined and based on the length of Δv_{45}, the variable $\bar{a}_4$ can be determined. The variables $\bar{a}_3$ and $\bar{a}_4$ are in turn searched until the errors of the variables $\bar{a}_3$ and $\bar{a}_4$ are less than critical values. The algorithm used for searching for the values of $\bar{a}_3$ and $\bar{a}_4$ is the same as the algorithm for a single-variable increasing continuous function that has been discussed in Section 8.2. The initial values of $\bar{a}_3$ and $\bar{a}_4$ are given as

$$\bar{a}_3 = \bar{a}_1$$

$$\bar{a}_4 = \bar{a}_2$$

in the search program.

8.4 Simulation and the Results

Simulation was carried out to prove the feasibility of the algorithm given above. The results of the simulation also present many advantages for robotic positioning.

8.4.1 Simulation

The computer hardware platform of the simulation is a PC (Pentium(r) II, 64.0M RAM). The computer software platform of the simulation is MATLAB 5.3 with Microsoft Windows 98. The parallel mechanism applied in this simulation is the 6-6 Stewart platform used through out this thesis (see Section 5.3.2). The simulations are divided into two groups. One is used to prove the PCA based algorithm. The other one is used to test the sensitivity of the positional variables to the link lengths. The results of the simulation are as follows.

8.4.2 The results of the simulation

Result 1: Forward displacement

In this simulation, a set of given data for different values of ($\alpha_1, \alpha_2, \alpha_3, \alpha_4, \alpha_5, lm$) was used. The corresponding lengths of the links ($l_1\ l_2, l_3, l_4, l_5, l_6$) were directly calculated using the different values of ($\alpha_1, \alpha_2, \alpha_3, \alpha_4, \alpha_5, lm$). The lengths of the links ($l_1\ l_2, l_3, l_4, l_5, l_6$) were used as the input data of the program for the forward

displacement problem. The following table presents a part of the simulation results. The cases in the table generally cover all situations, which were discussed in the previous sections.

Table 2.4-1 Computational results of the PCA based algorithm for the forward displacement problem.

	Given positional variables	Lengths of the links	Computational results of the positional variables	Computational errors of the positional variables
Case 1	$\alpha_1 = 0$	l_1 =158.6805	α_1 =0.0000	e_1 = 0.0000
	$\alpha_2 = 0$	l_2 =158.6805	α_2 = 0.0000	e_2 = 0.0000
	$\alpha_3 = 0$	l_3 =158.6805	α_3 = 0.0000	e_3 = 0.0000
	$\alpha_4 = 0$	l_4 =158.6805	α_4 = 0.0000	e_4 = 0.0000
	$\alpha_5 = 0$	l_5 =158.6805	α_5 = 0.0000	e_5 = 0.0000
	lm= 150	l_6 =158.6805	lm=150.0000	e_{lm} = 0.0000
Case 2	$\alpha_1 = \pi/8$	l_1 =118.1035	α_1 =0.3927	e_1 =-1.4466e-005
	$\alpha_2 = 0$	l_2 =131.1300	α_2 = 0.0001	e_2 = 0.0001
	$\alpha_3 = 0$	l_3 =172.8063	α_3 = 0.0000	e_3 = 0.0000
	$\alpha_4 = 0$	l_4 =194.6343	α_4 = 4.8793	e_4 = 4.8793
	$\alpha_5 = \pi/24$	l_5 =174.2601	α_5 =0.1309	e_5 = 1.0126e-005
	lm= 150	l_6 =163.1960	lm=149.9980	e_{lm} = 0.0020
Case 3	$\alpha_1 = \pi/4$	l_1 =95.0755	α_1 =0.7854	e_1 = 5.6663e-006
	$\alpha_2 = 0$	l_2 =96.6688	α_2 =0.0001	e_2 = 0.0001
	$\alpha_3 = 0$	l_3 =189.1721	α_3 =0.0001	e_3 = 0.0001
	$\alpha_4 = 0$	l_4 =220.5079	α_4 = 1.8002	e_4 = 1.8002
	$\alpha_5 = 0$	l_5 =195.7616	α_5 =-0.0000	e_5 = 0.0000
	lm= 150	l_6 =158.6805	lm=150.0047	e_{lm} = 0.0047
Case 4	$\alpha_1 = 0$	l_1 =121.7470	α_1 =0.0002	e_1 =0.0002
	$\alpha_2 = 0$	l_2 =150.8114	α_2 = 3.0588	e_2 =3.0588
	$\alpha_3 = \pi/8$	l_3 =160.0633	α_3 =0.3925	e_3 = 1.5796e-004
	$\alpha_4 = 0$	l_4 =198.2987	α_4 = 6.2830	e_4 = 1.6976e-004
	$\alpha_5 = \pi/24$	l_5 =183.6693	α_5 =0.1309	e_5 =3.3740e-006
	lm= 150	l_6 =140.1572	lm=149.9973	e_{lm} =0.0027
Case 5	$\alpha_1 = \pi/8$	l_1 =127.4624	α_1 =0.3927	e_1 =3.1331e-005
	$\alpha_2 = 0$	l_2 =173.0679	α_2 =0.0005	e_2 =0.005
	$\alpha_3 = \pi/8$	l_3 =230.3368	α_3 =0.3929	e_3 =-1.5765e-004
	$\alpha_4 = 0$	l_4 =280.7140	α_4 = 6.2831	e_4 =1.1614e-004
	$\alpha_5 = \pi/12$	l_5 =247.4473	α_5 =0.2618	e_5 =2.6292e-005
	lm= 200	l_6 =187.1736	lm=199.9988	e_{lm} =0.0013

Case 6	$\alpha_1 = \pi/8$ $\alpha_2 = \pi/2$ $\alpha_3 = \pi/8$ $\alpha_4 = \pi$ $\alpha_5 = \pi/24$ $lm = 150$	l_1 =140.1036 l_2 =177.4804 l_3 =159.5691 l_4 =139.2630 l_5 =164.2435 l_6 =170.3095	α_1 =0.3927 α_2 =1.5706 α_3 =0.3927 α_4 = 3.1420 α_5 =0.1309 lm=150.0013	e_1 =3.8401e-005 e_2 =2.0764e-004 e_3 =3.6016e-005 e_4 =-3.9550e-004 e_5 =-1.0643e-005 e_{lm} =0.0013

The above table shows that the PCA based algorithm has a high accuracy. In this simulation, the computational accuracy required that the angular errors are less than 0.001 radians and the error of the M-bar length is less 0.01mm. All computational results achieved the required accuracy. It should be noted that the error e_4 in Case 2 and Case3 is very large. This is because in Case 2 and Case 3, α_3 equals 0. In this situation, α_4 is uncertain and normally can be defined as zero, so the computational results of α_4 also satisfy the accuracy requirement.

Result 2: Impact of the errors of the links for the computation of the forward displacement

The impact of the errors of the link lengths for the computation of the forward displacement is very important for a positioning system. The following table only lists the situations relative to Case 1 and Case 6 in Table 2.4-1. In these cases, it is assumed that there are errors during the sensor measurement of the link lengths. Case 1-1 in Table 2.4-2 is similar to Case 1 in Table 2.4-1, but the measured length l_1 is 1 mm longer than the actual length. Case 6-1 in Table 2.4-2 is similar to Case 6 in Table 2.4-1, but the measured length l_1 is 1 mm longer than the actual length. Case 1-2 is similar to Case 1, but the measured lengths l_1 and l_2 are 1 mm longer than the actual lengths.

Table 2.4-2 The impact of the errors of the links

	Link lengths (actual lengths)	**Errors of the link lengths**	**Computational results**	**Errors of the positional variables**
Case 1-1	l_1 =122.5456 l_2 =126.0806 l_3 =175.8401 l_4 =190.8935	l_1 +1	$\alpha_1 = 0.0071$ $\alpha_2 = 4.1752$ $\alpha_3 = 0.0071$ $\alpha_4 = 3.6901$	$e_1 = 0.0071$ $e_2 = 4.1752$ $e_3 = 0.0071$ $e_4 = 3.6901$

	l_5=177.7047 l_6=158.6805		α_5= -0.0053 *lm*=150.1758	e_5= -0.0053 e_{lm} = 0.1758
Case 1-2	l_1 =122.5456 l_2 =126.0806 l_3 =175.8401 l_4 =190.8935 l_5 =177.7047 l_6 =158.6805	l_1 +1 l_2 +1	α_1 = 0.0099 α_2 =3.4038 α_3 = 0.0037 α_4 = 3.1400 α_5 = -0.0000 *lm*=150.3527	e_1 = 0.0071 e_2 = 4.1752 e_3 = 0.0071 e_4 = 3.6901 e_5 = -0.0053 e_{lm} = 0.1758
Case 1-3	l_1 =122.5456 l_2 =126.0806 l_3 =175.8401 l_4 =190.8935 l_5 =177.7047 l_6 =158.6805	l_1 +1 l_2 +1 l_3 +1	α_1 = 0.0037 α_2 =3.9575 α_3 = 0.0037 α_4 = 6.2686 α_5 = -0.0053 *lm*=150.5281	e_1 = 0.0071 e_2 = 4.1752 e_3 = 0.0071 e_4 = 3.6901 e_5 = -0.0053 e_{lm} = 0.1758
Case 1-4	l_1 =122.5456 l_2 =126.0806 l_3 =175.8401 l_4 =190.8935 l_5 =177.7047 l_6 =158.6805	l_1 +1 l_2 +1 l_3 +1 l_4 +1	α_1 = 0.0100 α_2 = 4.4388 α_3 = 0.0037 α_4 = 3.1860 α_5 = 0.0000 *lm*=150.7052	e_1 = 0.0071 e_2 = 4.1752 e_3 = 0.0071 e_4 = 3.6901 e_5 = -0.0053 e_{lm} = 0.1758
Case 1-5	l_1 =122.5456 l_2 =126.0806 l_3 =175.8401 l_4 =190.8935 l_5 =177.7047 l_6 =158.6805	l_1 +1 l_2 +1 l_3 +1 l_4 +1 l_5 +1	α_1 = 0.0070 α_2 = 3.6551 α_3 = 0.0070 α_4 = 2.6340 α_5 = -0.0053 *lm*=150.8807	e_1 = 0.0070 e_2 = 3.6551 e_3 = 0.0070 e_4 = 2.6340 e_5 = -0.0053 e_{lm} = 0.1758
Case 1-6	l_1 =122.5456 l_2 =126.0806 l_3 =175.8401 l_4 =190.8935 l_5 =177.7047 l_6 =158.6805	l_1 +1 l_2 +1 l_3 +1 l_4 +1 l_5 +1 l_6 +1	α_1 = 0.0000 α_2 = 5.4978 α_3 = 0.0000 α_4 = 0.0000 α_5 = 0.0000 *lm*=151.0575	e_1 = 0.0071 e_2 = 5.4978 e_3 = 0.0000 e_4 = 0.0000 e_5 = 0.0000 e_{lm} = 0.1758
Case 6-1	l_1 =140.1036 l_2 =177.4804 l_3 =159.5691 l_4 =139.2630 l_5 =164.2435 l_6 =170.3095	l_1 +1	α_1 = 0.3863 α_2 =1.5787 α_3 = 0.3855 α_4 = 3.1260 α_5 = 0.1250 *lm*=150.1916	e_1 = 0.0064 e_2 = 0.0079 e_3 = 0.0072 e_4 = 0.0156 e_5 = 0.0059 e_{lm} = 0.1916
Case 6-2	l_1 =140.1036 l_2 =177.4804	l_1 +1 l_2 +1	α_1 = 0.3903 α_2 =1.5966	e_1 = 0.0024 e_2 = 0.0258

	l_3=159.5691 l_4=139.2630 l_5=164.2435 l_6=170.3095		α_3 = 0.3918 α_4 = 3.1265 α_5 = 0.1310 *lm*=150.3448	e_3 = 8.7320e-004 e_4 = 0.0151 e_5 = 8.8654e-005 e_{lm} = 0.1916
Case 6-3	l_1 =140.1036 l_2=177.4804 l_3=159.5691 l_4=139.2630 l_5=164.2435 l_6=170.3095	l_1 +1 l_2+1 l_3+1	α_1 = 0.3895 α_2 =1.5780 α_3 = 0.3959 α_4 = 3.1248 α_5 = 0.1255 *lm*=150.5616	e_1 = 0.0032 e_2 = -0.0072 e_3 = -0.0032 e_4 = 0.0168 e_5 = 0.0054 e_{lm} = 0. 5616
Case 6-4	l_1 =140.1036 l_2=177.4804 l_3=159.5691 l_4=139.2630 l_5=164.2435 l_6=170.3095	l_1 +1 l_2+1 l_3+1 l_4+1	α_1 = 0.3825 α_2 =1.5782 α_3 = 0.3894 α_4 = 3.1364 α_5 = 0.1311 *lm*=150.6817	e_1 = 0.0102 e_2 = -0.0072 e_3 = 0.0033 e_4 = 0.0052 e_5 = -1.7745e-004 e_{lm} = 0.6817
Case 6-5	l_1 =140.1036 l_2=177.4804 l_3=159.5691 l_4=139.2630 l_5=164.2435 l_6=170.3095	l_1 +1 l_2+1 l_3+1 l_4+1 l_5+1	α_1 = 0.3888 α_2 =1.5876 α_3 = 0.3918 α_4 = 3.1394 α_5 = 0.1257 *lm*=150.9054	e_1 = 0.0039 e_2 = -0.0168 e_3 = 8.6050e-004 e_4 = 0.0022 e_5 = 0.0052 e_{lm} = 0.9054
Case 6-6	l_1 =140.1036 l_2=177.4804 l_3=159.5691 l_4=139.2630 l_5=164.2435 l_6=170.3095	l_1 +1 l_2+1 l_3+1 l_4+1 l_5+1 l_6+1	α_1 = 0.3924 α_2 =1.5705 α_3 = 0.3924 α_4 = 3.1429 α_5 = 0.1318 *lm*=151.0458	e_1 = 2.6414e-004 e_2 = 3.3873e-004 e_3 = 2.6400e-004 e_4 = -0.0013 e_5 = -8.5193e-004 e_{lm} = 1.0458

The above table shows that if the link lengths have errors of 1 mm, the errors of the positional variables ($\alpha_1, \alpha_2, \alpha_3, \alpha_4, \alpha_5$) will be less than 0.02 radians and in most situation will be less than 0.005 radians. These angular errors are still very small. If filter techniques are applied in a real system, the angular errors will become even.

Conclusions for the simulations:

The results of the simulation show the feasibility and advantages of the application of the parallel mechanism and the PCA based algorithm. Result 1 shows the feasibility and accuracy of the algorithm. The PCA based algorithm provides satisfactory accuracy for a positioning system. In addition, Result 2 shows the advantage of the

Parallel mechanism in terms of measurement accuracy. Normally, it is not difficult to ensure the measurement error of the link lengths is less than 1mm. Under this accuracy, the angular errors of the 6-6 Stewart platform are less 0.02 radians and, in most situations, the angular errors are less than 0.005 radians. Considering impact of the accumulation of the angular error for a long-term positioning system, the angular accuracy presented in this simulation is very important.

Although, much further discussion is necessary the results of this simulation have illustrated the feasibility and advantage of the parallel mechanism based approach for a positioning system for a stepwise robot.

Chapter 9

Further Discussions

In Chapter 7, a particular parallel linkage mechanism has been analysed by using the PCA approach. The analytical result was used in Chapter 8 to build up a numerical algorithm to compute the position and orientation of the platform. This particular parallel mechanism presents high measurement accuracy for the forward displacement problem through a computation simulation. However, the results presented in Chapter 7 and 8 are only for a particular parallel linkage mechanism for a particular range of the position and orientation of the platform. If the range of the position and orientation of the platform is extended, the forward displacement problem will become more complex than that discussed in Chapter 7 and 8. If the assembly configuration of the parallel linkage mechanism is changed, the measurement accuracy of the position and orientation of the platform may be different. To know the change of the solutions caused by the extension of the range of the position and orientation of the platform or by the change of the assembly configuration is very important for the research of the application of parallel linkage mechanisms to underground robot positioning system. In this section, a further discussion on these problems is given.

9.1 The Solutions in the Whole Range of the Positional Variables

It is known that the forward displacement problem has at most 40 non-singular solutions in the complex domain. However, the question of maximum number of real solutions still remains. In this context, 16 real solutions for a particular mechanism have been found. In the particular case discussed in Chapter 7 and 8, it is assumed that there is a unique solution for any given set of link lengths in the given range of the position and orientation of the platform. In the simulations used in this work, more than two hundred examples were tested only single solution for a given set of link lengths was found. The following discussions illustrate that there will be multiple solutions for one given set of link lengths if the range of the position and orientation of the platform is extended. It is obvious that if the range of the angle α_1 is extended

from [0, π/2] to [0, π], the number of the solutions will be doubled. Geometrically, any position and orientation of platform that is above the base has a mirrored position and orientation of platform that is below the base, in which the link lengths of the mirrored platform are the same as that of the original platform (see Figure 9-1).

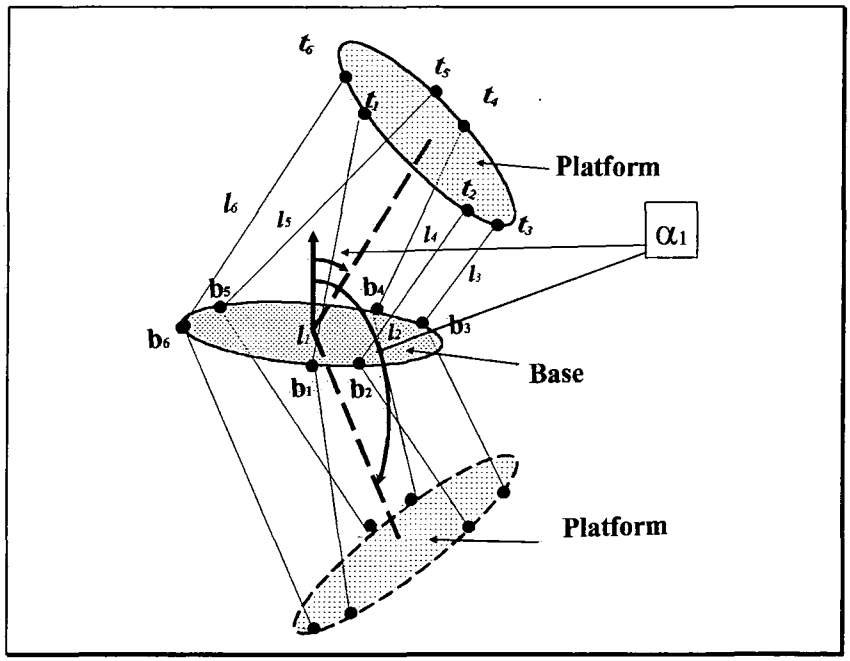

Figure 9-1

Therefore, when the angle α_1 is extended from [0, π/2] to [0, π], it corresponds to the fact that the movement range of the platform is extended from the platform above the base to the platform both above and below the base. Hence, the following discussion is only for the range of the angle α_1 is in the range [0, π/2]. The ranges of the positional variables are assumed as follows.

The angle α_1 is in the range [0, π/2].

The angle α_3 is in the range [0, π];

The angle α_5 is in the range [-π, π];

The angles α_2 and α_4 are in the range [0, 2π];

The length of the m-bar *lm* is in the range [150, 200].

It was found that the general relationship between the positional variables and the principal components are the same as discussed in Chapter 7. That is, the first principal component (Y_1) mainly relates to the positional variable lm. The sixth principal component (Y_6) mainly relates to the positional variable α_5. The principal components (Y_2, Y_3, Y_4, Y_5) mainly relate to the positional variables (α_1, α_2, α_3, α_4). However, the value range of the positional variables and the principal components have been extended compared with Chapter 7. In the extended range, the property of every one-to-one and pair-to-pair basic relationship is changed. The following discussions cover the details for the extended basic relationships.

The one-to-one relationship between Y_6 and α_5

(a) The case where the values of the positional variables α_1, α_2, α_3, α_4 are zero and *lm* equals 150.

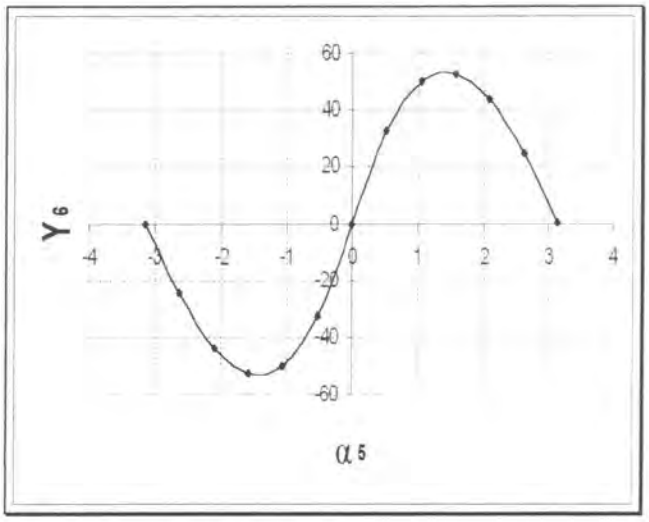

(b) The cases where the positional variables α_1, α_2, α_3, α_4 and *lm* have given different values.

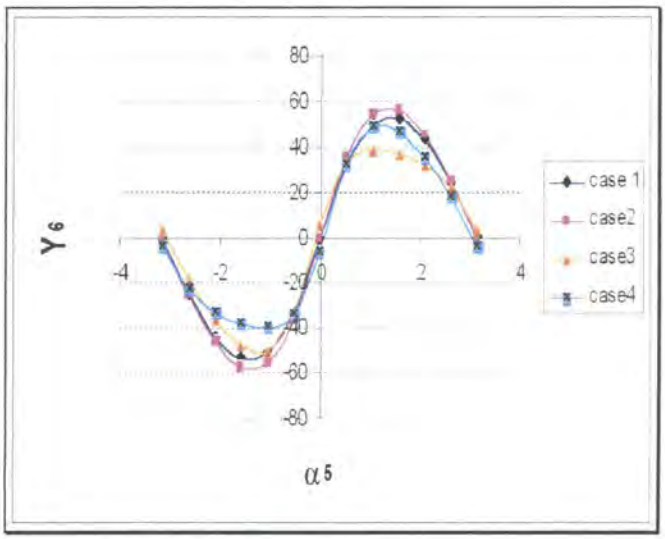

Figure 9-2 the relationship between Y_1 and α_5

In the discussion in Chapter 7, it was shown that the one-to-one relationship between the sixth principal component Y_6 and the positional variable α_5 is a single value function if the values of the other positional variables α_1, α_2, α_3, α_4 and lm are given.

However, if the value range of α_5 is extended to $[-\pi, \pi]$, a given value of Y_6 normally corresponds to two different values of α_5. Figure 9-2 illustrates the relationship between the sixth principal component Y_6 and the positional variable α_5. Figure 9-2 (a) is the situation where the other positional variables (α_1, α_2, α_3, α_4, *lm*) are given particular values. That is, the values of the positional variables α_1, α_2,

(a) At the initial position of the platform, $\alpha_5=0$ and $Y_6=0$.

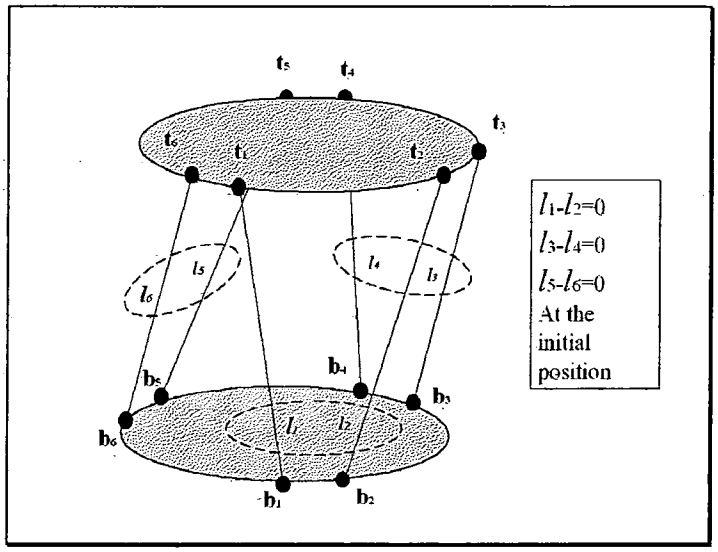

(b) The situation where $\alpha_5=\pi$ and $Y_6=0$.

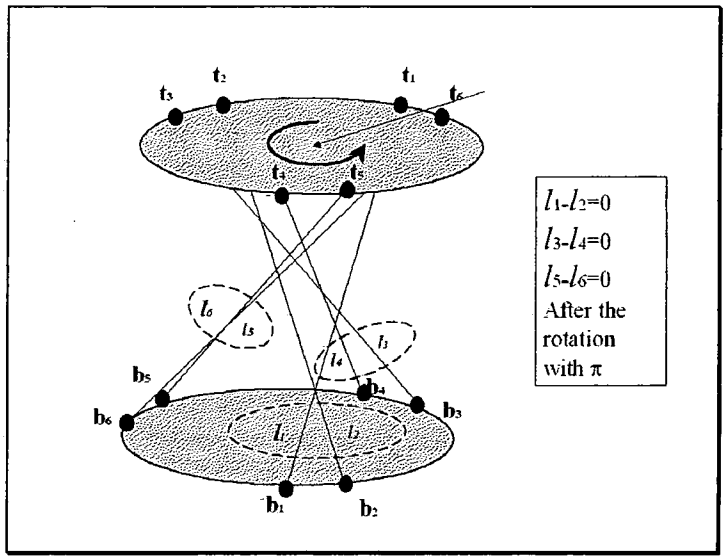

Figure 9-3 An example where to different values of α_5 correspond to one value of $Y_6=0$

α_3, α_4 are zero and lm equals 150. Figure 9-2 (a) shows that only when the principal component Y_6 gets to its maximum or minimum values, does Y_6 correspond to a unique value of α_5. Normally, a given value of Y_6 corresponds to two different values of α_5. This is a property of the relationship between Y_6 and α_5 after the range of α_5 is extended. Although for different particular values of the positional variables (α_1, α_2, α_3, α_4, *lm*) there are different particular relationship between Y_6 and α_5, this property of the relationship is true for all situations. Figure 9-2 (b), shows a few particular relationships for different particular values of the positional variables (α_1, α_2, α_3, α_4, *lm*).

Figure 9-3 shows an example where two different values of α_5 correspond to one value of Y_6.

The relationship between (Y_2,Y_3) and (α_1, α_2, α_3, α_4)

If the value range of α_1 is extended from [0, π/4] to [0, π/2] and the value range of α_3 is extended from [0, π/4] to [0, π], the relationship between (Y_2,Y_3) and (α_1, α_2, α_3, α_4) in the extension range of α_1 and α_3 may be different from that in the range discussed in Chapter 7.

As mentioned in Chapter 7, the values of the principal components Y_2 and Y_3 are mainly related to the values of (α_1, α_2, α_3, α_4). If the values of (α_1, α_2) are given, the values of the principal components Y_2 and Y_3 are mainly related to the values of (α_3, α_4). Especially, if (α_1, α_2) are given values (0,0), the relationship between (Y_2, Y_3) and (α_3, α_4) is called the basic pair-to-pair relationship of (Y_2,Y_3)-to-(α_3, α_4) Similarly, if (α_3, α_4) are given values (0,0), the relationship between (Y_2, Y_3) and (α_1, α_2) is called the basic pair-to-pair relationship of (Y_2,Y_3)-to-(α_1, α_2). The relationship between (Y_2,Y_3) and (α_1, α_2, α_3, α_4) can be viewed as the linear combination of the basic relationship of (Y_2,Y_3)-to-(α_1, α_2) and the basic relationship of (Y_2,Y_3)-to-(α_3, α_4). The analysis for the relationship between

(Y_2, Y_3) and $(\alpha_1, \alpha_2, \alpha_3, \alpha_4)$ will start by the analysis for these two basic relationships. Then, the combination of the basic relationships will be discussed.

-The basic pair-to-pair relationship of (Y_2, Y_3)-to-(α_1, α_2)

Figure 9-4 illustrates the basic relationship of (Y_2, Y_3)–to-(α_1, α_2) using the sample data which corresponds to α_3, α_4, α_5 given the value zero and *lm* equals 150. In Figure 9-4, different value pairs of (α_1, α_2) correspond to different points in the plane Y_2-Y_3 and the dash curves illustrate the track of the point movement as the values of (α_1, α_2) are varying. Compared with the discussion in Chapter 7, it was found that the characteristics of the basic relationship are not changed after the value range of α_1 is extended from [0, π/4] to [0, π/2].

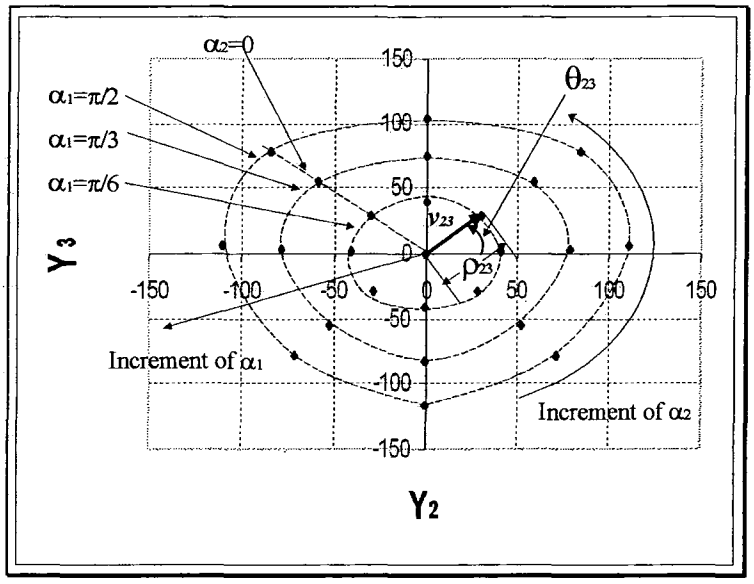

Figure 9-4 the basic relationship of (Y_2, Y_3)–to-(α_1, α_2)

As mentioned in Chapter 7, there is a vector (ν_{23}) from the origin of the plane Y_2-Y_3 to any given point corresponding to a given values of (α_1, α_2). The length of the vector $(\rho_{23} = |\nu_{23}| = \sqrt{Y_2^2 + Y_3^2})$ corresponds to the value of α_1 and the angle of the vector to the Y_3 axis $(\theta_{23} = \text{atan}(Y_3/Y_2))$ corresponds to the value of α_2. Thus, the length of the vector (ρ_{23}) can be mainly used to estimate the value of α_1 and the polar angle of the vector (θ_{23}) can be mainly used to estimate the value of α_2. Compared with the situation discussed in Section2.3, the relationship between ρ_{23} and α_1 for the

value range, $0 \le \alpha_1 \le \pi/2$, can be viewed as a linear extension of that for the value range, $0 \le \alpha_1 \le \pi/4$. The relationship between θ_{23} and α_2 for the value range, $0 \le \alpha_1 \le \pi/2$, is almost not different from that for the value range, $0 \le \alpha_1 \le \pi/4$.

-The basic pair-to-pair relationship of (Y_2, Y_3)-to-(α_3, α_4)

To show the relationship in the value range of α_3 $[0,\pi]$ more clearly, Figure 9-5

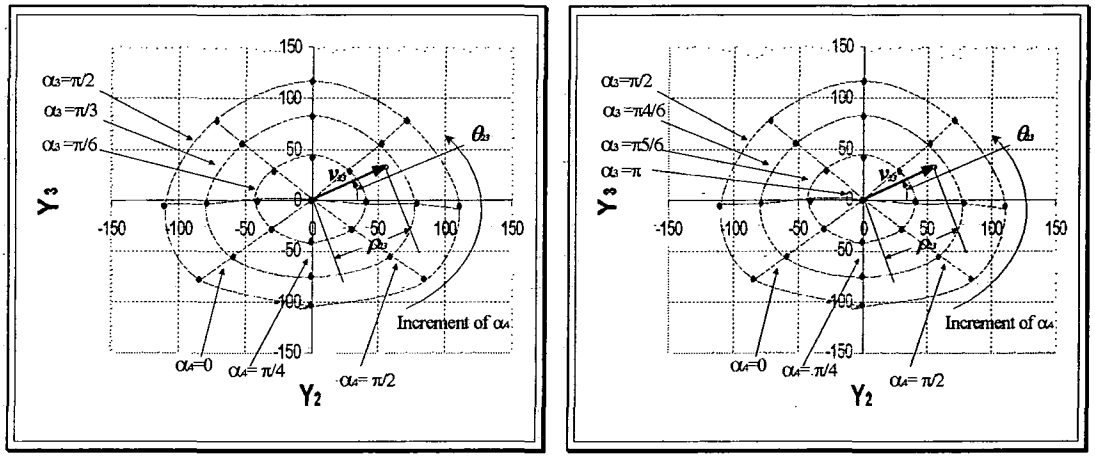

(a) α_3 is in the range $[0,\pi/2]$ **(b)** α_3 is in the range $[\pi/2, \pi]$

Figure 9-5 the basic relationship of (Y_2, Y_3)–to(α_3, α_4)

shows the basic relationship of (Y_2, Y_3)-to-(α_3, α_4) in the ranges of α_3, $[0,\pi/2]$ (see Figure 9-5 (a)) and $[\pi/2, \pi]$ (see Figure 9-5 (b)). Figure 9-5 illustrates the basic relationship of (Y_2, Y_3)–to-(α_3, α_4) using the sample data which corresponds to α_1, α_2, α_5 given the value zero and *lm* equals 150. In Figure 9-5, different value pairs of (α_3, α_4) correspond to different points in the plane Y_2-Y_3 and the dash curves illustrate the track of the point movement as the values of (α_3, α_4) vary. If the value range of α_3 is only extend from the range $[0,\pi/4]$ to $[0,\pi/2]$, the situation is similar to the previous discussion for the relationship between (Y_2, Y_3) and (α_1, α_2). The basic relationship of (Y_2, Y_3)–to-(α_3, α_4) is not changed if the value range of α_3 is only extended to the range $[0,\pi/2]$. In a manner similar to the previous discussion, there is a vector (v_{23}) from the origin of the plane Y_2-Y_3 to any point corresponding to a given pair of values (α_3, α_4). The length of the vector $(\rho_{23} = |v_{23}|)$ can be mainly used to estimate the value of α_3 and the polar angle of the vector (θ_{23}) can be mainly used

to estimate the value of α_4. Figure 9-5(b) shows the situation where α_3 is in the range [π/2, π]. The positions of the points and the dash curves in Figure 9-5(b) are similar to that in Figure 9-5(a). The same analysis was also carried out in the situation shown in Figure 9-5(b). However, any given same point in the plane Y_2-Y_3 in Figure 9-5(a) and Figure 9-5(b) correspond to different values of (α_3, α_4) respectively. This indicates that for any given pair of values (Y_2,Y_3), there are two pairs of different values (α_3, α_4), which come from different value ranges of α_3 shown in Figure 9-5(a) and (b) respectively. Considering the situations shown in Figure 9-5(a) and (b) together, it was found that if α_3 is fixed and α_4 varies, the corresponding point will move along an approximate circle. The counter clockwise direction along the circle is the direction of increment of α_4. If α_4 is fixed and α_3 varies, the corresponding point will moves along an approximate line which passes through the origin of the plane Y_2-Y_3. If the value of α_3 is less than π/2, the outward direction along the line is the direction of increment of α_3 (see Figure 9-5(a)). However, if the value of α_3 is greater than π/2, the direction along the line from the outside to the origin of the plane Y_2-Y_3 is the direction of increment of α_3 (see Figure 9-5(b))[†]. This is an important property of the basic relationship of (Y_2,Y_3)-to-(α_3, α_4) in the range $\alpha_3 \in$ [0, π]. This indicates that if $\alpha_3 \neq \pi/2$, there are two pairs of different values (α_3, α_4) for any given pair of values (Y_2,Y_3). These two different values of (α_3, α_4) geometrically correspond to two different orientations of the platform, which are mirrored each by the plane of the platform where $\alpha_3 = \pi/2$. Figure 9-6 shows the positions and orientations of these two solutions corresponding to one pair of given values (Y_2,Y_3). Figure 9-6 (a) is the situation where α_3 is less than π/2, in which the top side of the platform is facing up. Figure 9-6 (b) is the situation where α_3 is greater than π/2, in which the top side of the platform is facing down.

[†] Here, π/2 is the result of the analysis based on the sample data. To obtain higher accuracy value, more sample data around π/2 should be collected.

(a) The situation where α_3 is less than $\pi/2$, in which the top side of the platform is facing up.

(b) The situation where α_3 is greater than $\pi/2$, in which the top side of the platform is facing down

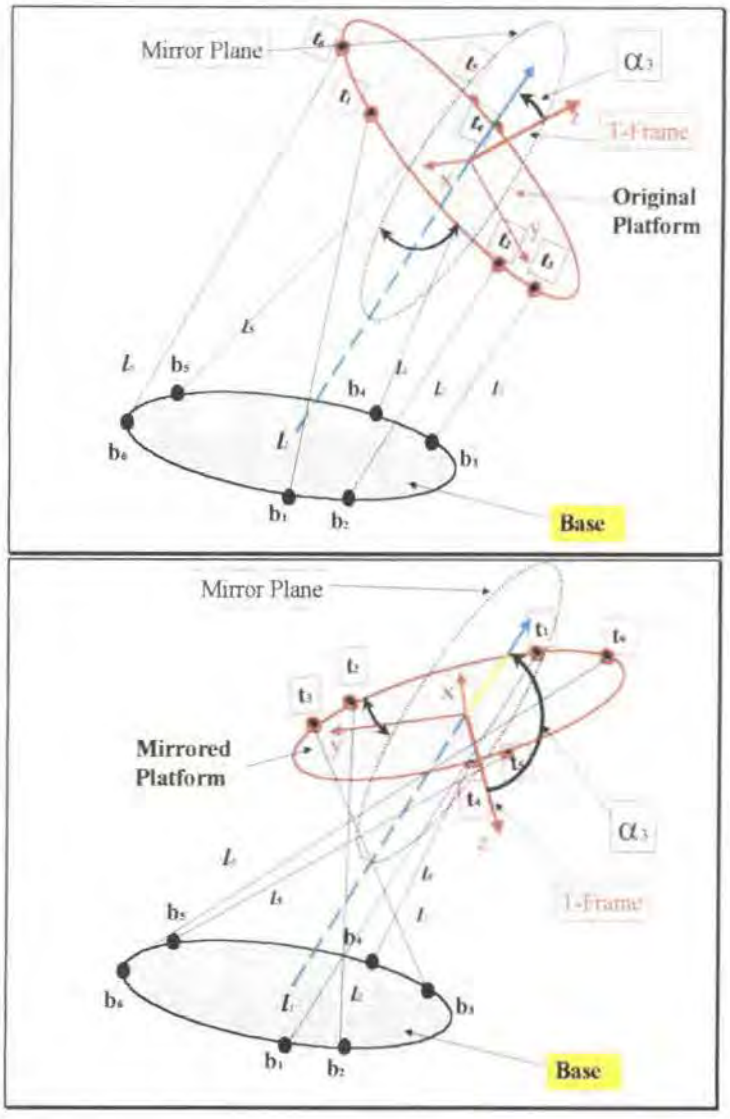

Figure 9-6 The two solutions corresponding to one given pair of values (Y_2, Y_3) geometrically mirrored each other by the platform plane of $\alpha_3 = \pi/2$.

-The combination of the basic relationship between (Y_2, Y_3)-to-(α_1, α_2) and the basic relationship between (Y_2, Y_3)-to-(α_3, α_4)

The relationship between (Y_2, Y_3) and $(\alpha_1, \alpha_2, \alpha_3, \alpha_4)$ can be viewed as the combination of the above two basic relationships, which are the relationship of (Y_2, Y_3)-to-(α_1, α_2) and the relationship of (Y_2, Y_3)-to-(α_3, α_4). Figure 9-7 shows the combination of the two basic relationships using the sample data which corresponds to $\alpha_1, \alpha_2, \alpha_5$ given the value zero and *lm* equals 150.

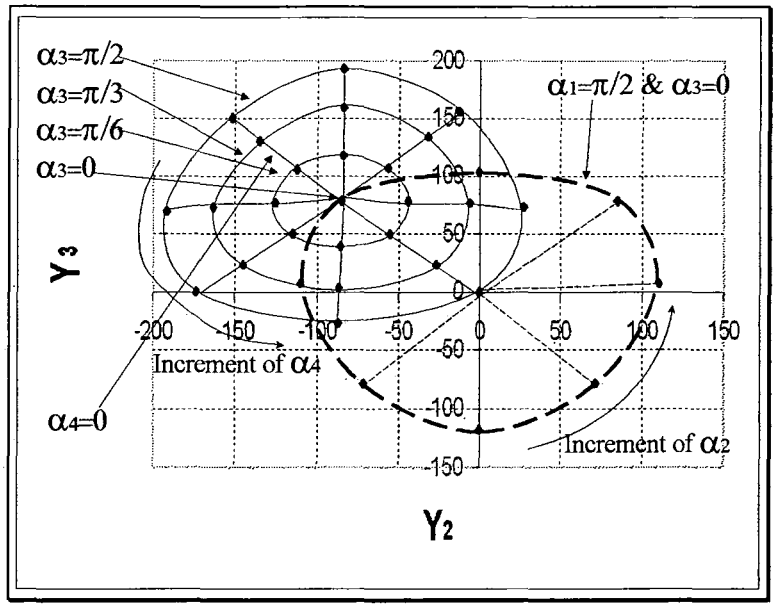

Figure 9-7 The combination of the two basic relationships

It was found through Figure 9-7 that the combination of the two basic relationships is no difference from the discussion in Chapter 7. If one of (α_1, α_2) and (α_3, α_4) is (0,0), the values of (Y_2, Y_3) can be determined by one of these two basic relationships. If both of (α_1, α_2) and (α_3, α_4) are not (0,0), the values of (Y_2, Y_3) can be determined by the linear combination of the two basic relationships.

The relationship between (Y_4, Y_5) and $(\alpha_1, \alpha_2, \alpha_3, \alpha_4)$

If the value range of α_1 is extended from [0, π/4] to [0, π/2] and the value range of α_3 is extended from [0, π/4] to [0, π], the relationship between (Y_4, Y_5) and $(\alpha_1, \alpha_2, \alpha_3, \alpha_4)$ in the extension range of α_1 and α_3 may be different from that in the range discussed in Chapter 7.

Similar to the discussion for the relationship between (Y_2, Y_3) and $(\alpha_1, \alpha_2, \alpha_3, \alpha_4)$, the relationship between (Y_4, Y_5) and $(\alpha_1, \alpha_2, \alpha_3, \alpha_4)$ can be viewed as the linear combination of the basic relationship of (Y_4, Y_5)-to-(α_1, α_2) and the basic relationship of (Y_4, Y_5)-to-(α_3, α_4). The analysis for the relationship between (Y_4, Y_5) and $(\alpha_1, \alpha_2, \alpha_3, \alpha_4)$ started by the analysis for these two basic relationships. Then, the combination of the basic relationships was analysed. Because

the procedure of the analysis is the same as the analysis for the relationship between (Y_2,Y_3) and $(\alpha_1, \alpha_2, \alpha_3, \alpha_4)$, the following section only gives the discussion for the issues that are different from the previous discussion and their conclusions.

-The basic pair-to-pair relationship of (Y_4,Y_5)-to-(α_3, α_4)

As discussed in Chapter 7, if $\alpha_3<\pi/4$, the property of the basic relationship of (Y_4,Y_5)-to-(α_3, α_4) is similar to the basic relationship of (Y_2,Y_3)-to-(α_3, α_4). That is, if the positional variable α_3 is fixed and α_4 varies in the range $[0,2\pi]$, the corresponding points (Y_4,Y_5) in the plane Y_4-Y_5 form a closed curve which is an approximate circle. When α_3 increases, the diameter of the closed curve will increase. However, if α_3 is greater than $\pi/4$ the closed curve in the plane Y_4-Y_5 is not like a circle. If α_3 is greater than $\pi/2$ the closed curve in the plane Y_4-Y_5 becomes more complex. This is different from the discussion for the basic relationship of (Y_2,Y_3)-to-(α_3,α_4), in which, if α_3 is greater than $\pi/2$ the closed curves are still similar to that where α_3 is less than $\pi/2$. Figure 9-8 shows the basic relationship of (Y_4,Y_5)-to-(α_3, α_4) using the sample data in the situation where α_5 equals zero and *lm* equals 150. The points 1 to 8 in Figure 9-8 correspond to the values of α_4, (0, $\pi/4$, $\pi/2$, $\pi3/4$, π, $\pi5/4$, $\pi6/4$, $\pi7/4$) respectively.

(a) the situation where α_3 is $\pi/6$,

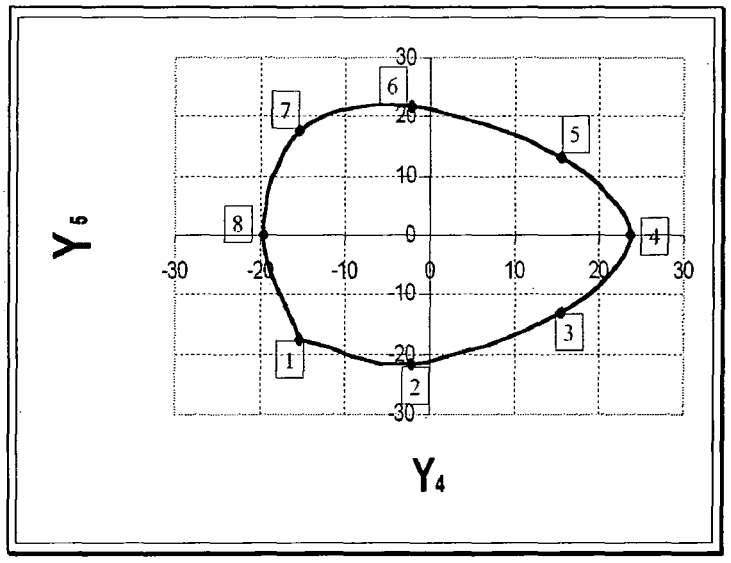

(b) The situation where α_3 is $\pi 2/6$

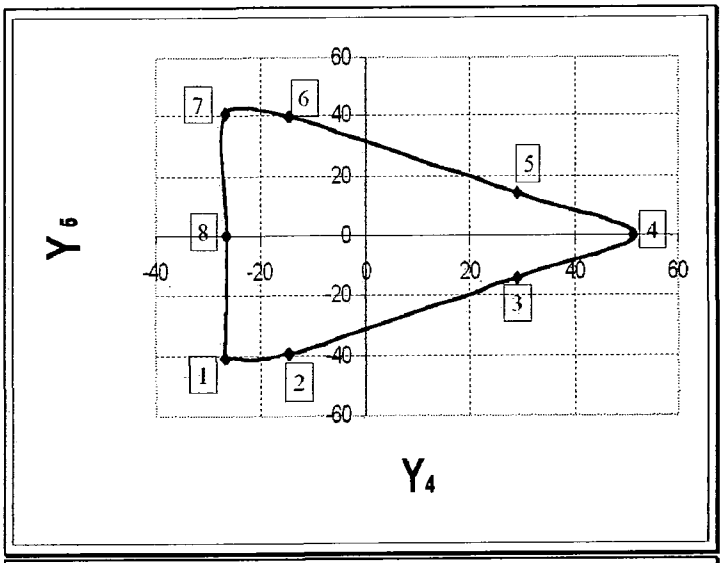

(c) The situation where α_3 is $\pi 3/6$

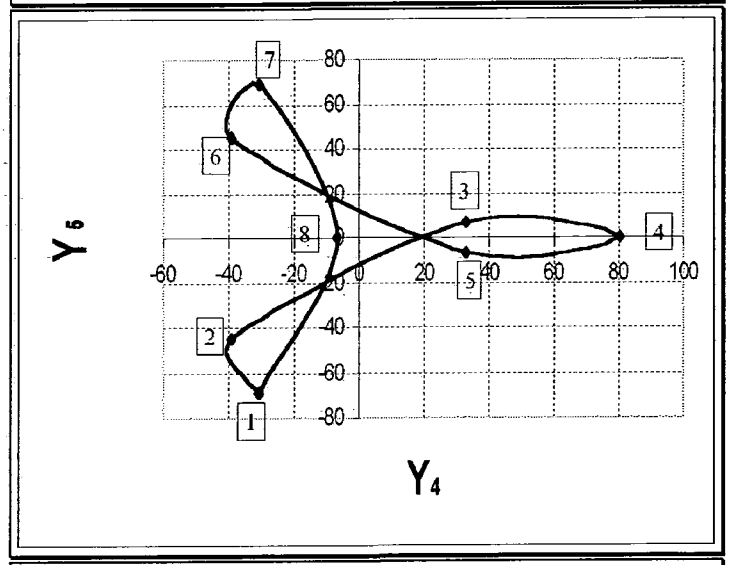

(d) The situation where α_3 is $\pi 4/6$

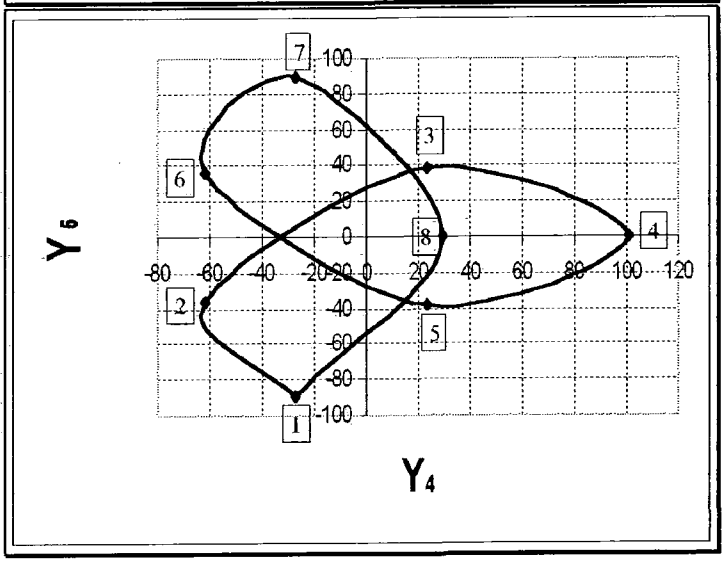

(e) The situation where α_3 is π5/6

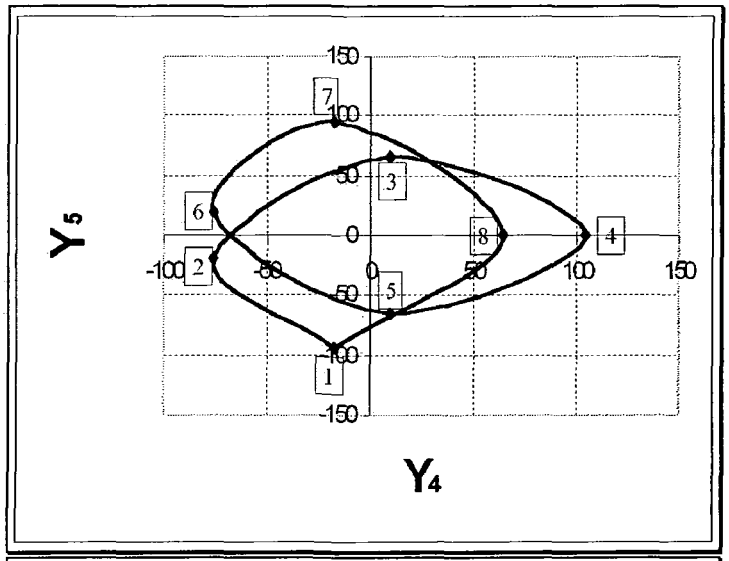

(f) The situation where α_3 is π

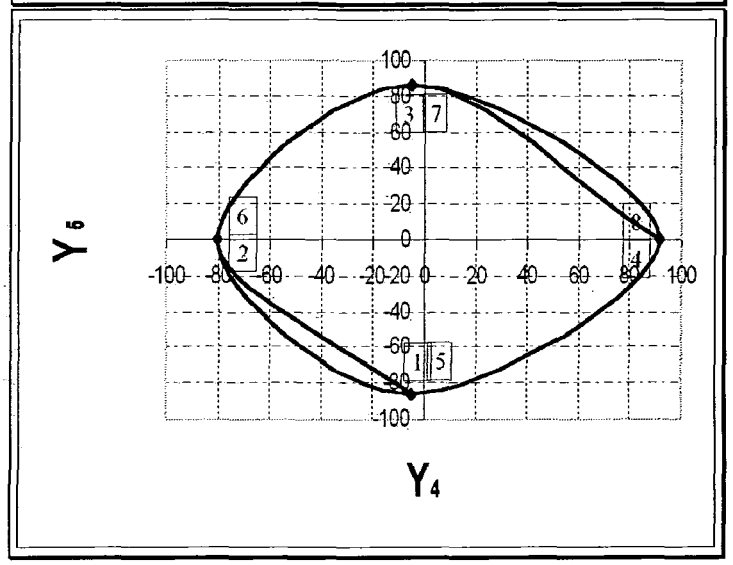

Figure 9-8 The basic relationship of (Y_4, Y_5)-to-(α_3, α_4)

Figure 9-8 (a) shows the situation where α_3 is π/6, which is in the range [0, π/4]. Figure 9-8 (b) shows the situation where α_3 is π/3 which is out of the range [0, π/4]. In this situation, the closed curve is not like a circle. Figure 9-8 (c) (d) (e) (f) show the change of the closed curve as α_3 increases.

Since the basic relationship of (Y_4, Y_5)-to-(α_3, α_4) in the value range $\alpha_3 \in [\pi/2, \pi]$ is very different from that in the value range $\alpha_3 \in [0, \pi/2]$, it is difficult to find which condition one pair of values(Y_4, Y_5) correspond to two or more pairs of values (α_3, α_4). However, it was found that some pairs of values (Y_4, Y_5) correspond to two

pairs of values (α_3, α_4). As an example, Point 8 in Figure 9-8 (b), (c), (d), (e), (f) corresponds to α_4 given π7/4 and α_3 given different values π2/6, π3/6, π4/6, π5/6, π. It was found that Point 8 moves on the Y_4-axis from left hand side to right hand side as α_3 increase. However, in the situation where α_3 is less than π/4, which was discussed in Chapter 7 (see Figure 2.3-26), the left half Y_4-axis corresponds to α_4 given π7/4 and α_3 given different values, where α_3 is less than π/4. The right half Y_4-axis corresponds to α_4 given π3/4 and α_3 given different values, where α_3 is less than π/4. From Figure 2.3-26, it was known that any given value (Y_4,Y_5) on Y_4-axis where $-25<Y_4<35$ corresponds to a pair of value (α_3, α_4) where α_3 is less than π/4. From Figure 9-8, it is known that any given value (Y_4,Y_5) on Y_4-axis where $-25<Y_4<35$ corresponds to a pair of value (α_3, α_4) where α_3 is greater than π/3. Considering these two situations together, if $-25<Y_4<35$, any given values (Y_4,Y_5) on Y_4-axis correspond to two pairs of values (α_3, α_4) that come from two different value ranges of α_3, [0, π/4] and [π/3, π] respectively. In addition, even if α_3 is fixed, one pair of values (Y_4,Y_5) may correspond to two different values of α_4. As an example, in Figure 9-8 (f) points 1 and 5 correspond to one pair of values (Y_4,Y_5). That is, the pairs of values (α_3, α_4) = (π, 0) [point 1] and (α_3, α_4) = (π, π) [point 5] correspond to one pair of values (Y_4,Y_5) = (-5.2237,-85.9018). Similarly, it is not difficult to find other pairs of points corresponding to one pair of values (Y_4,Y_5).

-The basic pair-to-pair relationship of (Y_4,Y_5)-to-(α_1, α_2)

As in the previous discussion for the basic relationship of (Y_2,Y_3)–to-(α_1, α_2), the basic relationship of (Y_4,Y_5)-to-(α_1, α_2) is not changed if the value range of α_1 is extended from [0, π/4] to [0, π/2].

-The combination of the basic relationship between (Y_4,Y_5)--to-(α_1, α_2) and the basic relationship between (Y_4,Y_5)-to-(α_3, α_4)

As in the previous discussion for the relationship between (Y_2, Y_3) and $(\alpha_1, \alpha_2, \alpha_3, \alpha_4)$, the relationship between (Y_4, Y_5) and $(\alpha_1, \alpha_2, \alpha_3, \alpha_4)$, can be viewed as the linear combination of the basic relationship of (Y_4, Y_5)-to-(α_1, α_2) and the basic relationship of (Y_4, Y_5)-to-(α_3, α_4).

The relationship between Y_1 and lm

The property of the relationship between Y_1 and *lm* is not changed if the ranges of the positional variables are extended. The first principal component and the length of the m-bar maintain an approximate linear relationship if the values of $\alpha_1, \alpha_2, \alpha_3, \alpha_4$ and α_5 are given.

Multiple solutions for the forward displacement of the Stewart Platform in the whole solution range

Based on the above discussion, some conclusions of the multiple solutions for the particular parallel mechanism discussed in Chapter 7 were obtained. Because the discussion of the problem of the multiple solutions is not the main task of this project, some problems still remain. The following discussions give some conclusions and the remaining problems.

Generally, there are multiple solutions with in the whole of the solution range for any given six link-lengths. Between these solutions corresponding to given six link-lengths, there are some inter-relationships.

- For any given solution for α_1, if α_1 is less than $\pi/2$ there must be at least one other solution where α_1 is greater than $\pi/2$.
- For any given solution for α_5, if α_5 is less than $\pi/2$ there must be at least one other solution where α_5 is greater than $\pi/2$.
- For any given solution for α_3, if α_3 is less than $\pi/2$ there may be at least one other solution where α_3 is greater than $\pi/2$.

Therefore, the whole value range of the positional variables $(\alpha_1, \alpha_2, \alpha_3, \alpha_4 \alpha_5, lm)$ can be divided into eight solution sub-ranges as shown in Table 5.2.1.

Table 5.2.1 The sub-ranges of the solutions

Value range (α_1)	Value range (α_3)	Value range (α_5)	Value range (α_2 α_4 & *lm*)	Solution sub-ranges
[0, π/2]	[0, π/2]	[-π/2, π/2]	All	**1**
[0, π/2]	[0, π/2]	[-π, -π/2] & [π/2, π]	All	**2**
[0, π/2]	[π/2, π]	[-π/2, π/2]	All	**3**
[0, π/2]	[π/2, π]	[-π, -π/2] & [π/2, π]	All	**4**
[π/2, π]	[0, π/2]	[-π/2, π/2]	All	**5**
[π/2, π]	[0, π/2]	[-π, -π/2] & [π/2,π]	All	**6**
[π/2, π]	[π/2, π]	[-π/2, π/2]	All	**7**
[π/2, π]	[π/2, π]	[-π, -π/2] & [π/2, π]	All	**8**

Here, the sub-ranges of the solutions are categorised by the value of the positional variables (α_1, α_2, α_3, α_4, α_5, *lm*). Through the above analysis, it is shown that for the whole range for any given six link-lengths there may be eight solutions.

Through the above discussion, it was found that if an actual solution is near to a boundary of two sub-ranges of solutions, the numerical approach for the forward displacement problem needs a good starting point to find one actual solution and cannot guarantee that the computing result is the actual solution. For example, if an actual solution of the problem where α_1 is greater than but near π/2, it cannot guarantee that the starting point of α_1 is greater than π/2. If the starting point of α_1 is less than π/2, the computing result should be that α_1 is less than π/2. Therefore, if it cannot be guaranteed that the computed result is the actual solution of the problem, more sensors are necessary.

In the particular positional variable range discussed in Chapter 7, no multiple solutions have been found but it is still not proved that there is only one solution in the particular range. The number of the solutions in a given range of the positional

variables remains unknown. Hence, if the parallel mechanism discussed in Chapter 7 is applied to a real positioning system, it is suggested that one or more redundant sensors may be needed.

9.2 Comparing Measurement Accuracy for Different Parallel Mechanisms

Comparing measurement accuracy for different parallel mechanisms is another important problem for positioning system design. Since the PCA based analysis is carried out based on figures, in which the relationships between the principal components and the position and orientation of the top platform are illustrated using sample data, the measurement accuracy for different mechanisms can be compared using the corresponding figures.

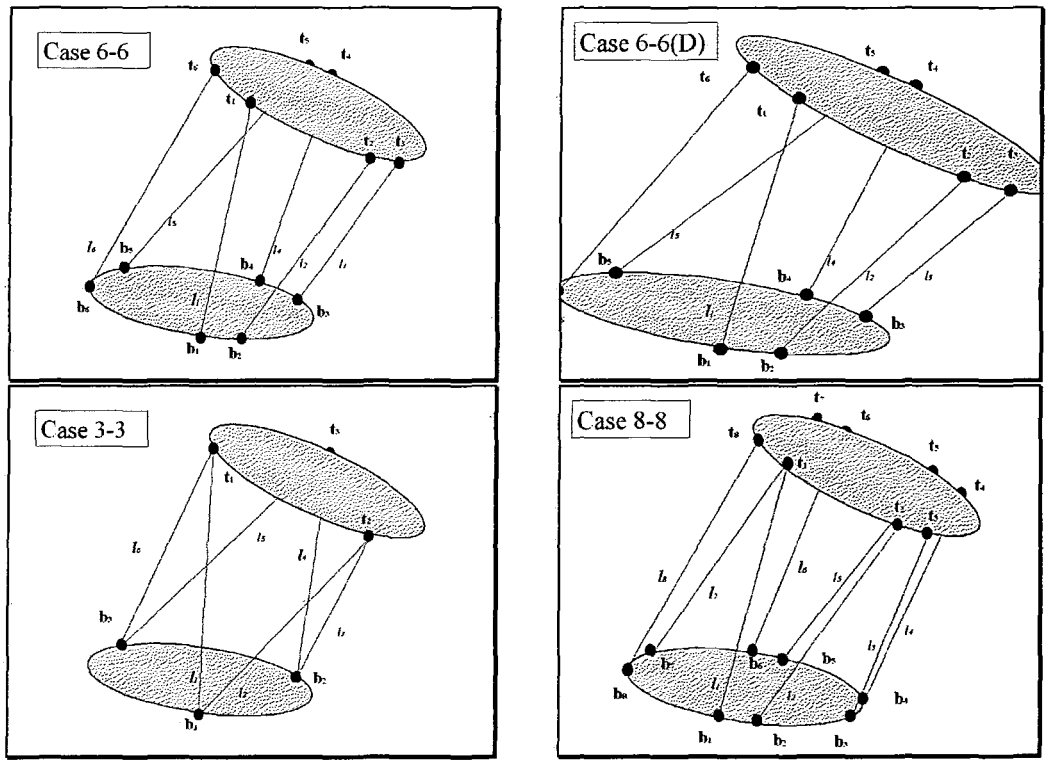

Figure 9-10 Different cases used to compare measurement accuracy

Normally, if a small change in link lengths leads to a big change in the positional variables, the accuracy of this positioning system will be low. If a big change in the link lengths only leads to a small change in the positional variables, the accuracy of this positioning system will be high. Measurement accuracy of every positional variable of a parallel mechanism cannot be evaluated by every linkage. Instead,

measurement accuracy of every positional variable of a parallel mechanism should be evaluated by a group of linkages. The PCA based approach can be used to evaluate the measurement accuracy for a particular mechanism. The following discussions are comparison analyses of the case discussed in Chapter 7, with another three given cases, as shown in Figure 9-10. Since the comparison analysis in the whole solution range is very complex, the following discussions are only to some special ranges. However, the general procedure and results of analysis will be illustrated as preparatory work.

Here, the case discussed in Chapter 7 and Chapter 8 is denoted as Case 6-6. The other cases are denoted as Case 6-6 (D), Case 3-3 and Case 8-8 respectively, which have different assembly configurations as follows.

Case 6-6 (D): This case is similar to the 6-6 case discussed in Chapter 7, but the diameter of the base and the platform is doubled. The joints on the base and on the platform are $\mathbf{b}=\{\mathbf{b}_x\,\mathbf{b}_y\,\mathbf{b}_z\}$ and $\mathbf{t}=\{\mathbf{t}_x\,\mathbf{t}_y\,\mathbf{t}_z\}$ respectively as follows.

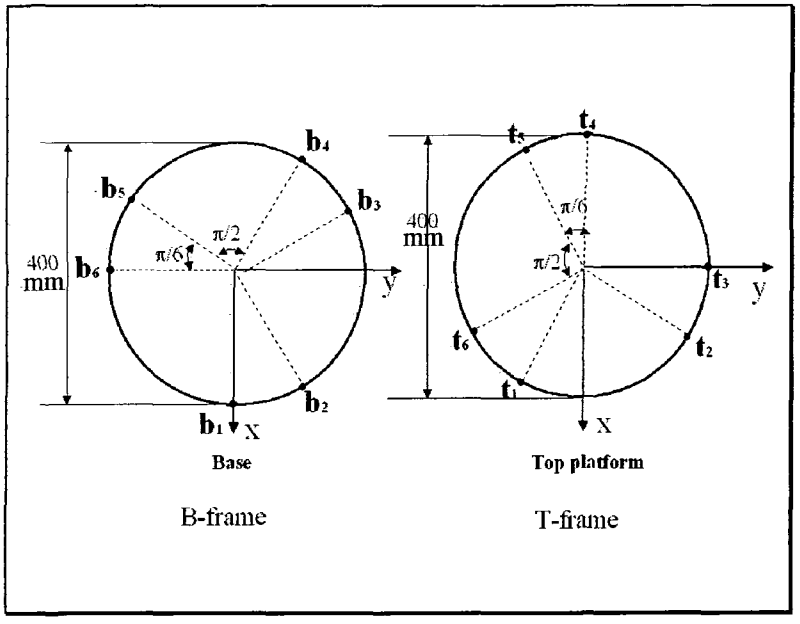

Figure 9-11 The positions of the joint points of the links in Case 6-6(D)

$$\mathbf{b}_x = (b_{x1}, b_{x2}, b_{x3}, b_{x4}, b_{x5}, b_{x6})$$

$$=200\cos(0, \pi/6, \pi*4/6, \pi*5/6, \pi*8/6, \pi*9/6)$$

$$\mathbf{b}_y = (b_{y1}, b_{y2}, b_{y3}, b_{y4}, b_{y5}, b_{y6})$$

$$=200\sin(0, \pi/6, \pi*4/6, \pi*5/6, \pi*8/6, \pi*9/6)$$

$\mathbf{b}_z = (b_{z1}, b_{z2}, b_{z3}, b_{z4}, b_{z5}, b_{z6})$

$=200(0, 0, 0, 0, 0, 0)$

$\mathbf{t}_x = (t_{x1}, t_{x2}, t_{x3}, t_{x4}, t_{x5}, t_{x6})$

$=200\cos(-\pi/6, \pi*2/6, \pi*3/6, \pi*6/6, \pi*7/6, \pi*10/6)$

$\mathbf{t}_y = (t_{y1}, t_{y2}, t_{y3}, t_{y4}, t_{y5}, t_{y6})$

$=200\sin(-\pi/6, \pi*2/6, \pi*3/6, \pi*6/6, \pi*7/6, \pi*10/6)$

$\mathbf{t}_z = (t_{z1}, t_{z2}, t_{z3}, t_{z4}, t_{z5}, t_{z6})$

$=(0, 0, 0, 0, 0, 0)$

Here, b_{x2} is for example the x coordinate of the second joint point $\mathbf{b}_2$, which is $200\cos(\pi/6)$. Similar, b_{zi} (i=1,2,3,4,5,6) is the x coordinate of the ith joint point $\mathbf{b}_i$; b_{yi} is the y coordinate of the ith joint point $\mathbf{b}_i$; b_{zi} is the z coordinate of the ith join point $\mathbf{b}_i$. The definitions of t_{zi}, t_{yi}, t_{zi} (i=1,2,3,4,5,6) are similar.

Case 3-3: This case is similar to the 6-6 case discussed in Chapter 7, but there are only three joints on the base and three joints on the platform rather than six. The link joint positions on the base and on the platform are given as follows.

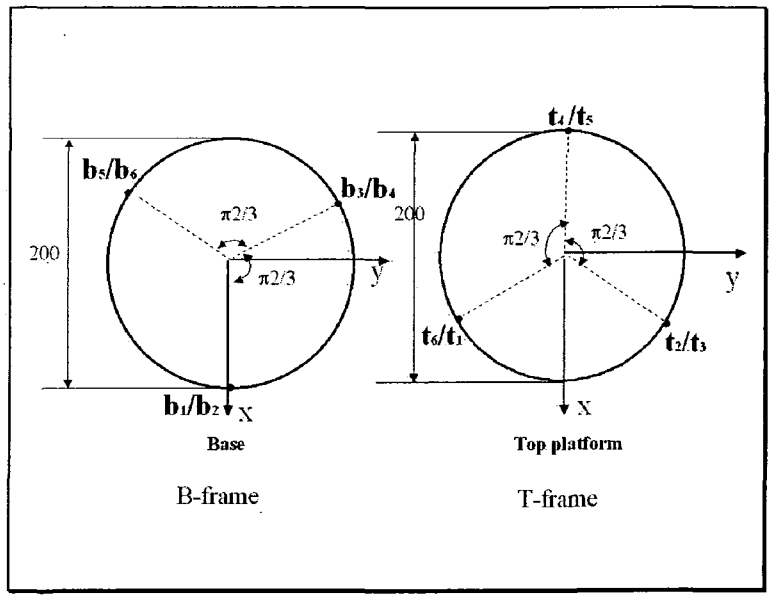

Figure 9-12 The positions of the joint points of the links in Case 3-3

$\mathbf{b}_x = (b_{x1}, b_{x2}, b_{x3}, b_{x4}, b_{x5}, b_{x6})$

$=100\cos(0, 0, \pi*2/3, \pi*2/3, \pi*4/3, \pi*4/3)$

$$\mathbf{b}_y = (b_{y1}, b_{y2}, b_{y3}, b_{y4}, b_{y5}, b_{y6})$$

$$=100\sin(0, 0, \pi*2/3, \pi*2/3, \pi*4/3, \pi*4/3)$$

$$\mathbf{b}_z = (b_{z1}, b_{z2}, b_{z3}, b_{z4}, b_{z5}, b_{z6})$$

$$=(0, 0, \mathbf{0}, \mathbf{0}, \mathbf{0}, \mathbf{0})$$

$$\mathbf{t}_x = (t_{x1}, t_{x2}, t_{x3}, t_{x4}, t_{x5}, t_{x6})$$

$$=100\cos(-\pi/3, \pi/3, \pi/3, \pi, \pi, -\pi/3)$$

$$\mathbf{t}_y = (t_{y1}, t_{y2}, t_{y3}, t_{y4}, t_{y5}, t_{y6})$$

$$=100\sin(-\pi/3, \pi/3, \pi/3, \pi, \pi, -\pi/3)$$

$$\mathbf{t}_z = (t_{z1}, t_{z2}, t_{z3}, t_{z4}, t_{z5}, t_{z6})$$

$$=(0, 0, \mathbf{0}, \mathbf{0}, \mathbf{0}, \mathbf{0})$$

Here the definitions of b_{zi}, b_{yi}, b_{zi} t_{zi}, t_{yi}, t_{zi} (i=1,2,3,4,5,6) are the same as the previous case.

Case 8-8: This is an 8-8 parallel mechanism, in which the link joint positions on the base and on the platform are given as follows.

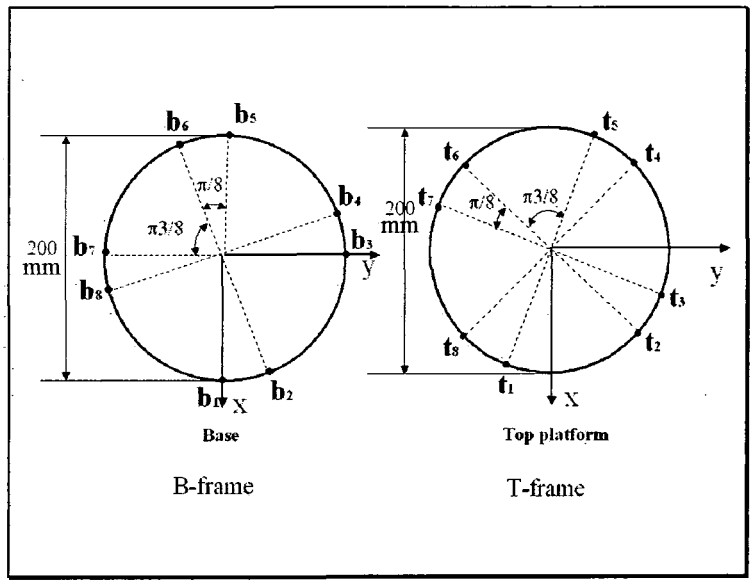

Figure 9-13 The positions of the joint points of the links in Case 8-8

$$\mathbf{b}_x = (b_{x1}, b_{x2}, b_{x3}, b_{x4}, b_{x5}, b_{x6}, b_{x7}, b_{x8})$$

$$=100\cos(0, \pi/8, \pi*4/8, \pi*5/8, \pi*8/8, \pi*9/8, \pi*12/8, \pi*13/8)$$

$$\mathbf{b}_y = (b_{y1}, b_{y2}, b_{y3}, b_{y4}, b_{y5}, b_{y6}, b_{y7}, b_{y8})$$

$=100\sin(0, \pi/8, \pi*4/8, \pi*5/8, \pi*8/8, \pi*9/8, \pi*12/8, \pi*13/8)$

$\mathbf{b}_z = (b_{z1}, b_{z2}, b_{z3}, b_{z4}, b_{z5}, b_{z6}\ b_{z7}, b_{z8})$

$=(0, 0, 0, 0, 0, 0, 0, 0)$

$\mathbf{t}_x = (t_{x1}, t_{x2}, t_{x3}, t_{x4}, t_{x5}, t_{x6}\ t_{x7}, t_{x8}))$

$=100\cos(-\pi/8, \pi*2/8, \pi*3/8, \pi*6/8, \pi*7/8, \pi*10/8, \pi*11/8, \pi*14/8)$

$\mathbf{t}_y = (t_{y1}, t_{y2}, t_{y3}, t_{y4}, t_{y5}, t_{y6}\ t_{y7}, t_{y8})$

$=100\sin(-\pi/8, \pi*2/8, \pi*3/8, \pi*6/8, \pi*7/8, \pi*10/8, \pi*11/8, \pi*14/8)$

$\mathbf{t}_z = (t_{z1}, t_{z2}, t_{z3}, t_{z4}, t_{z5}, t_{z6}, t_{z7}, t_{z8})$

$=(0, 0, 0, 0, 0, 0, 0, 0)$

The eigenvalues and eigenvectors for the different case are as follows

Case 6-6 (D):

Eigenvalues	Eigenvectors
λ_1 =1715207278	$\mathbf{a}_1$ = { 0.40825, 0.40825, 40825, 0.40825, 0.40825, 0.40825}
λ_2 =107547545	$\mathbf{a}_2$ = {-0.28878, -0.5773, -0.28867, 0.28867, -0.5773, 0.28878}
λ_3 =107475243	$\mathbf{a}_3$ = {0.50003, -0.000058743, -0.49997, -0.49997, -0.000058743, 0.50003}
λ_4 =13271868	$\mathbf{a}_4$ = {0.50003, -0.000058743, -0.49997, -0.49997, -0.000058743, 0.50003}
λ_5 =13263309	$\mathbf{a}_5$ = {-0.28869, 0.57735, -0.28873, -0.28873, 0.57735, 0.28862}
λ_6 =7746475	$\mathbf{a}_6$ = {-0.40826, 0.40826, -40824, 0.40824, -0.40824, 0.40824}

Case 3-3:

Eigenvalues	Eigenvectors
λ_1 =1527871656	$\mathbf{a}_1$ = { 0.40825, 0.40825, 40825, 0.40825, 0.40825, 0.40825}
λ_2 =27359239	$\mathbf{a}_2$ = {-0.28866, 0.28866, 0.57735, 0.28866, -0.28868, -0.57735}
λ_3 =27356025	$\mathbf{a}_3$ = {0.49999, 0.49999, 0.000013144, -0.50001, 0.50001,0.000013144}
λ_4 =9831822	$\mathbf{a}_4$ = {0.5, -0.5, -0.000019732, 0.5, -0.5, 0.000019733}
λ_5 =9831386	$\mathbf{a}_5$ = {0.28869, 0.28869,-0.57735, 0.28866, 0.28866, -0.57735}
λ_6 =1185659	$\mathbf{a}_6$ = {0.40826, -0.40826, 40824, -0.40824, 0.40824, -0.40824}

Case 8-8

Eigenvalues	Eigenvectors
λ_1 =1655283236	$\mathbf{a}_1$ = { 0.35355, 0.35355, 0.35355, 0.35355, 0.35355, 0.35355, 0.35355, 0.35355}
λ_2 =58346685	$\mathbf{a}_2$ = {0.43654, 0.13633,-0.24375, -0.48107,-0.43654,-0.13633,0.24375, 0.48107}

λ_3 =58346685	$\mathbf{a}_3$ = {0.24375, 0.48107, 0.43654, 0.13633,-0.24375, -0.48107,-0.43654, -0.13633}
λ_4 =2521346	$\mathbf{a}_4$ = {0.46741, -0.45607, 0.17762, 0.2049, -0.46741, 0.45607, -0.17762, -0.2049}
λ_5 =2521346	$\mathbf{a}_5$ = {-0.17762, -0.2049, 0.46741, -0.45607, 0.17762, 0.2049, -0.46741, 0.45607}
λ_6 =400481.9	$\mathbf{a}_6$ = {-0.35355, 0.35355, -0.35355, 0.35355, -0.35355, 0.35355, -0.35355, 0.35355}
λ_7 =130269.6	$\mathbf{a}_7$ = {-0.00459, 0.49998, 0.00459, -0.49998, -0.00459, 0.49998, 0.00459, -0.49998}
λ_8 =129786.5	$\mathbf{a}_8$ = {-0.49998, -0.00459, 0.49998, 0.00459, -0.49998, -0.00459, 0.49998, 0.00459}

The PCA based analysis was applied to the above three cases (Case 6-6 (D), Case 3-3 and Case 8-8). It was found that the general relationships between the principal components and the positional variables are similar to the case discussed in Chapter 7. That is, the first principal component (Y_1) mainly relates to the positional variable *lm*. The sixth principal component (Y_6) mainly relates to the positional variable α_5. The principal components (Y_2, Y_3, Y_4, Y_5) mainly relate to the positional variables (α_1, α_2, α_3, α_4).

The accuracy for the measurement of *lm*

The first principal components (Y_1) in these four cases are similar to each other, which are the average of the six, or eight in Case 8-8, link lengths with a scale factor.

Case 6-6: $Y_1 = 0.40825\,(l_1 + l_2 + l_3 + l_4 + l_5 + l_6)$

Case 6-6(D): $Y_1 = 0.40825\,(l_1 + l_2 + l_3 + l_4 + l_5 + l_6)$

Case 3-3: $Y_1 = 0.40825\,(l_1 + l_2 + l_3 + l_4 + l_5 + l_6)$

Case 8-8: $Y_1 = 0.35355(l_1 + l_2 + l_3 + l_4 + l_5 + l_6 + l_7 + l_8)$

Figure 9-14 shows the relationships between Y_1 and lm when α_1, α_2, α_3, α_4 $_4$ and α_5 equal zero in the different cases.

Here, the four lines express the four relationships for the different cases. The absolute values of the slopes of the lines determine the measurement accuracy. Here, Case 8-8

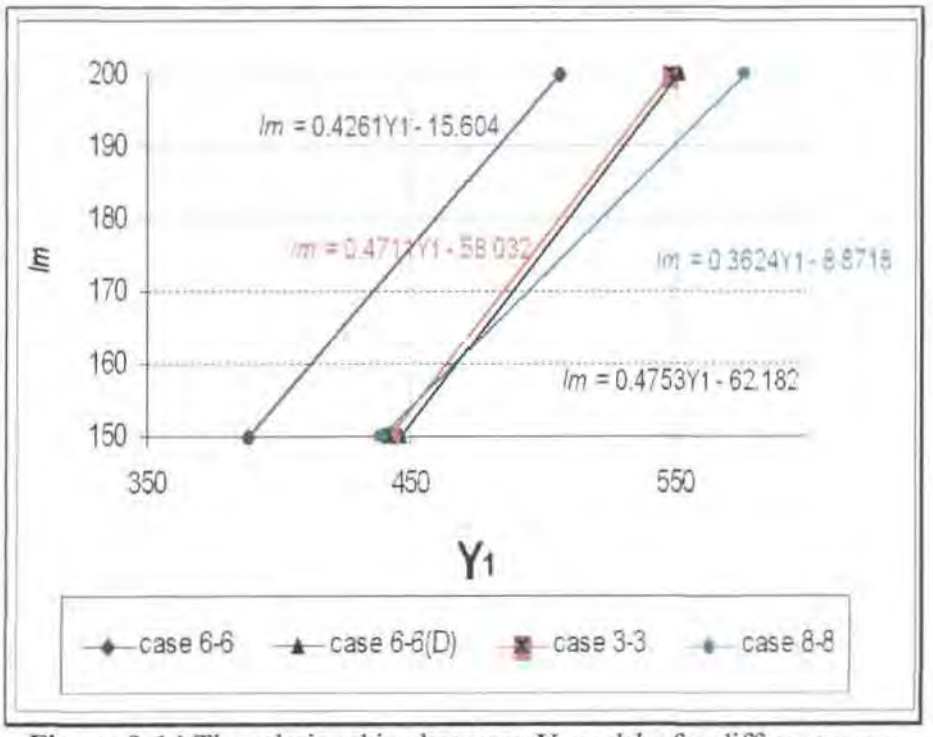

Figure 9-14 The relationships between Y_1 and *lm* for different cases

has the highest accuracy because the absolute value of the slopes of the line is the smallest (0.3624) in these four cases. In the other three cases, there is not much difference in terms of the measurement accuracy for *lm*. The rank of the accuracy is Case 6-6 (0.426), Case3-3 (0.4711) and Case 6-6(D) (0.4753).

The relationships between Y_1 and *lm* will be changed if the values of (α_1, α_2, α_3, α_4, α_5) are changed. Generally, the conclusions for accuracy comparison analysis are the same as the above situation where the values of (α_1, α_2, α_3, α_4, α_5) are zero.

The accuracy for the measurement of α_5

It was found that the sixth principal component mainly relates to the positional variable α_5 in every case.

The sixth principal components (Y_6) in these four cases are similar to each other, which are given as follows.

Case 6-6: $Y_6 = 0.40825(-l_1 + l_2 - l_3 + l_4 - l_5 + l_6)$

Case 6-6(D): $Y_6 = 0.40825(-l_1 + l_2 - l_3 + l_4 - l_5 + l_6)$

Case 3-3: $Y_6 = -0.40825(-l_1 + l_2 - l_3 + l_4 - l_5 + l_6)$

Case 8-8: $Y_6 = 0.35355\,(-l_1 + l_2 - l_3 + l_4 - l_5 + l_6 - l_7 + l_8)$

Through the above formulas for the sixth principal component, it is clear that the sixth principal components of the different cases are similar. The sixth principal components of Case 6-6 and Case 6-6(D) are the same. The difference of the sixth principal component between Case 6-6 and Case 3-3 is only with a scale factor (-1).

Figure 9-15 shows the relationships between Y_6 and α_5 when α_1, α_2, α_3, α_4 equal zero and *lm* =150 in the different cases.

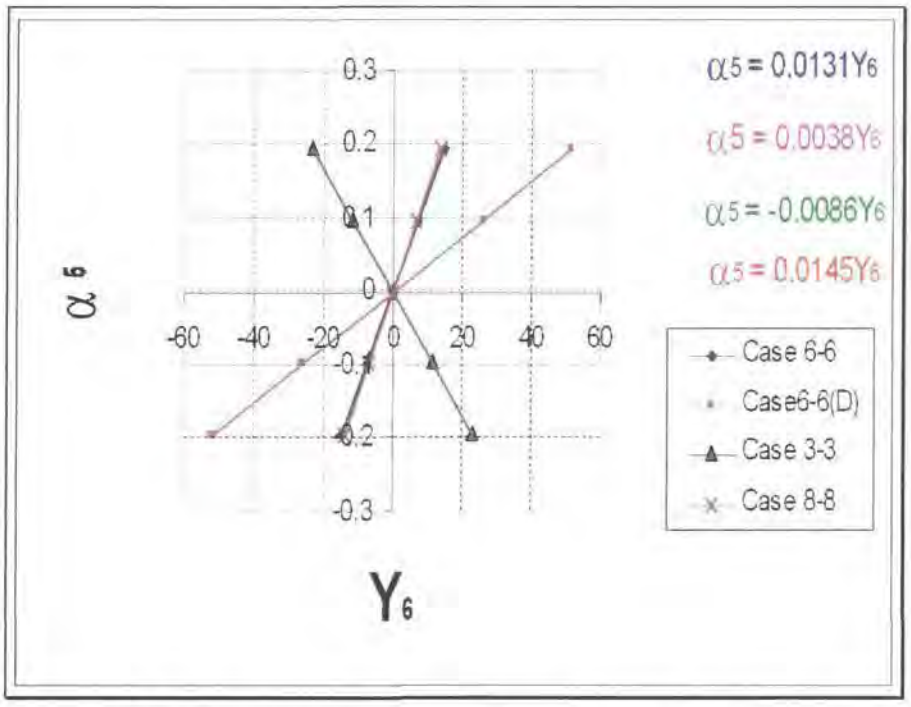

Figure 9-15 The relationships between Y_6 and α_5 for different cases

Here, the four lines express the four relationships for the different cases. The absolute values of the slopes of the lines determine the measurement accuracy. It is clear that Case 6-6(D) has the highest accuracy because the absolute value of the slopes of the line is the smallest (0.0038) in these four cases. Case 3-3 has the second the highest accuracy. Its absolute value of the slopes of the line is 0.0086. The other two cases, Case 6-6 and Case 8-8, have lower accuracy. These two cases have almost the same accuracy because the values of the slopes are very close (0.0131 for Case 6-6 and 0.0145 for Case 8-8).

The relationships between Y_6 and α_5 will be changed if the values of (α_1, α_2, α_3, α_4, *lm*) are changed. Generally, the conclusions for accuracy comparison analysis are the same as the above situation where the values of (α_1, α_2, α_3, α_4, *lm*) are zero.

The accuracy for the measurement of α_1, α_2, α_3, α_4

In the discussion in Chapter 8, it was known that the measurements of (α_1, α_2, α_3, α_4) are dependent upon the relationship between (Y_2, Y_3, Y_4, Y_5) and (α_1, α_2, α_3, α_4). Because the relationship between (Y_2, Y_3, Y_4, Y_5) and (α_1, α_2, α_3, α_4) is very complex, during computing the values (α_1, α_2, α_3, α_4), the basic relationships between (Y_2, Y_3, Y_4, Y_5) and (α_1, α_2, α_3, α_4) are used. Because of the complexity of the relationship between (Y_2, Y_3, Y_4, Y_5) and (α_1, α_2, α_3, α_4), the problem of accuracy analysis for the measurement of (α_1, α_2, α_3, α_4) for different cases remains. However, in some particular situations the comparison analyses were carried out as a preparatory discussion. The following discussion shows the measurement accuracy for α_3 and α_4 using the basic relationships between (Y_2, Y_3, Y_4, Y_5)-(α_3, α_4). Here, the basic relationship (Y_2, Y_3, Y_4, Y_5)-(α_3, α_4) means the basic relationships of (Y_2, Y_3)-to-(α_3, α_4) and (Y_4, Y_5)-to-(α_3, α_4) defined in Chapter 7. As mentioned in Chapter 7, the basic relationships of (Y_2, Y_3)-to-(α_3, α_4) and (Y_4, Y_5)-to-(α_3, α_4) are the pair-to-pair relationships (Y_2, Y_3)-(α_3, α_4) and (Y_4, Y_5)-(α_3, α_4) in the situation where α_1 and α_2 are zero. Hence, the following accuracy analysis for the measurements of α_3 and α_4 is based on the situation where α_1 and α_2 are zero. The same analysis can be carried out for the measurement accuracy of α_1 and α_2. Since the procedure and results of the accuracy analysis for the measurements of α_1 and α_2 are similar to that for the measurements accuracy of α_3 and α_4, the accuracy analysis for the measurements of α_1 and α_2 will not be discussed in this thesis.

Accuracy analysis for the measurements of α_3 and α_4 using the basic relationship of (Y_2, Y_3)-to-(α_3, α_4)

Figure 9-16 shows different values of (α_3, α_4) corresponding to different values of (Y_2, Y_3) where α_1, α_2 and α_5 equal zero, and *lm* equal 200. As mentioned in Chapter 7, there is a vector (v_{23}) from the origin of the plane Y_2-Y_3 to any given point corresponding to given values of (α_3, α_4). The length of the vector $(\rho_{23}=|v_{23}|=\sqrt{Y_2^2+Y_3^2})$ corresponds to the value of α_3 and the angle of the vector to the Y_3 axis ($\theta_{23}=\text{atan}(Y_3/Y_2)$ corresponds to the value of α_4. Thus, the length of the vector (ρ_{23}) can be mainly used to estimate the value of α_3 and the polar angle of the vector (θ_{23}) can be mainly used to estimate the value of α_4 However, the relationships between ρ_{23} and α_3 are different for the different cases. The relationships between θ_{23} and α_4 are also different for the different cases. These can illustrate the difference of the measurement accuracy between the different cases.

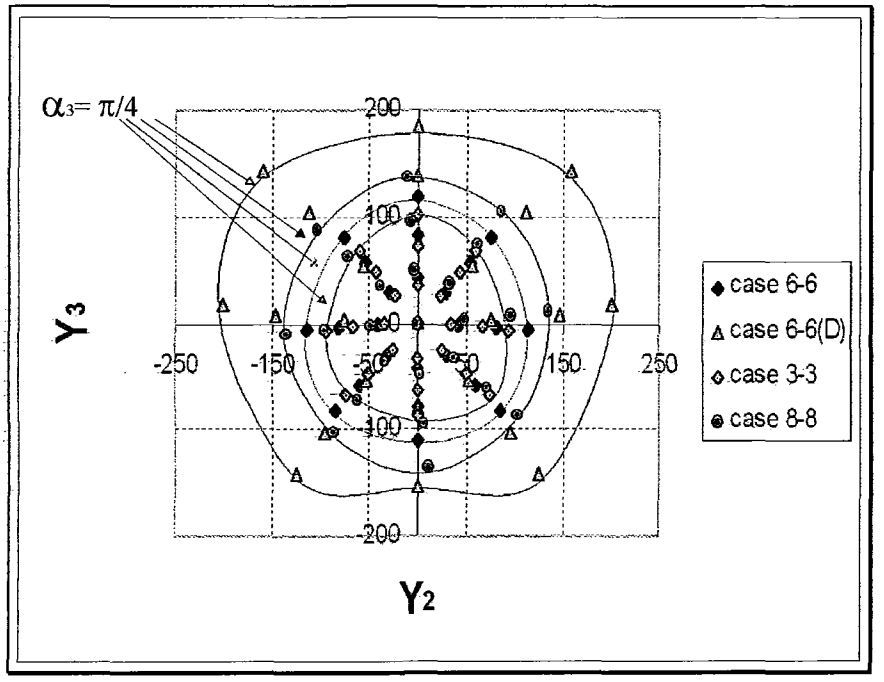

Figure 9-16 Different values (α_3, α_4) correspond to different values (Y_2, Y_3)

Figure 9-17 shows the relationships between ρ_{23} and α_3 in the different cases in the situation where α_1, α_2 and α_5 equal zero; *lm* equal 200 and α_4=0. It was found through Figure 9-17 that Case 6-6(D) has the highest measurement accuracy of α_3. Case 8-8 has the second highest measurement accuracy of α_3. Case 3-3 has the lowest

measurement accuracy of α_3. Case 6-6 is better than Case 3-3 but worse than case 6-6(D) and Case 8-8.

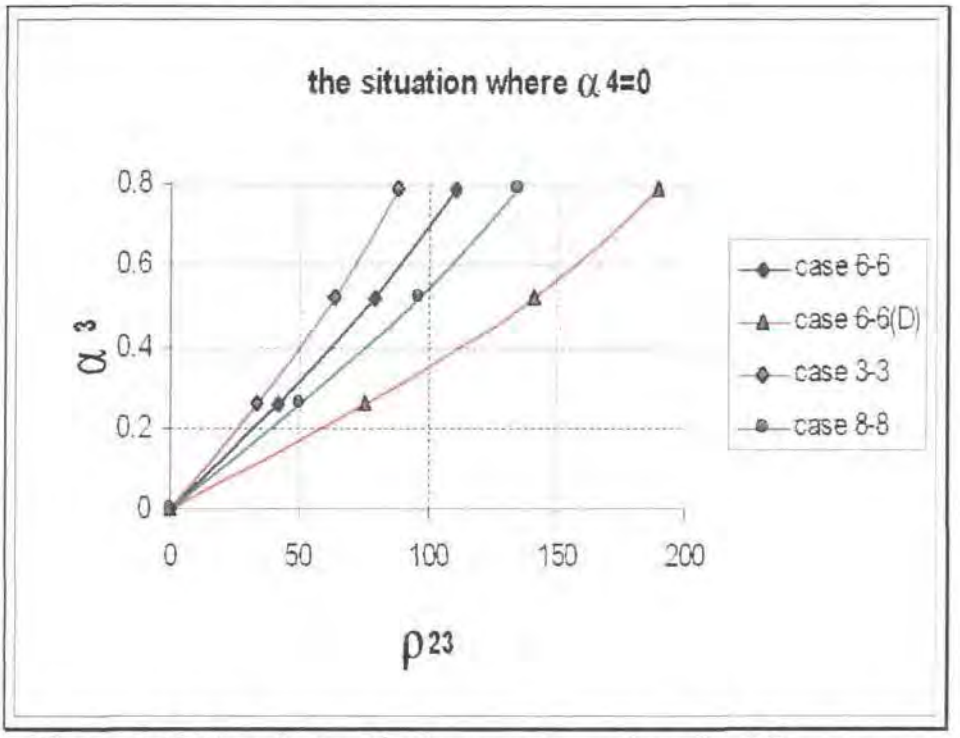

Figure 9-17 The relationships between ρ_{23} and α_3 for different cases

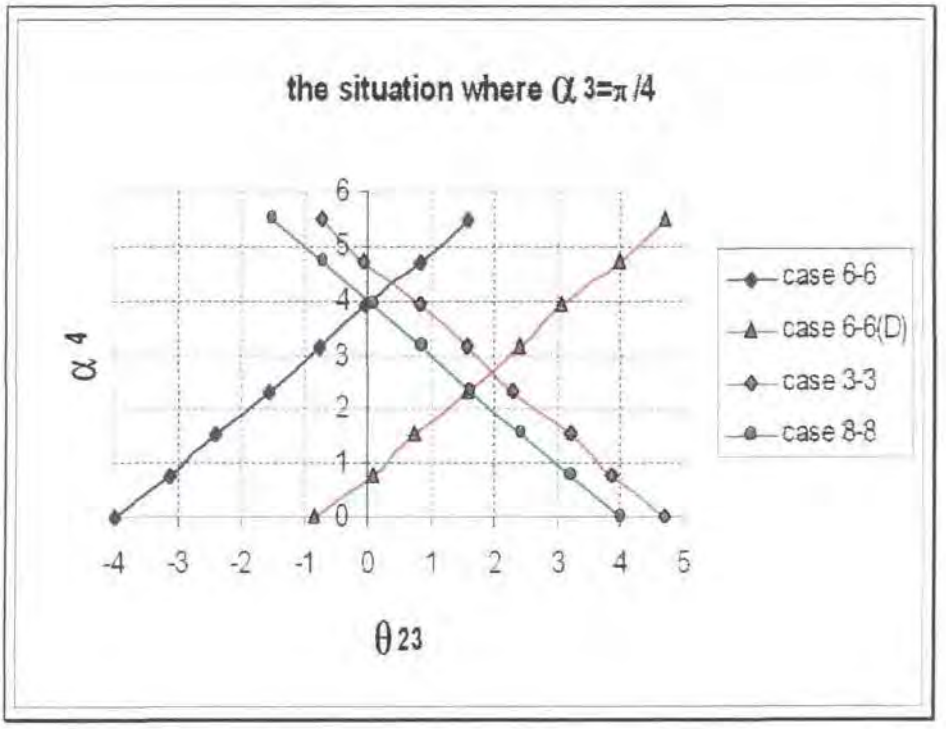

Figure 9-18 The relationships between θ_{23} and α_4 for different cases

Figure 9-18 shows the relationships between θ_{23} and α_4 in the different cases in the situation where α_1, α_2 and α_5 equal zero; *lm* equal 200 and $\alpha_3 = \pi/4$. It was found through Figure 9-18 that if there is a difference in the value of θ_{23}, there will be almost the same difference in the value of α_4. Hence the measurement accuracy of α_4 for the different cases are almost the same. It should be noted that if α_4 has a change of 2π, θ_{23} will also have a change of 2π. Hence, if the wave of the relationship curve in Figure 9-18 is smaller, the measurement accuracy of α_4 in the whole value range of α_4 are more even. Consequently, the minimum measurement accuracy in the whole range will be higher. Therefore, Case 8-8 has highest measurement accuracy in the whole value range of α_4.

Accuracy analysis for the measurements of α_3 and α_4 using the basic relationship (Y_4, Y_5)-(α_3, α_4)

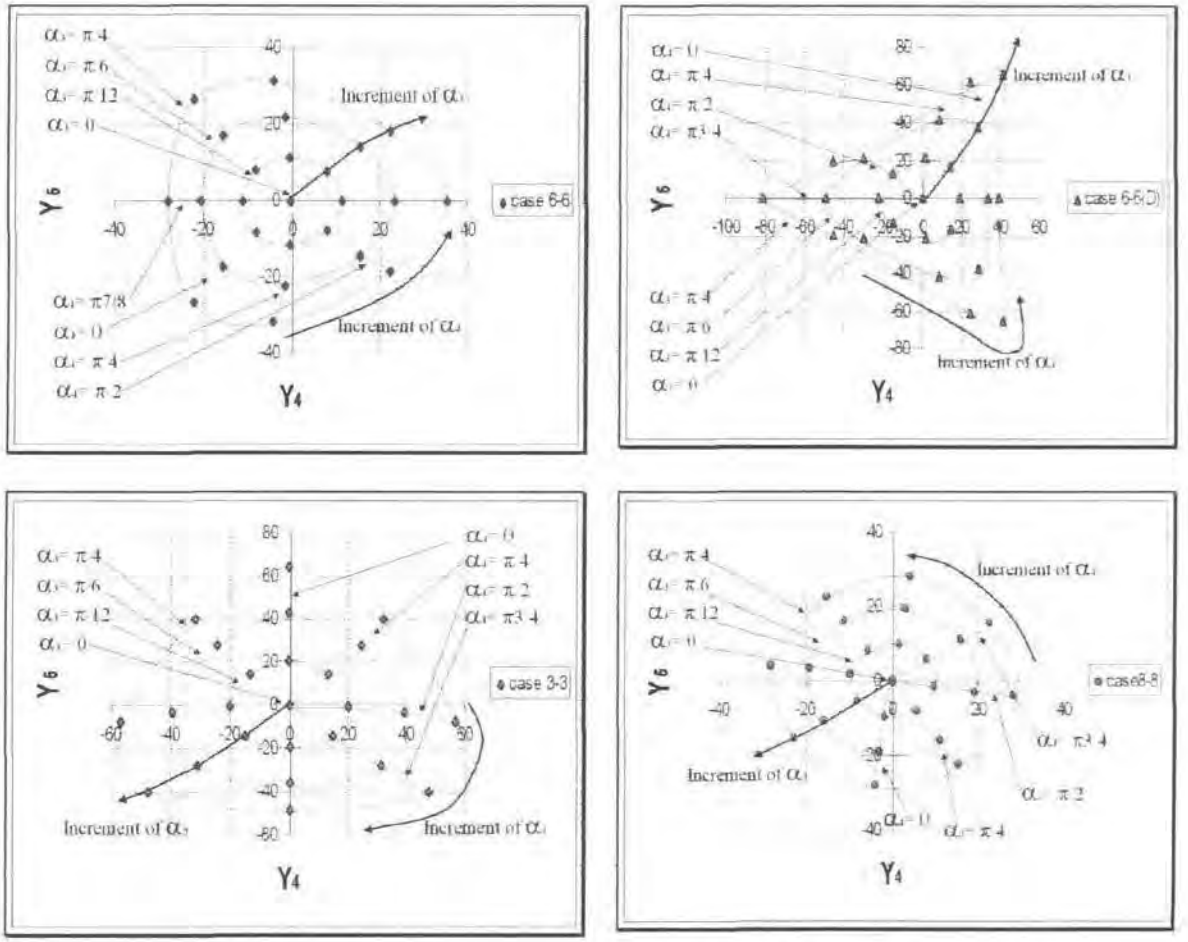

Figure 9-19 Different values (α_3, α_4) correspond to different values (Y_4, Y_5)

Because the values of (α_3, α_4) not only depend on the values of (Y_2,Y_3) but also depend on the values of (Y_4, Y_5), accuracy analysis for the measurements of α_3 and α_4 by using the basic relationship (Y_4, Y_5)-(α_3, α_4) is necessary.

Figure 9-19 shows different values of (α_3, α_4) corresponding to different values of (Y_4, Y_5) where α_1, α_2 and α_5 equal zero, and *lm* equal 200.

As in the previous discussion for the basic relationship of (Y_2, Y_3)-to-(α_3, α_4) there is a vector (v_{45}) from the origin of the plane Y_2-Y_3 to any given point corresponding to given values of (α_3, α_4). The length of the vector ($\rho_{45}=|v_{45}|=\sqrt{Y_4^2+Y_5^2}$) corresponds to the value of α_3 and the angle of the vector to the Y_3 axis (θ_{45} = atan(Y_5/Y_4)) corresponds to the value of α_4. Thus length of the vector (ρ_{45}) can be mainly used to estimate the value of α_3 and the polar angle of the vector (θ_{45})

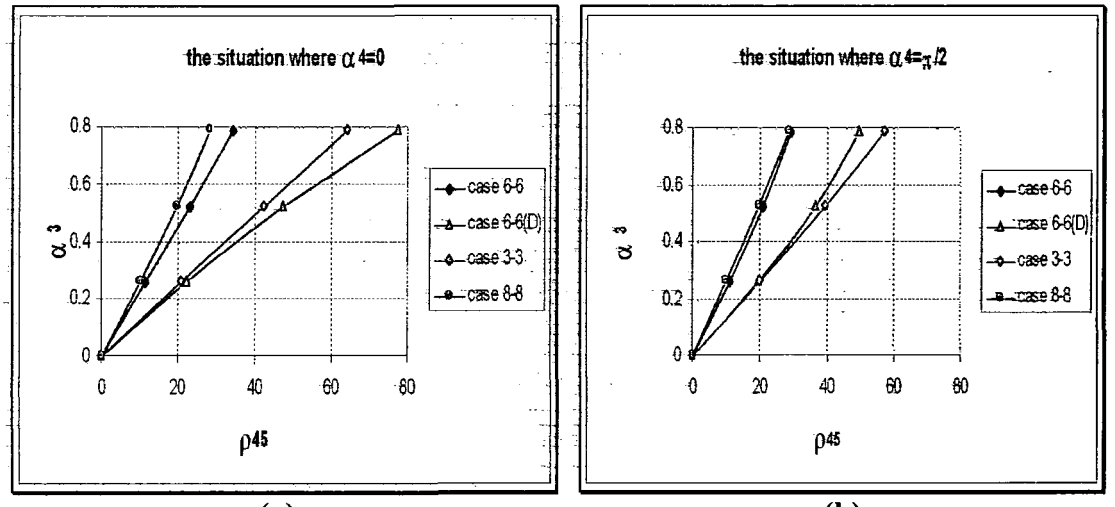

(a) **(b)**

Figure 9-20 the relationships between ρ_{45} and α_3 indifferent cases

can be mainly used to estimate the value of α_4 However, the relationships between ρ_{45} and α_3 are different for the different cases. The relationships between θ_{45} and α_4 are also different for the different cases. These can illustrate the difference of the measurement accuracy between the different cases.

Figure 9-20 shows the relationships between ρ_{45} and α_3 in the different cases, in the situation where α_1, α_2 and α_5 equal zero; *lm* equal 200. Figure 9-20(a) is for the situation α_4=0. Figure 9-20(b) is for the situation α_4=π/2. It was found that for

different values of α_4, the measurement accuracy of α_3 in different cases are different. When α_4=0, the rank of the measurement accuracy of α_3 from high to low is Case6-6(D), Case3-3, Case6-6 and Case8-8. When $\alpha_4 = \pi/2.$, the rank of the measurement accuracy of α_3 from high to low is Case3-3, Case6-6(D), Case6-6 and Case8-8.

Figure 9-21 shows the relationships between θ_{45} and α_4 in the different cases in the situation where α_1, α_2 and α_5 equal zero; *lm* equals 200. Figure 9-21(a) is for the situation $\alpha_3 = \pi/4$. Figure 9-20(b) is for the situation $\alpha_3 = \pi/12$. It should be noted that if α_4 has a change of 2π, θ_{45} will also have a change of 2π. Hence, if the wave of the relationship curve in Figure 9-21 is smaller, the measurement accuracy of α_4 in the whole value range of α_4 are more even. Consequently, the minimum measurement accuracy in the whole range will be higher. Therefore, two conclusions were obtained.

- The highest measurement accuracy of α_4 is Case8-8. The lowest

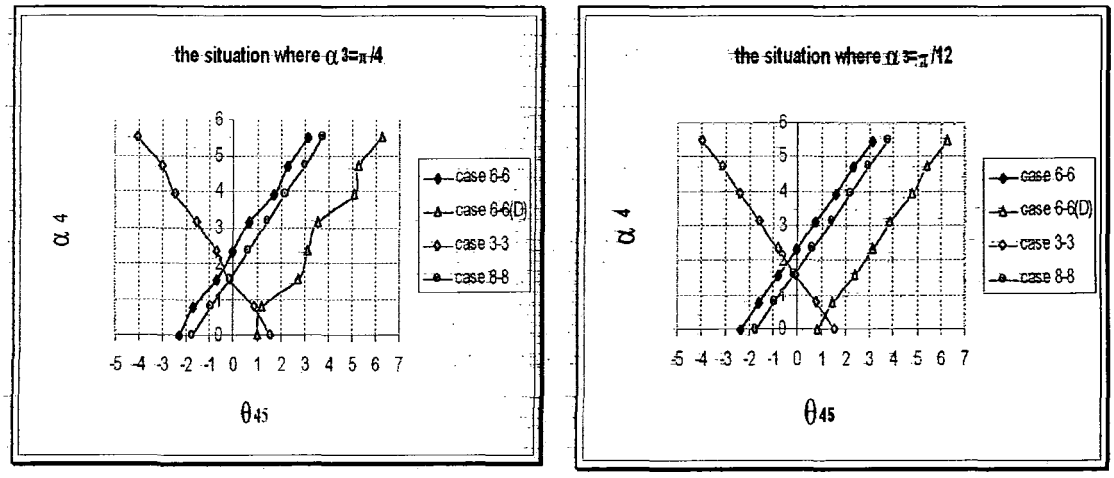

Figure 9-21 the relationships between θ_{45} and α_4 indifferent cases

measurement accuracy of α_4 is Case6-6(D). Case6-6 and Case3-3 are located in the middle.

- When α_3 becomes smaller, the measurement accuracy of α_4 for the different cases will approach the same value.

Through the above analysis, it was shown that the measurement accuracy is different for the different cases and different situations. Therefore, during the period of designing a parallel mechanism for a positioning system, identification of the

application situations and analysis for the corresponding measurement accuracy are required.

Chapter 10

Summary of Part II

The forward displacement problem for a 6-6 parallel mechanism was discussed in Part II. The target of this project is to improve accuracy of a positioning system, for stepwise robots, using parallel mechanisms, Not only a solution for the forward displacement problem is needed but also the accuracy of the solution needs to be determined. In Part II, the PCA based approach was introduced to analyse the relationship between the six link-lengths and the position and orientation of the top platform. Consequently, a numerical algorithm based on the result of the relationship analysis was given. The results of the computing simulation showed that the proposed system has very high accuracy.

The technical key to the PCA based approach is the transformation from the six link-lengths to the six principal components. This transformation directly comes from the result of PCA, which depends upon sample data. Because of the complexity of the parallel mechanism, any one or two linkages cannot express any part of the position and orientation of the platform. However, if the transformation from the six link-lengths to the six principal components is successful, every principal component can more easily express one part of the position and orientation of the platform. In this project, the transformation is successful, so that the relationship between the principal components and the position variables of the platform was identified. The success of this transformation not only makes the analysis for the particular parallel mechanism discussed in Section 2.3 possible but also benefits the same analysis for different mechanisms. In Section 9.2, for example, the transformations from the link-lengths to the principal components for different mechanisms were successfully obtained, by simply following the set procedures and sample rules.

The PCA based approach is a statistical approach. The results of the PCA based analysis depend on the sample data. Hence, the relationship identified by the PCA based approach is true in a certain range in which the sample data is valid. The discussions in Section 2.3 showed that when one of the six position variables varies and the other five are fixed, the varied variable can be determined by one or two

principal components. For example, *lm* can be determined by Y . Also, α can be determined by (Y , Y) or (Y , Y). In this situation, the quantity relationships between the position variables and the principal components can be determined. Based on this situation, if the five fixed variables are changed, the quantity relationship between the varied variable and the principal or principals will be changed. However, if the five fixed position variables are changed in the range discussed in Section 2.3, the quality relationship between the varied variable and the principal or principals will not be changed. That is, if the quantity relationship is viewed as a function, the properties of the function will not be changed. That is, the function is a Single-variable, Increasing and Continuous function in any situation. It should be noted that if the five fixed position variables are changed in the whole solution range discussed in Section 9.1, the quality relationship between the varied variable and the principal or principals will also be changed.

The PCA based approach can be used to investigate the different properties of the relationship between the linkages and the position variables in different solution ranges. This is one of the advantages of this approach. Because of this advantage, the searching paths in the numerical algorithm for the forward displacement problem can be optimised in a certain solution range. The measurement accuracy for any given position variable of the parallel mechanism can also be analysed in a certain solution range. Consequently, the assembly configuration of a parallel mechanism can be optimised, and/or what sensors are needed to improve the accuracy of the positioning system can be identified.

The numerical algorithm given in Chapter 8 is based on the quality relationship between the linkage and the position variables. The simulation results of the numerical algorithm given in Chapter 8 showed the advantages of parallel mechanism based approach for positioning systems. The algorithm is still not optimised, but the computing performance was very good. This shows the potential for industrial application of this positioning technique. Since the PCA based numerical algorithm is based on the result of the relationship analysis for a particular parallel mechanism, the numerical algorithm can be significantly optimised after the further analyses and assembly configuration optimisation for the parallel mechanism.

The parallel mechanism based positioning approach with the PCA based analysis methodology takes shape of a new positioning technique for stepwise robots. This technique is based on the signals of the lengths of the linkages but does not exclude uses of other signals from other sensors in a real industrial application. Any sensor may be added into the parallel mechanism based positioning system, as long as the results of the PCA based analysis show the use of the added sensor can improve the accuracy. In summary, a new positioning technique has been proposed and shows its advantages, but in this area, further work is also needed.

Chapter 11

Conclusions and Further Research Problems

11.1 Conclusions

In this thesis, positioning technology for stepwise underground robots was discussed. This is a theoretical preparatory work for industrial application of underground robotic positioning systems. During the research, Durham University stepwise robots were used as real case study.

Because of lack of research on underground robotic positioning, some fundamental issues were discussed in the first chapters of this thesis. Underground environment highly constrains the use of existing position measurement technologies. The main constraint is that only relative position measurement techniques are available for underground robot. Consequently, whether the accuracy of positioning systems for underground robots can meet application requirements becomes problematic. To answer this question, two-dimensional error model, exact and statistical models, were given in this thesis, which are also suitable for three-dimensional cases. These models show that:-

- Angular measurement errors are the dominant error sources for the positioning system. Comparing with the dominant error, Step-length measurement errors can be ignored.
- Theoretically, existing sensors and measurement technologies cannot ensure satisfactory long-term (1000 meters or longer travel distance) positioning accuracy for industrial applications because of the accumulation of the orientation errors. However, if the angular measurement errors are random error and the means of the errors are zero, under very high confidence, such as 99.9%, positioning systems can provide high long-term accuracy. This makes improvement of long-term positioning accuracy for industrial applications possible. The exact and estimate error models given tin this thesis are very

helpful to judge the feasibility of a particular accuracy requirement for a positioning system.

Based on the fundamental discussions, it was known that improvement of angular measurement accuracy is the most important for improving long-term positioning accuracy. Consequently, parallel linkage mechanism based approach for a positioning system was proposed. The aim of this proposal is to improve angular measurement accuracy. In fact, this proposal is an approach to improve the measurement accuracy by choosing an assembly configuration of parallel linkage mechanism. This approach is suitable for underground robots working in narrow space. The simulation of a real case study shown that the combination of six linear sensors, which have normal measurement accuracy (errors < 1mm), can provide very high angular measurement accuracy (<0.006 radians) in most situations and normal accuracy (<0.01 radians) in very few situations. Considering the accumulation of orientation error, which was discussed in this thesis, this property of the parallel linkage mechanism can be used to improve long-term positioning accuracy.

To design and improve a parallel linkage mechanism based positioning system, investigating the accuracy for different assembly configurations is also very important. The PCA based analysis method was shown its advantage in this aspect. The PCA based analysis method can also be used to investigate the characteristics of the solution, such as multiple-solutions. Therefore, the methodology in this thesis provides a new approach to investigate parallel linkage mechanisms. The procedure and the results of the PCA based analysis shown in this thesis can be referred by other researchers of parallel linkage mechanism.

11.2 Further Research Problems

In this research, a parallel mechanism based approach to improve accuracy of a positioning system for stepwise robots has been proposed. In addition, the PCA based approach to solve the problems of forward displacement has been proposed and shows its advantages in terms of accuracy analysis and the computational performance. The result of this research has shown to be of potential commercial value for industrial applications. However, some further research is required before applying this study to real industrial applications, which are listed as follows:

- Experiment based research for the parallel mechanism based approach is required to compare with the theoretical analysis. In this research, computer simulation has shown very good results for the proposed approach. The simulation results need to be verified by experimental results. Experimental research may find new problems in manufacture and operation. This is very important for industrial application. Experimental results may also provide further problems for future theoretical research.

- Analysis for the relationship between the linkages and the position and orientation of the platform is required to extend to the whole solution range. In this project, the solution range for the forward displacement problem of the 6-6 parallel mechanism was identified, based on a particular robotic application. The extension analysis can enhance the understanding of the properties of the parallel mechanism. It will not only benefit the further research for the positioning system using parallel mechanisms but also benefit other research on parallel mechanisms. Some preparatory work was done in Section 9.1, in this thesis.

- Comparison analysis of measurement accuracy for different assembly configurations of parallel mechanisms is very important for the design of a parallel mechanism based positioning system. This comparison analysis can provide the accuracy for using different mechanisms and in different solution ranges. Because the parallel mechanism based approach is an approach to improve the accuracy by improving structure rather than improving precision of individual sensors, a comparison analysis technique is of a critical importance in this approach.

- The PCA based numerical algorithm has great potential to be improved. If the PCA based analysis can identify the relationships between the linkages and the position and the orientation of the platform in more detail, the solution searching paths can be significantly improved.

- The parallel mechanism based solution for positioning system provides more space for the use of redundant sensors. This can improve the measurement accuracy not only by choosing a good assembly configuration in some situation

(see Section 9.2), but also by data fusion. Much work in this area remains to be done.

- The software development for the PCA based analysis for a parallel mechanism is also valuable for further research and industrial applications. The PCA based analysis needs further work on data comparison. In addition, this work needs knowledge from the PCA approach. If computer software was available for assisting analysis for the PCA analysis, the performance of the research and system design will be significantly improved.

All above further research problems can follow the methodology and results of this research project. Their potential value is also significant.

Appendix A

TABLE A.1

Test Result of the Error Estimate Function (1-5)

D	E_o	n	nD	nE_o	$49nE_o$	$(e_o/nD)\%$	$49nE_o-100(e_o/nD)$
0.1	0.00025	1000	100	0.25	12.25	12.49077	-0.24077
0.1	0.00025	2000	200	0.5	24.5	24.83917	-0.33917
0.1	0.00025	3000	300	0.75	36.75	36.92982	-0.17982
0.1	0.00025	4000	400	1	49	48.63831	0.361694
0.1	0.0005	1000	100	0.5	24.5	24.85156	-0.35156
0.1	0.0005	2000	200	1	49	48.65011	0.349893
0.1	0.001	1000	100	1	49	48.67371	0.326291
0.2	0.00025	1000	100	0.125	6.125	6.259744	-0.13474
0.2	0.00025	2000	200	0.25	12.25	12.49077	-0.24077
0.2	0.00025	3000	300	0.375	18.375	18.68926	-0.31426
0.2	0.00025	4000	400	0.5	24.5	24.8392	-0.3392
0.2	0.00025	5000	500	0.625	30.625	30.92461	-0.29961
0.2	0.00025	6000	600	0.75	36.75	36.92983	-0.17983
0.2	0.00025	7000	700	0.875	42.875	42.83942	0.035579
0.2	0.00025	8000	800	1	49	48.63829	0.361706
0.2	0.0005	1000	100	0.25	12.25	12.50325	-0.25325
0.2	0.0005	2000	200	0.5	24.5	24.85151	-0.35151
0.2	0.0005	3000	300	0.75	36.75	36.94193	-0.19193
0.2	0.0005	4000	400	1	49	48.65011	0.349893
0.2	0.001	1000	100	0.5	24.5	24.87614	-0.37614
0.2	0.001	2000	200	1	49	48.67376	0.326244
0.4	0.00025	1000	100	0.0625	3.0625	3.137184	-0.07468
0.4	0.00025	2000	200	0.125	6.125	6.259794	-0.13479
0.4	0.00025	3000	300	0.1875	9.1875	9.37833	-0.19083
0.4	0.00025	4000	400	0.25	12.25	12.49077	-0.24077
0.4	0.00025	5000	500	0.3125	15.3125	15.5951	-0.2826
0.4	0.00025	6000	600	0.375	18.375	18.68928	-0.31428
0.4	0.00025	7000	700	0.4375	21.4375	21.7713	-0.3338
0.4	0.00025	8000	800	0.5	24.5	24.8392	-0.3392
0.4	0.00025	9000	900	0.5625	27.5625	27.89096	-0.32846
0.4	0.00025	10000	1000	0.625	30.625	30.92461	-0.29961
0.4	0.0005	1000	100	0.125	6.125	6.272266	-0.14727
0.4	0.0005	2000	200	0.25	12.25	12.50321	-0.25321
0.4	0.0005	3000	300	0.375	18.375	18.70169	-0.32869
0.4	0.0005	4000	400	0.5	24.5	24.85152	-0.35152
0.4	0.0005	5000	500	0.625	30.625	30.93684	-0.31184
0.4	0.0005	6000	600	0.75	36.75	36.94194	-0.19194
0.4	0.0005	7000	700	0.875	42.875	42.85139	0.023611
0.4	0.0005	8000	800	1	49	48.65011	0.349893
0.4	0.001	1000	100	0.25	12.25	12.52813	-0.27813
0.4	0.001	2000	200	0.5	24.5	24.8762	-0.3762
0.4	0.001	3000	300	0.75	36.75	36.96618	-0.21618
0.4	0.001	4000	400	1	49	48.67376	0.326244
						Min	**-0.3762**
						Max	**0.361706**

TABLE A.2

The Rate e_{oy}/e_o and e_{ox}/e_o in Different Situation

D	E_o	n	nD	nE_o	x	y	e_o	e_{oy}/e_o	e_{ox}/e_o
0.1	0.00025	1000	100	0.25	98.96	12.4474	12.49077	0.996528	0.083261
0.1	0.00025	2000	200	0.5	191.7841	48.9909	49.67835	0.986162	0.165784
0.1	0.00025	3000	300	0.75	272.6421	107.3585	110.7894	0.969032	0.246936
0.1	0.00025	4000	400	1	336.5654	183.9212	194.5532	0.945352	0.326053
0.1	0.0005	1000	100	0.5	95.879	24.5075	24.85156	0.986155	0.165825
0.1	0.0005	2000	200	1	168.2712	91.9816	97.30021	0.945338	0.326092
0.1	0.001	1000	100	1	84.1241	46.0118	48.67371	0.945311	0.32617
0.2	0.00025	1000	100	0.125	99.739	6.2543	6.259744	0.99913	0.041695
0.2	0.00025	2000	200	0.25	197.9201	24.8948	24.98153	0.996528	0.083257
0.2	0.00025	3000	300	0.375	293.0111	55.6305	56.06779	0.992201	0.124651
0.2	0.00025	4000	400	0.5	383.5282	97.9819	99.3568	0.986162	0.165784
0.2	0.00025	5000	500	0.625	468.0589	151.288	154.6231	0.978431	0.206574
0.2	0.00025	6000	600	0.75	545.2842	214.7171	221.579	0.969032	0.246936
0.2	0.00025	7000	700	0.875	613.9989	287.2793	299.876	0.957994	0.286789
0.2	0.00025	8000	800	1	673.1308	367.8423	389.1063	0.945352	0.326053
0.2	0.0005	1000	100	0.25	98.9585	12.4598	12.50325	0.996525	0.083298
0.2	0.0005	2000	200	0.5	191.758	49.0149	49.70303	0.986155	0.165825
0.2	0.0005	3000	300	0.75	272.6287	107.3926	110.8258	0.969022	0.246976
0.2	0.0005	4000	400	1	336.5424	183.9632	194.6004	0.945338	0.326092
0.2	0.001	1000	100	0.5	95.8729	24.5314	24.87614	0.986142	0.165906
0.2	0.001	2000	200	1	168.2482	92.0237	97.34751	0.945311	0.32617
0.4	0.00025	1000	100	0.0625	99.9345	3.1365	3.137184	0.999782	0.020879
0.4	0.00025	2000	200	0.125	199.478	12.5087	12.51959	0.99913	0.041695
0.4	0.00025	3000	300	0.1875	298.2418	28.08	28.13499	0.998845	0.062492
0.4	0.00025	4000	400	0.25	395.8401	49.7896	49.96308	0.996528	0.083259
0.4	0.00025	5000	500	0.3125	491.8919	77.5528	77.9755	0.994579	0.103983
0.4	0.00025	6000	600	0.375	586.0221	111.2611	112.1357	0.992201	0.124652
0.4	0.00025	7000	700	0.4375	677.8632	150.7828	152.3991	0.989394	0.145255
0.4	0.00025	8000	800	0.5	767.0564	195.9638	198.7136	0.986162	0.165784
0.4	0.00025	9000	900	0.5625	853.2535	246.6275	251.0186	0.982507	0.186227
0.4	0.00025	10000	1000	0.625	936.1178	302.576	309.2461	0.978431	0.206574
0.4	0.0005	1000	100	0.125	99.7382	6.2668	6.272266	0.999129	0.041739
0.4	0.0005	2000	200	0.25	197.9169	24.9195	25.00641	0.996524	0.083303
0.4	0.0005	3000	300	0.375	293.0041	55.6672	56.10508	0.992195	0.124693
0.4	0.0005	4000	400	0.5	383.5159	98.0298	99.40607	0.986155	0.165826
0.4	0.0005	5000	500	0.625	468.04	151.3465	154.6842	0.978422	0.206614
0.4	0.0005	6000	600	0.75	545.2573	214.7852	221.6516	0.969022	0.246976
0.4	0.0005	7000	700	0.875	613.963	287.356	299.9597	0.957982	0.286829
0.4	0.0005	8000	800	1	673.0848	367.9264	389.2009	0.945338	0.326092
0.4	0.001	1000	100	0.25	98.9554	12.4845	12.52813	0.996518	0.08338
0.4	0.001	2000	200	0.5	191.7457	49.0629	49.7524	0.986141	0.165908
0.4	0.001	3000	300	0.75	272.6018	107.4608	110.8985	0.969001	0.247056
0.4	0.001	4000	400	1	336.4964	184.0474	194.695	0.945311	0.32617
							Max	**0.999782**	**0.32617**
							Min	**0.945311**	**0.020879**

TABLE A3

Descriptions and Critical Values

D	Eo	n	nD	mean(y)	Std Dev (y)	Critical value (99.9% conf.)
0.1	0.00025	0	0	0	0	0
0.1	0.00025	1000	100	0.0046201	0.27192459	0.897351147
0.1	0.00025	2000	200	0.162046	0.7849972	2.59049076
0.1	0.00025	3000	300	0.0281082	1.428437	4.7138421
0.1	0.00025	4000	400	0.0484781	2.196338	7.2479154
0.1	0.00025	5000	500	0.0855699	3.065313	10.1155329
0.1	0.00025	6000	600	0.1282263	4.022257	13.2734481
0.1	0.00025	7000	700	0.1488998	5.068258	16.7252514
0.1	0.00025	8000	800	0.1595498	6.200332	20.4610956
0.1	0.00025	9000	900	0.1690676	7.402619	24.4286427
0.1	0.00025	10000	1000	0.170381	8.669147	28.6081851
0.1	0.0005	0	0	0	0	0
0.1	0.0005	1000	100	0.0092397	0.54383748	1.794663684
0.1	0.0005	2000	200	0.0324086	1.569928	5.1807624
0.1	0.0005	3000	300	0.0562141	2.856692	9.4270836
0.1	0.0005	4000	400	0.969453	4.3923	14.49459
0.1	0.0005	5000	500	0.1711188	6.129985	20.2289505
0.1	0.0005	6000	600	0.2564143	8.043523	26.5436259
0.1	0.0005	7000	700	0.2977423	10.13507	33.445731
0.1	0.0005	8000	800	0.3190179	12.39863	40.915479
0.1	0.0005	9000	900	0.3380218	14.80249	48.848217
0.1	0.0005	10000	1000	0.3406196	17.33474	57.204642
0.1	0.001	0	0	0	0	0
0.1	0.001	1000	100	0.0184801	1.087586	3.5890338
0.1	0.001	2000	200	0.648104	3.13933	10.359789
0.1	0.001	3000	300	0.112391	5.71192	18.849336
0.1	0.001	4000	400	0.1937944	8.781617	28.9793361
0.1	0.001	5000	500	0.3420512	12.25484	40.440972
0.1	0.001	6000	600	0.5125174	16.07913	53.061129
0.1	0.001	7000	700	0.5950634	20.25855	66.853215
0.1	0.001	8000	800	0.6373955	24.78095	81.777135
0.1	0.001	9000	900	0.6751322	29.58305	97.624065
0.1	0.001	10000	1000	0.6801131	34.64108	114.315564
0.2	0.00025	0	0	0	0	0
0.2	0.00025	500	100	0.0079628	0.18129945	0.598288185
0.2	0.00025	1000	200	0.0131417	0.52535013	1.733655429
0.2	0.00025	1500	300	0.0288099	0.98068668	3.236266044
0.2	0.00025	2000	400	0.0368944	1.516123	5.0032059
0.2	0.00025	2500	500	0.0355849	2.129233	7.0264689
0.2	0.00025	3000	600	0.0275424	2.812428	9.2810124
0.2	0.00025	3500	700	0.0234714	3.547285	11.7060405
0.2	0.00025	4000	800	0.0215808	4.330353	14.2901649
0.2	0.00025	4500	900	0.27459	5.168052	17.0545716
0.2	0.00025	5000	1000	0.0379768	6.060675	20.0002275
0.2	0.0005	0	0	0	0	0
0.2	0.0005	500	100	0.0159259	0.3625952	1.19656416
0.2	0.0005	1000	200	0.0262838	1.050679	3.4672407
0.2	0.0005	1500	300	0.0576185	1.961314	6.4723362

0.2	0.0005	2000	400	0.0737897	3.032123	10.0060059
0.2	0.0005	2500	500	0.0711696	4.258247	14.0522151
0.2	0.0005	3000	600	0.550871	5.624504	18.5608632
0.2	0.0005	3500	700	0.0469423	7.094058	23.4103914
0.2	0.0005	4000	800	0.0431522	8.659998	28.5779934
0.2	0.0005	4500	900	0.0548964	10.33517	34.106061
0.2	0.0005	5000	1000	0.0759232	12.12014	39.996462
0.2	0.001	0	0	0	0	0
0.2	0.001	500	100	0.0318513	0.72516199	2.393034567
0.2	0.001	1000	200	0.0525714	2.101184	6.9339072
0.2	0.001	1500	300	0.1152375	3.922147	12.9430851
0.2	0.001	2000	400	0.1475728	6.063259	20.0087547
0.2	0.001	2500	500	0.1423426	8.514741	28.0986453
0.2	0.001	3000	600	0.1101581	11.2462	37.11246
0.2	0.001	3500	700	0.0938457	14.18404	46.807332
0.2	0.001	4000	800	0.086211	17.31436	57.137388
0.2	0.001	4500	900	0.1096186	20.66284	68.187372
0.2	0.001	5000	1000	0.1515682	24.23056	79.960848
0.4	0.00025	0	0	0	0	0
0.4	0.00025	250	100	-0.0028494	0.1372351	0.45287583
0.4	0.00025	500	200	-0.0074349	0.38729162	1.278062346
0.4	0.00025	750	300	-0.0062026	0.71133353	2.347400649
0.4	0.00025	1000	400	-0.0000456	1.080263	3.5648679
0.4	0.00025	1250	500	0.0119584	1.500478	4.9515774
0.4	0.00025	1500	600	0.0203678	1.968074	6.4946442
0.4	0.00025	1750	700	0.0412512	2.485471	8.2020543
0.4	0.00025	2000	800	0.0805871	3.04281	10.041273
0.4	0.00025	2250	900	0.1319978	3.632001	11.9856033
0.4	0.00025	2500	1000	0.1756502	4.242228	13.9993524
0.4	0.00025	0	0	0	0	0
0.4	0.00025	250	100	-0.0056985	0.27446881	0.905747073
0.4	0.00025	500	200	-0.0148693	0.77457659	2.556102747
0.4	0.00025	750	300	-0.0124045	1.422646	4.6947318
0.4	0.00025	1000	400	-0.0000905	2.160488	7.1296104
0.4	0.00025	1250	500	0.0239154	3.000882	9.9029106
0.4	0.00025	1500	600	0.0407392	3.936034	12.9889122
0.4	0.00025	1750	700	0.0825054	4.970772	16.4035476
0.4	0.00025	2000	800	0.1611684	6.085385	20.0817705
0.4	0.00025	2250	900	0.2639887	7.263687	23.9701671
0.4	0.00025	2500	1000	0.3512863	8.484048	27.9973584
0.4	0.00025	0	0	0	0	0
0.4	0.00025	250	100	-0.0113962	0.54892605	1.811455965
0.4	0.00025	500	200	-0.0297359	1.54909	5.111997
0.4	0.00025	750	300	-0.0248018	2.845123	9.3889059
0.4	0.00025	1000	400	-0.0001707	4.320643	14.2581219
0.4	0.00025	1250	500	0.0478444	6.001194	19.8039402
0.4	0.00025	1500	600	0.0814995	7.871162	25.9748346
0.4	0.00025	1750	700	0.1650262	9.940206	32.8026798
0.4	0.00025	2000	800	0.3223227	12.16889	40.157337
0.4	0.00025	2250	900	0.5279128	14.52484	47.931972
0.4	0.00025	2500	1000	0.7024703	16.96485	55.984005

TABLE A.4

Test Result of the Estimate Model

D	Eo	n	nD	Critical Values (99.9% confi) (CV)	Estimated Critical Values (ECV)	100×(CV-EVC)/nD
0.1	0.00025		0	0	0	0
0.1	0.00025	1000	100	0.897351147	0.757841	0.13951
0.1	0.00025	2000	200	2.59049076	1.956364	0.317063
0.1	0.00025	3000	300	4.7138421	3.595569	0.372758
0.1	0.00025	4000	400	7.2479154	5.675456	0.393115
0.1	0.00025	5000	500	10.1155329	8.198025	0.383902
0.1	0.00025	6000	600	13.2734481	11.15728	0.352695
0.1	0.00025	7000	700	16.7252514	14.55921	0.309435
0.1	0.00025	8000	800	20.4610956	18.40182	0.257409
0.1	0.00025	9000	900	24.4286427	22.68512	0.193725
0.1	0.00025	10000	1000	28.6081851	27.4091	0.119909
0.1	0.0005	0	0	0	0	0
0.1	0.0005	1000	100	1.794663684	1.515682	0.278982
0.1	0.0005	2000	200	5.1807624	3.912728	0.634017
0.1	0.0005	3000	300	9.4270836	7.191138	0.745315
0.1	0.0005	4000	400	14.49459	11.35091	0.786919
0.1	0.0005	5000	500	20.2289505	16.39205	0.76738
0.1	0.0005	6000	600	26.5436259	22.31455	0.704846
0.1	0.0005	7000	700	33.445731	29.11842	0.618188
0.1	0.0005	8000	800	40.915479	36.80365	0.513979
0.1	0.0005	9000	900	48.848217	45.37024	0.386442
0.1	0.0005	10000	1000	57.204642	54.8182	0.238644
0.1	0.001	0	0	0	0	0
0.1	0.001	1000	100	3.5890338	3.031364	0.55767
0.1	0.001	2000	200	10.359789	7.825456	1.267167
0.1	0.001	3000	300	18.849336	14.38228	1.48902
0.1	0.001	4000	400	28.9793361	22.70182	1.569378
0.1	0.001	5000	500	40.440972	32.7841	1.531374
0.1	0.001	6000	600	53.061129	44.6291	1.405338
0.1	0.001	7000	700	66.853215	58.23684	1.230911
0.1	0.001	8000	800	81.777135	73.6073	1.02123
0.1	0.001	9000	900	97.624065	90.74048	0.764842
0.1	0.001	10000	1000	114.315564	109.6364	0.467916
0.2	0.00025	0	0	0	0	0
0.2	0.00025	500	100	0.598288185	0.630202	-0.03191
0.2	0.00025	1000	200	1.733655429	1.520806	0.106425
0.2	0.00025	1500	300	3.236266044	2.671814	0.188151
0.2	0.00025	2000	400	5.0032059	4.083224	0.229995
0.2	0.00025	2500	500	7.0264689	5.755038	0.254286
0.2	0.00025	3000	600	9.2810124	7.687254	0.265626
0.2	0.00025	3500	700	11.7060405	9.879874	0.260881
0.2	0.00025	4000	800	14.2901649	12.3329	0.244659
0.2	0.00025	4500	900	17.0545716	15.04632	0.223139
0.2	0.00025	5000	1000	20.0002275	18.02015	0.198008
0.2	0.0005	0	0	0	0	0
0.2	0.0005	500	100	1.19656416	1.260403	-0.06384

0.2	0.0005	1000	200	3.4672407	3.041612	0.212814
0.2	0.0005	1500	300	6.4723362	5.343627	0.376236
0.2	0.0005	2000	400	10.0060059	8.166448	0.459889
0.2	0.0005	2500	500	14.0522151	11.51008	0.508428
0.2	0.0005	3000	600	18.5608632	15.37451	0.531059
0.2	0.0005	3500	700	23.4103914	19.75975	0.521521
0.2	0.0005	4000	800	28.5779934	24.66579	0.489025
0.2	0.0005	4500	900	34.106061	30.09264	0.445935
0.2	0.0005	5000	1000	39.996462	36.0403	0.395616
0.2	0.001	0	0	0	0	0
0.2	0.001	500	100	2.393034507	2.520806	-0.12777
0.2	0.001	1000	200	6.9339072	6.083224	0.425342
0.2	0.001	1500	300	12.9430851	10.68725	0.751944
0.2	0.001	2000	400	20.0087547	16.3329	0.918965
0.2	0.001	2500	500	28.0986453	23.02015	1.015699
0.2	0.001	3000	600	37.11246	30.74902	1.060574
0.2	0.001	3500	700	46.807332	39.51949	1.04112
0.2	0.001	4000	800	57.137388	49.33158	0.975725
0.2	0.001	4500	900	68.187372	60.18529	0.889121
0.2	0.001	5000	1000	79.960848	72.0806	0.788025
0.4	0.00025	0	0	0	0	0
0.4	0.00025	250	100	0.45287583	0.510132	-0.05726
0.4	0.00025	500	200	1.278062346	1.190527	0.043768
0.4	0.00025	750	300	2.347400649	2.041186	0.102072
0.4	0.00025	1000	400	3.5648679	3.062108	0.12569
0.4	0.00025	1250	500	4.9515774	4.253294	0.139657
0.4	0.00025	1500	600	6.4046442	5.614743	0.14665
0.4	0.00025	1750	700	8.2020543	7.140450	0.1508
0.4	0.00025	2000	800	10.041273	8.848432	0.149105
0.4	0.00025	2250	900	11.9856033	10.72067	0.140548
0.4	0.00025	2500	1000	13.9993524	12.76318	0.123618
0.4	0.0005	0	0	0	0	0
0.4	0.0005	250	100	0.905747073	1.020264	-0.11452
0.4	0.0005	500	200	2.556102747	2.381054	0.087524
0.4	0.0005	750	300	4.6947318	4.082372	0.20412
0.4	0.0005	1000	400	7.1296104	6.124216	0.251349
0.4	0.0005	1250	500	9.9029106	8.506588	0.279265
0.4	0.0005	1500	600	12.9880122	11.22940	0.293238
0.4	0.0005	1750	700	16.4035478	14.29291	0.301519
0.4	0.0005	2000	800	20.0817705	17.69686	0.298113
0.4	0.0005	2250	900	23.9701671	21.44134	0.28098
0.4	0.0005	2500	1000	27.9973584	25.52635	0.247101
0.4	0.001	0	0	0	0	0
0.4	0.001	250	100	1.811455965	2.040527	-0.22907
0.4	0.001	500	200	5.111997	4.762108	0.174945
0.4	0.001	750	300	9.3889059	8.164743	0.408054
0.4	0.001	1000	400	14.2581219	12.24843	0.502422
0.4	0.001	1250	500	19.8039402	17.01318	0.558153
0.4	0.001	1500	600	25.9748346	22.45807	0.585977
0.4	0.001	1750	700	32.8026798	28.58582	0.602408
0.4	0.001	2000	800	40.157337	35.39373	0.595451

0.4	0.001	2250	900	47.931972	42.88269	0.561032
0.4	0.001	2500	1000	55.984005	51.0527	0.49313
					Min	**-0.22907**
					Max	**0.602408**

Appendix B

TABLE B

Areas Under the Normal Curve

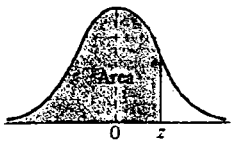

z	0.00	0.01	0.02	0.03	0.04	0.05	0.06	0.07	0.08	0.09
−3.4	0.0003	0.0003	0.0003	0.0003	0.0003	0.0003	0.0003	0.0003	0.0003	0.0002
−3.3	0.0005	0.0005	0.0005	0.0004	0.0004	0.0004	0.0004	0.0004	0.0004	0.0003
−3.2	0.0007	0.0007	0.0006	0.0006	0.0006	0.0006	0.0006	0.0005	0.0005	0.0005
−3.1	0.0010	0.0009	0.0009	0.0009	0.0008	0.0008	0.0008	0.0008	0.0007	0.0007
−3.0	0.0013	0.0013	0.0013	0.0012	0.0012	0.0011	0.0011	0.0011	0.0010	0.0010
−2.9	0.0019	0.0018	0.0017	0.0017	0.0016	0.0016	0.0015	0.0015	0.0014	0.0014
−2.8	0.0026	0.0025	0.0024	0.0023	0.0023	0.0022	0.0021	0.0021	0.0020	0.0019
−2.7	0.0035	0.0034	0.0033	0.0032	0.0031	0.0030	0.0029	0.0028	0.0027	0.0026
−2.6	0.0047	0.0045	0.0044	0.0043	0.0041	0.0040	0.0039	0.0038	0.0037	0.0036
−2.5	0.0062	0.0060	0.0059	0.0057	0.0055	0.0054	0.0052	0.0051	0.0049	0.0048
−2.4	0.0082	0.0080	0.0078	0.0075	0.0073	0.0071	0.0069	0.0068	0.0066	0.0064
−2.3	0.0107	0.0104	0.0102	0.0099	0.0096	0.0094	0.0091	0.0089	0.0087	0.0084
−2.2	0.0139	0.0136	0.0132	0.0129	0.0125	0.0122	0.0119	0.0116	0.0113	0.0110
−2.1	0.0179	0.0174	0.0170	0.0166	0.0162	0.0158	0.0154	0.0150	0.0146	0.0143
−2.0	0.0228	0.0222	0.0217	0.0212	0.0207	0.0202	0.0197	0.0192	0.0188	0.0183
−1.9	0.0287	0.0281	0.0274	0.0268	0.0262	0.0256	0.0250	0.0244	0.0239	0.0233
−1.8	0.0359	0.0352	0.0344	0.0336	0.0329	0.0322	0.0314	0.0307	0.0301	0.0294
−1.7	0.0446	0.0436	0.0427	0.0418	0.0409	0.0401	0.0392	0.0384	0.0375	0.0367
−1.6	0.0548	0.0537	0.0526	0.0516	0.0505	0.0495	0.0485	0.0475	0.0465	0.0455
−1.5	0.0668	0.0655	0.0643	0.0630	0.0618	0.0606	0.0594	0.0582	0.0571	0.0559
−1.4	0.0808	0.0793	0.0778	0.0764	0.0749	0.0735	0.0722	0.0708	0.0694	0.0681
−1.3	0.0968	0.0951	0.0934	0.0918	0.0901	0.0885	0.0869	0.0853	0.0838	0.0823
−1.2	0.1151	0.1131	0.1112	0.1093	0.1075	0.1056	0.1038	0.1020	0.1003	0.0985
−1.1	0.1357	0.1335	0.1314	0.1292	0.1271	0.1251	0.1230	0.1210	0.1190	0.1170
−1.0	0.1587	0.1562	0.1539	0.1515	0.1492	0.1469	0.1446	0.1423	0.1401	0.1379
−0.9	0.1841	0.1814	0.1788	0.1762	0.1736	0.1711	0.1685	0.1660	0.1635	0.1611
−0.8	0.2119	0.2090	0.2061	0.2033	0.2005	0.1977	0.1949	0.1922	0.1894	0.1867
−0.7	0.2420	0.2389	0.2358	0.2327	0.2296	0.2266	0.2236	0.2206	0.2177	0.2148
−0.6	0.2743	0.2709	0.2676	0.2643	0.2611	0.2578	0.2546	0.2514	0.2483	0.2451
−0.5	0.3085	0.3050	0.3015	0.2981	0.2946	0.2912	0.2877	0.2843	0.2810	0.2776
−0.4	0.3446	0.3409	0.3372	0.3336	0.3300	0.3264	0.3228	0.3192	0.3156	0.3121
−0.3	0.3821	0.3783	0.3745	0.3707	0.3669	0.3632	0.3594	0.3557	0.3520	0.3483
−0.2	0.4207	0.4168	0.4129	0.4090	0.4052	0.4013	0.3974	0.3936	0.3897	0.3859
−0.1	0.4602	0.4562	0.4522	0.4483	0.4443	0.4404	0.4364	0.4325	0.4286	0.4247
−0.0	0.5000	0.4960	0.4920	0.4880	0.4840	0.4801	0.4761	0.4721	0.4681	0.4641
0.0	0.5000	0.5040	0.5080	0.5120	0.5160	0.5199	0.5239	0.5279	0.5319	0.5359
0.1	0.5398	0.5438	0.5478	0.5517	0.5557	0.5596	0.5636	0.5675	0.5714	0.5753
0.2	0.5793	0.5832	0.5871	0.5910	0.5948	0.5987	0.6026	0.6064	0.6103	0.6141
0.3	0.6179	0.6217	0.6255	0.6293	0.6331	0.6368	0.6406	0.6443	0.6480	0.6517
0.4	0.6554	0.6591	0.6628	0.6664	0.6700	0.6736	0.6772	0.6808	0.6844	0.6879
0.5	0.6915	0.6950	0.6985	0.7019	0.7054	0.7088	0.7123	0.7157	0.7190	0.7224
0.6	0.7257	0.7291	0.7324	0.7357	0.7389	0.7422	0.7454	0.7486	0.7517	0.7549
0.7	0.7580	0.7611	0.7642	0.7673	0.7704	0.7734	0.7764	0.7794	0.7823	0.7852
0.8	0.7881	0.7910	0.7939	0.7967	0.7995	0.8023	0.8051	0.8078	0.8106	0.8133
0.9	0.8159	0.8186	0.8212	0.8238	0.8264	0.8289	0.8315	0.8340	0.8365	0.8389
1.0	0.8413	0.8438	0.8461	0.8485	0.8508	0.8531	0.8554	0.8577	0.8599	0.8621
1.1	0.8643	0.8665	0.8686	0.8708	0.8729	0.8749	0.8770	0.8790	0.8810	0.8830
1.2	0.8849	0.8869	0.8888	0.8907	0.8925	0.8944	0.8962	0.8980	0.8997	0.9015
1.3	0.9032	0.9049	0.9066	0.9082	0.9099	0.9115	0.9131	0.9147	0.9162	0.9177
1.4	0.9192	0.9207	0.9222	0.9236	0.9251	0.9265	0.9278	0.9292	0.9306	0.9319
1.5	0.9332	0.9345	0.9357	0.9370	0.9382	0.9394	0.9406	0.9418	0.9429	0.9441
1.6	0.9452	0.9463	0.9474	0.9484	0.9495	0.9505	0.9515	0.9525	0.9535	0.9545
1.7	0.9554	0.9564	0.9573	0.9582	0.9591	0.9599	0.9608	0.9616	0.9625	0.9633
1.8	0.9641	0.9649	0.9656	0.9664	0.9671	0.9678	0.9686	0.9693	0.9699	0.9706
1.9	0.9713	0.9719	0.9726	0.9732	0.9738	0.9744	0.9750	0.9756	0.9761	0.9767
2.0	0.9772	0.9778	0.9783	0.9788	0.9793	0.9798	0.9803	0.9808	0.9812	0.9817
2.1	0.9821	0.9826	0.9830	0.9834	0.9838	0.9842	0.9846	0.9850	0.9854	0.9857
2.2	0.9861	0.9864	0.9868	0.9871	0.9875	0.9878	0.9881	0.9884	0.9887	0.9890
2.3	0.9893	0.9896	0.9898	0.9901	0.9904	0.9906	0.9909	0.9911	0.9913	0.9916
2.4	0.9918	0.9920	0.9922	0.9925	0.9927	0.9929	0.9931	0.9932	0.9934	0.9936
2.5	0.9938	0.9940	0.9941	0.9943	0.9945	0.9946	0.9948	0.9949	0.9951	0.9952
2.6	0.9953	0.9955	0.9956	0.9957	0.9959	0.9960	0.9961	0.9962	0.9963	0.9964
2.7	0.9965	0.9966	0.9967	0.9968	0.9969	0.9970	0.9971	0.9972	0.9973	0.9974
2.8	0.9974	0.9975	0.9976	0.9977	0.9977	0.9978	0.9979	0.9979	0.9980	0.9981
2.9	0.9981	0.9982	0.9982	0.9983	0.9984	0.9984	0.9985	0.9985	0.9986	0.9986
3.0	0.9987	0.9987	0.9987	0.9988	0.9988	0.9989	0.9989	0.9989	0.9990	0.9990
3.1	0.9990	0.9991	0.9991	0.9991	0.9992	0.9992	0.9992	0.9992	0.9993	0.9993
3.2	0.9993	0.9993	0.9994	0.9994	0.9994	0.9994	0.9994	0.9994	0.9995	0.9995
3.3	0.9995	0.9995	0.9995	0.9996	0.9996	0.9996	0.9996	0.9996	0.9996	0.9997
3.4	0.9997	0.9997	0.9997	0.9997	0.9997	0.9997	0.9997	0.9997	0.9997	0.9998

References

1 M. Ait-Ahmed, M. Renaud, M. Vidyasagar (Ed.), Proc. Int. Symp. Intel. Robot., Intelligent robotics, Tata MeGraw-Hill, New Delhi, 1993, pp. 13-24.

2 L. Baron, J. Angeles, Advances in Design Automation ASME-69-2 (1994) 467-474. (*1)

3 L. Baron, J. Angeles, in: Proc. IEEE Int. Conf. Robot. Automn, 1994, pp. 974-979. (*2)

4 L. Baron, J. Angeles, in: Proc. IEEE Int. Conf. Robot. Automn, 1995, pp. 1541-1546. (*1)

5 L. Baron, J. Angeles, in: Proc. 9th Wld Congr. Theory Mach. Mech, 1995, pp. 1925-1929. (*2)

6 J. Borenstein, H.R. Everett, L. Feng, D. Wehe, J. Robotic Sys 14 (4) (1997) pp231-249

7 N.-X. Chen, S.-M. Song, Trans. ASME, J. Mech. Des. 116 (1994) 61-66.

8 J.J. Craig, Introduction to Robotics: Mechanics & Control. Addison-Wesley, USA 1986, pp.3-5

9 B. Dasgupta, T.S. Mruthyunjaya, Mech. Mach. Theory 29 (6) (1994) 819-827.

10 B. Dasgupta, T.S. Mruthyunjaya, Mech. Mach. Theory 31 (6) (1996) 799-81 1.

11 B. Dasgupta, Mech. Machi. Theory 35 (2000)15-40

12 G. Deshmukh, M. Pecht, Computers and Structures 34 (3) (1990) 485-491.

13 A. Dhingra, D. Kohli, Y.-X. Xu, Robotics, Spatial Mechanisms and Mechanical Systems ASME-45 (1992) 107-112.

14 J.C. Faugare, D. Lazard, Mech. Mach. Theory 30 (6) (1995) 765-776.

15 Z. Geng, L. Haynes, in: Proc. IEEE Int. Conf. Robot. Automn, 1991, pp. 2650-2655.

16 M. Griffis, J. Duffy, J. Robot. Sys. 6 (6) (1989) 703-720.

17 W. Guozhen, Robotics, Spatial Mechanisms and Mechanical Systems ASME-45 (1992) 113-117.

18 K. Han, W. Chung, Y. Youm, Trans. ASME, J. Mech. Des. 118 (1996) 214-219.

19 K.H. Hunt, E.J.F. Primrose, Mech. Mach. Theory 28 (1) (1993) 31-42.

20 M. Husain, K.J. Waldron, Trans. ASME, J. Mech. Des. 116 (1994) 1102-1107.

21 M.L. Husty, Mech. Mach. Theory 31 (4) (1996) 365-379.

22 C. Innocenti, V. Parenti-Castelli, Mech. Mach. Theory 25 (6) (1990) 611-621.

23 C. Innocenti, V. Parenti-Castelli, Meecanica 26 (1991) 247-252(*1).

24 C. Innocenti, V. Parenti-Castelli, in: Proc. IEEE Sth Int. Conf. Advanced Robotics, Pisa, Italy, 1991, pp. 851- 855. (*2)

25 C. Innocenti, V. Parenti-Castelli, in: Ninth CISM-IF-roMM Symposium on Theory and Practice of Robots and Manipulators, Udine, Italy, 1992.

26 C. Innocenti, V. Parenti-Castelli, Trans. ASME, J. Mech. Des. 115 (1993) 515--521. (*1)

27 C. Innocenti, V. Parenti-Castelli, Trans. ASME, J. Mech. Des. 115 (1993) 932-937 (*2).

28 C. Innocenti, V. Parenti-Castelli, Mech. Mach. Theory 28 (4) (1993) 553-561. (*3)

29 C. Innocenti, Trans. ASME, J. Mech. Des. 117 (1995) 89-95.

30 W.J. Krzanowski *Principles of multivariate analysis : a user's perspective* 1988

31 Q. Liao, L.D. Seneviratne, S.W.E. Earles, Proc. Instn Mech. Engrs 209 (Pt C) (1995) 55-67.

32 W. Lin, C.D. Crane, J. Duffy, Trans. ASME, J. Mech. Des. 116 (1994) 47-53.

33 W. Lin, M. Griffis, J. Duffy, Trans. ASME, J. Mech. Des. 114 (1992) 444-450.

34 H. McCallion, P.D. Truong, in: Proc. 5th Wld Congr, Theory Mach. Mech., 1979 pp611-616

35 J.-P. Meriet, Int. J. Robot. Res. 11 (2) (1992) 150-162.

36 A. Morgan, Solving Polynomial Systems using Continuation for Engineering and Scientific Problems, Prentice-Hall, Englewood Cliffs, NJ, 1987.

37 V. Murthy, K.J. Waldron, Trans. ASME, J. Mech. Des. 114 (1992) 406-413.

38 R. Nair, J.H. Maddocks, Int. J. Robot. Res. 13 (2) (1994) 171-188.

39 P. Nanua, K.J. Waldron, V. Murthy, IEEE Trans. Robot. Automn 6 (4) (1990) 438-444.

40 C.C. Nguyen, Z.-L. Zhou, S.S. Antrazi, C.E. Campbell Jr., in: Proc. IEEE SOUTHEASTCON, 1991, pp. 869-874.

41 V. Parenti-Castelli, R. Di Gregorio, J. Mech. Des. 121 (1999) 21-25

42 M. Raghavan, Trans. ASME, J. Mech. Des. 115 (1993) 277-282.

43 Y.L. Sarkissian, T.F. Padkian, in: Proc. 9th Wld Congr. Theory Mach. Mech, 1995, pp. 1614-1618.

44 S.V. Sreenivasan, K.J. Waldron, P. Nanua, Mech. Mach. Theory 29 (6) (1994) 855-864.

45 S.V. Srinivasan, P. Nanua, Robotics, Spatial Mechanisms and Mechanical Systems ASME-45 (1992) 99-106.

46 D. Stewart, A platform with six degrees of freedom. Proc. Inst. Mech. Engineers, London,180, (1),1965, pp.371-386

47 C.W. Wampler, Mech. Mach. Theory 31 (3) (1996) 331'-337.

48 L.-C.T. Wang, C.C. Chen, IEEE Trans. Robot. Automn 9 (3) (1993) 272-285.

49 F. Wen, C. Liang, Mech. Mach. Theory 29 (4) (1994) 547-557.

50 K. Wohlhart, Mech. Mach. Theory 29 (4) (1994) 581-589.

51 J.P. Yin, C.G. Liang, Mech. Mach. Theory 29 (1) (1994) 1-9.

52 C-de Zhang, 5.-M. Song, in: Proc. IEEE Int. Conf. Robot. Automn, (1991) 2676-2681.

53 C-de Zhang, 5.-M. Song, Trans. ASME, J. Mech. Des 116 (1994) 54-60.